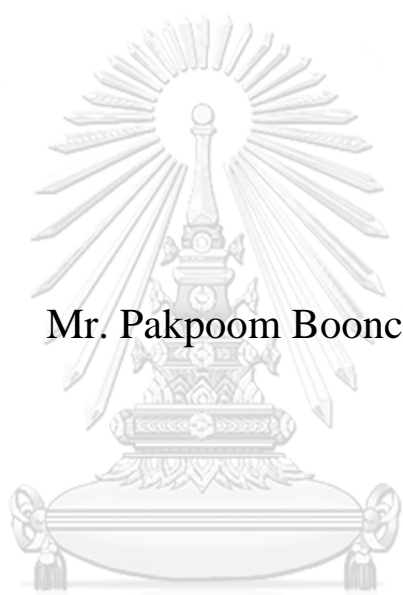


Identification and functional characterization of genes and
microRNAs from *Penaeus vannamei* in response to
pathogens and heat stress



Mr. Pakpoom Boonchuen

จุฬาลงกรณ์มหาวิทยาลัย
CHULALONGKORN UNIVERSITY

A Dissertation Submitted in Partial Fulfillment of the Requirements
for the Degree of Doctor of Philosophy in Biochemistry and Molecular
Biology

Department of Biochemistry

Faculty of Science

Chulalongkorn University

Academic Year 2018

Copyright of Chulalongkorn University

การระบุและลักษณะสมบัติเชิงหน้าที่ของยีนและไมโครอาร์เอ็นเอจาก *Penaeus vannamei* ที่ตอบสนองต่อการติดเชื้อก่อโรคและความเครียดจากความร้อน



วิทยานิพนธ์นี้เป็นส่วนหนึ่งของการศึกษาตามหลักสูตรปริญญาวิทยาศาสตรดุษฎีบัณฑิต
สาขาวิชาชีวเคมีและชีววิทยาโมเลกุล ภาควิชาชีวเคมี
คณะวิทยาศาสตร์ จุฬาลงกรณ์มหาวิทยาลัย
ปีการศึกษา 2561
ลิขสิทธิ์ของจุฬาลงกรณ์มหาวิทยาลัย

Thesis Title	Identification and functional characterization of genes and microRNAs from <i>Penaeus vannamei</i> in response to pathogens and heat stress
By	Mr. Pakpoom Boonchuen
Field of Study	Biochemistry and Molecular Biology
Thesis Advisor	Associate Professor Dr. KUNLAYA SOMBOONWIWAT
Thesis Co Advisor	Professor Dr. Anchalee Tassanakajon Professor Dr. Peter Sarnow

Accepted by the Faculty of Science, Chulalongkorn University in Partial Fulfillment of the Requirement for the Doctor of Philosophy

..... Dean of the Faculty of Science
(Professor Dr. POLKIT SANGVANICH)

DISSERTATION COMMITTEE

..... Chairman
(Assistant Professor Dr. Rath Pichyangkura)

..... Thesis Advisor
(Associate Professor Dr. KUNLAYA SOMBOONWIWAT)

..... Thesis Co-Advisor
(Professor Dr. Anchalee Tassanakajon)

..... Thesis Co-Advisor
(Professor Dr. Peter Sarnow)

..... Examiner
(Associate Professor Dr. TEERAPONG BUABOOCHA)

..... Examiner
(Associate Professor Dr. SUPAART SIRIKANTARAMAS)

..... External Examiner
(Associate Professor Dr. Chalernporn Ongvarrasopone)

ภาคภูมิ บุญชื่น : การระบุและลักษณะสมบัติเชิงหน้าที่ของยีนและไมโครอาร์เอ็นเอจาก *Penaeus vannamei* ที่ตอบสนองต่อการติดเชื้อก่อโรคและความเครียดจากความร้อน. (Identification and functional characterization of genes and microRNAs from *Penaeus vannamei* in response to pathogens and heat stress) อ.ที่ปรึกษาหลัก : รศ. ดร.กุลยา สมบูรณ์วิวัฒน์, อ.ที่ปรึกษาร่วม : ศ. ดร.อัญชลี ทัศนชาจร, ศ. ดร.ปีเตอร์ ชาร์นาว

ในปัจจุบัน เทคนิค high-throughput (HT) sequencing สามารถให้ข้อมูลเชิงลึกเกี่ยวกับการแสดงออกและการควบคุมการแสดงออกของยีน และในงานวิจัยนี้จะนำไปใช้วิธีการตอบสนองของระบบภูมิคุ้มกันของกุ้งต่อสิ่งเร้าต่าง ๆ ในปัจจุบันโรคตายด่วน หรือ acute hepatopancreatic necrosis disease (AHPND) ในกุ้ง เกิดจากเชื้อแบคทีเรีย *Vibrio parahaemolyticus* (VP_{AHPND}) ที่สามารถผลิตโปรตีนสารพิษ Pir มีการระบาดรุนแรงในกุ้ง การศึกษานี้ใช้เทคนิค suppression subtractive hybridization (SSH) เพื่อระบุยีนที่มีการแสดงออกเปลี่ยนแปลงไปในระดับและเซลล์เม็ดเลือดกุ้งหลังจากติดเชื้อ VP_{AHPND} พบว่ายีน *hemocyanin* และยีน *Vago5* เป็นยีนที่มีการแสดงออกมากขึ้นในระดับและเซลล์เม็ดเลือด ตามลำดับ และนำมาศึกษาหน้าที่ในระบบภูมิคุ้มกันต่อเชื้อ VP_{AHPND} โดยโปรตีน hemocyanin ที่ได้จากการทำบริสุทธิ์จากน้ำเลือดสามารถเหนี่ยวนำให้เกิดการเกาะกลุ่มของเซลล์แบคทีเรีย (agglutination) และลดความเป็นพิษ (Neutralization) ของโปรตีนสารพิษ Pir โดยการเกิดปฏิสัมพันธ์กับโปรตีน PirA จากการศึกษาหน้าที่ของยีน *Vago5* ในกุ้งขาวที่ติดเชื้อ VP_{AHPND} ด้วยเทคนิค RNA interference พบว่าการยับยั้งการแสดงออกของยีน *Vago5* ส่งผลให้กุ้งมีการตายสะสมและจำนวนแบคทีเรียในกระเพาะและลำไส้มากขึ้น นอกจากนี้การยับยั้งการแสดงออกของยีน *Vago5* ยังส่งผลให้ยีน PEN4 PO2 และ TNF มีการแสดงออกลดลงอย่างมีนัยสำคัญ แสดงว่า *Vago5* น่าจะเป็นยีนที่สำคัญทำหน้าที่เกี่ยวข้องกับการควบคุมการตอบสนองของระบบภูมิคุ้มกันต่อเชื้อแบคทีเรียในกุ้ง จากการศึกษาเบื้องต้นพบว่าการทำให้กุ้งเครียดด้วยความร้อน (non-lethal heat shock; NLHS) ส่งผลให้กุ้งรอดตายจากการติดเชื้อ VP_{AHPND} มากขึ้นและมีการแสดงออกของยีนในระบบภูมิคุ้มกันมากขึ้น จากการศึกษา mRNA และ miRNA ที่ตอบสนองต่อการติดเชื้อ VP_{AHPND} ภายใต้สภาวะ NLHS และสภาวะปกติ (NH) และทำการวิเคราะห์ปฏิสัมพันธ์ของ miRNA และ mRNA พบว่าสภาวะ NLHS สามารถเหนี่ยวนำยีนในกระบวนการ prophenoloxidase (proPO) วิถีธำรงก่อกูลของเซลล์เม็ดเลือด และกระบวนการผลิตเปปไทด์ต้านจุลชีพให้มีการแสดงออกเปลี่ยนแปลงไป จากผลการศึกษา miRNA ที่ตอบสนองต่อการติดเชื้อ VP_{AHPND} ที่น่าสนใจ พบว่า Iva-miR-4850 สามารถจับบริเวณ 3'-UTR ของยีน PO2 ส่งผลให้เกิดการยับยั้งการแสดงออกของยีน PO2 และกระบวนการ proPO แต่มีการเพิ่มขึ้นของจำนวนแบคทีเรียในกุ้งภายหลังจากการฉีด Iva-miR-4850 ได้ นอกจากนี้โรคตัวแดงดวงขาวซึ่งเกิดจากเชื้อไวรัสตัวแดงดวงขาว (WSSV) ซึ่งเป็นโรคติดเชื้อที่ส่งผลในกุ้งตายเป็นจำนวนมาก ในการทดลองนี้จึงใช้เทคนิค psoralen analysis of RNA interactions and structures (PARIS) เพื่อระบุปฏิสัมพันธ์ของ RNA ในเซลล์เม็ดเลือดของกุ้งที่ติดเชื้อ WSSV ถึงแม้ว่ายังไม่ได้ลำดับนิวคลีโอไทด์ แต่ในการทดลองพบที่สามารถตรวจ RNA ในเซลล์เม็ดเลือดของกุ้งด้วย psoralen เป็นผลสำเร็จ จากผลการวิจัยข้างต้นจึงสรุปได้ว่า จากการศึกษาข้อมูลทรานสคริปโตมของกุ้งที่ติดเชื้อก่อโรคหรือ NLHS ด้วยเทคนิค HT ร่วมกับการศึกษาหน้าที่ของโปรตีนในระบบภูมิคุ้มกัน แสดงให้เห็นถึงความซับซ้อนของการตอบสนองภูมิคุ้มกันของกุ้งเพื่อส่งเสริมการป้องกันตัวเองอย่างมีประสิทธิภาพ

จุฬาลงกรณ์มหาวิทยาลัย
CHULALONGKORN UNIVERSITY

สาขาวิชา	ชีวเคมีและชีววิทยาโมเลกุล	ลายมือชื่อนิติ
ปีการศึกษา	2561
		ลายมือชื่อ อ.ที่ปรึกษาหลัก
		ลายมือชื่อ อ.ที่ปรึกษาร่วม
		ลายมือชื่อ อ.ที่ปรึกษาร่วม

5772835623 : MAJOR BIOCHEMISTRY AND MOLECULAR BIOLOGY

KEYWORD: *Vibrio parahaemolyticus*, Non-lethal heat shock, microRNA, *Penaeus vannamei*, Shrimp immunity, White spot syndrome virus

Pakpoom Boonchuen : Identification and functional characterization of genes and microRNAs from *Penaeus vannamei* in response to pathogens and heat stress. Advisor: Assoc. Prof. Dr. KUNLAYA SOMBOONWIWAT Co-advisor: Prof. Dr. Anchalee Tassanakajon, Prof. Dr. Peter Sarnow

In the present day, high-throughput (HT) sequencing techniques provide in-depth data on how the transcripts are expressed and regulated and in this case shed light on how innate immunity responds to different stimuli. Acute Hepatopancreatic Necrosis Disease (AHPND) caused by *Vibrio parahaemolyticus* producing Pir toxin (VP_{AHPND}) is a current severe bacterial disease in shrimp. Suppression subtractive hybridization (SSH) was used to identify differentially expressed genes (DEGs) in hepatopancreas and hemocyte of VP_{AHPND}-challenged *Penaeus vannamei*. The *hemocyanin* and *Vago5* were found as up-regulated genes in hepatopancreas and hemocyte of VP_{AHPND}-infected *P. vannamei*, respectively. Their functions in shrimp immunity against VP_{AHPND} infection were then characterized. The native hemocyanin protein purified from hemolymph was able to agglutinate VP_{AHPND} *in vitro* and neutralize of VP_{AHPND} secreted toxin via direct interaction with the PirA protein. The *Vago5*, the early VP_{AHPND}-responsive gene in *P. vannamei* hemocyte, was functionally characterized by RNA interference. *Vago5* knockdown in VP_{AHPND}-infected *P. vannamei* resulted in the increase in shrimp mortality and the number of bacteria in stomach and hepatopancreas. Moreover, *Vago5* knockdown caused a significant decrease in *PEN4*, *PO2* and *TNF* expression suggesting its role in modulating antibacterial responses. As reported previously, non-lethal heat shock (NLHS) could enhance the resistance of *P. vannamei* to VP_{AHPND} infection and induce expression of immune-related genes. Herein, HT-sequencing of total RNAs and small RNAs from *P. vannamei* hemocyte challenged with VP_{AHPND} under NLHS and non-heat stress (NH) conditions brought about the data on NLHS-induced DEGs and differentially expressed miRNAs (DEMs) and the miRNA-mRNA regulatory network. Furthermore, pathway analysis of the NLHS-induced DEMs and their target DEGs which have immune-related functions, demonstrated that NLHS induces changes in expression of genes involved in prophenoloxidase system, hemocyte homeostasis and antimicrobial peptide production of VP_{AHPND}-infected *P. vannamei*. Focusing on VP_{AHPND}-responsive miRNAs targeting immune genes, lva-miR-4850 was studied for its function in regulating prophenoloxidase 2 (*PO2*) gene expression. Introducing the lva-miR-4850 mimic into the VP_{AHPND}-infected shrimp caused the reduction of the *PO2* transcript and the PO activity but significantly increased the number of bacteria in the VP_{AHPND}-targeted shrimp tissues. White spot disease caused by white spot syndrome virus (WSSV), is highly contagious and lethal in shrimp. The method called, Psoralen Analysis of RNA Interactions and Structures (PARIS) was performed to determine the transcriptome-wide base pairing interactions in hemocyte of WSSV-infected *P. vannamei*. Although the sequencing data have not yet obtained, we demonstrated for the first time the success of psoralen-induced RNA cross-linking in invertebrates tissues. In conclusions, the *P. vannamei* transcriptome-wide interactions during pathogen infections and NLHS elucidated by HT sequencing based technologies and protein function analysis, revealed the complexity of the shrimp innate immune responses to promote effective host defense.

CHULALONGKORN UNIVERSITY

Field of Study:	Biochemistry and Molecular Biology	Student's Signature
Academic Year:	2018	Advisor's Signature
		Co-advisor's Signature
		Co-advisor's Signature

ACKNOWLEDGEMENTS

On the completion of my thesis, I would like to express my deepest gratitude to my superlative supervisor, Assoc. Prof. Kunlaya Somboonwiwat, for her excellent guidance, supervision, encouragement and supports throughout my 5-year study. The great suggestion and discussion with you have become essential keys for developing my research outcome. Especially, I have to thank you very much for your hard effort to teach, improve and inspire me into an efficient researcher. I would like to appreciate Prof. Anchalee Tassanakajon, my co-supervisor, for giving a chance to join a warm, huge, and excellent laboratory research group.

To Prof. Peter Sarnow, my co-supervisor, thank you for your warm welcome in Stanford University as well as your great supports and advises all the time while I was studying in USA. Moreover, I did not only gain a lot of knowledge of science from you but I also got your worth experiences of science that you kindly shared to me. I also would like to thank Sarnow's lab members for their valuable suggestion and discussion on my works in USA.

I also thank Dr. Phattarunda Jaree and Prof. Vichien Rimphanitchayakit for their suggestion and help in my research experiment. The Marine Shrimp Broodstock Research Center II (MSBRC-2), Charoen Pokphand Foods PCL for providing *V. parahaemolyticus* AHPND strains is acknowledged. Dr. Premruethai Supungul and all of my friends in Thailand and USA are greatly appreciated for their helpful suggestion and discussion.

Additional great appreciation is extended to Assist. Prof. Rath Pichyangkura, Assoc. Prof. Teerapong Buaboocha, Assoc. Prof. Supaart Sirikantaramas and Assoc. Prof. Chalernporn Ongvarrasopone for giving me your precious time on being my thesis's defense committee.

I wish to acknowledge the Royal Golden Jubilee Ph.D. program, Thailand Research Fund, the 100th Anniversary Chulalongkorn University Fund for Doctoral Scholarship, and the 90th Anniversary of Chulalongkorn University Fund (Ratchadaphiseksomphot Endowment Fund) for my student fellowship as well as the financial supports from the National Research University Project, Office of Higher Education Commission (WCU-58-009-FW), Thailand Research Fund to KS (Grant No.

RSA5980055), Chulalongkorn University under the Ratchadaphisek Somphot Endowment to the Center of Excellence for Molecular Biology and Genomics of Shrimp and the Outstanding Research Performance Program: Chulalongkorn Academic Advancement into Its 2nd Century Project (CUAASC).

Finally, I would like to express my deepest gratitude to indispensable people including my parents and all members in my family for their guidance, understanding, encouragement, endless love, care and support along my lifetime.

Pakpoom Boonchuen



TABLE OF CONTENTS

	Page
ABSTRACT (THAI)	iii
ABSTRACT (ENGLISH).....	iv
ACKNOWLEDGEMENTS.....	v
TABLE OF CONTENTS.....	vii
LIST OF TABLES.....	xiii
LIST OF FIGURES	xv
LIST OF ABBREVIATIONS.....	xx
CHAPTER I.....	1
1.1 General introduction.....	2
1.2 Taxonomy of the pacific white shrimp, <i>Penaeus vannamei</i>	3
1.3 Disease in shrimp.....	4
1.3.1 Viral diseases.....	5
1.3.1.1 White spot syndrome.....	5
1.3.1.2 Taura syndrome.....	6
1.3.1.3 Yellow head disease.....	7
1.3.2 Bacterial diseases.....	8
1.3.2.1 Vibriosis.....	8
1.3.2.2 Early Mortality Syndrome (EMS).....	9
1.4 The immune responses in shrimp.....	11
1.4.1 The prophenoloxidase system.....	12
1.4.2 Pattern recognition proteins.....	14
1.4.3 Antimicrobial peptides (AMPs).....	14
1.5 RNA interference pathway.....	15
1.6 Non-lethal heat shock.....	16
1.7 Purpose of this thesis research.....	17

CHAPTER II.....	20
2.1 Introduction.....	21
2.2 Materials	22
2.2.1 Equipment	22
2.2.2 Chemicals and reagents	22
2.2.3 Enzymes and kits.....	24
2.2.4 Experimental shrimp, microorganisms, cells and viruses	24
2.2.5 Software.....	24
2.2.6 Animal cultivation.....	25
2.2.7 <i>Vibrio parahaemolyticus</i> (VP _{AHPND}) challenge.....	25
2.2.8 Partially purified VP _{AHPND} toxin challenge.....	25
2.2.9 The detection of VP _{AHPND} from cultures or infected shrimp.....	26
2.2.10 Total RNA extraction by GENEzol™ reagent and DNase I treatment.....	27
2.2.11 Single-stranded cDNA synthesis using the RevertAid First-strand cDNA Synthesis Kit (Thermo Fisher Scientific).....	28
2.2.12 Hemocyte and hepatopancreas collection and RNA preparation.....	28
2.2.13 Suppression subtractive hybridization (SSH).....	28
2.2.14 Evaluation of Suppression subtractive hybridization efficiency	30
2.2.15 cDNA cloning, sequencing, and homology analysis.....	31
2.2.16 Confirmation of gene up-regulation in response to VP _{AHPND} infection by qRT-PCR.....	31
2.2.17 Expression analysis of hemocyanin genes in response to VP _{AHPND} toxin infection by qRT-PCR.....	32
2.2.18 Native hemocyanin purification	33
2.2.19 Biological activity of hemocyanin on VP _{AHPND}	34
2.2.19.1 <i>In vitro</i> antibacterial activity of hemocyanin on VP _{AHPND}	34
2.2.19.2 <i>In vivo</i> antibacterial activity of hemocyanin on VP _{AHPND}	34
2.2.20 Biological activity of hemocyanin on VP _{AHPND} TOXIN.....	35
2.2.20.1 ELISA-based binding assay of hemocyanin and VP _{AHPND} toxin.....	35
2.2.20.2 Neutralization of VP _{AHPND} toxin by hemocyanin.....	36

2.2.21 Functional analysis of <i>Vago5</i> by RNAi-mediated double-stranded RNA	37
2.2.21.1 Preparation of double-stranded RNA (dsRNA)	37
2.2.21.2 <i>In vivo</i> gene knockdown of <i>Vago5</i>	38
2.2.21.3 <i>In vivo</i> gene knockdown of <i>Vago5</i> upon VP _{AHPND} infection.....	38
2.2.21.4 Effect of <i>Vago5</i> gene silencing on the mRNA levels of the shrimp immune-related pathway	39
2.3 Results.....	41
2.3.1 Diagnosis of <i>Vibrio parahaemolyticus</i> AHPND (VP _{AHPND}) infection in shrimp.....	41
2.3.2 Evaluation of SSH efficiency	41
2.3.3 Identification of VP _{AHPND} -responsive genes in shrimp hepatopancreas and hemocytes by SSH.....	42
2.3.4 Gene expression analysis in VP _{AHPND} - and toxin-challenged shrimp hepatopancreas by qRT-PCR	52
2.3.5 Functional characterization of hemocyanin in shrimp upon VP _{AHPND} infection.....	55
2.3.5.1 Purification of hemocyanin protein from <i>P. vannamei</i> hemolymph	55
2.3.5.2 Bacterial agglutination	57
2.3.5.3 Effect of hemocyanin protein on VP _{AHPND} clearance.....	58
2.3.5.4 Partial purification of VP _{AHPND} toxin	59
2.3.5.5 Neutralizing activity of hemocyanin protein on the VP _{AHPND} toxin	60
2.3.5.6 Protein-protein interaction assay between rPirA and B proteins and purified native hemocyanin using the ELISA technique	62
2.3.6 Confirmation of the differentially expressed genes in VP _{AHPND} -challenged shrimp hemocyte by qRT-PCR	63
2.3.7 Functional characterization of <i>Vago5</i> in shrimp upon VP _{AHPND} infection.....	64
2.3.7.1 Gene silencing of <i>Vago5</i> using dsRNA.....	64
2.3.7.2 Effect of <i>Vago5</i> gene silencing in <i>P. vannamei</i> upon VP _{AHPND} infection	66

2.3.7.3 Effect of <i>Vago5</i> gene silencing on the bacterial count in VP _{AHPND} infected <i>P. vannamei</i>	67
2.3.7.4 Effects of <i>Vago5</i> gene silencing on the mRNA levels of the shrimp immune-related genes.....	69
2.4 Discussions	71
2.4.1 Identification of genes in response to <i>Vibrio parahaemolyticus</i> AHPND (VP _{AHPND}) infection by suppression subtractive hybridization (SSH).	71
2.4.2 Functional characterization of hemocyanin in response to <i>Vibrio parahaemolyticus</i> AHPND (VP _{AHPND}) infection.	72
CHAPTER III	77
3.1 Introduction.....	78
3.2 Materials	80
3.2.1 Chemicals, reagents, enzymes and kits	80
3.2.2 Experimental shrimp, microorganisms, cells and viruses	80
3.2.3 Software.....	80
3.2.4 Animal cultivation.....	81
3.2.5 Non-lethal heat shock (NLHS) of <i>P. vannamei</i>	81
3.2.6 Single-stranded cDNA synthesis using the RevertAid First-strand cDNA Synthesis Kit (Thermo Fisher Scientific).....	81
3.2.7 Small RNA library sequencing using the MiSeq instrument (Illumina) ..	82
3.2.7.1 Sample preparation.....	82
3.2.7.2 Small RNA library preparation and sequencing.....	83
3.2.7.3 Small RNA library preparation	86
3.2.7.4 Stem-loop quantitative Real-time PCR analysis	87
3.2.7.5 miRNA target prediction	89
3.2.7.6 miRNA/mRNA interaction network analysis.....	90
3.3 Results.....	91
3.3.1 Effect of NLHS on shrimp survival upon VP _{AHPND} challenge.....	91
3.3.2 Total small RNA preparation	92
3.3.3 Sequence analysis of shrimp miRNAs	92

3.3.4 Integrated analysis of miRNA and gene expression in the hemocytes of shrimp under the NLHS-VP condition	97
3.3.4.1 qRT-PCR validation of significant differentially expressed miRNAs (DEMs) and differentially expressed genes (DEGs)	98
3.3.4.2 Correlation of DEMs and DEGs of shrimp in response to VP _{AHPND} infection under the heat stress condition	101
3.4 Discussion	106
CHAPTER IV	110
4.1 Introduction	111
4.2 Materials	114
4.2.1 Chemicals, reagents, enzymes and kits	114
4.2.2 Experimental shrimp, microorganisms, cells and viruses	114
4.2.3 Software	114
4.2.4 miRNA target prediction	114
4.2.5 miRNA/mRNA interaction network analysis	115
4.2.6 Dual-luciferase reporter assay	115
4.2.7 Mimic, scramble mimic, anti-miRNA oligonucleotide (AMO), and AMO scramble	116
4.2.8 <i>In vivo</i> lva-miR-4850 introducing and silencing in shrimp	117
4.2.9 Phenoloxidase activity assay	117
4.3 Results	118
4.3.1 miRNA expression analysis upon VP _{AHPND} infection using stem-loop real-time PCR	118
4.3.2 miRNA target prediction	119
4.3.3 Expression analysis of the target mRNA of lva-miR4850 in <i>P. vannamei</i> shrimp by qRT-PCR	122
4.3.4 Confirmation of target mRNA of lva-miR4850 by dual-luciferase reporter assay	123
4.3.5 Regulation of <i>PO2</i> gene and proPO activating system by lva-miR-4850 in VP _{AHPND} -infected shrimp	125
4.3.6 Effect of mimic and AMO lva-miR-4850 on the number of bacteria in stomach and hepatopancreas of VP _{AHPND} -infected shrimp	127

4.4 Discussion.....	128
CHAPTER V	131
5.1 Introduction.....	132
5.2 Materials	133
5.2.1 Equipment	133
5.2.2 Chemicals and reagents	133
5.2.3 Enzymes and kits.....	134
5.2.4 Experimental shrimp, microorganisms, cells and viruses	135
5.2.5 PARIS library construction	135
5.3 Results.....	142
5.3.1 Establishment of mRNAs and small RNA of WSSV-infected <i>P. vannamei</i> hemocyte by the Next generation sequencing and used as reference.....	142
5.3.1.1 Next generation sequencing	142
5.3.1.2 Differential expression of genes in <i>P. vannamei</i> hemocyte upon WSSV infection.....	143
5.3.1.3 Small RNA-Seq data analysis	145
5.3.2 PARIS library construction	149
5.4 Discussion.....	154
CHAPTER VI CONCLUSIONS	155
REFERENCES	158
CURRICULUM VITAE.....	170
REFERENCES	175
VITA.....	177

LIST OF TABLES

	Page
Table 1 Primer used for the detection of VP _{AHPND} in shrimp and bacterial isolates....	27
Table 2 Primers used for qRT-PCR.....	32
Table 3 Primers used for qRT-PCR in Vago5 knockdown shrimp	40
Table 4 Up-regulated genes at 3/6 h post challenge in the hepatopancreas of VP _{AHPND} -infected <i>P. vannamei</i> identified from suppression subtractive hybridization.	45
Table 5 Up-regulated genes at 48 h post challenge in the hepatopancreas of VP _{AHPND} -infected <i>P. vannamei</i> identified from suppression subtractive hybridization.....	47
Table 6 Up-regulated genes at 3/6 h post challenge in the hemocyte of VP _{AHPND} -infected <i>P. vannamei</i> identified from suppression subtractive hybridization.....	49
Table 7 Up-regulated genes at 48 h post challenge in the hemocyte of VP _{AHPND} -infected <i>P. vannamei</i> identified from suppression subtractive hybridization.....	51
Table 8 Primer used for the first-strand cDNA synthesis of miRNAs	82
Table 9 Primers used for qRT-PCR in stem-loop qRT-PCR.....	89
Table 10 Summary of sequences identified from the small RNA libraries of <i>P. vannamei</i> hemocyte in the NLHS-VP condition at 0, 6, and 24 hpi, and in the NH-VP condition at 0 and 6 hpi.....	94
Table 11 Nucleotide sequences of differentially expressed miRNA homologs identified in NLHS-VP-infected <i>P. vannamei</i> hemocytes.....	95
Table 12 Nucleotide sequences of differentially expressed miRNA homologs identified in NH-VP-infected <i>P. vannamei</i> hemocytes.....	97
Table 13 Mimic, scramble mimic, anti-miRNA oligonucleotide (AMO), and AMO scramble RNA sequences	116
Table 14 The custom RT primer sequence	140
Table 15 Differentially expressed genes from shrimp hemocyte upon WSSV infection that were involved in shrimp immunity.....	145
Table 16 Summary of sequences identified from the small RNA libraries of <i>P. vannamei</i> hemocyte infected with WSSV at 24 hpi	146

Table 17 Nucleotide sequences of differentially expressed miRNA homologs identified in WSSV-infected *P. vannamei* hemocytes.....147



LIST OF FIGURES

	Page
Figure 1 Shrimp aquaculture production by (A) world region and (B) in Asia by species during 1995-2018.	3
Figure 2 GOAL 2017 survey in issues and challenges of shrimp aquaculture in all countries. The 17 issues were rearranged by survey and indicated in tree level (not important, moderately important, and extremely important). The major challenge issues that show the extremely important level in shrimp aquaculture are diseases. (Source: GOAL 2017).....	5
Figure 3 White spot syndrome disease.	6
Figure 4 Purified TSV suspension.	6
Figure 5 Yellow head disease in shrimp.	8
Figure 6 The colonies of luminescent bacteria, <i>V. harveyi</i> are grown on selective media (left) and <i>V. harveyi</i> infected shrimp (right).	9
Figure 7 The infected shrimp caused by early mortality syndrome or Acute Hepatopancreatic Necrosis Disease (EMS/AHPND). The black arrow indicated the pale hepatopancreas of infected shrimp (left) compared to the brown hepatopancreas of normal shrimp (right) (Tran et al., 2013).....	9
Figure 8 Structural comparison of PirA ^{VP} and PirB ^{VP} with Cry.	10
Figure 9 The model of shrimp immune system (Tassanakajon et al. 2013).....	12
Figure 10 The prophenoloxidase (proPO)-activating system in arthropods.....	13
Figure 11 The miRNA processing pathway (Winter et al., 2009).....	16
Figure 12 The PCR-Select™ cDNA Subtraction procedure (Clontech).	30
Figure 13 The experimental design for neutralization activity assay (Boonchuen et al., 2017).	37
Figure 14 Analysis of VP and VP _{AHPND} infections in the experimental <i>P. vannamei</i> . TLH, AP2, and TUMSAT-Vp3 fragments were amplified by PCR in VP- and VP _{AHPND} -challenged shrimp at 48 h post-infection. Lanes Neg are the negative control.	41
Figure 15 Analysis of the SSH efficiency of VP _{AHPND} -challenged shrimp Hc (3/6Hc and 48Hc) and Hp (3/6Hp and 48Hp) SSH libraries by comparing the transcript	

abundance of EF-1 α in the unsorted and sorted cDNA samples amplified by PCR.....	42
Figure 16 Percentages of gene groups identified from SSH libraries. Clones from the SSH libraries of <i>P. vannamei</i> hepatopancreas and hemocyte infected with VP _{AHPND} at 3/6 h post challenge and 48 h post challenge, respectively, were obtained from sequencing followed by annotation and categorization into nine groups of genes according to their function.....	44
Figure 17 Expression of hemocyanin genes identified from SSH libraries in VP _{AHPND} ⁻ and VP _{AHPND} toxin-infected <i>P. vannamei</i> shrimp.....	54
Figure 18 Purification of the putative native hemocyanin protein by Blue-Sepharose column chromatography.....	55
Figure 19 Purification of the native hemocyanin protein by DEAE Sepharose Fast Flow column chromatography.....	56
Figure 20 The purified hemocyanin protein was separated by Coomassie blue stained-10% SDS-PAGE and 10% Native-PAGE. The amino acid sequences of two hemocyanin (bands indicated by arrows) were analyzed by nano LC-MS/MS using the MASCOT program. The best hits for both hemocyanin amino acid sequences are shown in the table below.....	57
Figure 21 VP _{AHPND} agglutination by hemocyanin. VP _{AHPND} was mixed and incubated with 40 μ g/ml hemocyanin overnight at 30°C, placed on a microscope slide, and then Gram-stained. The 40 μ g/ml BSA and 20 mM Tris-HCl (pH 8.0) were used as control treatments. Agglutination was observed under a light microscope at 100 \times magnification. Scale bar indicates 10 μ m.....	58
Figure 22 The effect of hemocyanin treatment on the number of VP _{AHPND} counts (CFU/ml).....	59
Figure 23 The partially purified VP _{AHPND} toxin protein separated by Coomassie blue stained-12.5% SDS-PAGE. Arrows indicate the expected bands of rPirA and rPirB proteins.....	60
Figure 24 Survival of shrimp challenged with hemocyanin-neutralized VP _{AHPND} toxin.....	61
Figure 25 Hepatopancreatic histology of shrimp injected with hemocyanin-neutralized VP _{AHPND} toxin.....	61
Figure 26 Analysis of recombinant proteins of PirA (rPirA) and PirB (rPirB) by 12.5% SDS-PAGE staining with Coomassie brilliant blue.....	62

Figure 27 Binding ability of rPirA (●) and rPirB (■) on the immobilized hemocyanin, as determined by ELISA.....	63
Figure 28 Expression of differentially expressed immune-related genes identified from Hemocyte SSH libraries in the VP _{AHPND} -infected hemocyte of <i>P. vannamei</i> . 64	
Figure 29 Analysis of purified dsVago5 and dsGFP using 2% agarose gel electrophoresis.	65
Figure 30 The efficiency of dsRNA-mediated gene knockdown of Vago5 gene at 24 h post-dsRNA injection.....	65
Figure 31 Effect of <i>Vago5</i> gene knockdown in VP _{AHPND} infected <i>P. vannamei</i>	66
Figure 32 Effect of <i>Vago5</i> gene knockdown on VP _{AHPND} infection on total Vibrio count.....	68
Figure 33 VP _{AHPND} verification by colony PCR.	69
Figure 34 Expression analysis of <i>Vago5</i> and other shrimp immune-related genes in dsVago5, dsGFP, and 0.85% NaCl-injected shrimp challenged with VP _{AHPND}	70
Figure 35 Small RNA library preparation workflow using the TruSeq® Small RNA Sample Preparation Kit.	84
Figure 36 Small RNA data analysis workflow.	87
Figure 37 Effect of chronic heat stress on the survival of AHPND-challenged shrimp. The final observation of survival was performed at 53 h post immersion. All experiments were performed in triplicate. Survival percentage was calculated as mean ± 1 S.E. at each time point.	91
Figure 38 Verification of total small RNA quality by denaturing 15% acrylamide gel.	92
Figure 39 Length distribution and abundance of small RNAs in the small RNA libraries of 0 NLHS-VP, 6 NLHS-VP, 24 NLHS-VP, 0 NH-VP, and 6 NH-VP.	93
Figure 40 Composition of small RNAs in the small RNA NGS libraries.	94
Figure 41 Validation of RNA-Seq using qRT-PCR	99
Figure 42 Relative expression analysis of miRNAs in response to VP _{AHPND} infection under heat and non-heat stress conditions. Total RNA from VP _{AHPND} -infected <i>P. vannamei</i> hemocyte under heat and non-heat stress conditions was used as a template for specific stem-loop first-strand cDNA synthesis. The relative expression levels of 10 miRNAs were determined by qRT-PCR and standardized against U6 as the internal reference at 0, 6, and 24 hpi. The results were derived from triplicate	

experiments. Data are presented as means \pm standard deviations. Asterisks indicate significant differences at $P < 0.05$	100
Figure 43 Venn diagrams represent unique and common shrimp mRNAs and miRNAs in response to VP _{AHPND} infection under heat and non-heat stress conditions.	102
Figure 44 The miRNA-mRNA negative correlation network based on predicted miRNA target function (A) and unique isotig (B).	102
Figure 45 Relative expression analysis of genes in the NLSH modulated immune pathways processes.	104
Figure 46 A schematic representation of the predicted interactions between the miRNAs and target immune genes of <i>P. vannamei</i> under the NLHS-VP condition.	105
Figure 47 Relative expression analysis of miRNAs in response to VP _{AHPND} infection.	119
Figure 48 The predicted interactions between miRNAs and target <i>P. vannamei</i> immune genes.	121
Figure 49 Prediction of target genes, miRNA binding site and expression analysis of lva-miR-4850.	122
Figure 50 Sequence alignment of the lva-miR-4850 binding site for the PO2 gene between the wild type and mutated seed sequence. Yellow highlight represents the lva-miR-4850 binding sequence.	124
Figure 51 <i>In vitro</i> miRNA/target interaction analysis.	124
Figure 52 Regulation of <i>PO2</i> gene by lva-miR-4850 in VP _{AHPND} infected shrimp.	126
Figure 53 Regulation of proPO activating system by lva-miR-4850 in VP _{AHPND} infected shrimp.....	126
Figure 54 Effects of mimic and AMO lva-miR-4850 on the number of bacteria in stomach and hepatopancreas of VP _{AHPND} -infected shrimp.....	127
Figure 55 Outline of the PARIS experimental strategy. Major steps are explained on the right side (Lu et al., 2018).....	136
Figure 56 Diagram and example result for 2D gel purification of crosslinked and digested RNA.....	138
Figure 57 Analysis of total RNA quality using a Bioanalyzer.	142
Figure 58 Sample correlation analysis by Pearson correlation. The differences in gene expression between NaCl and WSSV libraries that were differentially expressed ($P < 0.05$) by at least 2-fold were generated as a matrix table. The unigenes from each	

library were counted. Sample correlations were calculated using ENCODE software.	143
Figure 59 The overall results of FPKM cluster analysis based on clustering using the $\log_{10}(\text{FPKM}+1)$ value.	144
Figure 60 Hierarchy-clustered heatmap of (TMM-normalized) FPKM expression values for miRNAs (represented in rows) that were at least 2-fold differentially expressed ($P < 0.05$).	146
Figure 61 Analysis of crosslinked RNA quality using a Bioanalyzer. The crosslinked RNA of WSSV- or 0.85% NaCl-injected shrimp at 24 h were analyzed by Agilent RNA 6000 Pico Kit on a bioanalyzer instrument. The un-crosslinked RNA was used as a control.	150
Figure 62 Analysis of purified RNase III-treated RNA quality using a Bioanalyzer.	150
Figure 63 Analysis of crosslinked RNA libraries constructed by 2D gel.....	151
Figure 64 Analysis of extracted RNA quality using a Bioanalyzer.....	152
Figure 65 Quantitative analysis of PARIS libraries using bioanalyzer. The amplified products of PARIS libraries (WSSV-1, WSSV-2, WSSV-3, NaCl-1, NaCl-2, and NaCl-3) were electrophoresed using an Agilent High-sensitivity DNA Kit.	153

LIST OF ABBREVIATIONS

AHPND	Acute hepatopancreatic necrosis disease
bp	Base pair
Da	Dalton
DNA	Deoxyribonucleic acid
dsRNA	Double-stranded RNA
ELISA	Enzyme-linked immunosorbent assay
EMS	Early mortality syndrome
EST	Expressed sequence tag
FBS	Fetal bovine serum
g	Gram
GFP	Green fluorescence protein
h	Hour, Hours
HMC	hemocyanin
K	Kilo
l	Liter
LB	Luria-Bertani
LD ₅₀	Lethal Dose fifty
LHM	Lobster hemolymph medium
LPS	Lipopolysaccharide
m	Milli
M	Molar
min	Minute, Minutes
miRNA	MicroRNA
NGS	Next generation sequencing
nt	Nucleotide
PAGE	polyacrylamide electrophoresis
PARIS	psoralen analysis of RNA interactions and structures
PCR	Polymerase chain reaction

PBS	1x phosphate buffered saline
<i>Pl</i>	<i>Pacifastacus leniusculus</i>
<i>Pv</i>	<i>Penaeus vannamei</i>
RACE	Rapid amplification of cDNA end
RNA	Ribonucleic acid
RNAi	RNA interference
RT	Reverse transcription
SD	Standard deviation
SE	Standard error
sec	Seconds
SPF	Specific pathogen free
SPI	Serine proteinase inhibitor
SSH	Suppression subtractive hybridization
ssRNA	Single-stranded RNA
TBS	Tris buffer saline
TBST	Tris buffer saline containing Tween 20
TCBS	Thiosulfate-citrate-bile salts-sucrose agar
TSV	Taura syndrome virus
μ	Micro
UV	Ultraviolet
VP _{AHPND}	<i>Vibrio parahaemolyticus</i> AHPND
WSSV	White spot syndrome virus
YHV	Yellow head virus

CHAPTER I
INTRODUCTION, LITERATURE REVIEW
& RESEARCH OBJECTIVE



จุฬาลงกรณ์มหาวิทยาลัย
CHULALONGKORN UNIVERSITY

1.1 General introduction

Shrimp farming is a very important aquaculture industry in many countries. In 1976, commercial culture of *Penaeus vannamei* began in South and Central America. Subsequent development of intensive breeding and rearing techniques led to its culture in Hawaii, mainland United States of America, and much of Central and South America by the early 1980s (FAO, 2006). Asia has seen a phenomenal increase in the production of *P. vannamei*. Although no production was reported to FAO in 1999, it was nearly 1,116,000 tonnes by 2004 and had overtaken the production of *Penaeus monodon* in China, Taiwan Province of China and Thailand, due to a number of favorable factors.

Thailand has been the world's leading exporter of cultured shrimp since 1992, and used to be the largest producer of the black tiger shrimp supplying 20 percent of the world trade in shrimp and prawn (Wyban, 2007). Unfortunately, the production of the black tiger shrimp *P. monodon* had rapidly been decreased because the outbreaks of bacterial and viral diseases (Mohan et al., 1998). Due to the serious problems of the black tiger shrimp production loss, Thailand had switched to culture the pacific white shrimp, *P. vannamei*.

However, shrimp farming has been continuing affected by serious infectious disease outbreaks caused mainly by viruses and bacteria especially the white spot syndrome virus (WSSV) and *Vibrio* species. In 2013, Thai shrimp production has declined nearly 50 per cent because of the spread of a deadly disease outbreak named 'early mortality syndrome' (EMS) or acute hepatopancreatic necrosis disease (AHPND) (Figure 1). Although it is expected that the shrimp production in Thailand was improved as shrimp farmers adopt several strategies to cope with the disease, the research to support disease control and prevention in shrimp farming remains very important for the sustainability of the industry.

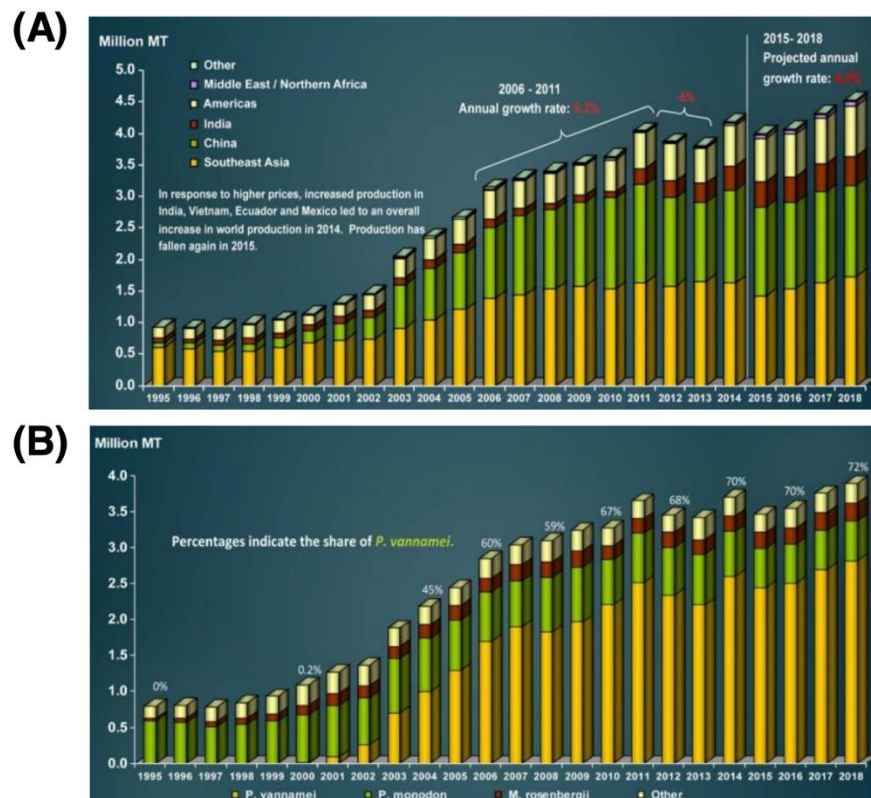


Figure 1 Shrimp aquaculture production by (A) world region and (B) in Asia by species during 1995-2018.

Sources: FAO (2016) for 1995-2011; FAO (2016) and GOAL (2014) for 2012-2014; GOAL (2016) for 2014-2018 (Anderson et al., Shrimp production review, GOAL 2016.)

1.2 Taxonomy of the pacific white shrimp, *Penaeus vannamei*

Penaeid shrimp are classified into the largest phylum in the animal kingdom, the Arthropoda. This group of animal is characterized by the presence of pair appendages and a protective cuticle or exoskeleton that covers the whole animal. The subphylum Crustacea is made up of 42,000, predominantly aquatic species, which belong to the 10 classes. Within the class Malacostraca; shrimp, crayfish, lobster and crab belong to the order Decapoda. The taxonomic definition of the Pacific white shrimp, *P. vannamei* is as follows (Boone, 1931):

Domain: Eukarya

Kingdom: Animalia

Phylum: Arthropoda

Subphylum: Crustacea
Class: Malacostraca
Subclass: Eumalacostraca
Superorder: Eucarida
Order: Decapoda
Suborder: Dendrobranchiata
Superfamily: Penaeoidea
Family: Penaeidae
Genus: Penaeus
Species: *Penaeus vannamei*

Scientific name: *Penaeus vannamei*

Common name: Pacific white shrimp (USA), White shrimp (Peru), Whiteleg shrimp (UK, USA), Valkokatkarapu (Finland), Crevette pattes blanches (France), Mazzancolla tropicale (Italy), Camarón blanco (Ecuador and Mexico), Camarón café (Columbia), Camarón ecuatoriano o penaeus (Chile), Camarón patiblanco (Spain) and Kung-kao (Thailand)

F.A.O. Names: Whiteleg shrimp, Crevette pattes blanches, Camarón patiblanco

1.3 Disease in shrimp

Infectious diseases especially new emerging diseases have contributed to a major loss of shrimp production in recent years (Lai et al., 2015). According to the GOAL 2017 survey, the diseases are the most important issues and challenges in shrimp aquaculture (Figure 2). Viruses and bacteria are the major cause of the infectious diseases in shrimp.

GOAL 2017 Survey: Issues & Challenges in Shrimp Aquaculture - All Countries

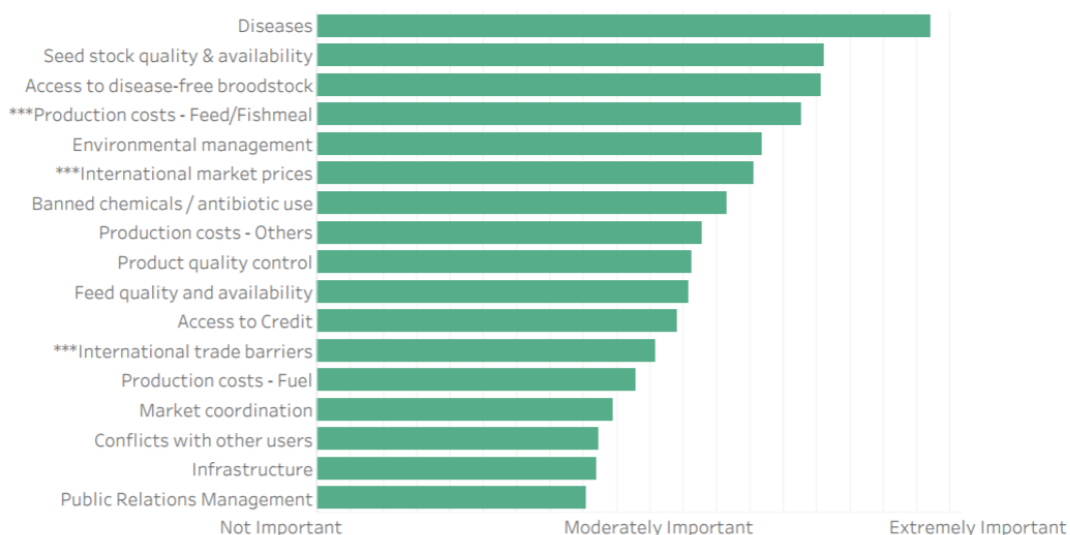


Figure 2 GOAL 2017 survey in issues and challenges of shrimp aquaculture in all countries. The 17 issues were rearranged by survey and indicated in tree level (not important, moderately important, and extremely important). The major challenge issues that show the extremely important level in shrimp aquaculture are diseases. (Source: GOAL 2017)

1.3.1 Viral diseases

1.3.1.1 White spot syndrome

White spot syndrome virus (WSSV) is a pathogen of the major economic importance. Usually, WSSV infection of shrimp leads to cumulative mortality of nearly 100% within 3-10 days after the first signs of disease (Lightner, 1996), causing dramatic economic losses on farms (Figure 3). WSSV virions are ovoid to bacilliform in shape and are enveloped but not occluded by a protein matrix as found in baculoviruses. The size of intact virion ranges between 250-380 nm in length and 80-120 nm in width. The WSSV genome is a large circular double-stranded DNA of approximately 300 kbp. It was completely sequenced in three different isolates from Thailand (WSSV-TH, accession number AF369029), China (WSSV-CN, accession number AF332093), and Taiwan (WSSV-TW, accession number AF440570). It had been proposed to encode 181 functional open reading frames (ORFs) (Yang et al., 2001).

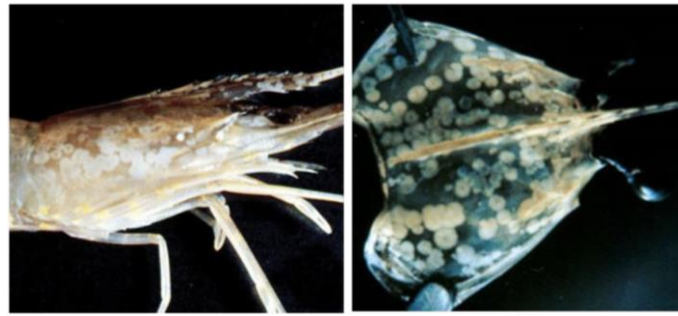


Figure 3 White spot syndrome disease.

(Left) and (Right) The white spots occur on the cuticle of infected shrimp at the late phase of infection (Lightner, 1996).

1.3.1.2 Taura syndrome

Taura syndrome virus (TSV), the shrimp disease that caused by Taura virus (Figure 4). It is a cytoplasmic virus containing a single-stranded positive sense RNA consist of 10,205 nucleotides with a diameter of 32 nm (Jimenes, 1992). It was classified as a possible member of genus *Cripavirus* in new family *Dicistroviridae* (in the superfamily of *Picornaviruses*) (Bonami et al. 1997; Mari et al. 2002). Seriously, this disease is a causative of shrimp mortality in *P. monodon* and *P. vannamei*. The symptoms of Taura syndrome virus in shrimp are tail fan and pleopods particularly were red, soft cuticle, darkening of body from infection.

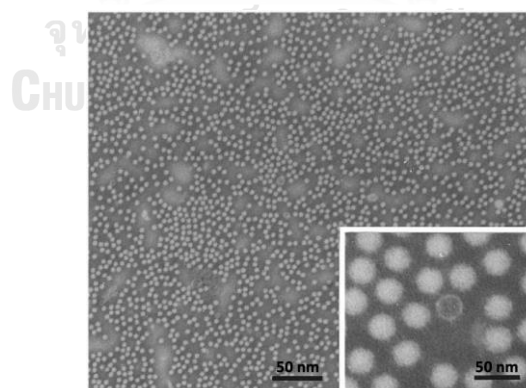


Figure 4 Purified TSV suspension.

Negative staining, 2% PTA. Bar represents 300 nm. At higher magnification (inset), virions appear icosahedral in shape (Bonami et al, 1997).

1.3.1.3 Yellow head disease

Yellow head virus (YHV) disease was first observed in the black tiger shrimp *P. monodon* in central Thailand in 1990 (Limsuwan, 1991) and since then, the disease has been commonly found throughout shrimp farming areas in Thailand (Flegel, 1997). Clinical signs of YHV disease include a pale body appearance and a yellowish discoloration of the cephalothorax (Figure 5). The original YHV type-1 reported from Thailand causes severe mortality of *P. monodon* while the second type (YHV-2), named as gill-associated virus (GAV), and other geographical types are considered to be less or non-virulent (Wijegoonawardane et al., 2008). Age and shrimp species also affects the severity of the disease symptoms (Spann et al., 2000; Spann et al., 2003). Juvenile to subadult shrimp are susceptible to YHV disease. It appears that *P. monodon* is a major natural host of YHV; however, the virus can also infect other shrimp species e.g. *Euphasia superba*, *Palaemon setiferus* (Flegel, 1997), *P. merguensis*, *Metapenaeus ensis* (Chantanachookin et al., 1993), *P. vannamei*, *P. stylostris* (Lightner et al., 1998; Lu et al., 1994; Lu et al., 1997), *P. setiferus*, *P. aztecus* and *P. duorarum* (Lightner et al., 1998).

YHV is a rod-shaped, single-stranded, positive-sense RNA virus with a spiked envelope. YHV genome is approximately 27 kb and the virus belongs to a new family *Roniviridae*, genus *Okavirus* (Walker et al., 2005; Wongteerasupaya et al., 1995). After YHV infection, a widespread necrosis was observed in the lymphoid organ, gills, connective tissues, hemocytes and hematopoietic organs of shrimps (Wang et al., 1996). Histopathological and YHV receptor studies suggested that the lymphoid organ is probably the primary target of YHV (Assavalapsakul et al., 2006; Lu et al., 1995). Three YHV structural proteins, including two-envelope glycoproteins gp116 and gp64 and a nucleocapsid protein p20, have been described (Assavalapsakul et al., 2005; Jitrapakdee et al., 2003; Sittidilokratna et al., 2008). Neutralization assays showed that antibodies against gp116 inhibited YHV infection while anti-gp64 did not (Assavalapsakul et al., 2005). Electron microscopy has shown that gp116 forms the projections on envelope of the virions (Soowannayan et al., 2003).



Figure 5 Yellow head disease in shrimp.

The black arrow indicated the YHV-infected shrimp which shows a yellowish discoloration of the cephalothorax compare to the black color of normal shrimp (left).

(Source: AGDAFF-NACA (Photo D. V. Lightner))

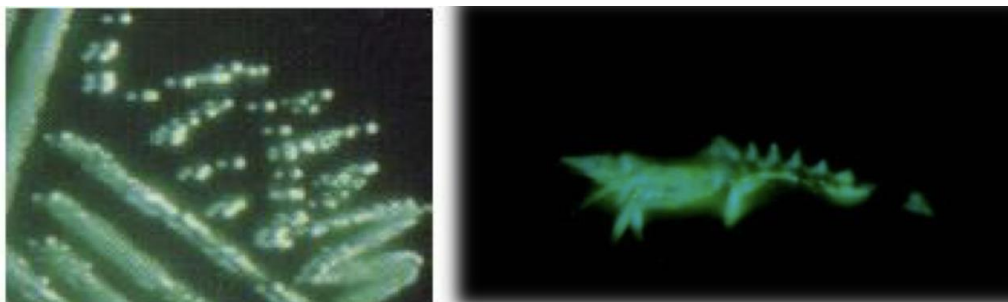
1.3.2 Bacterial diseases

1.3.2.1 Vibriosis

Vibriosis is one of the major bacterial disease problems in shrimp aquaculture. It is responsible for mortality of cultured shrimp worldwide (Lightner & Lewis, 1975; Adams, 1991; Lightner et al., 1992; Lavilla-Pitogo et al., 1996; Lavilla-Pitogo et al., 1998; Chen et al., 2000). Vibriosis, caused by gram-negative bacteria species, is widely distributed in culture facilities throughout in the family *Vibrionaceae*, including *V. harveyi*, *V. vulnificus*, *V. parahaemolyticus*, *V. alginolyticus*, *V. penaeicida* (Brock and Lightner 1990; Shimaru et al. 1995). There were occasional reports of vibriosis caused by *V. damsela*, *V. fluvialis* and other undefined *Vibrio* species (Lightner 1996).

V. harveyi, a Gram-negative, luminous bacterium, is one of the important etiologic agents of mass mortalities of shrimp larval rearing systems. It is a rod-shaped, 0.5-0.8 μm in width and 1.4-2.6 μm in length. It is capable to emit light of a blue-green color. This bacterial outbreak causes mortality of the affected shrimp up to 100% (Lightner, 1993). Presumptive diagnosis is made on the basis of clinical sign and culture of the suspensions of hepatopancreas or blood on tryptic plate

supplemented with 2% (w/v) NaCl. After incubation at 30 °C overnight, colonies of *V. harveyi* show strong luminescence in a dim light (Figure 6). Other features of the infected shrimps are the milky white body and appendages, weakness, disoriented swimming, lethargy and loss of appetite. Eventually, these lead to death.



(Source: www.thailandshrimp.com)

Figure 6 The colonies of luminescent bacteria, *V. harveyi* are grown on selective media (left) and *V. harveyi* infected shrimp (right).

1.3.2.2 Early Mortality Syndrome (EMS)

AHPND is an emerging disease, which causes severe mortalities (up to 100%) in farmed shrimp such as *P. vannamei* and *P. monodon* (Figure 7). With the spread of the disease to Thailand, shrimp production in 2013 has dropped by 33% percent since 2012 (<http://www.fisheries.go.th/ems/>).

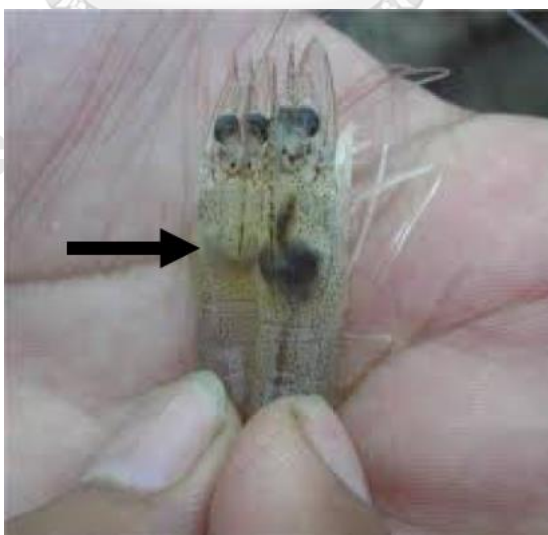


Figure 7 The infected shrimp caused by early mortality syndrome or Acute Hepatopancreatic Necrosis Disease (EMS/AHPND). The black arrow indicated the pale hepatopancreas of infected shrimp (left) compared to the brown hepatopancreas of normal shrimp (right) (Tran et al., 2013).

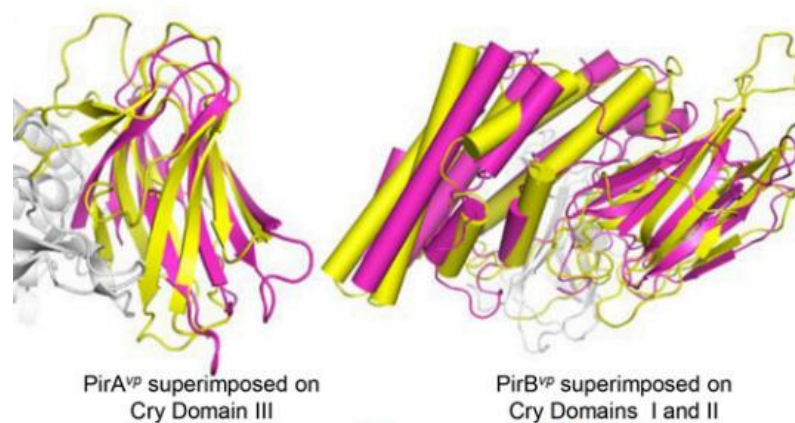


Figure 8 Structural comparison of PirA^{VP} and PirB^{VP} with Cry.

(Left) PirA^{VP} (magenta) is superimposed on domain III of Cry (yellow). (Right) PirB^{VP} (magenta) is compared with domains I and II of Cry. PirA^{VP} has a rmsd of 3.2 Å for 88 matched C α atoms in CRY domain III, and PirB^{VP} superimposes with Cry domain I and II with an rmsd of 2.8 Å for 320 matched C α atoms. (PDB ID codes: PirA^{VP}, 3X0T; PirB^{VP}, 3X0U) (Lee et al., 2015).

So far, the causative agents of AHPND has been identified as a unique strain of the bacterium *Vibrio parahaemolyticus* (VP_{AHPND}) containing a 69-kb plasmid that has 2 genes coding for Pir toxin-like proteins, pirA and pirB (Han et al., 2015b; Tran et al., 2013; Yang et al., 2014) (Figure 8). These two toxin proteins were confirmed to be the key factors that cause AHPND symptoms by Lee et al., 2015 who demonstrated that PirA^{VP}/PirB^{VP} are sufficient to induce the typical symptoms of AHPND by feeding shrimp with either the recombinant PirA^{VP}/PirB^{VP} proteins or with *E. coli* that expressed both PirA^{VP} and PirB^{VP}. In addition, they showed that PirA^{VP} and PirB^{VP} form a complex similar to that of the *Bacillus thuringiensis* Cry insecticidal toxins: the N-terminus and C-terminus of PirB^{VP} correspond to the pore-forming domain I and the receptor-binding domain II of Cry protein, respectively, while PirA^{VP} corresponds to Cry toxin domain III, which is the sugar-binding domain. In the case of *B. thuringiensis* Cry1A toxin, domain III first interacts with the GalNAc sugar on the aminopeptidase N (APN) receptor and facilitates further binding of domain II to another region of the same receptor (Knowles et al., 1987; Bravo et al., 2004; Zhang et al., 2006). This binding promotes localization and concentration of the activated

toxins. The APN-bound Cry toxin subsequently binds to another receptor, cadherin, which facilitates the proteolytic cleavage of its domain I α 1 helix. This cleavage induces the formation of Cry oligomer, which has pore-forming activity (Knowles et al., 1987; Bravo et al., 2004; Zhang et al., 2006). Interestingly, when Cry toxin binds only to cadherin, it triggers an alternative signal transduction pathway. By activating protein G and adenylyl cyclase, cellular cAMP concentration is increased and protein kinase A is activated. This will destabilize the cytoskeleton and ion channels on the membrane, and induce cell death (Oppert et al., 1997; Keller et al., 1996). In the present day, the detection methods for AHPND are available by means of histological examinations and laboratory bioassays (Tran et al., 2013), molecular diagnostics such as a conventional PCR (Han et al., 2015b; Sirikharin et al., 2015), a quantitative PCR (Han et al., 2015a) and loop-mediated isothermal amplification (LAMP) (Kongrueng et al., 2015). Early diagnosis and detection of AHPND makes control and prevention of AHPND in shrimp possible.

1.4 The immune responses in shrimp

Shrimp immunity is innate immunity that can be divided into 2 groups of cellular and humoral immunities. The humoral responses of shrimp are the important part of shrimp immune defense system for they are a first line of defense against pathogens. The responses to microbial infections are rapid and very strong involving the secretion of immune proteins from the granular hemocytes into the circulating system and, then, the re-synthesis of said proteins in the immune cells. The humoral responses arise when the extracellular signal molecules from pathogens, such as the pathogen-associated molecular patterns (PAMPs) or the viral protein antigens, are detected by the cell-surface receptors or pattern recognition proteins (PRPs) resulting in the activation of NF- κ B signaling pathways (Janeway, 1989; Li and Xiang, 2013; Shaukat et al., 2015). The activation triggers the secretion of circulating antimicrobial peptides and other immune proteins to eradicate the infection. Two major signaling immune pathways are directly involved in these responses, known as Toll and Imd (immune deficiency) pathways. These two distinct signaling pathways regulate the expression of different sets of AMPs (Leclerc and Reichhart, 2004; Naitza and

Ligoxygakis, 2004; Tanji and Ip, 2005). They may also act in parallel in response to different kinds of microorganisms (Li and Xiang, 2013b) (Figure 9).

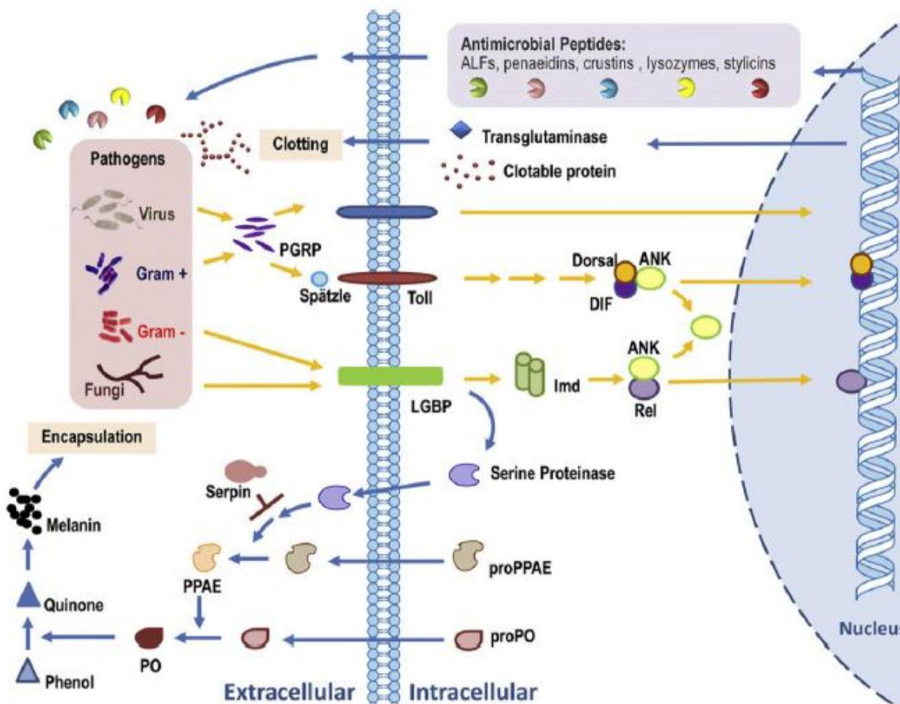


Figure 9 The model of shrimp immune system (Tassanakajon et al. 2013)

1.4.1 The prophenoloxidase system

Melanization by the activation of proPO system is the major innate immune responses in shrimp. Upon infection, pathogens are recognized by host PRRs and this leads to activation of serine proteinase cascade. The last proteinase then cleaves the proPO zymogen to the active PO enzyme that is required for melanin biosynthesis (Amparyup et al., 2013; Cerenius and Söderhäll 2004) (Figure 10). In shrimp, PRRs function to activate the proPO cascade have been characterized, however their role in antiviral immune response remain largely unknown.

In shrimp *P. monodon*, a lipopolysaccharide (LPS) and β -1,3-glucan-binding protein (*PmLGBP*) and clip-domain serine proteinase (*PmClipSP2*) were characterized as PRRs for LPS and glucan (Amparyup et al., 2012, 2013b). Recently, two serine proteinase homologues (*PmMasSPH1* and *PmMasSPH2*) were also shown to act as PRRs for *P. monodon* proPO system (Jitvaropas et al., 2009; Jearaphunt et al., 2015). *PmMasSPH1* displays the binding activities toward LPS, *V. harveyi* and PGN, whereas *PmMasSPH2* showed the binding activity to PGN (Jitvaropas et al.,

2009; Jearaphunt et al., 2015). With respect to the viral response, *P. stylirostris* LGBP transcripts was demonstrated to be up-regulated after WSSV infection (Roux et al., 2002). *PmMasSPH1* was also shown to interact with protein from yellow head virus (YHV) (Sriphaijit et al., 2007).

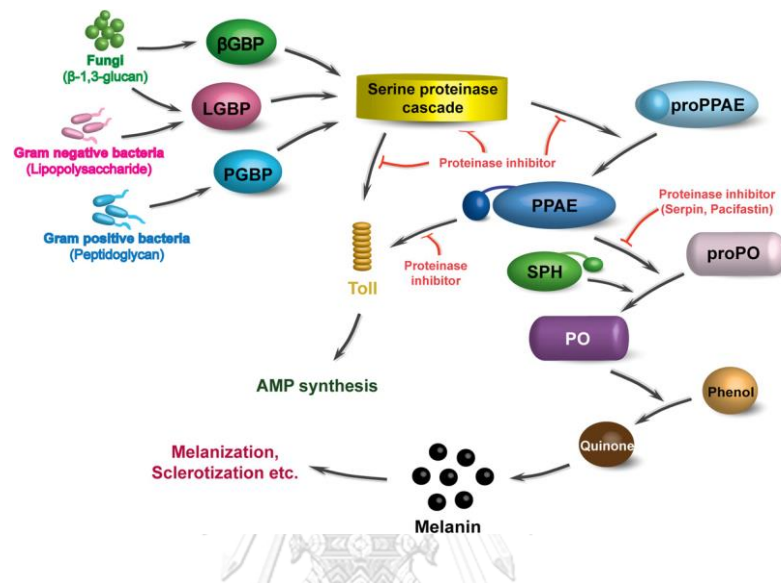


Figure 10 The prophenoloxidase (proPO)-activating system in arthropods.

The system is activated by recognition of microbe-specific molecules (LPS, PGN and β -1,3-glucan) by the pattern recognition proteins (peptidoglycan-binding protein (PGBP), LPS and β -1,3-glucan-binding protein (LGBP) and β -1,3-glucan-binding protein (β GBP)). A cascade of serine proteinases is then activated, resulting in the cleavage of a final clip-domain serine proteinase (clip-SP) designated as a proPO-activating enzyme (PPAE). The PPAE subsequently changes the inactive proPO to active PO which is required for the quinone production. The quinones can cross-link neighboring molecules to form melanin around invading microorganisms. The molecular cross-talk between the proPO system and the Toll signaling pathway that leads to the production of antimicrobial peptides (AMPs) has been described in some insects, *Tenebrio molitor* and *Manduca sexta* (Amparyup et al., 2013a).

1.4.2 Pattern recognition proteins

The innate immune response to viral pathogens is critical in order to mobilize protective immunity. Cells of the innate immune system detect and identify viral pathogens by engaging pathogen-associated molecular patterns (PAMPs) through the pattern recognition receptors (PRRs). The role of PRRs and associated signaling pathways in detecting viral pathogens may help to convey a greater understanding of how viruses activate PRR signaling and how this interaction shapes the anti-viral immune response. To date, many PRRs and virus-binding proteins have been identified in shrimp (Sritunyalucksana et al., 2013). However, the reported shrimp proteins do not recognize common patterns among viral proteins and thus it might not fit the criteria of PRRs such as those that interact with unique bacterial and fungal cell wall components.

1.4.3 Antimicrobial peptides (AMPs)

The AMPs are the first-line defense which play a key role in defense mechanism by killing/controlling the microorganisms and the secondary roles in modulating other immune responses. Therefore, the AMPs are considered as major humoral immune effectors. The shrimp AMPs are gene-encoded peptides and the cleaved peptides derived from larger proteins. The gene-encoded AMPs are produced as precursor proteins, stored in granule-containing hemocytes, and released upon induction. Like other organisms, a number of families of gene-encoded AMPs in shrimp have been reported. They are penaeidins, crustins, anti-lipopolysaccharide factors (ALFs), and stylicins (Liu et al., 2015a; Tassanakajon et al., 2013). For the cleaved peptides, the precursor proteins, hemocyanin and histones, undergo proteolysis in response to infection releasing the active cleaved-AMPs (Destoumieux-Garzon et al., 2001). According to the net charge, the shrimp AMPs can be classified as cationic and anionic AMPs. The cationic AMPs are commonly found whereas the anionic AMPs in shrimp are fewer; only stylicin, hemocyanin derived peptide and some ALFs are anionic AMPs.

1.5 RNA interference pathway

Double-stranded RNA (dsRNA) from intracellular and extracellular cells is involved in RNA interference pathway (RNAi). This is a biological process in which RNA molecules inhibit gene expression, typically by causing the destruction of specific mRNA molecules (Kim et al., 2006). The key regulators of RNAi pathway are siRNA and miRNA.

MicroRNAs (miRNAs) are small non-coding RNA molecules that function in RNA silencing and post-transcriptional regulation of gene expression. miRNAs play an important function in several biological processes including development, cellular differentiation, proliferation, apoptosis, hematopoiesis and immune system (Bartel et al., 2004). According to Figure 11, the biogenesis of miRNAs has been described in *Drosophila* where primary transcripts (pri-miRNA) that contain hairpin loop domains are transcribed by RNA polymerase II. The pri-miRNA is cut by the RNase III enzyme Drosha to a 60–70 nucleotide-long precursor miRNA (pre-miRNA), which is then exported to the cytoplasm by Exportin-5. Cleavage of these pre-miRNAs by the RNase-III enzyme, Dicer produces miRNAs composed of 18-24 double-stranded oligonucleotides. Newly generated mature miRNAs, which are now single-stranded RNA, become guide strands that are eventually integrated into RNA-induced silencing complexes (RISC). Specific interactions between the miRNA-RISC (miRISC) and mRNA targets involve binding between the “seed” region of the miRNA (typically nucleotides 2-8) and the complementary target sequence on the mRNA inducing mRNA degradation and translational repression (Azzam et al., 2012). As mentioned, miRNAs are known to have diverse functions including development. In a study using river prawn *Macrobrachium nipponense*, 3 miRNAs have been identified to have functional roles in sex differentiation and determination due to their possible interactions to 11 target genes. Not only targeted to sex differentiation genes, the *M. nipponense* miRNA homologs were identified and predicted as targeted to the innate immune genes (Jin et al., 2017). Previously, the next generation sequencing was used to identify differentially miRNA expression from *P. vannamei* hemocyte upon VP_{AHPND} infection. Among them, 47 up-regulated and 36 down-regulated were found and might target to 222 target genes involved in biological functions and shrimp immune-related genes such as proteinase inhibitor,

apoptosis and heat shock protein (Zheng et al., 2018). Determination of miRNA expression profiles in response to bacterial infections have revealed miRNAs as players in the host innate immune response (Eulalio et al., 2012) thus, providing key evidence on the general role of miRNAs in shrimp immunity.

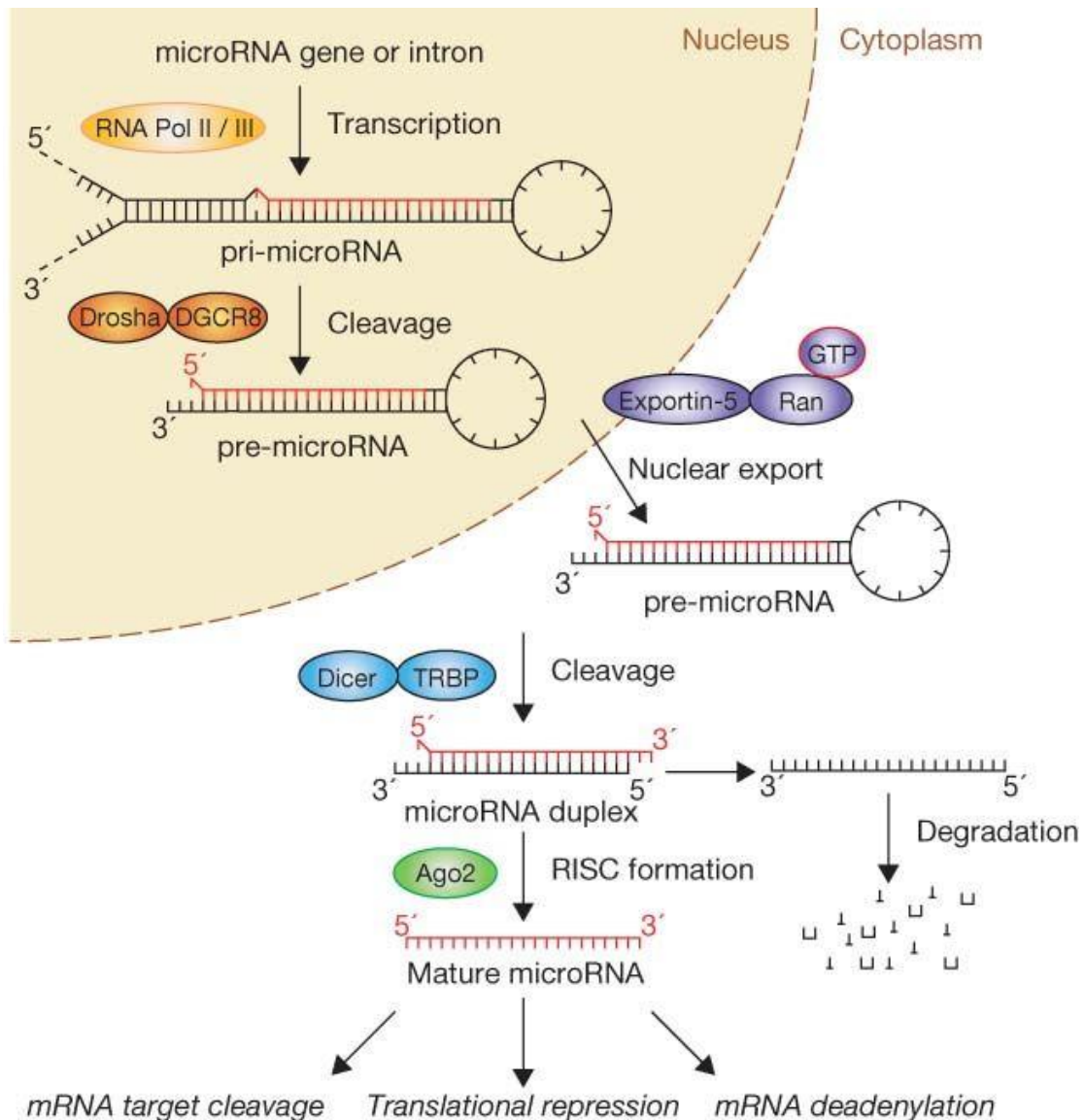


Figure 11 The miRNA processing pathway (Winter et al., 2009)

1.6 Non-lethal heat shock

It has been proven that heat shock proteins and other immune-related genes become upregulated after non-lethal heat shock, which facilitates some form of tolerance or resistance to *Vibrio spp* (Yik-Sung et al., 2007; Loc et al., 2013). In

aquatic animals, different families of heat shock proteins (Hsps) function as molecular chaperones protecting cells during stress. Increase in Hsps in *Artemia* induces protective effects against infection by *Vibrio campbellii* highlighting their important roles in disease resistance. The molecular mechanisms of Hsps to improve resistance to pathogens are thought to be their stimulating effects on the host innate immunity (Baruah et al., 2014). In shrimp, Hsps are likewise expected to be expressed in response to pathogen infection. Particularly, Hsp70 transcript has been shown to increase in the hepatopancreas of Chinese shrimp *Fenneropenaeus chinensis* after white spot syndrome virus (WSSV) infection (Wang et al., 2006). More specifically, Hsp70 and Hsp90 mRNAs become up-regulated in the gills of black tiger shrimp *Penaeus monodon* upon *Vibrio harveyi* infection (Rungrassamee et al., 2010). In another species, *P. vannamei*, LvHsp60 protein was significantly up-regulated in the gills, hepatopancreas and hemocyte after bacterial challenge (Zhou et al., 2010). These observations in different shrimp species indicate the conserved functional role of Hsps in shrimp, which also highlights the presence of an organized system of resistance to *Vibrio* spp. related to heat stress in shrimp and perhaps invertebrates in general.

1.7 Purpose of this thesis research

The objectives of this study are divided into four parts. Firstly, we aimed to identify genes that might be involved in VP_{AHPND} infection by suppression subtractive hybridization (SSH). The functions of genes/proteins related to immune response against VP_{AHPND} infection, likewise, be further characterized.

Secondly, the functions of miRNAs and genes in shrimp immunity and stress response were explored by looking at the global expression of mRNA and miRNA populations in *P. vannamei* upon VP_{AHPND} infection under NLHS and NH conditions. We then applied the next generation sequencing (NGS) for differentially expressed genes and miRNAs identification. The inferred relationships of the identified genes and miRNAs were investigated to reveal important aspects of miRNA and their targets in relation to AHPND resistance/tolerance. The so-called non-lethal heat stress-modulated immune pathways were identified.

Next, to identify the miRNAs involved in *P. vannamei* response to VP_{AHPND} infection, sequences and expression profiles of miRNAs in the hemocyte *P. vannamei* challenged with VP_{AHPND} were identified through the Illumina MiSeq high-throughput NGS technique. Differentially expressed miRNAs were further verified by the real-time RT-PCR technique. The regulatory role of miRNA involved in the VP_{AHPND} response in *P. vannamei* was studied.

Lastly, transcriptome-wide base pairing interaction in shrimp hemocytes of WSSV-infected *P. vannamei* was elucidated using the psoralen analysis of RNA interactions and structures (PARIS) technique. The next generation sequencing was performed to identify differentially expressed genes and miRNAs in shrimp upon WSSV challenge for being a reference sequences of PARIS data.

The research is presented in four chapters:

Chapter II: Identification and functional characterization of genes in response to *Vibrio parahaemolyticus* AHPND (VP_{AHPND}) infection by suppression subtractive hybridization (SSH)

Chapter III: Transcriptomic profiling and immune response against non-lethal heat shock (NLHS) of VP_{AHPND} infected shrimp

Chapter IV: Identification and functional characterization of miRNA in shrimp hemocyte in response to *Vibrio parahaemolyticus* AHPND (VP_{AHPND}) infection

Chapter V: Identification of miRNAs and their interacting partners from WSSV-infected *P. vannamei* hemocyte using psoralen analysis of RNA interactions and structures (PARIS)



จุฬาลงกรณ์มหาวิทยาลัย
CHULALONGKORN UNIVERSITY

CHAPTER II

Identification and functional characterization of genes in response to *Vibrio parahaemolyticus* AHPND (VP_{AHPND}) infection by suppression subtractive hybridization (SSH)



จุฬาลงกรณ์มหาวิทยาลัย
CHULALONGKORN UNIVERSITY

2.1 Introduction

Since 2013, Thai shrimp production has encountered several severe outbreaks of a disease called “early mortality syndrome” (EMS) or “Acute Hepatopancreatic Necrosis Disease” (AHPND). So far, the causative agent of AHPND has been identified as a unique strain of the bacterium *Vibrio parahaemolyticus*(VP_{AHPND}) containing a 69-kb plasmid that has 2 genes coding for Pir toxin-like proteins, PirA^{VP} and PirB^{VP} (Han et al., 2015; Tran et al., 2013; Yang et al., 2014). It was reported that the increase of VP_{AHPND} in the shrimp stomach and secretion of Pir toxins were the cause of hepatopancreatic cell damage (Tran et al., 2013). The structural alignment of VP_{AHPND} Pir toxin proteins showed a high similarity to the *Bacillus* Cry insecticidal toxin-like proteins which can induce cell death through a series of processes including receptor binding, oligomerization, and pore formation(Lee et al., 2015). However, at present, there is no effective way to control AHPND outbreaks in shrimp. Therefore, it is imperative to better understand shrimp immune response to pathogenic VP_{AHPND}.

Transcriptome data is a source of information that could help uncovering the nature of the shrimp immune response against VP_{AHPND} infection. Previously, 141 immune-related unigenes were found from a transcriptional analysis of *P. monodon* stomach in response to VP_{AHPND} infection using Ion Torrent sequencing (Soonthornchai et al., 2016). Recently, a study has demonstrated up-regulation of several immune-related genes in *P. vannamei* hemolymph after being challenged with VP_{AHPND} in which Lysozyme and Toll-like receptors (TLRs) showed statistically significant up-regulation (Hong et al., 2016).

In the present study, we identified differentially expressed genes using suppression subtractive hybridization from *P. vannamei* shrimp hepatopancreas infected by VP_{AHPND}. In addition, the role of selected immune genes involved in VP_{AHPND} infection was determined in order to provide insight into host-pathogen interactions.

2.2 Materials

2.2.1 Equipment

- 20 °C Freezer (Whirlpool), - 80 °C Freezer (ThermoForma)
 Amicon Ultra-4 concentrators (Millipore).
 Automatic micropipette (Gilson Medical Electrical S.A.)
 Centrifuge 5804R (Eppendorf), Centrifuge Avanti™ J-301 (Beckman Coulter)
 CX31 Biological Microscope (Olympus)
 Gel documentation (SYNGENE)
 Gene Pulser (Bio-RAD)
 Hybridization oven (Hybrid)
 iCycler iQ™ Real-Time Detection System (Bio-Rad)
 Incubator (Mettler)
 Innova 4080 incubator shaker (New Brunswick Scientific)
 LABO Autoclave (SANYO)
 Laminar Airflow Biological Safety Cabinets (NuAire, Inc.)
 Microcentrifuge tubes 0.5 ml and 1.5 ml (Bio-RAD Laboratories)
 PCR Mastercycler (Eppendorf AG)
 pH meter Model # SA720 (Orion)
 Spectrophotometer (Eppendorf)
 Sterring hot plate (Fisher Scientific)
 Trans-Blot® SD (Bio-RAD Laboratories)
 Ultra Sonicator (SONICS Vibracell)
 Vertical electrophoresis system (Hofer™ miniVE)
 Water bath (Mettler)

2.2.2 Chemicals and reagents

100 mM dATP, dCTP, dGTP and dTTP (Thermo Scientific)
 2-Mercaptoethanol (AppliChem)
 30% (wt/vol) acrylamide/Bis solution, 29:1 (Bio-Rad)
 5-bromo-4-chloro-3-indolyl-b-D-galactopyranoside (X-gal) (Fermentas)
 Absolute ethanol, CH₃CH₂OH (HAYMAN)

Agar powder (HIMEDIA)
Agarose (Research organics)
Ammonium persulfate (APS; Thomas Scientific)
Ampicillin sodium salt (BIO BASIC INC.)
Ammonium sulfate (Ajax)
Boric acid, BH_3O_3 (MERCK)
Bromophenolblue sodium salt (USB)
Bovine serum albumin (SIGMA-ALDRICH)
Calcium chloride, CaCl_2 (MERCK)
Coomassie brilliant blue R250 (BIO BASIC INC.)
Chloroform, CHCl_3 (RCI Labscan)
Diethyl pyrocarbonate (DEPC), $\text{C}_6\text{H}_{10}\text{O}_5$ (SIGMA)
Dithiothreitol (DTT), $\text{C}_4\text{H}_{10}\text{O}_2\text{S}_2$ (BIO BASIC INC.)
Ethylene diaminetetraacetic acid disodium salt dehydrate, EDTA (Ajax Finechem)
Genezol reagent (Geneaid)
Glacial acetic acid, CH_3COOH (MERCK)
Glycerol, $\text{C}_3\text{H}_8\text{O}_3$ (Scharlau)
Hydrochloric acid, HCl (MERCK)
Isopropanol, $\text{C}_3\text{H}_7\text{OH}$ (MERCK)
Isopropyl- β -D-thiogalactoside (IPTG), $\text{C}_9\text{H}_{18}\text{O}_5\text{S}$ (Thermo Scientific)
Magnesium chloride, MgCl_2 (MERCK)
Methanol, CH_3OH (Burdick&Jackson)
N-N dimethyl formamide (Carlo Erba)
N-Lauroylsarcosine sodium salt solution (20%, for molecular biology; Sigma-Aldrich)
Opti-MEM (Life Technologies)
Paraformaldehyde (SIGMA)
PBS (Life Technologies)
Potassium chloride, KCl (Ajax Finechem)
Potassium dihydrogen orthophosphate (Ajax Finechem)
RedSafe™ Nucleic Acid Staining Solution (iNtRON Biotechnology)

Sodium acetate, CH₃COONa (Carlo Erba)
 Sodium citrate (Ajax Finechem)
 Sodium chloride, NaCl (Ajax Finechem)
 Sodium dihydrogen orthophosphate, NaH₂PO₄.H₂O (Carlo Erba)
 Sodium hydroxide, NaOH (MERCK)
 Thermo Scientific™ GeneRuler 100 bp Plus DNA Ladder
 Thermo Scientific™ GeneRuler 1 kb DNA Ladder
 Tris-(hydroxyl methyl)-aminomethane, NH₂C(CH₂OH)₃ (Vivantis)
 Tryptone type I (HIMEDIA)
 Ultrapure TEMED (Invitrogen)
 Yeast extract powder (HIMEDIA)

2.2.3 Enzymes and kits

Advantage[®] 2 Polymerase Mix (Clontech)
 DEAE Sepharose[®] Fast Flow (GE Healthcare)
 DNase I (RNase-free) (NEB)
 FavorPrep™ GEL/PCR Purification Kit
 FavorPrep™ Plasmid DNA Extraction Mini Kit
 Luna[®] Universal qPCR Master Mix (NEB)
 SMARTer™ RACE cDNA Amplification Kit (Takara Bio)
 RBC T&A Cloning Kit (RBC Bioscience)
 RBC *Taq* DNA polymerase (RBC Bioscience)
 RiboLock RNase inhibitor (Thermo Scientific)
 T7 RiboMAX™ Express Large Scale RNA Production System (Promega)
 Thermo Scientific™ RevertAid First Strand cDNA Synthesis Kit

2.2.4 Experimental shrimp, microorganisms, cells and viruses

Pacific white shrimp *Penaeus vannamei*
Escherichia coli strain Top10
Vibrio parahaemolyticus (AHPND)

2.2.5 Software

BLAST[®] (<https://blast.ncbi.nlm.nih.gov/Blast.cgi>)

Clustal Omega (<https://www.ebi.ac.uk/Tools/mas/clustalo/>)

ExPASy-Translate tool (<https://web.expasy.org/translate/>)

Geneious R11 (Biomatters, Ltd)

GraphPad Prism 6 (GraphPad Software)

SMART 8.0 (<http://smart.embl-heidelberg.de/>)

2.2.6 Animal cultivation

Healthy *P. vannamei* shrimp weighing 2-5 g (for VP_{AHPND} challenge, VP_{AHPND} toxin challenge, RNAi injection) were purchased from commercial farms in Samut Songkhram Province and Chachoengsao Province, Thailand. The shrimp were acclimatized in laboratory aquaria at 28 ± 4 °C with a salinity of 20 ppt for a minimum of 2 weeks prior to use in experiments.

2.2.7 *Vibrio parahaemolyticus* (VP_{AHPND}) challenge

For bacterial preparation, the acute hepatopancreatic necrosis disease (AHPND)-causing strain of *Vibrio parahaemolyticus* (VP_{AHPND}) was isolated from Thamai, Chanthaburi province, Thailand, and was further verified for AHPND pathogenesis by an immersion challenge test modified from Tran et al. (2013). The bacteria were cultured overnight in 3 mL of tryptic soy broth (TSB) containing 1.5% NaCl at 250 rpm and 30 °C. The starter culture was then transferred to a new culture flask containing 100 mL TSB with 1.5% NaCl and incubated at 30 °C at 220 rpm until the OD₆₀₀ reached 2.0 (approximately 10⁸ CFU/ml). Bacterial inoculant (final concentration: 10⁶ CFU/ml) was added to seawater tanks containing twenty shrimp (LD₅₀=24 hpi).

2.2.8 Partially purified VP_{AHPND} toxin challenge

Crude VP_{AHPND} toxin was prepared from VP_{AHPND} culture supernatant and subjected to the purification process using ammonium sulfate precipitation as described by Sirikharin et al. (2015). A total of 200 ml of cultured supernatant was precipitated in 40% (w/v) ammonium sulfate at 4 °C overnight. Then, the supernatant was separated by centrifugation at 12,000×g at 4 °C for 20 min. Ammonium sulfate was then added to a concentration of 60% (w/v) and incubated overnight at 4 °C. The pellet was collected by centrifugation at 12,000×g at 4 °C for 20 min. The pellet was

dissolved in $1 \times$ PBS at pH 7.4 and dialyzed against $1 \times$ PBS at pH 7.4. The partially purified VP_{AHPND} toxin was assessed using 15% SDS-PAGE to determine the presence of PirAB toxin protein and was subsequently used for further VP_{AHPND} toxin challenge experiments.

Ten shrimp of 3-5 g were used for each group. For each shrimp, 0.2 μ g of partially purified VP_{AHPND} toxin/g of shrimp ($LD_{50} = 1$ day) (adjusted volume to 50 μ l with $1 \times$ PBS at pH 7.4) was intramuscularly injected into the second abdominal segment of the shrimp. The 1% red food dye (Winner, Thailand) was added to the solution prior to injection into shrimp in order to observe its transportation into the shrimp hepatopancreas. The shrimp survival rate was observed every 12 h post injection for a duration of 7 days.

2.2.9 The detection of VP_{AHPND} from cultures or infected shrimp

PCR was performed to diagnose whether VP_{AHPND} in VP_{AHPND}-infected shrimp stomach, hepatopancreatic tissue, or bacterial isolates. For shrimp tissues, stomach or hepatopancreas was added to 3 ml of TSB containing 1.5% NaCl for 3 h at 250 rpm and 30 °C. Then, 1 ml of cultured media was collected and resuspended in 100 μ l of water. For bacterial isolates, a single colony was picked up and resuspended in 10 μ l of water. Then, the resuspended cells from cultured TSB containing shrimp tissue or bacterial isolates were boiled for 2 min. The supernatant was diluted 10-fold in water and used as a template for PCR reactions. Three primer sets including AP2, Tumsat-Vp3, and TLH were used for the amplification of AHPND bacterial DNA fragments (Table 1). The cycling reactions were conducted for 5 min at 94 °C, followed by 25~30 cycles of 94 °C for 30 sec, 55 °C for 30 sec, 72 °C for 30 sec, and then a final extension at 72 °C for 5 min. Subsequently, the PCR products were run using a TBE-2% (w/v) agarose gel followed by RedSafe Nucleic Acid Staining Solution (iNtRON Biotechnology) for staining and UV transillumination.

Table 1 Primer used for the detection of VP_{AHPND} in shrimp and bacterial isolates

Primer	Sequences (5'-3')
TLH-F	AAAGCGGATTATGCAGAAGCACTG
TLH-R	GCTACTTTCTAGCATTTTCTCTGC
TUMSAT-Vp3-F	GTGTTGCATAATTTTGTGCA
TUMSAT-Vp3-R	TTGTACAGAAACCACGACTA
AP2-F	TCACCCGAATGCTCGCTTGTGG
AP2-R	CGTCGCTACTGTCTAGCTGAAG

2.2.10 Total RNA extraction by GENEzol™ reagent and DNase I treatment

Cells or tissues harvested from shrimp were homogenized in 1 ml of GENEzol™ reagent (Geneaid). Subsequently, 200 µl of chloroform was added and vigorously shaken for 30 sec. After incubation at room temperature for 10 min, the mixtures were centrifuged at 12,000 x g for 15 min at 4 °C and then transferred to the RNA-containing aqueous (upper) phase in a fresh tube. Total RNA was precipitated by adding an equal volume of isopropanol, followed by incubation at -20 °C for 15 min. The supernatant was removed by centrifugation at 12,000 x g for 15 min at 4 °C. The RNA pellet was washed with 1 ml of 75% (v/v) ethanol in diethyl pyrocarbonate (DEPC)-treated water. The total RNA was stored in 75% (v/v) ethanol at -80 °C until use. The ethanol supernatant was completely removed by centrifugation at 12,000 x g for 15 min at 4 °C. The RNA pellet was air-dried at room temperature for 10 - 15 min and dissolved in 20 µl of DEPC-treated water. The obtained total RNA was further treated with DNase I (RNase-free) (NEB) (1 unit/5 µg of total RNA) at 37 °C for 30 min to remove any contaminating chromosomal DNA. Then, the RNA pellet was purified using GENEzol™ reagent (as previously described).

2.2.11 Single-stranded cDNA synthesis using the RevertAid First-strand cDNA Synthesis Kit (Thermo Fisher Scientific)

The DNase-treated total RNA (1 µg) was combined with 0.5 µg of Oligo(dT)₁₅ primer in nuclease-free water for a final volume of 12 µl per reverse transcription reaction. The sample was heated at 65 °C for 5 min and then immediately chilled in ice water for at least 5 min. Then, 8 µl of the reverse transcription reaction mix, containing 4 µl of 5X reaction buffer, 2 µl of 10 mM dNTP mix, 1 µl of RiboLock RNase Inhibitor (20 U/µL), and 1 µl of RevertAid M-MuLV RT (200 U/µL), was added to the total RNA sample. The mixture was incubated in a temperature series of 42 °C for 60 min and 70 °C for 5 min.

2.2.12 Hemocyte and hepatopancreas collection and RNA preparation

Hepatopancreas tissue samples were collected from VP_{AHPND}-infected shrimp at 0, 3, 6, and 48 h post challenge. The hemolymphs of VP_{AHPND}-infected (surviving) shrimp were drawn at 0, 3, 6, and 48 h post challenge by immersion (LD₅₀ = 48 h). Hemolymphs were collected and centrifuged immediately at 800 × g for 10 min at 4 °C to separate the hemocytes from plasma. Total RNAs were isolated from the hemocytes using the FavorPrep™ Tissue/Cultured Cells Total RNA Mini Kit (Favorgen). The eluted RNA was stored at -80 °C until use.

2.2.13 Suppression subtractive hybridization (SSH)

Hepatopancreas tissue and hemocyte samples of VP_{AHPND}-infected shrimp were collected at 0, 3, 6, and 48 h post challenge and RNA extraction was performed (as previously described). The total RNA from 3 and 6 h post challenge for each hemocyte or hepatopancreas were pooled at an equal amount of 2 µg. cDNA was synthesized using a SMARTer™ PCR cDNA Synthesis Kit (Clontech) following the manufacturer's protocol. To identify genes that are differentially expressed in VP_{AHPND}-infected shrimp hepatopancreas and hemocyte at early (3 and 6 h post challenge) and late periods (48 h post challenge) of infection, four SSH libraries (Hepatopancreas 3/6, Hepatopancreas 48, Hemocyte 3/6 and Hemocyte 48) were constructed using a PCR-Select™ cDNA Subtraction Kit (Clontech). The tester

cDNA for the Hemocyte 3/6, Hemocyte 48, Hepatopancreas 3/6, and Hepatopancreas 48 libraries were isolated from VP_{AHPND}-infected shrimp hemocyte at 3 and 6 h post challenge, hemocyte at 48 h post challenge, hepatopancreas at 3 and 6 h post challenge, and 48 h post challenge, respectively. The total cDNA of VP_{AHPND}-infected shrimp hemocyte at 0 h post challenge and hepatopancreas at 0 h post challenge were used as the templates for the driver cDNA of hemocyte and hepatopancreas libraries, respectively. Briefly, the double-stranded cDNAs of tester and driver were digested with *RsaI* to generate short, blunt-ended double-stranded cDNA. Thereafter, *RsaI*-digested tester cDNA was subdivided into two portions and each was ligated with a different adaptor (adaptor 1 and adaptor 2R) at the 5' ends of the cDNA, while the driver cDNA had no adaptor ligation. The adaptor 1-ligated and adaptor 2R-ligated tester cDNAs were then separately hybridized with an excess of the driver cDNA at 68 °C for 8 h after denaturation at 98 °C for 90 sec. The two hybridization samples were mixed together without denaturation and hybridized at 68°C overnight with an excess of fresh denatured driver cDNA. The resulting mixture was diluted in 200 ml of dilution buffer (Clontech) composed of 20 mM HEPES, 20 mM NaCl, and 0.2 mM EDTA followed by nested PCR amplification. In the primary PCR, primers against adaptor 1 and adaptor 2R were used to selectively amplify differentially expressed cDNA, with the product of the first PCR then being used as a template for the second PCR with nested primers to generate subtracted cDNA (Figure 12).

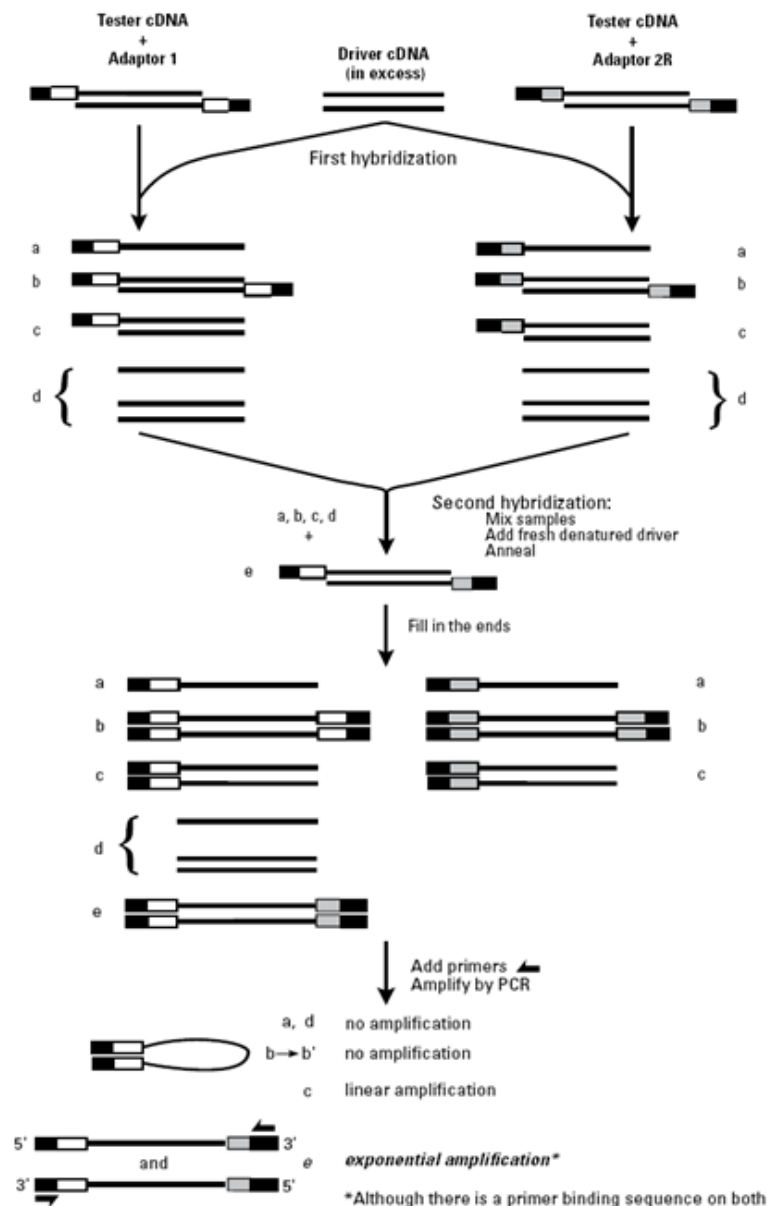


Figure 12 The PCR-Select™ cDNA Subtraction procedure (Clontech).

2.2.14 Evaluation of Suppression subtractive hybridization efficiency

SSH efficiency was evaluated by PCR using the EF-1 α primer pair (forward: 5'-CGCAAGAGCGACA ACTATGA-3' and reverse: 5'-TGGCTTCAGGATA ACCAGTCT-3') performed on unsubtracted and subtracted cDNAs under the following conditions: 94 °C for 3 min, 24 cycles of 94 °C for 30 sec, 55 °C for 30 sec, 72 °C for 30 sec, and then a final extension at 72 °C for 5 min. Subsequently, the abundance of PCR products between unsubtracted and subtracted samples was compared using a TBE-1.5% (w/v) agarose gel followed by RedSafe Nucleic Acid Staining Solution (iNtRON Biotechnology) and UV transillumination.

2.2.15 cDNA cloning, sequencing, and homology analysis

The subtracted cDNA products were cloned into the RBC T&A Cloning Vector (RBC Bioscience) and then transformed into *E. coli* XL1-Blue competent cells (Stratagene), followed by the standard blue/white screening method. Recombinant plasmids were isolated from the positive clones using the FavorPrep Plasmid Extraction Mini Kit (Favorgen) according to the manufacturer's instructions and sequenced using T7 promoter and/or M13 reverse primer at Macrogen Inc., South Korea. The consensus sequences obtained were searched against the NCBI GenBank database for homology using the BLASTN and BLASTX programs (<http://www.ncbi.nlm.nih.gov/BLAST/>). Significant matches presented *E*-values lower than 1×10^{-4} .

2.2.16 Confirmation of gene up-regulation in response to VP_{AHPND} infection by qRT-PCR

The control and VP_{AHPND}-infected shrimp were prepared as previously described in section 2.3. The hemocytes and hepatopancreas of shrimp (three individuals each) were collected at 0, 3, 6, and 48 h post challenge. Total RNA was extracted, and then the first-strand cDNA synthesis subsequently being performed. The transcription level of target genes was identified by qRT-PCR using an equal amount of cDNA template with gene-specific primers (Table 2). EF-1 α was used as an internal control. qRT-PCR analysis was performed using an appropriate amount of cDNA for each gene, specific oligonucleotide primers (Table 2). PCR was performed using the Luna[®] Universal qPCR Master Mix (NEB) with the CFX96 Touch[™] Real-time PCR System (Bio-Rad) under the following conditions: 95 °C for 3 min, 40 cycles at 95 °C for 30 s, 60 °C for 30 s, and 72 °C for 30 s. Each qRT-PCR reaction was performed in triplicate. Relative expression was calculated using the mathematical model of Pfaffl (2001). Data were analyzed using one-way ANOVA followed by Duncan's new multiple ranges test and presented as means \pm standard deviations. The level of statistical significance was set at $P < 0.05$.

Table 2 Primers used for qRT-PCR

Primer name	Sequence
<i>LvVago5-F</i>	AATGGTACCGGTAAATTAGCCCTTTACCAAT
<i>LvVago5-R</i>	TTCAGATCTCTCCTCCAAAGGGAAAATG
Profilin-F	GGGCAAAAAGTTTGTGCACATG
Profilin-R	GACGACCCATGACACAGAAGAT
SeLeuPro-F	TCACGCGAGCAAAGCTTTTC
SeLeuPro-R	GTTCCACGCACTTCTTTCCG
<i>LvKunitz-F</i>	ACAGAGCCACCAACATGCTT
<i>LvKunitz-R</i>	CACACAACCTTGCATTCCCG
Hemocyanin-F	TAGGCAGCTACAGTGATGGT
Hemocyanin-R	GAGTGGATCACGGCAACATA
Hemocyanin subunit L1-F	CAAGTTCACCTTTGACGAAGGC
Hemocyanin subunit L1-R	CTCGATATGGTGTGTTCCACC
Hemocyanin subunit L2-F	GTAGAAGACCTAAGATTCAACGAG
Hemocyanin subunit L2-R	GGTTGCTAAGGCTTCGCCAC
Hemocyanin subunit L3-F	AAGGAACAACCTGACATTCAATGGT
Hemocyanin subunit L3-R	GACTGTTGTCAGAACTTCCTTG
Hemocyanin subunit L4-F	GACGCAGGAGTGCCTGGT
Hemocyanin subunit L4-R	GGAATACCAGTGGCACTCTCG
EF-1 α -F	CGCAAGAGCGACAACCTATGA
EF-1 α -R	TGGCTTCAGGATACCAGTCT

2.2.17 Expression analysis of hemocyanin genes in response to VP_{AHPND} toxin infection by qRT-PCR

To study the effect of VP_{AHPND} toxin on the expression of the genes under study, shrimp were injected with 1 × PBS (pH 7.4) or 0.2 µg/g per shrimp of partially purified VP_{AHPND} toxin containing 1% red color food grade dye (Winner, Thailand). The hepatopancreas of three shrimp from each group were collected at 0, 1, 3, 6, 12, and 24 h post injection (hpi). Total RNA was isolated using a FavorPrep™ Tissue Total RNA Mini Kit (Favorgen) and cDNA was synthesized using a RevertAid First-strand cDNA Synthesis Kit (Thermo Fisher Scientific). The transcription level of target genes was identified by qRT-PCR using an equal amount of cDNA template

with gene-specific primers (Table 2). EF-1 α was used as an internal control. qRT-PCR analysis was performed using an appropriate amount of cDNA for each gene using specific oligonucleotide primers (Table 2.3). PCR was performed using the Luna[®] Universal qPCR Master Mix (NEB) with the CFX96 Touch[™] Real-time PCR System (Bio-Rad) under the following conditions: 95 °C for 3 min, 40 cycles at 95 °C for 30 s, 60 °C for 30 s, and 72 °C for 30 s. Each qRT-PCR reaction was performed in triplicate. Relative expression was calculated using the mathematical model of Pfaffl (2001). Data were analyzed using one-way ANOVA followed by Duncan's new multiple ranges test and presented as means \pm standard deviations. The level of statistical significance was set at $P < 0.05$.

2.2.18 Native hemocyanin purification

Native hemocyanin protein was purified from shrimp hemolymph collected from the ventral sinus of healthy shrimp using a sterile 1 ml syringe pre-loaded with 500 μ l of anticoagulant (50% (v/v) MAS solution). After centrifugation at 800 \times g for 10 min (4 °C) to separate the hemocytes, 2 ml of cell-free hemolymph was applied to a Blue-Sepharose column (10 ml) pre-equilibrated with 20 mM Tris, pH 8.0 (Gollas-Galván et al., 2003). Then, the Blue-Sepharose column was washed with 5x the column volume using 20 mM Tris-HCl, pH 8.0. The flow-through and wash containing hemocyanin fractions were pooled and further purified using 2 ml of DEAE Sepharose Fast Flow (GE Healthcare) equilibrated with 10x the column volume of binding buffer (20 mM Tris-HCl at a pH of 8.0 containing 150 mM NaCl). Then, the immobilized DEAE Sepharose was washed with 10x the column volume of binding buffer. The bound protein was eluted with 10 ml of 20 mM Tris-HCl (pH 8.0) containing 300 mM NaCl. The fractions containing hemocyanin protein were pooled and dialyzed against 20 mM Tris-HCl (pH 8.0). The purified hemocyanin was then run on 10% SDS-PAGE and 10% native-PAGE.

In order to verify purification success, 5 μ g of purified protein was separated with 10% SDS-PAGE. The gel was stained with colloidal Coomassie Brilliant Blue G250 and the protein bands (whose sizes corresponded to hemocyanin) were analyzed using LC-QTOF Impact[™] II (Bruker Daltonics, Bremen, Germany). Obtained results obtained were searched against the protein-NCBI database using MASCOT software

to identify and annotate the protein. The native purified hemocyanin protein was subsequently used to test the biological activity and neutralization of VP_{AHPND} toxin.

2.2.19 Biological activity of hemocyanin on VP_{AHPND}

2.2.19.1 *In vitro* antibacterial activity of hemocyanin on VP_{AHPND}

Liquid growth inhibition and agglutination activity assays of the purified native hemocyanin against VP_{AHPND} were performed as previously described by Somboonwiwat et al. (2005) and Kamsaeng et al. (2017), respectively. Briefly, VP_{AHPND} was cultured overnight at 30 °C and shaken at 250 rpm (as previously described in section 2.3). Then, this culture was diluted to 1:100 with TSB containing 1.5% NaCl. At an OD₆₀₀ of 0.1, the bacterial culture was diluted 1000-fold by marine poor broth. The liquid growth inhibition assay was performed by mixing various concentrations of purified native hemocyanin protein (20 µg/ml to 100 µg/ml final concentration) with the poor broth-diluted VP_{AHPND} culture in a 96-well plate incubated at 30 °C and shaken at 120 rpm. The optical density at OD₆₀₀ was measured after incubation for 12 h. As a positive control, sterile water was used instead of purified native hemocyanin protein.

Moreover, to further investigate how hemocyanin inhibited the growth of VP_{AHPND}, the VP_{AHPND}-purified native hemocyanin mixture was placed on a microscope slide and Gram staining was performed (Kamsaeng et al., 2017). Bacterial agglutination was then observed under a 100× magnification light microscope (Olympus CX31). As a control reaction, the bovine serum albumin (BSA) protein was used instead of purified native hemocyanin. The experiment was performed in triplicate.

2.2.19.2 *In vivo* antibacterial activity of hemocyanin on VP_{AHPND}

To examine the involvement of hemocyanin in the mechanism of shrimp bacterial clearance, VP_{AHPND} was cultured as previously described in section 2.3. Then, the VP_{AHPND} cells were washed three times using 0.85% NaCl. VP_{AHPND} cells were then resuspended in 0.85% NaCl. Three *P. vannamei* samples (4–6 g) were intramuscularly injected with 100 µl of sterile 0.85% NaCl containing 50 µg of purified native hemocyanin (20 µl) mixed with VP_{AHPND} (1×10^6 CFU). Shrimp

injected with 100 μ l 0.85% NaCl containing 20 μ l of 20 mM Tris-HCl (pH 8.0) mixed with 1×10^6 CFU of VP_{AHPND} were used as a control. The hemolymph was collected from each shrimp at 0, 15, 30, and 60 min after challenge, and then serially 10-fold diluted in sterile 0.85% NaCl. The diluted hemolymph samples at 10- to 10⁴-fold were dropped onto Thiosulfate-citrate-bile salts-sucrose (TCBS) agar and incubated at 30 °C for 12-14 h. The bacterial colonies were then counted and calculated as CFU/ml. All experiments were performed in triplicate and statistical analysis was performed using one-way ANOVA followed by Duncan's new multiple ranges test. Results are presented as means \pm standard deviations. Statistical significance was set at $P < 0.05$.

2.2.20 Biological activity of hemocyanin on VP_{AHPND} toxin

2.2.20.1 ELISA-based binding assay of hemocyanin and VP_{AHPND} toxin

To study the interaction between VP_{AHPND} toxin proteins (PirA and PirB) and purified native hemocyanin, the recombinant PirA and PirB proteins and their specific antibodies for rPirA and rPirB were provided by Professor Dr. Chu Fang Lo, Department of Biotechnology and Bioindustry Sciences, National Cheng Kung University, Tainan, Taiwan.

The interaction of recombinant proteins (rPirA and rPirB) and purified native hemocyanin was determined using a modified version of the ELISA technique described by Amparyup et al. (2012). Briefly, 20 μ g of purified native hemocyanin was coated overnight in a 96-well microtiter plate (Costar) at 4 °C. The wells were washed 4 times with TBS (20 mM Tris-HCl, 150 mM NaCl, pH 8.0) containing 0.1% (v/v) Tween 20 (TBST) for 15 min at room temperature. Then, the coated hemocyanin was fixed for 1 h at 60 °C and blocked with TBS (pH 8.0) containing 0.5% (w/v) BSA (Sigma Aldrich) for 3 h. After being washed 4 times with TBST, 100 μ l of either rPirA or rPirB at various concentration (0-10 μ M in TBS) were incubated in the hemocyanin-coated 96-well plate and incubated at 4 °C for overnight. The wells were washed with TBST. Bound proteins (rPirA and rPirB) were detected using the specific primary antibodies rabbit anti-PirA polyclonal antibody and rabbit anti-PirB polyclonal antibody, diluted to 1:5000 fold. A secondary antibody, alkaline phosphatase-conjugated goat anti-rabbit IgG (Jackson ImmunoResearch Inc.), was

diluted to 1:5000. The alkaline phosphatase substrate was added, and A_{405} was then measured by spectrophotometer. All assays were performed in triplicate. TBS was used instead of rPirA and rPirB as a negative control. Statistical tests were performed using GraphPad Prism[®] 6 software (GraphPad Software, Inc.), where the data were fitted with a one-site binding specific binding model, and the K_d value was determined from the nonlinear curve fitting as $A = A_{max} [L]/(K_d + [L])$, where A is the absorbance, which is proportional to the bound concentration, A_{max} is the maximum binding, and $[L]$ is the concentration of the recombinant proteins.

2.2.20.2 Neutralization of VP_{AHPND} toxin by hemocyanin

In this experiment, 10 shrimp of 3-5 g were used for each group. For the VP_{AHPND} toxin-challenged group, 0.2 μ g of partially purified VP_{AHPND} toxin/g of shrimp ($LD_{50} = 1$ day) (adjusted volume to 50 μ l with $1 \times$ PBS at pH 7.4) was intramuscularly injected into the second abdominal segment of each shrimp. The test groups were incubated with mixtures of 50 μ l partially purified VP_{AHPND} toxin and purified native hemocyanin (50 and 100 μ g) in $1 \times$ PBS for 10 min before being injected into the shrimp. Control shrimp were injected with 30 μ l of 20 mM Tris-HCl (pH 8.0) adjusted to 50 μ l with $1 \times$ PBS (pH 7.4). The highest amount of purified native hemocyanin (100 μ g) was used as a control protein for the test groups. Then, 1% red food dye (Winner, Thailand) was added to the solution before injection into the shrimp in order to observe its transportation into the shrimp hepatopancreas. Thereafter, 100 μ g BSA was used in place of purified native hemocyanin as a control protein for the test group. The shrimp survival rate was observed every 12 h post injection for a duration of 7 days. The experiment was performed in triplicate. A flowchart outlining the experimental groups is provided in Figure 13.

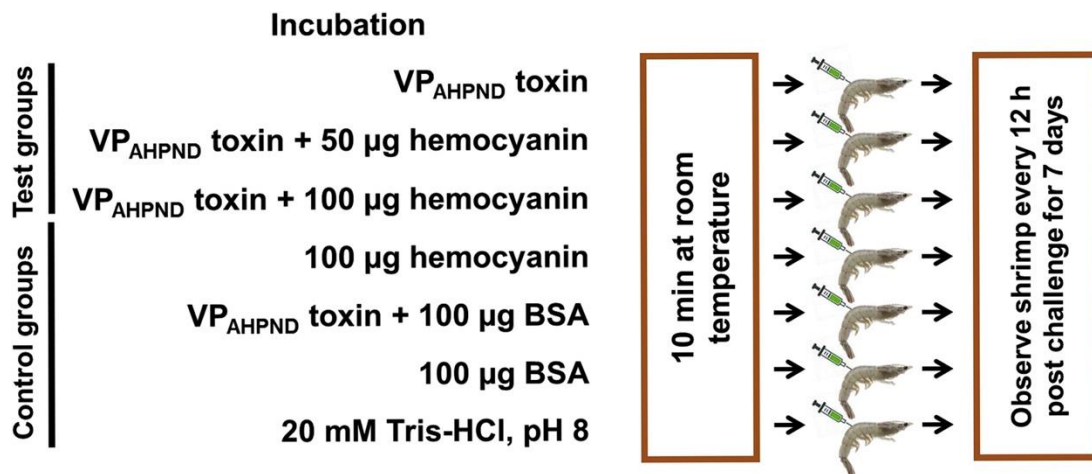


Figure 13 The experimental design for neutralization activity assay (Boonchuen et al., 2017).

To test the VP_{AHPND} toxin-neutralizing activity of hemocyanin, shrimp were divided into 7 groups of 10 shrimp each. In this experiment, VP_{AHPND} toxin at a dose of 0.2 µg of partially purified VP_{AHPND} toxin/g shrimp (LD₅₀ = 1 day) was used. VP_{AHPND} toxin alone or VP_{AHPND} toxin with 50 µg or 100 µg hemocyanin were mixed and incubated for 10 min before injection into shrimp. The control groups included shrimp injected with 100 µg hemocyanin alone, VP_{AHPND} toxin with 100 µg BSA, 100 µg BSA alone, or 20 mM Tris-HCl (pH 8.0). After pre-incubating the mixtures at room temperature for 10 min, they were injected into the tested shrimp groups (10 shrimp per group). The shrimp survival rate was observed every 12 h after challenge for 7 days.

2.2.21 Functional analysis of Vago5 by RNAi-mediated double-stranded RNA

2.2.21.1 Preparation of double-stranded RNA (dsRNA)

To investigate whether Vago5 is involved in antibacterial immunity in shrimp, *in vivo* RNAi experiments were performed. The recombinant dsRNA of Vago5 (dsVago5) was cloned, expressed, and purified by Miss Hafeezaa Sakhor. The recombinant dsRNA of GFP (dsGFP) was also expressed, and purified by Miss Hafeezaa Sakhor. The dsRNA quality was verified by agarose gel electrophoresis with UV visualization followed by staining using the RedSafe Nucleic Acid Staining Solution (iNtRON Biotechnology) and quantification by UV spectrophotometer.

2.2.21.2 *In vivo* gene knockdown of Vago5

Shrimp were divided into three groups of three individuals each. Shrimp were intramuscularly injected with 50 μ l of 0.85% NaCl solution containing 10 μ g of dsVago5, while the control group was injected with 10 μ g of dsGFP or 50 μ l of 0.85% NaCl. At 24 h post-dsRNA injection, hemocytes were collected and subjected to total RNA extraction (described in Section 2.8). In order to determine the efficiency of Vago5 gene transcript silencing, RT-PCR was performed to assess gene transcription using specific primers for the Vago5 gene (Table 2.3). One microliter of 10-fold diluted cDNA was used as a template for PCR amplification, while a fragment of the EF-1 α gene was amplified and used as an internal control. The PCR conditions were 94 °C for 2 min, followed by 28 cycles (for Vago5) or 25 cycles (for EF-1 α) of 94 °C for 30 s, 60 °C for 30 s, 72 °C for 30 s, and then a final extension at 72 °C for 5 min. The PCR products were analyzed by 1.5% (w/v) agarose gel electrophoresis and visualized by UV transillumination.

2.2.21.3 *In vivo* gene knockdown of Vago5 upon VP_{AHPND} infection

To study the involvement of the Vago5 gene during VP_{AHPND} infection in shrimp, the percentage of cumulative mortality of VP_{AHPND}-infected Vago5 knockdown shrimp was compared to VP_{AHPND}-infected dsGFP or 0.85% NaCl-injected shrimp (control groups). Ten *P. vannamei* shrimp of approximately 3 g body weight per group were injected with dsVago5, dsGFP, or 0.85% NaCl as above (Section 2.19.2). After 24 incubation, the cultured VP_{AHPND} was transferred 1:100 fold to a new culture flask containing 400 mL TSB with 1.5% NaCl, and then incubated at 30 °C and 220 rpm until OD₆₀₀ = 2.0 (approximately 10⁸ CFU/ml). Bacterial inoculant, at a final concentration of 5x10⁵ CFU/ml, was added to seawater tanks containing twenty shrimp (LD₅₀ =48 hpi). Shrimp mortality was observed every 6 h after VP_{AHPND} infection. This experiment was performed in triplicate. The dsVago5, dsGFP, or 0.85% NaCl only injection (without VP_{AHPND} challenge) were used as the experimental controls.

Moreover, hemocyte from 3 shrimp was collected at 0, 6, 12, 24, and 48 h after VP_{AHPND} infection. Stomach and hepatopancreas were individually collected from three shrimp in each group, crushed, and serially 10-fold diluted in sterile 0.85%

NaCl. The diluted hemolymph samples at 10- to 10⁶-fold were dropped onto TCBS agar and incubated at 30 °C for 12-14 h. The bacterial colonies were then counted and calculated as CFU/ml. All experiments were performed in triplicate, and statistical analysis was performed using one-way ANOVA followed by Duncan's new multiple ranges test and presented as means ± standard deviations. Statistical significance was set at $P < 0.05$. The green colonies were picked up and diagnosed for VP_{AHPND} (as described in Section 2.7) using TLH and TUMSAT-Vp3 primers.

2.2.21.4 Effect of Vago5 gene silencing on the mRNA levels of the shrimp immune-related pathway

To determine whether Vago5 is involved in the regulation of the immune-related pathway in shrimp, *in vitro* RNAi experiments of Vago5 was conducted. Shrimp were injected with either dsRNA or 0.85% NaCl as described above. Then, total RNA was extracted from the hemocyte at 24 h post VP_{AHPND} challenge and subjected to qRT-PCR analysis using specific primers (Table 3). The qRT-PCR analysis was performed using an appropriate amount of cDNA for each gene, specific oligonucleotide primers. The qPCR was performed using the Luna[®] Universal qPCR Master Mix (NEB) with the CFX96 Touch[™] Real-time PCR System (Bio-Rad) under the following conditions: 95 °C for 3 min, 40 cycles at 95 °C for 30 s, 60 °C for 30 s, and 72 °C for 30 s. EF-1 α was used as an internal control. Each qRT-PCR reaction was performed in triplicate. Relative expression was calculated using the mathematical model of Pfaffl (2001). Data were analyzed using one-way ANOVA followed by Duncan's new multiple ranges test and presented as means ± standard deviations. The level of statistical significance was set at $P < 0.05$.

Table 3 Primers used for qRT-PCR in Vago5 knockdown shrimp

Primer name	Sequence
LvPPO-F	ACTGACCTGGAAATCTGGCG
LvPPO-R	TCCTCCTTGTGAGCGTTGTC
LvPPO2-F	CCGTGAACAACCTCCGGAAGA
LvPPO2-R	CTGAGATTCGAGTCGGCCTC
Lv_Vago5-F	AATGGTACCGGTAAATTAGCCCTTTTACCAAT
Lv_Vago5-R	TTCAGATCTCTCCTCCAAAGGGAAAATG
PEN4-F	ATGCTACGGAATTCCCTCCT
PEN4-R	ATCCTTGCAACGCATAGACC
TNF-F	ATCTCCTTCTTGCCACACC
TNF-R	TCCTCCCATCTTCCTTCCC
EF-1 α -F	CGCAAGAGCGACAACATATGA
EF-1 α -R	TGGCTTCAGGATACCAGTCT

2.3 Results

2.3.1 Diagnosis of *Vibrio parahaemolyticus* AHPND (VP_{AHPND}) infection in shrimp

To determine the status of VP_{AHPND} infection in experimental shrimp, PCR was used to detect part of the PirAB expressed plasmid using primer pairs AP2 and TUMSAT-Vp3 or its genome using primer pair TLH, respectively, in non-pathogenic *V. parahaemolyticus* (VP)- or VP_{AHPND}-challenged shrimp. The results indicated that the PCR products of AP2 and TUMSAT-Vp3 were found only in the hepatopancreas of VP_{AHPND}-challenged shrimp, whereas when using TLH primer the expected product was detected in both VP- and VP_{AHPND}-challenged shrimp (Figure 14). These results imply that the systemic VP_{AHPND} challenge was successful.

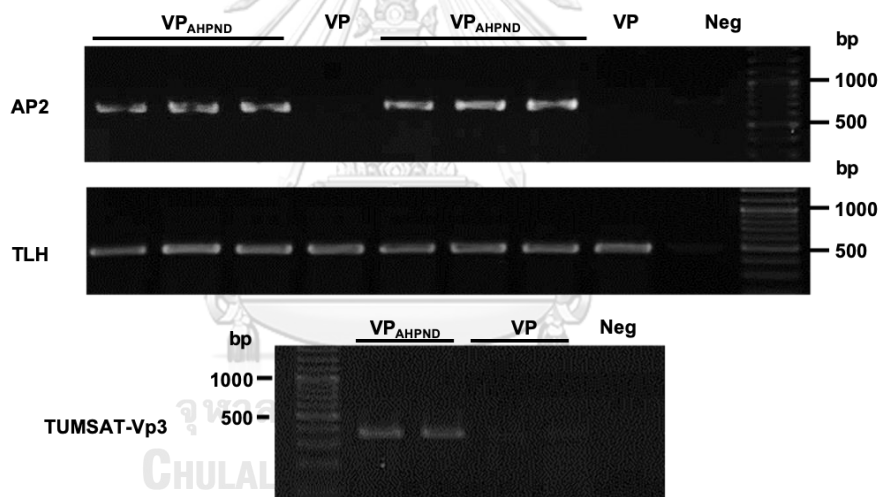


Figure 14 Analysis of VP and VP_{AHPND} infections in the experimental *P. vannamei*. TLH, AP2, and TUMSAT-Vp3 fragments were amplified by PCR in VP- and VP_{AHPND}-challenged shrimp at 48 h post-infection. Lanes Neg are the negative control.

2.3.2 Evaluation of SSH efficiency

Initially, the poly(A)+RNAs of uninfected *P. vannamei* hemocytes (Hc) and hepatopancreas (Hp), as well as VP_{AHPND}-infected Hc and Hp were collected at 3, 6, and 48 h post-infection and subjected to SSH library construction. Four SSH libraries (3/6Hc, 48Hc, 3/6Hp, and 48Hp) of the early and late phases of VP_{AHPND}-responsive

genes, respectively, were generated. A preliminary evaluation of SSH success was performed by comparing the transcript abundance of a house-keeping gene (EF-1 α) in the cDNA samples before and after subtraction. EF-1 α transcript was barely detectable in the subtracted cDNA samples of all SSH libraries whereas the high transcript level of EF-1 α was still detected in the un-subtracted cDNA samples—thus implying that the SSHs were successful (Figure 15).

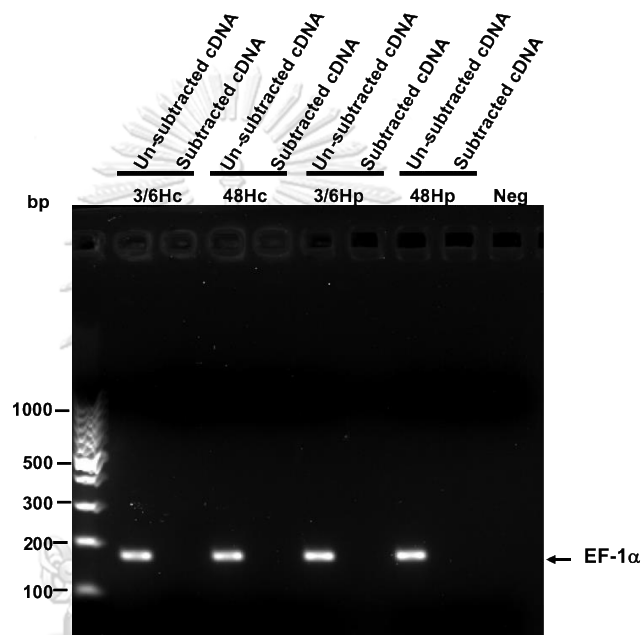


Figure 15 Analysis of the SSH efficiency of VP_{AHPND}-challenged shrimp Hc (3/6Hc and 48Hc) and Hp (3/6Hp and 48Hp) SSH libraries by comparing the transcript abundance of EF-1 α in the un-subtracted and subtracted cDNA samples amplified by PCR.

2.3.3 Identification of VP_{AHPND}-responsive genes in shrimp hepatopancreas and hemocytes by SSH

SSH was performed to identify VP_{AHPND}-responsive genes from the hemocytes and hepatopancreas of *P. vannamei*. As mentioned before, four SSH cDNA libraries were constructed to identify VP_{AHPND}-responsive genes in the early (3/6) and late (48) phases of VP_{AHPND} infection in hepatopancreas and hemocyte, respectively. The 142, 155, 162, and 153 clones from Hp 3/6 h post challenge, Hp 48

h post challenge, Hc 3/6 h post challenge, and Hc 48 h post challenge SSH libraries, respectively, were randomly selected and their sequences were analyzed. After searching for sequence homology against the NCBI GenBank database using BLASTN and BLASTX (E -values $< 1 \times 10^{-4}$), 75 (52.82%), 78 (50.32%), 93 (57.41%), and 92 (60.13%) clones were matched with known genes, while 67 (47.18%), 77 (49.68%), 69 (42.59%), and 61 (39.87%) clones were identified as hypothetical and unknown genes, respectively. The known genes were functionally categorized into nine groups, including defense and homeostasis; transport; gene expression, regulation, and protein synthesis; cell cycle/DNA synthesis, repair, and replication; energy and metabolism; signaling and communication; hypothetical proteins; and miscellaneous function (Figure 16). Of these, several genes with immune-related functions were identified (Tables 4-7). The highest expressed gene found in the hepatopancreas libraries was *hemocyanin* (HMC), while *vago5*, *kunitz*, *secretory leukocyte proteinase inhibitor*, and *profilin* were the highest expressed immune-related genes of the hemocyte libraries.

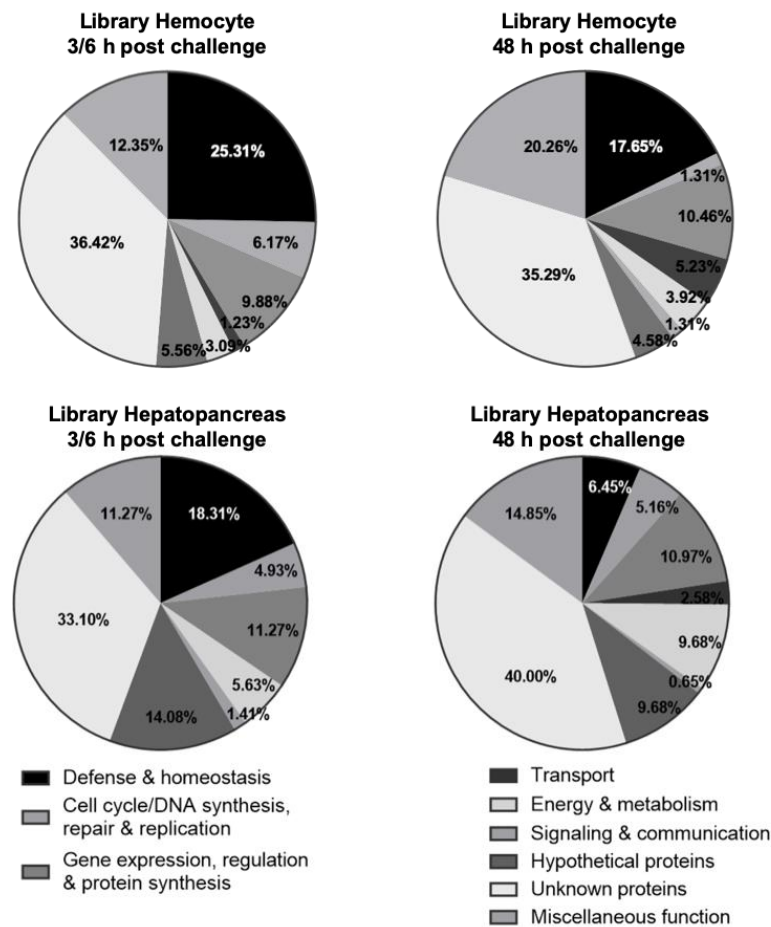


Figure 16 Percentages of gene groups identified from SSH libraries. Clones from the SSH libraries of *P. vannamei* hepatopancreas and hemocyte infected with VP_{AHPND} at 3/6 h post challenge and 48 h post challenge, respectively, were obtained from sequencing followed by annotation and categorization into nine groups of genes according to their function.

Table 4 Up-regulated genes at 3/6 h post challenge in the hepatopancreas of VP_{AHPND}-infected *P. vannamei* identified from suppression subtractive hybridization.

Highest homology	Accession no.	E Value	Closet species	No. of clones
Defense & homeostasis				
Chaperones				
PREDICTED: prefoldin subunit 6-like	XP_013060984	1.39E-14	<i>Biomphalaria glabrata</i>	1
Other defense and homeostasis proteins				
hemocyanin	AEA92687	1.13E-57	<i>Penaeus monodon</i>	2
hemocyanin	AHN85635	3.93E-69	<i>naeuspenaeus vannamei</i>	6
hemocyanin	CAA57880	8.06E-120	<i>Penaeus vannamei</i>	9
hemocyanin	ADZ15149	0	<i>Penaeus vannamei</i>	1
hemocyanin subunit L1, partial	AHY86475	1.62E-65	<i>Penaeus vannamei</i>	2
hemocyanin subunit L3, partial	AHY86477	1.50E-47	<i>Penaeus vannamei</i>	1
hemocyanin subunit L3, partial	AHY86473	2.20E-66	<i>Penaeus vannamei</i>	1
hemocyanin subunit L4, partial	AHY86474	1.79E-60	<i>Penaeus vannamei</i>	1
i-type lysozyme-like protein 1	ACZ63471	1.66E-33	<i>Penaeus monodon</i>	1
lectin B isoform 2	ADG85661	1.93E-24	<i>Marsupenaeus japonicus</i>	1
Cell cycle/DNA synthesis, repair & replication				
Apoptosis				
defender against apoptotic death	ABU54835	1.08E-25	<i>Penaeus monodon</i>	1
ferritin, partial	AGV55416	2.80E-58	<i>Penaeus monodon</i>	1
Cell cycle/DNA synthesis				
PREDICTED: 26S protease regulatory subunit 10B-like	XP_010789996	5.38E-37	<i>Notothenia coriiceps</i>	1
PREDICTED: 26S protease regulatory subunit 6B	XP_008479170	5.70E-87	<i>Diaphorina citri</i>	1
PREDICTED: polyubiquitin-B-like	XP_006892052	6.37E-40	<i>Elephantulus edwardii</i>	1
ubiquitin	KDB11907	5.60E-151	<i>Ustilaginoidea virens</i>	1
PREDICTED: structural maintenance of chromosomes protein 3-like, partial	XP_006821274	4.91E-40	<i>Saccoglossus kowalevskii</i>	1
Gene expression, regulation & protein synthesis				
Gene expression				
elongation factor 2	ADO51769	4.93E-42	<i>Penaeus vannamei</i>	1
Protein synthesis				
40S ribosomal protein S13	NP_001002079	1.18E-90	<i>Danio rerio</i>	1
40S ribosomal protein S20	ALE99171	2.08E-65	<i>Procambarus clarkii</i>	1
60S acidic ribosomal protein P2-like protein	ACY71124	6.00E-23	<i>Scylla paramamosain</i>	1
60S ribosomal protein L29	KDR09435	2.04E-20	<i>Zootermopsis nevadensis</i>	1
PREDICTED: 40S ribosomal protein S25 isoform X1	XP_008487718	3.05E-24	<i>Diaphorina citri</i>	2
PREDICTED: 40S ribosomal protein S5, partial	XP_002196941	1.16E-40	<i>Taeniopygia guttata</i>	1
PREDICTED: 60S ribosomal protein L14-like	XP_011433871	4.18E-32	<i>Crassostrea gigas</i>	1
RecName: Full=40S ribosomal protein S27	P55833	4.15E-51	<i>Homarus americanus</i>	2
ribosomal protein L13	AEB54639	2.61E-23	<i>Procambarus clarkii</i>	1
ribosomal protein L8	ABC48600	5.81E-67	<i>Penaeus vannamei</i>	1
ribosomal protein S17	AAN52389	1.46E-44	<i>Branchiostoma belcheri</i>	1
ribosomal protein S8	ACY95327	2.10E-21	<i>Manduca sexta</i>	1
tRNA (m(7)G46) methyltransferase subunit 1	XP_002650255	3.22E-75	<i>Enterocytozoon bieneusi</i>	1
Transport				
Energy & metabolism				
metabolism				
alpha-amylase	AHN91843	7.66E-08	<i>Marsupenaeus japonicus</i>	1
UDP-glucose:glycoprotein glucosyltransferase 2 precursor, putative	XP_002430541	3.32E-10	<i>Pediculus humanus</i>	1

Highest homology	Accession no.	E Value	Closest species	No. of clones
Energy				
cytochrome b	YP_001382118	3.57E-124	<i>Fenneropenaeus chinensis</i>	2
cytochrome c oxidase subunit III	YP_001315037	1.84E-55	<i>Penaeus vannamei</i>	2
ATP synthase F0 subunit 6	ABF58009	9.90E-61	<i>Penaeus vannamei</i>	1
PREDICTED: cytochrome b-c1 complex subunit 9	XP_971284	2.23E-16	<i>Tribolium castaneum</i>	1
Signaling & communication				
Rab8, partial	ABD65433	2.60E-31	<i>Suberites domuncula</i>	1
receptor accessory protein 5	AEB54634	9.26E-84	<i>Procambarus clarkii</i>	1
Hypothetical proteins				20
Unknown proteins				47
Other				15
Total				142



Table 5 Up-regulated genes at 48 h post challenge in the hepatopancreas of VP_{AHPND}-infected *P. vannamei* identified from suppression subtractive hybridization

Highest homology	Accession no.	E Value	Closet species	No. of clones
Defense & homeostasis				
Chaperones				
PREDICTED: prefoldin subunit 3	XP_015123702	4.22E-70	<i>Diachasma alloeum</i>	1
heat shock protein 90	AGC54636	6.05E-107	<i>Scylla paramamosain</i>	1
Other defense and homeostasis proteins				
chitinase 3 precursor	ADG22163	1.15E-29	<i>Penaeus monodon</i>	1
chitinase 4 precursor	ACR23314	2.37E-49	<i>Penaeus vannamei</i>	2
beta-thymosin 3	AFV39709	3.33E-76	<i>Pacifastacus leniusculus</i>	1
C-type lectin 2	AHA83583	2.29E-84	<i>Marsupenaeus japonicus</i>	1
Homeostasis				
calreticulin	AFC34501	1.45E-104	<i>Penaeus vannamei</i>	2
coronin-like protein 3	KPM06481	1.73E-18	<i>Sarcoptes scabiei</i>	1
Cell cycle/DNA synthesis, repair & replication				
Cell cycle/DNA synthesis,				
CHK1 checkpoint-like protein	ABK29471	2.11E-20	<i>Helicoverpa armigera</i>	1
proteasome subunit beta type-1-like protein	KPM09618	2.97E-24	<i>Sarcoptes scabiei</i>	1
PREDICTED: proteasome subunit alpha type-2-like	XP_002740669	6.55E-36	<i>Saccoglossus kowalevskii</i>	1
septin-2-like protein	ACY66493	2.27E-48	<i>Scylla paramamosain</i>	1
PREDICTED: ATP-dependent RNA helicase WM6-like	XP_014096660	1.53E-162	<i>Bactrocera oleae</i>	1
PREDICTED: ubiquitin-60S ribosomal protein L40 isoform X3	XP_011845882	1.89E-55	<i>Mandrilus leucophaeus</i>	1
TBC1 domain family member 20	AHX25870	2.51E-38	<i>Penaeus monodon</i>	1
Apoptosis				
caspase 4	AGL61584	1.06E-42	<i>Penaeus vannamei</i>	1
Gene expression, regulation & protein synthesis				
Gene expression				
PREDICTED: DNA-directed RNA polymerase II subunit RPB3	XP_012257186	2.92E-72	<i>Athalia rosae</i>	1
Protein synthesis				
40S ribosomal protein S20	ALE99171	1.49E-70	<i>Procambarus clarkii</i>	1
60S ribosomal protein L35a	ALS05024	1.34E-35	<i>Centropages dorsispinatus</i>	1
PREDICTED: 40S ribosomal protein S2	XP_012587306	1.28E-68	<i>Condylura cristata</i>	1
PREDICTED: 40S ribosomal protein S5	XP_014943501	1.37E-51	<i>Acinonyx jubatus</i>	1
PREDICTED: 60S ribosomal protein L23, partial	XP_009483823	6.27E-60	<i>Pelecanus crispus</i>	2
ribosomal protein L12	AEL23104	4.11E-62	<i>Cherax quadricarinatus</i>	1
ribosomal protein L13	AEB54639	1.12E-22	<i>Procambarus clarkii</i>	1
ribosomal protein L35	AEB54642	1.69E-16	<i>Procambarus clarkii</i>	1
ribosomal protein L35A	ACR54138	8.77E-25	<i>Palaemon varians</i>	1
ribosomal protein S3a	ADY16617	2.54E-61	<i>Fenneropenaeus merguensis</i>	1
putative ribosomal protein L6	ABW90342	6.39E-39	<i>Sipunculus nudus</i>	1
translationally controlled tumor protein	ABY55541	3.95E-114	<i>Penaeus vannamei</i>	2
PREDICTED: eukaryotic translation initiation factor 3 subunit E-like	XP_012937991	2.18E-94	<i>Aplysia californica</i>	1
PREDICTED: aminoacyl tRNA synthase complex-interacting multifunctional protein 2-like	XP_013407676	2.24E-23	<i>Lingula anatina</i>	1
Transport				
tubulin alpha-1	AEI88094	4.42E-47	<i>Scylla paramamosain</i>	1
profilin	ABU97474	3.78E-34	<i>Penaeus monodon</i>	1

Highest homology	Accession no.	E Value	Closet species	No. of clones
dynactin subunit 5	ACD13590	5.91E-46	<i>Penaeus monodon</i>	1
charged multivesicular body protein 5	KMR04381	1.17E-78	<i>Lasius niger</i>	1
Energy & metabolism				
ATP synthase F0 subunit 6	ABF58009	2.41E-66	<i>Penaeus vannamei</i>	1
PREDICTED: ATP synthase subunit d, mitochondrial	XP_013100056	6.14E-17	<i>Stomoxys calcitrans</i>	1
PREDICTED: ATP synthase subunit O, mitochondrial	XP_013191410	8.16E-82	<i>Amyeloidis transitella</i>	1
cytochrome b	YP_001315043	3.43E-71	<i>Penaeus vannamei</i>	2
cytochrome b	YP_001382118	1.09E-117	<i>Fenneropenaeus chinensis</i>	1
cytochrome c oxidase subunit II	YP_001315034	2.59E-98	<i>Penaeus vannamei</i>	4
cytochrome c oxidase subunit III	YP_001315037	7.62E-156	<i>Penaeus vannamei</i>	1
cytochrome oxidase subunit I, partial (mitochondrion)	AGY36769	3.26E-121	<i>Alpheus polystictus</i>	1
cytochrome P450 enzyme, CYP330A1	JC8025	2.31E-37	<i>Carcinus maenas</i>	1
PREDICTED: cytochrome b-c1 complex subunit 9	XP_971284	1.64E-16	<i>Tribolium castaneum</i>	1
PREDICTED: cytochrome c1, heme protein, mitochondrial-like	XP_013772646	1.69E-22	<i>Limulus polyphemus</i>	1
Signaling & communication				
PREDICTED: COP9 signalosome complex subunit 8-like isoform X2	XP_007544445	1.17E-21	<i>Poecilia formosa</i>	1
Hypothetical proteins				15
Unknown proteins				62
Other				23
Total				155

Table 6 Up-regulated genes at 3/6 h post challenge in the hemocyte of VP_{AHPND}-infected *P. vannamei* identified from suppression subtractive hybridization

Highest homology	Accession no.	E Value	Closest species	No. of clones
Defense & homeostasis				
Antimicrobial proteins				
RecName: Full=Penaeidin-3j; Short=Pen-3j	Q963D9	1.06E-14	<i>Penaeus vannamei</i>	1
Chain A, Solution Structure Of The [t8a]-Penaeidin-3	1UEO_A	1.99E-20		1
antimicrobial peptide PEN3-11	ABA63167	2.36E-13	<i>Penaeus vannamei</i>	1
putative antimicrobial peptide	AAL36894	1.71E-66	<i>Penaeus vannamei</i>	1
saposin isoform 1	ADK94870	5.14E-173	<i>Penaeus monodon</i>	2
stylicine 2	ABW24769	4.24E-42	<i>Penaeus stylirostris</i>	1
Proteinases & their inhibitors				
secretory leukocyte proteinase inhibitor	ABR19819	4.96E-74	<i>Penaeus vannamei</i>	3
serpin 3	AIW39913	1.69E-168	<i>Penaeus vannamei</i>	2
Kunitz-type serine protease inhibitor	AGU16239	3.32E-25	<i>Fenneropenaeus chinensis</i>	5
Other defense and homeostasis proteins				
single VWC domain protein 5	AEB54795	7.22E-57	<i>Penaeus vannamei</i>	18
thymosin beta	AIW64741	2.22E-75	<i>Penaeus monodon</i>	2
relish	ABR14713	7.92E-147	<i>Penaeus vannamei</i>	1
selenoprotein M	ABI93178	3.13E-59	<i>Penaeus vannamei</i>	1
PREDICTED: annexin B9	XP_974030	2.23E-32	<i>Tribolium castaneum</i>	1
PREDICTED: LOW QUALITY PROTEIN: annexin-B12-like	XP_013773891	5.16E-43	<i>Limulus polyphemus</i>	1
15 kDa selenoprotein	ACR54144	4.27E-33	<i>Palaemon varians</i>	1
Cell cycle/DNA synthesis, repair & replication				
Cell cycle/DNA synthesis,				
septin	AEN94576	7.56E-10	<i>Scylla paramamosain</i>	1
Apoptosis				
fortilin binding protein 1	ACB87923	5.02E-20	<i>Penaeus monodon</i>	8
flotillin-1	AEN94568	1.38E-26	<i>Scylla paramamosain</i>	1
Gene expression, regulation & protein synthesis				
Gene expression				
PREDICTED: mediator of RNA polymerase II transcription subunit 18	XP_014239778	2.83E-30	<i>Cimex lectularius</i>	1
PREDICTED: elongation factor 1-beta-like	XP_002162369	6.2E-18	<i>Hydra vulgaris</i>	1
eukaryotic initiation factor 4A	ACY66442	4.73E-42	<i>Scylla paramamosain</i>	1
eukaryotic initiation factor 4A	AGZ89665	2.31E-124	<i>Penaeus vannamei</i>	1
elongation factor 2	ADO51769	2.29E-74	<i>Penaeus vannamei</i>	1
Protein synthesis				
ribosome like protein	BAB78484	5.91E-84	<i>Marsupenaeus japonicus</i>	1
ribosomal protein S3	ACR54109	4.01E-119	<i>Palaemon varians</i>	1
ribosomal protein P1	ACR54112	4.49E-31	<i>Palaemon varians</i>	1
ribosomal protein L13	AHM25603	9.98E-18	<i>Scylla paramamosain</i>	1
ribosomal protein L12	ACY66553	1.49E-77	<i>Scylla paramamosain</i>	1
PREDICTED: 60S ribosomal protein L14	XP_013874182	5.44E-41	<i>Austrofundulus limnaeus</i>	1
PREDICTED: 60S ribosomal protein L11	XP_014258513	1.75E-39	<i>Cimex lectularius</i>	1
PREDICTED: 40S ribosomal protein S4, X isoform	XP_003457778	3.46E-102	<i>Oreochromis niloticus</i>	1
putative ribosomal protein L6	ABW90342	5.15E-39	<i>Sipunculus nudus</i>	1
60S ribosomal protein L13A	AEL23133	4.22E-31	<i>Cherax quadricarinatus</i>	1
Transport				
profilin	ABU97474	1.02E-32	<i>Penaeus monodon</i>	1

Highest homology	Accession no.	E Value	Closet species	No. of clones
putative myosin regulatory light chain 2 smooth muscle	ACY66440	3.07E-08	<i>Scylla paramamosain</i>	1
Energy & metabolism				
metabolism				
PREDICTED: beta-mannosidase	XP_001945791	5.77E-15	<i>Acyrtosiphon pisum</i>	1
Energy				
cytochrome c oxidase subunit III	YP_001315037	7.18E-156	<i>Penaeus vannamei</i>	1
cytochrome c oxidase subunit 1, partial (mitochondrion)	AGT54729	8.34E-94	<i>Fenneropenaeus indicus</i>	1
cytochrome b	YP_001315043	1.01E-66	<i>Penaeus vannamei</i>	1
PREDICTED: ATP synthase subunit O, mitochondrial	XP_013191410	7.23E-82	<i>Amyeloidis transitella</i>	1
Signaling & communication				
Hypothetical proteins				9
Unknown proteins				59
Other				20
Total				162



Table 7 Up-regulated genes at 48 h post challenge in the hemocyte of VP_{AHPND}-infected *P. vannamei* identified from suppression subtractive hybridization

Highest homology	Accession no.	E Value	Closet species	No. of clones
Defense & homeostasis				
Antimicrobial proteins				
RecName: Full=Penaeidin-3j; Short=Pen-3j;	Q963D9	4.47E-24	<i>Penaeus vannamei</i>	3
RecName: Full=Penaeidin-2a; Short=P2; Short=Pen-2;	P81057	3.48E-09	<i>Penaeus vannamei</i>	1
Proteinases & their inhibitors				
secretory leukocyte proteinase inhibitor	ABR19819	3.27E-74	<i>Penaeus vannamei</i>	2
Kunitz-type serine protease inhibitor	AGU16239	3.55E-26	<i>Fenneropenaeus chinensis</i>	8
kazal type protease inhibitor	AGH68885	8.90E-07	<i>Penaeus monodon</i>	1
Other defense and homeostasis proteins				
single VWC domain protein 5	AEB54795	1.22E-43	<i>Penaeus vannamei</i>	4
cathepsin B	ADI80349	3.29E-136	<i>Penaeus vannamei</i>	1
calreticulin	AFC34501	1.41E-117	<i>Penaeus vannamei</i>	1
autophagy-related protein 8	AFV99179	6.16E-41	<i>Penaeus vannamei</i>	1
astakine variant 2	ADP06651	1.62E-25	<i>Penaeus vannamei</i>	1
C type lectin containing domain protein	AEH05998	9.37E-52	<i>Penaeus vannamei</i>	1
lysozyme	AAL23948	3.8E-51	<i>Penaeus vannamei</i>	3
Cell cycle/DNA synthesis, repair & replication				
Apoptosis				
fortilin binding protein 1	ACB87923	1.42E-19	<i>Penaeus monodon</i>	1
Cell cycle/DNA synthesis				
PREDICTED: probable E3 ubiquitin-protein ligase DTX2, partial	XP_010071922	2.02E-42	<i>Pterocles gutturalis</i>	1
Gene expression, regulation & protein synthesis				
Gene expression				
PREDICTED: negative elongation factor B	XP_015364222	1.27E-65	<i>Diuraphis noxia</i>	1
PREDICTED: eukaryotic translation initiation factor 3 subunit B-like	XP_013408544	1.11E-96	<i>Lingula anatina</i>	1
Protein synthesis				
ribosomal protein P1	ACR54112	1.21E-31	<i>Palaemon varians</i>	1
ribosomal protein L35	AEB54642	7.8E-18	<i>Procambarus clarkii</i>	1
ribosomal protein L32	AEB54641	8.24E-71	<i>Procambarus clarkii</i>	3
60s ribosomal protein I27a	ERG81655	1.11E-66	<i>Ascaris suum</i>	1
60S ribosomal protein L27	ACY66537	1.07E-46	<i>Scylla paramamosain</i>	1
PREDICTED: 60S ribosomal protein L37	XP_014260836	3.75E-43	<i>Cimex lectularius</i>	1
PREDICTED: 60S ribosomal protein L14-like	XP_011433871	3.57E-32	<i>Crassostrea gigas</i>	2
PREDICTED: 60S ribosomal protein L14	XP_013874182	2.73E-32	<i>Austrofundulus limnaeus</i>	1
Putative ribosome biogenesis protein RLP24, partial	EHB03557	9.08E-08	<i>Heterocephalus glaber</i>	1
putative ribosomal protein L6	ABW90342	6.27E-39	<i>Sipunculus nudus</i>	2
Transport				
profilin	ABU97474	1.87E-34	<i>Penaeus monodon</i>	1
profilin	ACQ90248	5.8E-17	<i>Fenneropenaeus chinensis</i>	3
putative myosin regulatory light chain 2 smooth muscle	ACY66440	1.05E-82	<i>Scylla paramamosain</i>	2
PREDICTED: actin, cytoplasmic 2-like	XP_008334771	4.82E-84	<i>Cynoglossus semilaevis</i>	1
keratinocyte associated protein 2	ABI93175	1.97E-53	<i>Penaeus vannamei</i>	1
Energy & metabolism				
metabolism				
glucose transporter 2	ALG65274	5E-67	<i>Penaeus vannamei</i>	1

Highest homology	Accession no.	E Value	Closest species	No. of clones
Energy				
cytochrome oxidase subunit I, partial (mitochondrion)	AGY36761	6.07E-122	<i>Alpheus polystictus</i>	1
cytochrome oxidase subunit I, partial (mitochondrion)	AGY36769	3.2E-121	<i>Alpheus polystictus</i>	2
mitochondrial cytochrome c oxidase subunit Va	AFW19996	8.24E-107	<i>Penaeus vannamei</i>	1
PREDICTED: mitochondrial carrier homolog 2-like isoform X2	XP_012257319	3.88E-38	<i>Athalia rosae</i>	1
Signaling & communication				
B-cell receptor-associated protein, putative	XP_002403043	6.7E-70	<i>Ixodes scapularis</i>	1
PREDICTED: renin receptor isoform X3	XP_011301396	2.17E-07	<i>Fopius arisanus</i>	1
Hypothetical proteins				7
Unknown proteins				54
Other				31
Total				153

2.3.4 Gene expression analysis in VP_{AHPND}- and toxin-challenged shrimp hepatopancreas by qRT-PCR

In order to validate the data from Hp-SSH libraries, qRT-PCR was used to determine the transcription levels of immune-related genes in shrimp hepatopancreas in response to VP_{AHPND} infection. Following the results presented in Section 2.3.3, the most abundant clone found in the Hepatopancreas SSH library was hemocyanin (HMC). Five hemocyanin isoforms, including HMC, hemocyanin subunit L1 (HMCL1), hemocyanin subunit L2 (HMCL2), hemocyanin subunit L3 (HMCL3), and hemocyanin subunit L4 (HMCL4) were found in Hepatopancreas SSH libraries.

To study the expression profile of hemocyanin transcripts, the gene expression levels of five hemocyanin isoforms (HMC, HMCL1, HMCL2, HMCL3, and HMCL4) were analyzed in VP_{AHPND}-infected *P. vannamei* hepatopancreas at 0, 3, 6, and 48 h post challenge. The EF-1 α gene was used as the internal control gene (Figure 17). The results indicate that the expression levels of hemocyanin genes were altered in shrimp hepatopancreas after VP_{AHPND} challenge. The expression level of the HMC gene was up-regulated approximately 5-fold and 2-fold at 3 and 6 h post challenge, respectively, and down-regulated by 4.8-fold at 48 h post challenge. This result highlights the positive correlation between qRT-PCR and SSH. Meanwhile, the expression levels of hemocyanin subunits HMCL1, HMCL2, HMCL3, and HMCL4 were down-regulated by 4.8-, 2.9-, 2.0-, and 2.2-fold at 48 h post challenge, respectively.

During VP_{AHPND} infection, VP_{AHPND} produces PirA and PirB toxin complexes, which are the cause of hepatopancreatic necrosis and subsequent shrimp death. The direct effect of VP_{AHPND} toxin on hemocyanin isoform expression in shrimp hepatopancreas was also investigated. The transcript levels of all hemocyanin subunits were analyzed in the hepatopancreas of VP_{AHPND}-injected shrimp at 0, 1, 3, 6, 12, and 24 hpi (Figure 17). The results show a decrease in HMC and HMCL1 gene expression of approximately 4-fold at 12 and 24 hpi. The expression level of HMCL2 was down-regulated at 12 hpi by approximately 4.4-fold and recovered at 24 hpi to the same level as at 0 hpi. On the other hand, HMCL3 and HMCL4 were up-regulated by 2.4- and 1.5-fold at 1 and 3 hpi, respectively; then, from 12 to 24 hpi, they were down-regulated by approximately 4- and 2-fold, respectively. These results indicate that genes of HMC and other HMC isoforms were expressed in response to VP_{AHPND} toxin challenge.

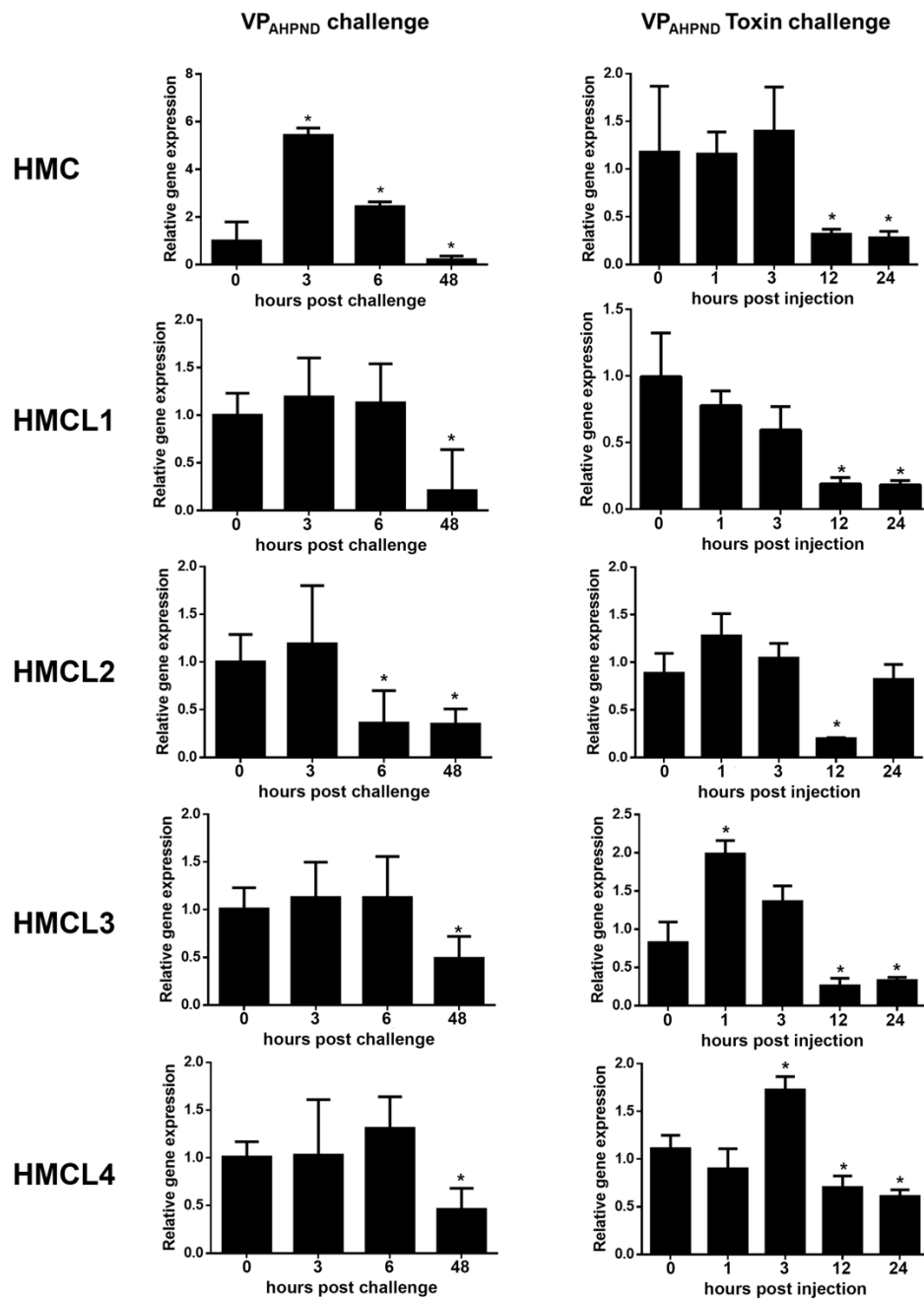


Figure 17 Expression of hemocyanin genes identified from SSH libraries in VP_{AHPND}- and VP_{AHPND} toxin-infected *P. vannamei* shrimp.

The transcription levels of each hemocyanin gene (HMC, HMCL1, HMCL2, HMCL3, and HMCL4) were analyzed at different time points during hepatopancreas VP_{AHPND} (left panel) or VP_{AHPND} toxin (right panel) challenge. The expression level was calculated relative to that of the control shrimp injected with 1×PBS at each time point. The experiment was performed in triplicate. Data are presented as means ± standard deviations. Asterisks indicate significant differences between data at 0 h post challenge ($P < 0.05$).

2.3.5 Functional characterization of hemocyanin in shrimp upon VP_{AHPND} infection

2.3.5.1 Purification of hemocyanin protein from *P. vannamei* hemolymph

To investigate the involvement of hemocyanin protein in VP_{AHPND} infection, the native hemocyanin was purified from healthy shrimp hemolymph and used for biological activity assay. The native hemocyanin protein was purified from shrimp hemolymph using a Blue-Sepharose column (GE Healthcare) and DEAE Sepharose Fast Flow (GE Healthcare). Then, 10% SDS-PAGE was used to analyze the purified protein. The expected bands of putative native hemocyanin protein (70 kDa) were observed (Figures 18-19).

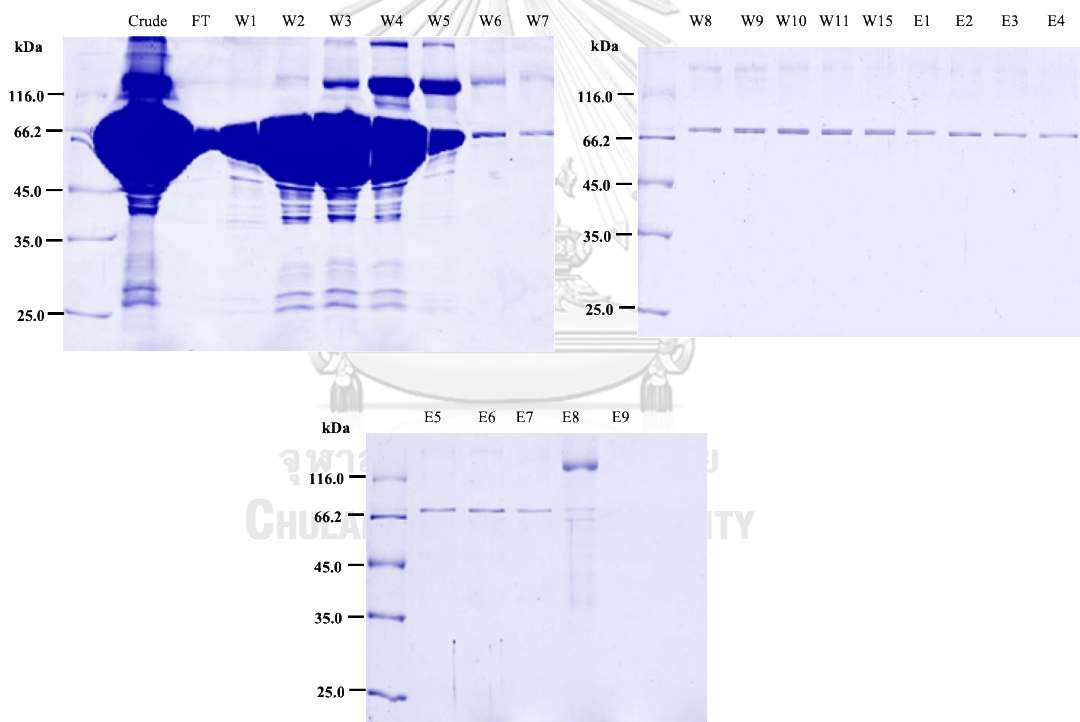


Figure 18 Purification of the putative native hemocyanin protein by Blue-Sepharose column chromatography.

The crude hemocyte-free hemolymph was passed through a Blue-Sepharose column calibrated with 20 mM Tris-HCl (pH 8.0). Then, the column was washed with 20 mM Tris-HCl (pH 8.0) and eluted with 20 mM Tris-HCl (pH 8.0) supplemented with 1 M NaCl. The fractions were then run on 10% SDS-PAGE. Lane crude: the hemocyte-free hemolymph. Lane FT: the flow-through fraction. Lane W: the wash fraction. Lane E: the elution fraction.

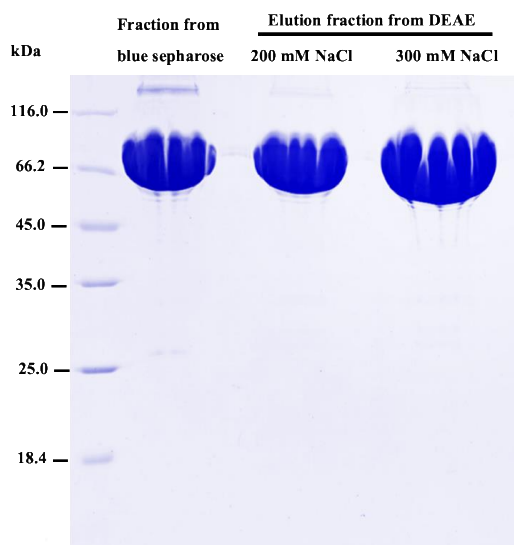
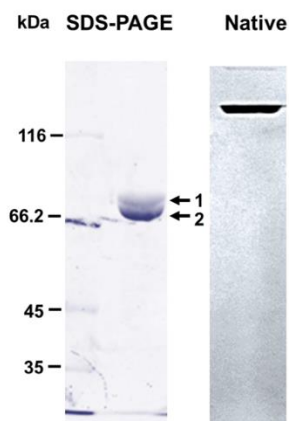


Figure 19 Purification of the native hemocyanin protein by DEAE Sepharose Fast Flow column chromatography.

The fractions containing hemocyanin protein from wash fraction were pooled and passed through a DEAE Sepharose column pre-calibrated with 20 mM Tris-HCl (pH 8.0). Then, the column was washed with 20 mM Tris-HCl (pH 8.0) and eluted with 20 mM Tris-HCl (pH 8.0) supplemented with 200 and 300 mM NaCl. The fractions were then run on 10% SDS-PAGE.

To analyze the purified putative hemocyanin protein, 10% SDS-PAGE and native-PAGE were analyzed. Only one band of purified hemocyanin was observed on native-PAGE and two protein bands of purified native hemocyanin of approximately 71 (lower band) and 75 (upper band) kDa were observed on SDS-PAGE. Both of these protein bands were analyzed by nano LC-MS/MS. The upper band was HMCL1 (AHY86475) and the lower band was HMC (CAA57880) (Figure 20). Comparing band HMC intensity of both HMC proteins purified from shrimp hemolymph, indicated that HMC (lower band) was the most abundant protein in the native hemocyanin purified from healthy shrimp hemolymph.



Protein band	Protein name	Sequence coverage (%)	pI	Molecular weight		NCBI accession no	Score
				Observed	Theory		
1	Hemocyanin subunit L1, partial	31	5.43	75	77.29	AHY86471	960
2	Hemocyanin	31	5.27	71	74.99	CAA57880	1065

Figure 20 The purified hemocyanin protein was separated by Coomassie blue stained-10% SDS-PAGE and 10% Native-PAGE. The amino acid sequences of two hemocyanin (bands indicated by arrows) were analyzed by nano LC-MS/MS using the MASCOT program. The best hits for both hemocyanin amino acid sequences are shown in the table below.

2.3.5.2 Bacterial agglutination

To investigate the defense function of hemocyanin against VP_{AHPND}, liquid growth inhibition assay and agglutination activity assay were performed. Different concentrations of purified native hemocyanin protein (0-40 $\mu\text{g/ml}$) were incubated with VP_{AHPND} in a 96-well plate overnight under vigorous shaking at 30 °C. Bacterial agglutination was observed under a light microscope after treatment with 40 $\mu\text{g/ml}$ purified native hemocyanin (Figure 21). Notably, no bacterial agglutination was observed in the control groups (BSA-treated VP_{AHPND} and 20 mM Tris-HCl (pH 8.0)-treated VP_{AHPND}).

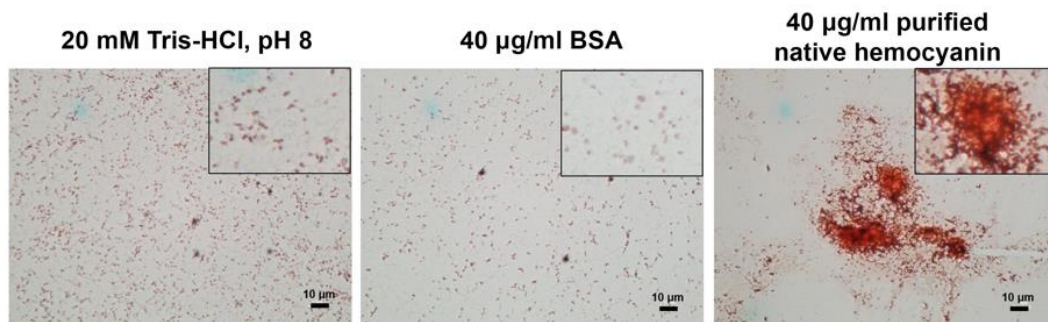


Figure 21 VP_{AHPND} agglutination by hemocyanin. VP_{AHPND} was mixed and incubated with 40 µg/ml hemocyanin overnight at 30°C, placed on a microscope slide, and then Gram-stained. The 40 µg/ml BSA and 20 mM Tris-HCl (pH 8.0) were used as control treatments. Agglutination was observed under a light microscope at 100× magnification. Scale bar indicates 10 µm.

2.3.5.3 Effect of hemocyanin protein on VP_{AHPND} clearance

To definitively determine whether the *hemocyanin* protein plays an important role in the shrimp immune response against VP_{AHPND}, the effect of *hemocyanin* protein on bacterial clearance was tested *in vivo*. In this experiment, hemolymph was collected from shrimp injected with VP_{AHPND} pre-incubated with 50 µg purified native hemocyanin at 0-60 min post injection (Figure 22) The total *Vibrio* species count was unchanged at 15 min post injection, but significantly decreased at 30 min post injection by approximately 2.2-fold when compared to the control shrimp. At 60 min post injection, the total *Vibrio* species count of shrimp injected with purified native hemocyanin-treated VP_{AHPND} was the same as the control. These results indicate that hemocyanin may induce bacterial agglutination and reduce the invasive VP_{AHPND} in shrimp during a short period of time but have no function on bacterial clearance.

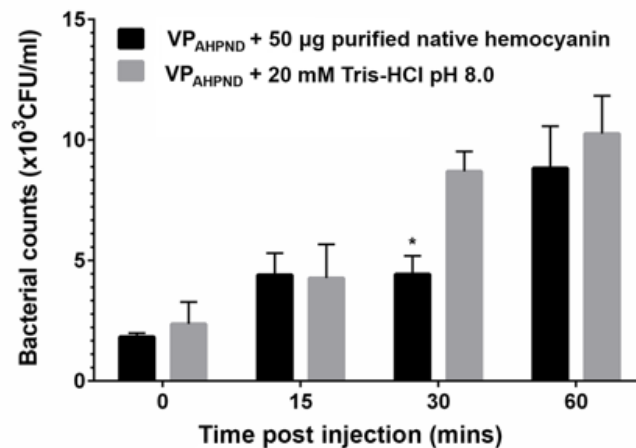


Figure 22 The effect of hemocyanin treatment on the number of VP_{AHPND} counts (CFU/ml).

VP_{AHPND} pre-incubation with 50 µg hemocyanin or 20 mM Tris-HCl (pH 8.0) (control) were injected into shrimp. At various time points after injection, hemolymph was drawn, diluted, and plated onto TCBS–NaCl agar plates. The number of VP_{AHPND} colonies was then counted. Results are expressed as mean ± SD of triplicate experiments. Asterisks indicate significant differences at $P < 0.05$ compared to the control group.

2.3.5.4 Partial purification of VP_{AHPND} toxin

Crude VP_{AHPND} toxin was prepared from VP_{AHPND} culture supernatant (as described above) and subjected to purification as described by Sirikharin et al. (2015). Following precipitation in 40% (w/v) ammonium sulfate, the supernatant was separated by centrifugation and ammonium sulfate was added to a concentration of 60% (w/v). The pellet was collected, dissolved in 1× PBS (pH 7.4), and dialyzed against 1×PBS (pH 7.4). The partially purified VP_{AHPND} toxin was checked using 12.5% SDS-PAGE for the presence of PirAB toxin protein (Figure 2.23).

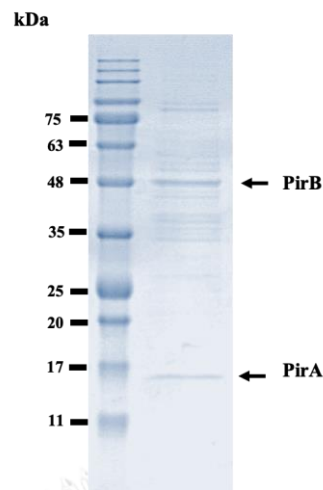


Figure 23 The partially purified VP_{AHPND} toxin protein separated by Coomassie blue stained-12.5% SDS-PAGE. Arrows indicate the expected bands of rPirA and rPirB proteins.

2.3.5.5 Neutralizing activity of hemocyanin protein on the VP_{AHPND} toxin

To determine the importance of hemocyanin in shrimp immune response against VP_{AHPND} toxin protein, a test of shrimp survival upon hemocyanin-neutralized VP_{AHPND} toxin infection was performed (Figure 24). The results indicate that no shrimp death was observed in control groups injected with either 20 mM Tris-HCl (pH 8.0) volume adjusted to 50 μ l with 1 \times PBS, 100 μ g purified native hemocyanin, or 100 μ g BSA. VP_{AHPND} toxin injection alone and BSA-treated VP_{AHPND} toxin injection caused shrimp survival to decrease to 0% within 4 days. Notably, the injection of the VP_{AHPND} toxin pre-incubated with 50 and 100 μ g the purified native hemocyanin caused a significant increase in shrimp survival rate (30% and 60%, respectively) at 4 days after injection. These results indicate that the purified native hemocyanin can neutralize VP_{AHPND} toxin. Furthermore, the effect of hemocyanin-VP_{AHPND} toxin neutralization on hepatopancreas morphology was observed. As expected, the hepatopancreas histology of shrimp challenged with VP_{AHPND} toxin showed signs of AHPND sloughed epithelial cells and cellular disruption, whereas shrimp challenged with purified native hemocyanin-neutralized VP_{AHPND} toxin exhibited no sign of AHPND infection (Figure 25).

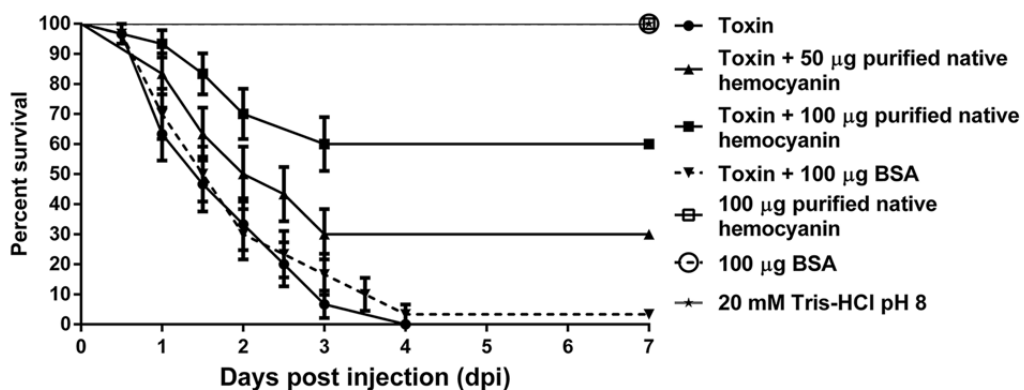


Figure 24 Survival of shrimp challenged with hemocyanin-neutralized VP_{AHPND} toxin.

Shrimp were challenged with VP_{AHPND} toxin alone (●), VP_{AHPND} toxin pre-incubated with 50 µg hemocyanin (▲), VP_{AHPND} toxin pre-incubated with 100 µg hemocyanin (■), 100 µg hemocyanin (□), 100 µg BSA (○), 100 µg BSA pre-incubated with VP_{AHPND} toxin protein (▼), and 20 mM Tris-HCl, pH 8.0 (*) (control). Shrimp survival was observed every 12 h post-treatment for 7 days. All experiments were performed in triplicate. Survival percentage was calculated as mean ± 1 standard error (S.E.) at each time point.

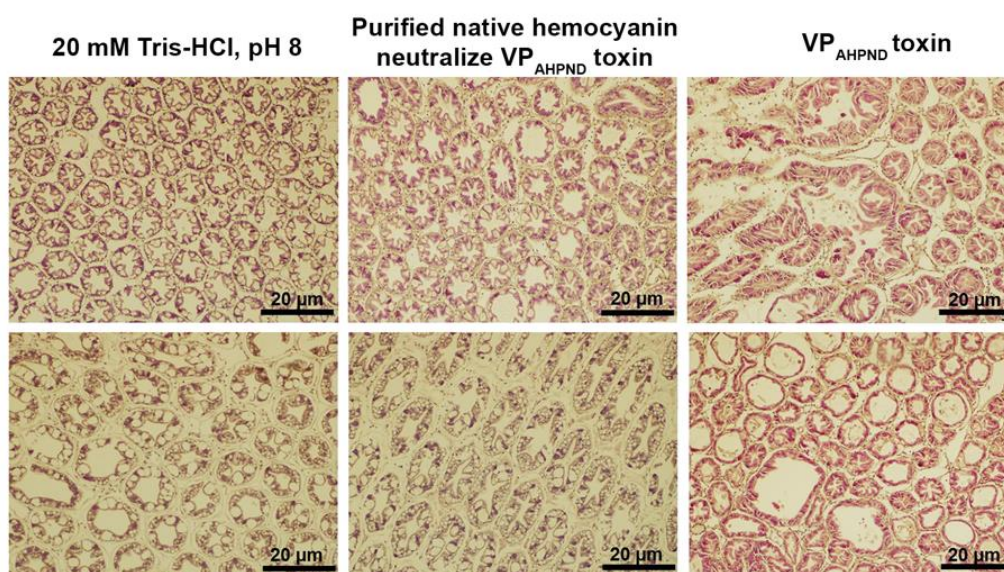


Figure 25 Hepatopancreatic histology of shrimp injected with hemocyanin-neutralized VP_{AHPND} toxin.

Sections of hepatopancreas of shrimp injected with VP_{AHPND} toxin only, hemocyanin pre-incubated VP_{AHPND} toxin and PBS were stained with H&E and subjected to histological examination. Scale bar indicates 20 µm.

2.3.5.6 Protein-protein interaction assay between rPirA and B proteins and purified native hemocyanin using the ELISA technique

The recombinant proteins of PirA (rPirA) and PirB (rPirB) expressed and purified by the Center for Shrimp Disease Control and Genetic Improvement, National Cheng Kung University, Taiwan, were used for protein-protein interaction assay (Figure 26). To determine how hemocyanin exhibits VP_{AHPND} toxin-neutralizing activity, the direct binding between each VP_{AHPND} toxin subunit to hemocyanin was tested using the ELISA technique. The purified native hemocyanin was coated onto a 96-well plate with either purified rPirA or rPirB (0-10 μ M) being added. The bound protein was then detected with each specific antibody. As shown in Figure 27, the purified native hemocyanin could directly bind to rPirA in a concentration-dependent manner, though rPirB could not. The apparent dissociation constant (K_d) of the native hemocyanin to rPirA calculated from the saturation curve fitting according to the one-site binding model was 6.83×10^{-6} M. These data suggest that native hemocyanin can neutralize VP_{AHPND} toxin via direct binding to PirA protein.

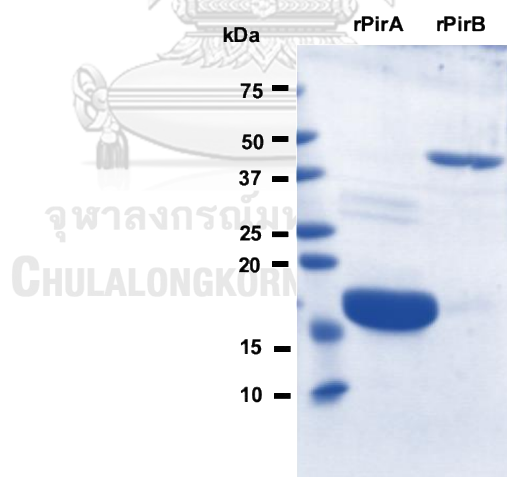


Figure 26 Analysis of recombinant proteins of PirA (rPirA) and PirB (rPirB) by 12.5% SDS-PAGE staining with Coomassie brilliant blue. Lane 1: the purified rPirA. Lane 2: the purified rPirB.

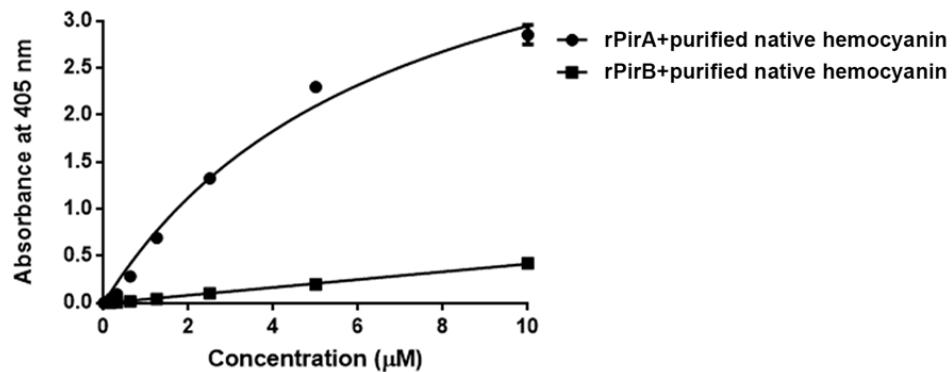


Figure 27 Binding ability of rPirA (●) and rPirB (■) on the immobilized hemocyanin, as determined by ELISA.

The purified rPirA or rPirB (0-10 µM) was added into hemocyanin-coated plate, followed by probing with the specific primary antibody and goat anti-rabbit-conjugated AP antibody as the secondary antibody. The substrate (p-nitrophenylphosphate) was finally added, and A_{405} was measured. Solid lines illustrate the fitted curves. The data are shown as the dissociation constant (K_d) near the line and the mean \pm 1 SEM, as derived from triplicate experiments.

2.3.6 Confirmation of the differentially expressed genes in VP_{AHPND}-challenged shrimp hemocyte by qRT-PCR

Based on the data obtained from Hc-SSH libraries, *Vago5*, *kunitz*, *secretory leukocyte proteinase inhibitor*, and *profilin* were identified as the up-regulated genes in *P. vannamei* hemocyte following VP_{AHPND} infection. To confirm this SSH result, qRT-PCR was used to analyze the expression of differentially expressed genes in the hemocytes of VP_{AHPND}-challenged shrimp at 0, 3, 6, and 48 h post challenge. The results revealed that *Vago5* was up-regulated at the early phases of VP_{AHPND} infection (3 and 6 h post challenge) by approximately 3.7- and 3-fold, respectively. *Kunitz*, *secretory leukocyte proteinase inhibitor*, and *profilin* were up-regulated at the late phase of VP_{AHPND} infection (48 h post challenge) by approximately 4- to 6-fold (Figure 28). These results confirmed the efficiency of the SSH, which suggests that some of these genes should be selected for further study in order to understand immune functions that might be related to VP_{AHPND} infection.

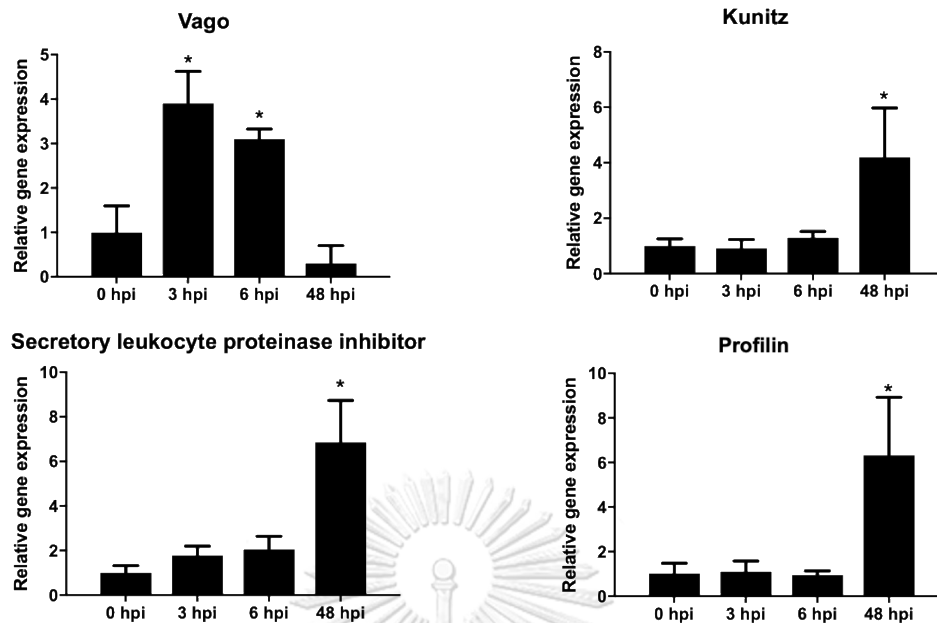


Figure 28 Expression of differentially expressed immune-related genes identified from Hemocyte SSH libraries in the VP_{AHPND}-infected hemocyte of *P. vannamei*. Gene expression level at each time post challenge of VP_{AHPND}-infected was calculated in relative to that of control shrimp at 0 h post challenge. The experiment was performed in triplicate. Data are presented as means \pm standard deviations. Asterisks indicate significant differences between data at each time point post challenge ($P < 0.05$).

2.3.7 Functional characterization of *Vago5* in shrimp upon VP_{AHPND} infection

Vago5 has also been identified in *P. vannamei* as an IFN-like molecule (Li et al., 2015). Notably, it could serve a role in antiviral immunity in shrimp. Previously, five *Vago5* genes were identified as up-regulated genes in immune responses against poly(C-G) and WSSV challenges (Chen et al., 2011). In this study, *Vago5* was identified by SSH as an up-regulated gene during the early phase of VP_{AHPND} infection. This result suggests that *Vago5* might play a role in antibacterial immunity in shrimp.

2.3.7.1 Gene silencing of *Vago5* using dsRNA

To investigate whether *Vago5* is involved in antibacterial immunity in shrimp, *in vitro* RNAi experiment was performed. The recombinant plasmid expressing dsRNA of *Vago5* (dsVago5) and GFP (dsGFP) were prepared by Miss Hafeezaa

Sakhor. The quality of dsVago5 and dsGFP was determined before used (Figure 29). Shrimp were injected with either 10 μ g of dsVago5, dsGFP (control), or 0.85% NaCl (control). Thereafter, hemocyte was collected and total RNA was extracted at 24 h and subjected to semi-quantitative RT-PCR analysis. The semi-quantitative RT-PCR analysis showed that the *Vago5* transcription level was specifically and significantly decreased in dsVago5-treated shrimp, whereas no change in *Vago5* gene expression was observed in dsGFP- and 0.85% NaCl-treated shrimp (Figure 30).

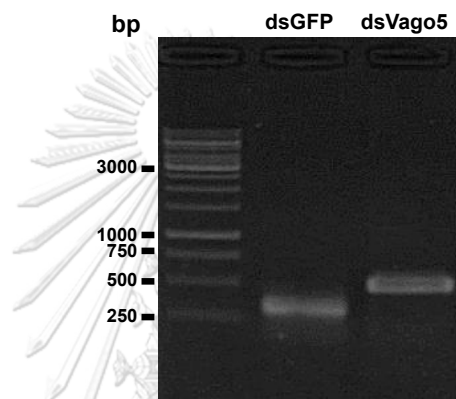


Figure 29 Analysis of purified dsVago5 and dsGFP using 2% agarose gel electrophoresis.

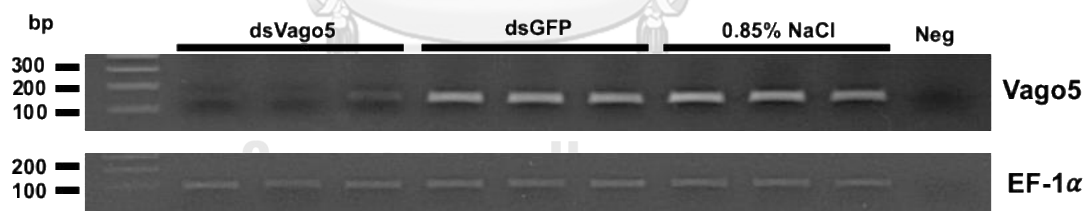


Figure 30 The efficiency of dsRNA-mediated gene knockdown of *Vago5* gene at 24 h post-dsRNA injection.

The *Vago5* transcript of dsVago5, dsGFP and 0.85%NaCl challenged *P. vannamei* at 24 h post injection was elucidated by semi-quantitative RT-PCR. EF-1 α served as the internal control gene.

2.3.7.2 Effect of *Vago5* gene silencing in *P. vannamei* upon VP_{AHPND} infection

To determine the importance of *Vago5* in shrimp antibacterial immunity, survival of shrimp injected with either dsVago5, dsGFP, or 0.85% NaCl prior to VP_{AHPND} infection was observed for 120 h post VP_{AHPND} infection (Figure 2.20). The results indicated that no shrimp death was observed in control unchallenged groups pre-injected with either 0.85% NaCl, 10 µg dsVago5, or 10 µg dsGFP and immersed with TSB media. In the VP_{AHPND} challenge control groups pre-injected with 0.85% NaCl or 10 µg dsGFP followed by VP_{AHPND} challenge, caused a decrease in shrimp survival to 50% within 108 and 120 hpi, respectively. Shrimp pre-injected with 10 µg dsVago5 before VP_{AHPND} challenge had a significant lower shrimp survival at 60 hpi (45%) to 120 hpi (25%) as compared to the both challenged control groups (Figure 2.20). These results indicate that *Vago5* might be involved in antibacterial immunity in shrimp.

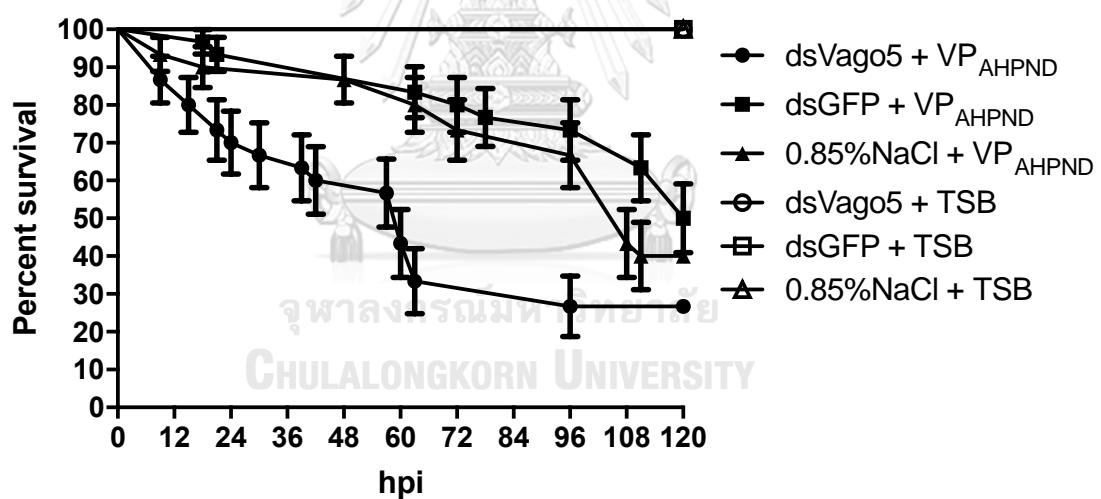


Figure 31 Effect of *Vago5* gene knockdown in VP_{AHPND} infected *P. vannamei*. Effect of *Vago5* gene knockdown in VP_{AHPND} infected *P. vannamei* pre-injected with 10 µg dsVago5 (●), 10 µg dsGFP (■), and 0.85% NaCl (▲) were challenged with VP_{AHPND} by immersion. Shrimp pre-injected with 10 µg dsVago5 (○), 10 µg dsGFP (□), and 0.85% NaCl (△) were immersed with TSB media as control experiments. Shrimp survival was observed every 12 h post-treatment for 120 h. All experiments were performed in triplicate. Survival percentage was calculated as mean ± 1 S.E. at each time point.

2.3.7.3 Effect of *Vago5* gene silencing on the bacterial count in VP_{AHPND} infected *P. vannamei*

We further investigated the effect of *Vago5* gene knockdown on VP_{AHPND} infection by determining the number of bacterial count. The total *Vibrio* count in shrimp stomach and hepatopancreas of 10 µg ds*Vago5*, 10 µg dsGFP, or 0.85% NaCl treated shrimp at 0, 6, 12, 24, and 48 h post VP_{AHPND} challenge was determined. In shrimp stomach, the significant higher (approximately 2.5-to 10-fold of total *Vibrio* count in ds*Vago5* treated shrimp than the controls was observed at 12 to 48 hpi (Figure 32a). The total *Vibrio* count in the VP_{AHPND}-infected shrimp hepatopancreas was 10- and 2.5-fold higher than the controls at 12 and 24 hpi, respectively (Figure 32b).

PCR analysis of the representative green colonies grown on the selective plates, using VP_{AHPND} specific primer (TUMSAT-Vp3; 350 bp), was used to confirm VP_{AHPND} infection. The results showed that TUMSAT-Vp3 and THL were found in both the stomach and hepatopancreas of VP_{AHPND}-challenged shrimp at 12 and 24 hpi (Figure 33). This indicated that the observed colonies were VP_{AHPND}.

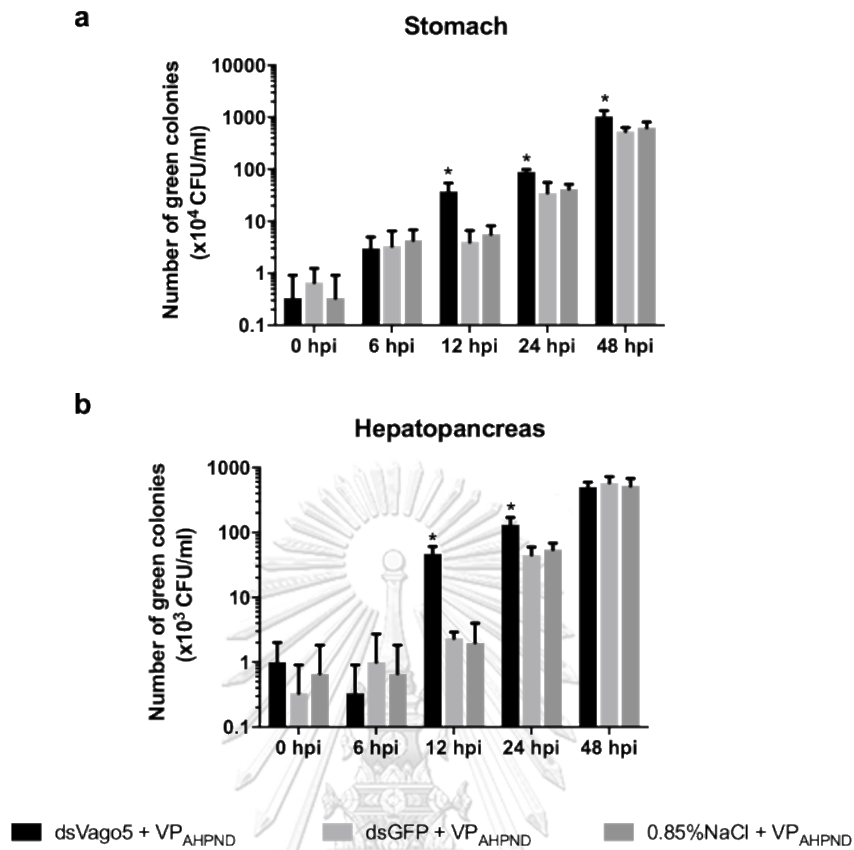


Figure 32 Effect of *Vago5* gene knockdown on VP_{AHPND} infection on total *Vibrio* count.

Shrimp were injected with dsVago5, dsGFP, and 0.85% NaCl. After 24 h, shrimp were immersed with 1×10^6 CFU/ml VP_{AHPND}. Stomach and hepatopancreas were individually collected to determine the amount of VP_{AHPND} by dotting on TCBS agar at various time points. After incubating overnight, the total numbers of viable green colonies (CFUs) were counted. The experiment was performed in triplicate. Data are presented as means \pm standard deviations. Asterisks indicate significant differences between data between dsVago5 knockdown and controls (dsGFP and 0.85% NaCl) groups ($P < 0.05$).

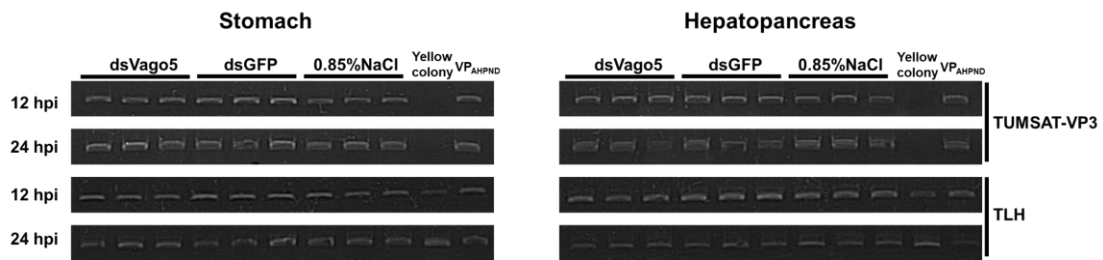


Figure 33 VP_{AHPND} verification by colony PCR.

Green colonies were used as a template for VP_{AHPND} identification using TUMSAT-Vp3 and TLH primers. VP_{AHPND} and yellow colony was used as positive control and a non-AHPND causing strain, respectively.

2.3.7.4 Effects of *Vago5* gene silencing on the mRNA levels of the shrimp immune-related genes

To investigate whether *Vago5* is involved in the regulation of the shrimp immune-related pathway, *in vitro* RNAi experiment of *Vago5* was conducted. Shrimp were injected with either dsRNA or 0.85% NaCl (as described in Section 2.2.19.3). Then, total RNA was extracted from hemocyte at 24 h post challenge and subjected to qRT-PCR analysis. The qRT-PCR analysis indicated that *Vago5* transcription level significantly decreased at 24 h post VP_{AHPND} challenge in dsVago5 pre-injected shrimp as compared to the dsGFP and 0.85% NaCl pre-injected shrimp. The transcription of immune-related genes was further analyzed in the *Vago5*-silenced shrimp in comparison to that of dsGFP and 0.85% NaCl-injected shrimp. Expression level of *PEN4*, *TNF* and *PO2* was significantly decreased in the *Vago5*-silenced shrimp. Though *Vago5* gene suppression has no significant effect on the transcriptional level of *PO1* (Figure 34).

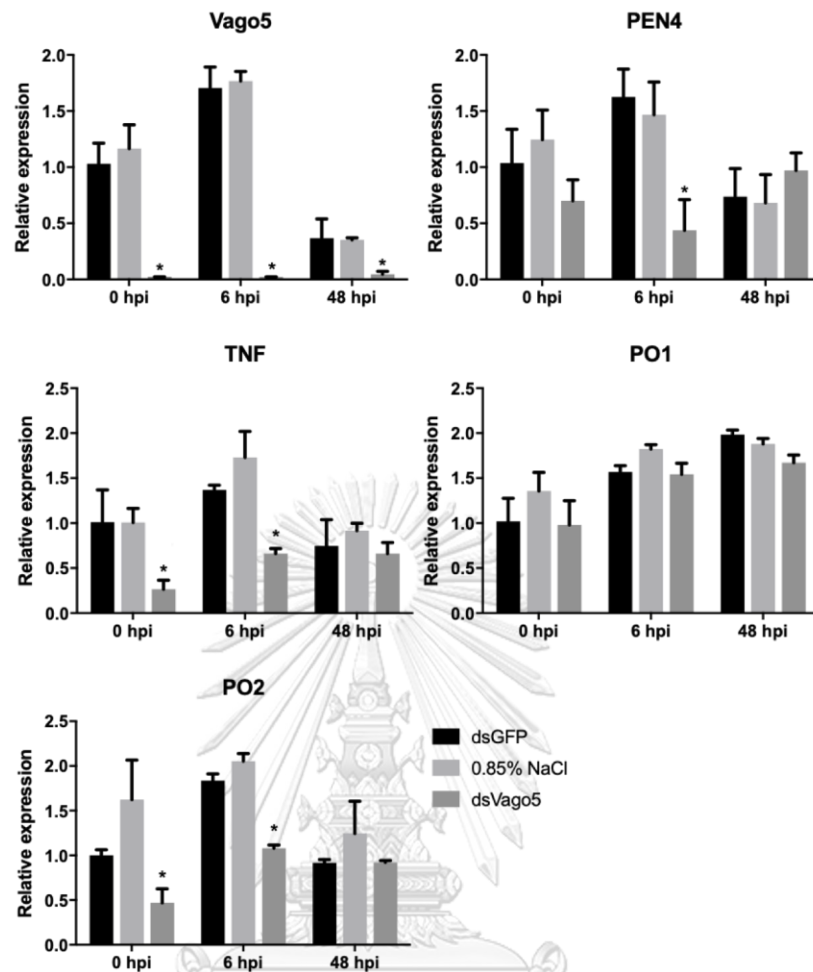


Figure 34 Expression analysis of *Vago5* and other shrimp immune-related genes in dsVago5, dsGFP, and 0.85% NaCl-injected shrimp challenged with VP_{AHPND}. The experiment was performed in triplicate. Data are presented as means \pm standard deviations. Asterisks indicate significant differences between the data of dsGFP-injected shrimp at each time point post challenge ($P < 0.05$).

2.4 Discussions

2.4.1 Identification of genes in response to *Vibrio parahaemolyticus* AHPND (VP_{AHPND}) infection by suppression subtractive hybridization (SSH).

AHPND, is known to be caused by VP_{AHPND}, which accumulates in the stomach and secretes PirA/B in the hepatopancreas (Lai et al., 2015). The mechanism by which AHPND kills shrimp is currently unclear but recent data demonstrated that genes of Toll and IMD pathways and their downstream antimicrobial peptides (AMPs) are suppressed in the stomach as well as the hemocytes but overexpressed in the hepatopancreas (Yeh et al., 2016). This suggests that while the stomach and hepatopancreas are major AHPND targets, the hemocytes, being the major immune organs of shrimp (Leu et al., 2011), may also give informative clues to the immune mechanisms to AHPND. This study reports the differentially-expressed genes identified from VP_{AHPND} infected *P. vannamei* hepatopancreas and hemocyte by suppression subtractive hybridization. They could be categorized into 9 groups based on their function. Of those, immune-related genes such as *hemocyanin*, *caspase 4*, *heat shock protein 90*, and *i-type lysozyme-like protein 1* have been identified in hepatopancreas whereas *Vago5* and *kunitz proteinase inhibitor* have been identified in hemocyte. This data provides information on how shrimp response to VP_{AHPND} infection. Like what we reported here, in *Macrobrachium rosenbergii* hepatopancreas VP_{AHPND} infection could activate genes that have function in immune defense such as *hemocyanin*, *arginine kinase*, *anti-lipopolysaccharide factor*, *apoptosis inhibitor*, *caspase*, *heat shock protein 21*, *lectin 1*, and *NF-kappa B inhibitor alpha* (Rao et al., 2015).

Generally, caspase is a key player in apoptosis (Fiandalo and Kyprianou , 2012). Five caspase genes have been reported in Penaeid shrimp and are extremely sensitive to WSSV infection (Leu et al., 2013). In *P. vannamei*, only *Lvcaspase-3* and *-4* were up-regulated upon WSSV and *V. alginolyticus* infections (Wang et al., 2008). However, caspase-3 from *P. vannamei* was activated by *Vibrio alginolyticus* infection to inactivate anti-apoptotic proteins, such as NF-κB or MAP-kinases, or to upregulate the endogenous receptor/ligand system, that induces apoptosis, on the surface of

infected cells (Chang et al., 2008). In our study, *Lvcaspase 4* was highly expressed in shrimp hepatopancreas upon VP_{AHPND} infection at 48 h (hpi).

Heat shock protein (HSP) is a protein family that is known to play role in protective mechanisms that animals developed in response to the stresses (Qian et al., 2012). In *P. vannamei*, up-regulation of HSPs such as *HSP60*, *HSP70*, and *HSP90* in shrimp hemocyte correlated to enhancement of shrimp tolerance to VP_{AHPND} infection (Junprung et al., 2017). In our study, HSP90 was up-regulated upon VP_{AHPND} infection at 48 hpi.

Kunitz-type protease inhibitor (KuPI) is one of serine proteases inhibitor family that plays vital roles in biological processes, physiological process (i.e. blood clotting and fibrinolysis) and shrimp immune responses (Vargas-Albores and Villalpando, 2012). According to Hung et al., 2017, Kunitz-type protease inhibitor from kuruma shrimp *Marsupenaeus japonicus* was identified and characterized. It was found that *MjKuPI* was mainly expressed in hemocytes. The mRNA level of *MjKuPI* was up-regulated after *Vibrio penaeicida* and white spot syndrome virus (WSSV) infection. In this study, *KuPI* in hemocyte was up-regulated upon VP_{AHPND} infection at 3, 6 and 48 hpi.

Single von Willebrand factor type C or Vago has two main functions, as part of the response pathway to pathogenic infection and in nutritional regulation (Sheldon et al., 2007, Zinke et al., 2002). Previously, five Vagos were identified as the up-regulation of gene expression after WSSV infection (Chen et al., 2011). In our study, *Vago5* was highly expressed in shrimp hemocyte upon VP_{AHPND} infection at 3 and 6 hpi

In conclusions, SSH could identified differentially expressed genes upon VP_{AHPND} infection in both hepatopancreas and hemocyte which might play an important role in anti-VP_{AHPND} infection in shrimp.

2.4.2 Functional characterization of hemocyanin in response to *Vibrio parahaemolyticus* AHPND (VP_{AHPND}) infection.

Hemocyanin is a molecule which play a significant role in oxygen transportation, molting regulation, and pathogen non-specific immune defense

(Coates and Nairn, 2014). In *P. vannamei*, 6 hemocyanins including HMC, HMCL1, HMCL2, HMCL3, HMCL4 (Xu et al., 2015), and HMCV4 (Lu et al., 2015) were reported to be highly up-regulated after WSSV (Xu et al., 2015), and *V. harveyi* infection (Chang et al., 2016). Many researchers have reported that the expression levels of hemocyanin genes varied greatly after bacteria or viral challenge (Wang, et al., 2015; Qiu et al., 2014). From SSH library Hepatopancreas 3/6, 5 hemocyanin transcripts were found. *HMC* appeared to be highly expressed in the early phase of *V. parahaemolyticus* AHPND-infected *P. vannamei* hepatopancreas. This result suggested that *HMC* plays role in shrimp bacterial response. qRT-PCR results showed that each hemocyanin isoform expressions were varied after VP_{AHPND}. *HMC* was highly up-regulated at 3 hpi. Similar to SSH library, only *HMC* was highly expressed at early phase of VP_{AHPND} infection but all hemocyanin subunits were down-regulated at late phase of VP_{AHPND} infection. Previously, hemocyanin expression profiles in WSSV-resistant *P. vannamei* show that *HMCL1*, *HMCL2*, *HMCL3*, and *HMCL4* were up-regulated at early phase of WSSV infection. *HMCL1*, *HMCL2*, and *HMCL4* were down-regulated at early phase and all isoforms were late phase down-regulated during WSSV infection in WSSV- susceptible shrimp (Xu et al., 2015). It suggested that hemocyanin isoforms might not only play role in antiviral immunity but also involved in shrimp bacterial response.

In Chinese mitten crab (*Eriocheir sinensis*), hemocyanin subunit 1, 2, and 3 were up-regulated at early phase of endotoxin, LPS and PNG injection (Huang et al., 2014). VP_{AHPND} toxin, PirA and PirB, plays a critical role in producing the characteristic symptoms of AHPND (Lee et al., 2015). In this study, the direct effect of VP_{AHPND} toxin on the expression of hemocyanin genes was studied. The hemocyanin genes expression analysis showed that *HMCL3* and *HMCL4* were up-regulated at early phase of VP_{AHPND} toxin injection and all isoforms were down-regulated at late phase of VP_{AHPND} toxin injection. Our results indicate that the VP_{AHPND} toxin itself induced expression levels of some hemocyanin genes.

Hemocyanin has been reported to play a significant role in oxygen transportation and immune defense (Coates and Nairn, 2014). Previous studies showed that, apart from its primary function as a respiratory protein for many arthropods, hemocyanin could be functionally converted into a phenoloxidase-like

enzyme by different substances, which would allow it to act as an antiviral agent against various viruses or to generate reactive oxygen species (ROS) as an antimicrobial strategy (Decker et al., 2001; Jiang et al., 2007; Nagai et al., 2001; Zhang et al., 2004). In this study, hemocyanin was purified from *P. vannamei* hemolymph. The MS/MS analysis showed that HMC and HMCL1 were found. SDS-PAGE analysis showed that HMC is the most abundant hemocyanin isoform purified from hemolymph. As reported previously that hemocyanin could aggregate *Vibrio* species such as *V. parahaemolyticus*, *V. alginolyticus*, *V. anguillarum* and *V. fluvialis* in *P. vannamei* (Zhang et al., 2006). We demonstrated that hemocyanin purified from *P. vannamei* hemolymph induced *V. parahaemolyticus* AHPND agglutination. Additionally, hemocyanin-derived antibacterial peptides were demonstrated to have a broad range of antimicrobial activity and it could inhibit fungal, Gram-positive and Gram-negative bacterial growth (Lee et al., 2003, Qiu et al., 2014). We further explored the immunological activities of hemocyanin protein *in vivo*. The result showed that hemocyanin could reduce amount of VP_{AHPND} at certain time. In support of this inference, Xianliang Zhao et al. and Xin Lu et al. found that the recombinant peptides of hemocyanins from *P. vannamei* including HMCL1, HMCL3, and HMCL4 showed antimicrobial activity against *V. parahaemolyticus* (Lu et al., 2015; Zhao et al., 2016). These results indicated that hemocyanins might play a functional role in inhibition of VP_{AHPND} infection.

The structural analysis of VP_{AHPND} toxin shows that PirA corresponds to domain III of the *Bacillus thuringiensis* Cry toxin and PirB corresponds to domains I and II, which induces cell death by pore formation in shrimp hepatopancreas (Lee et al., 2015). Previously, Keyhole Limpet Hemocyanin (KLH) was used as an adjuvant for Shiga toxin B-subunit vaccine production in mice. The result showed that the recombinant Shiga toxin B-subunit conjugated with KLH could reduce the cytotoxicity of Shiga toxin B-subunit by neutralize the apoptogenic activity of Shiga toxin (Marcato et al., 2005). In this study, after shrimp was injected with hemocyanin-neutralized VP_{AHPND} toxin, the shrimp mortality was lower than the VP_{AHPND} toxin only. We propose that hemocyanin might be able to neutralize VP_{AHPND} toxin activity by reducing the cytotoxicity of VP_{AHPND} toxin in shrimp. To confirm the hemocyanin neutralizing activity on VP_{AHPND} toxin, the histology of shrimp hepatopancreas

challenged with VP_{AHPND} toxin and hemocyanin- neutralized VP_{AHPND} toxin were observed. The histology of shrimp challenged with hemocyanin-neutralized VP_{AHPND} toxin showed cells without AHPND signs and hepatopancreas damage whereas the histopathology of VP_{AHPND} toxin challenged shrimp showed a dramatic decrease hepatopancreas damage.

In conclusion, abundant hemocyanins upon VP_{AHPND} infection were found from SSH technique. Our results implied that hemocyanin is also responsible for immunity against VP_{AHPND} in shrimp. Not only the VP_{AHPND} agglutination activity of hemocyanin was demonstrated, its neutralizing activity on VP_{AHPND} toxin was firstly reported.

2.4.3 Functional characterization of *Vago5* gene in shrimp hemocyte in response to *Vibrio parahaemolyticus* AHPND (VP_{AHPND}) infection.

Vagos are the antiviral genes that could be induced by triggering a Dicer-2 signaling pathway (Deddouche et al., 2018). In *Culex pipiens*, CxVago might be a stable, secreted cytokine that stimulates an insect cell-specific antiviral response by activating the Jak-STAT pathway (Paradkar et al., 2012). According to Chen et al., 2011, five Vago genes including *Vago1*, *Vago2*, *Vago3*, *Vago4* and *Vago5* were identified and characterized in shrimp *P. vannamei*. It was found that *Vago1*, *Vago4* and *Vago5* were activated by LvDicer2 in shrimp hemocyte. The expression analysis showed that Vagos were up-regulated in immune responses against Poly(C-G) or WSSV challenge. Not only Vago-Dicer2 activation, interferon regulatory factor (IRF) could bind to the 5'-UTR of *Vago4* and *Vago5* and activate their transcription (Li et al., 2015). This suggesting that shrimp Vagos might function as an IFN-like molecule in shrimp and possess an IFN system-like antiviral mechanism.

From SSH library (Hemocyte 3/6), *Vago5* was found to be highly expressed in *P. vannamei* hemocyte at the early phase of *V. parahaemolyticus* AHPND-infection. This result suggested that *Vago5* plays a crucial role in shrimp bacterial response. The qRT-PCR results showed that the expression of the abundance genes identified by SSH-hemocyte libraries were varied after VP_{AHPND} infection. *Vago5* was highly up-regulated at 3 and 6 hpi. Similar to SSH library, only *HMC* was highly expressed at early phase of VP_{AHPND} infection. Previously, Lv*Vago5* was up-regulated after WSSV,

Poly (G-C) (Chen et al., 2011) and Poly (I-C) challenge (Li et al., 2015). Previously, knocking down of *Vago* gene in *Culex quinquefasciatus* resulted in the increase of viral number (Paradkar et al., 2012). In our study, it was found that *Vago5* transcript in circulating hemocyte cells was down-regulated after dsVago5 injection. The *Vago5* depletion in shrimp has lower shrimp survival rate and the increasing amount of bacterial in stomach and hepatopancreas was observed in dsVago5 challenged shrimp upon VP_{AHPND} infection. Taken together, the evidence suggests that *Vago5* gene might not only play role in antiviral immunity but also involved in shrimp bacterial response.

Previously, in *Manduca sexta*, the interferon-like protein could activate prophenoloxidase activating proteinase-1 (PAP-1) expression leading to activate prophenoloxidase system by binding on the interferon-stimulated response element (ISRE) (Zho et al., 2005). In our study, the expression analysis of shrimp immune-related genes upon dsVago5 injection revealed that prophenoloxidase 2 gene (PO2) was down-regulated after Vago5 gene depletion. This result suggested that Vago5 was up-regulated upon VP_{AHPND} challenge and might activate shrimp proPO system via PO2 gene up-regulation to fight against VP_{AHPND} infection.



CHAPTER III

Transcriptomic profiling and immune response against non-lethal heat shock (NLHS) of VP_{AHPND} infected shrimp

จุฬาลงกรณ์มหาวิทยาลัย
CHULALONGKORN UNIVERSITY

3.1 Introduction

The devastating effect of EMS or AHPND in the global shrimp industry was primarily caused by the lack of information regarding the disease and its causative agent during its first outbreak (Leaño et al., 2012). Understanding the fundamental concepts of the AHPND pathogenesis and how the shrimp immune system work during diseased conditions will lead to the development of efficient management strategies to prevent AHPND infection. Likewise, the information on the molecular mechanism of AHPND tolerance enhanced by chronic non-lethal heat stress (NLHS) can lead to platforms for development of AHPND-resistant shrimp either through marker-assisted selective breeding or transcriptome analyses at different rearing conditions.

It has been proven that heat shock proteins and other immune-related genes become upregulated after non-lethal heat shock, which facilitates some form of tolerance or resistance to *Vibrio spp* (Yik Sung et al., 2007 and Loc et al., 2013). Hsp70 transcript has been shown to increase in the hepatopancreas of Chinese shrimp *F. chinensis* after WSSV infection (Wang et al., 2006). More specifically, Hsp70 and Hsp90 mRNAs become up-regulated in the gills of black tiger shrimp *P. monodon* upon *V. harveyi* infection. LvHsp60 protein was significantly up-regulated in the gills,

hepatopancreas and hemocyte after bacterial challenge (Zhou et al., 2010). The conserved role of Hsps in shrimp is evidenced, which also highlights the presence of an organized system of resistance to *Vibrio* ssp. related to heat stress in shrimp and perhaps invertebrates in general.

miRNAs are small non-coding RNA molecules that play an important function in biological processes by RNA silencing and post-transcriptional regulation (Bartel, 2004). Biogenesis of miRNAs has been described. The primary transcripts (pri-miRNA) that contain hairpin loop domains are cut by the RNase III enzyme Drosha to a 60–70 nucleotide-long precursor miRNA (pre-miRNA). After pre-miRNA exported to the cytoplasm by Exportin-5, the RNase-III enzyme, Dicer produces miRNAs composed of 18-24 double-stranded oligonucleotides by cleavage pre-miRNAs. Specific interactions between the miRNA-RISC (miRISC) and mRNA targets involve binding between the “seed” region of the miRNA (typically nucleotides 2-8) and the complementary target sequence on the mRNA inducing mRNA degradation and translational repression (Azzam et al., 2012). Previously, the next generation sequencing was used to identify differentially miRNA expression from *P. vannamei* hemocyte upon VP_{AHPND} infection. Among them, they have been shown to have 222 target genes involved in biological function and shrimp immune-related genes such as proteinase inhibitor, apoptosis and heat shock protein (Zheng et al., 2018). Determined miRNA expression profiles in response to bacterial infections have revealed miRNAs as players in the host innate immune response thus, providing key evidence on the general role of miRNAs in immunity (Eulalio et al., 2012).

In this study, the functional role of miRNAs in immunity and stress survival is further explored by looking at the global expression of mRNA and miRNA

populations in the hemocyte of shrimp under NLHS condition. Global gene expression analysis by high-throughput sequencing has been proven successful in a lot of previously described shrimp transcriptome studies ¹⁷. This study, thus, aims to identify mRNAs and miRNAs and analyze their expression in the hemocyte of shrimp under NLHS condition using next-generation sequencing. The inferred relationships of the identified genes and miRNAs are expected to reveal important aspects of miRNA and their targets in relation to AHPND resistance/tolerance. This information will give valuable insights on the so-called heat stress-modulated immune pathway.

3.2 Materials

3.2.1 Chemicals, reagents, enzymes and kits

Luna[®] Universal qPCR Master Mix (NEB)

Phusion high-fidelity (HF) PCR master mix with HF buffer (NEB)

Thermo Scientific[™] RevertAid First Strand cDNA Synthesis Kit

3.2.2 Experimental shrimp, microorganisms, cells and viruses

Pacific white shrimp *Penaeus vannamei*

Vibrio parahaemolyticus (AHPND)

3.2.3 Software

BLAST[®] (<https://blast.ncbi.nlm.nih.gov/Blast.cgi>)

Clustal Omega (<https://www.ebi.ac.uk/Tools/mas/clustalo/>)

Galaxy instance (<https://usegalaxy.org/>)

Geneious R11 (Biomatters, Ltd)

GraphPad Prism 6 (GraphPad Software)

miRBase 22.1 (<http://www.mirbase.org/>)

RNAhybrid (<http://bibiserv.techfak.uni-bielefeld.de/rnahybrid/>)

3.2.4 Animal cultivation

Healthy *P. vannamei* shrimp weighing 2-5 g (for VP_{AHPND} challenge, RNAi injection, next generation sequencing (NGS), and non-lethal heat shock) were purchased from commercial farms in Samut Songkhram Province and Chachoengsao Province, Thailand. The shrimp were acclimatized in laboratory aquaria at 28 ± 4 °C with a salinity of 20 ppt for a minimum of 2 weeks prior to use in experiments.

3.2.5 Non-lethal heat shock (NLHS) of *P. vannamei*

After acclimatization in rearing tanks with an ambient temperature of 30 °C, a total of 24 shrimp per treatment were placed in tanks containing 38 °C 20 ppt sea water for 5 min once daily over 7 days. The shrimp were allowed a 3-day recovery period from chronic heat stress in their respective rearing tanks.

3.2.6 Single-stranded cDNA synthesis using the RevertAid First-strand cDNA Synthesis Kit (Thermo Fisher Scientific)

To analyze the expression profile of miRNA in shrimp hemocyte, the stem-loop RT primer was used in cDNA synthesis. As previously described, the DNase-treated total with small RNA (1 µg) was combined with 1 µl of 10 µM stem-loop RT primer (Table 8) in nuclease-free water for a final volume of 12 µl per reverse transcription reaction. The sample was heated at 65 °C for 5 min and then immediately chilled in ice water for at least 5 min. Then, 8 µl of the reverse transcription reaction mix, containing 4 µl of 5X reaction buffer, 2 µl of 10 mM dNTP mix, 1 µl of RiboLock RNase Inhibitor (20 U/µL), and 1 µl of RevertAid M-MuLV RT (200 U/µL), was added to the total RNA sample. The mixture was incubated in a temperature series of 42 °C for 60 min and 70 °C for 5 min. The cDNA was used to analyze the expression level of interested genes by qRT-PCR.

Table 8 Primer used for the first-strand cDNA synthesis of miRNAs

Primer name	Sequence
miR-D9-3p	GTTGGCTCTGGTGCAGGGTCCGAGGTATTCGCACCAGAGCCAACAGTGGGA
miR-4850_RT	GTTGGCTCTGGTGCAGGGTCCGAGGTATTCGCACCAGAGCCAACAAATGT
miR-8552c_RT	GTTGGCTCTGGTGCAGGGTCCGAGGTATTCGCACCAGAGCCAACCACTAT
miR-317_RT	GTTGGCTCTGGTGCAGGGTCCGAGGTATTCGCACCAGAGCCAACCTGAGAT
miR-92b-5p_RT	GTTGGCTCTGGTGCAGGGTCCGAGGTATTCGCACCAGAGCCAACAAGCAC
miR-6090_RT	GTTGGCTCTGGTGCAGGGTCCGAGGTATTCGCACCAGAGCCAACCTGGCCG
miR-2898_RT	GTTGGCTCTGGTGCAGGGTCCGAGGTATTCGCACCAGAGCCAACCTACCCC
miR-2169-3p_RT	GTTGGCTCTGGTGCAGGGTCCGAGGTATTCGCACCAGAGCCAACCCAGCT
miR-7170-5p_RT	GTTGGCTCTGGTGCAGGGTCCGAGGTATTCGCACCAGAGCCAACAGTCGG
miR-92a-3p_RT	GTTGGCTCTGGTGCAGGGTCCGAGGTATTCGCACCAGAGCCAACCTAAGG
miR-4901_RT	GTTGGCTCTGGTGCAGGGTCCGAGGTATTCGCACCAGAGCCAACGTTTGT
miR-184_RT	GTTGGCTCTGGTGCAGGGTCCGAGGTATTCGCACCAGAGCCAACCCCTTA
miR-61_RT	GTTGGCTCTGGTGCAGGGTCCGAGGTATTCGCACCAGAGCCAACAGATGA
U6-qRTR	TGGAACGCTTCACGATTTTGC

3.2.7 Small RNA library sequencing using the MiSeq instrument (Illumina)

3.2.7.1 Sample preparation

The hemocyte was collected at 0, 6, and 24 h post VP_{AHPND} infection in shrimp from both NLHS and normal condition treatments (described in Section 2.3). Total small RNA was isolated from hemocyte using the mirVana™ miRNA Isolation Kit (Ambion, Life Technologies) following the manufacturer's protocol. Briefly, the hemocyte free of hemolymph was immediately added by lysis/binding buffer to a min. 1:10 ratio (w/v, added 1 ml lysis/binding buffer per 0.1 g hemocyte). After homogenization, 1/10 of the miRNA homogenate additive volume was added to hemocyte homogenate and mixed well by inversion several times, and then kept on ice for 10 min. Thereafter, organic extraction was performed by adding an equal volume of acid-phenol. Then, the chloroform was added to the homogenate followed by 1/10 of the miRNA homogenate additive volume being added to the mixture and being vigorously shaken for 30-60 sec. The mixture was centrifuged at 13,500 x g for 15 min at room temperature to separate the aqueous and organic phases. After centrifugation, the upper aqueous phase was transferred to a fresh 1.5 ml microcentrifuge tube without disturbing the lower organic phase.

For total small RNA extraction, 1/3 of the absolute ethanol volume was added to the aqueous phase and mixed thoroughly by inversion several times. The lysate/ethanol mixture was applied to a filter cartridge and centrifuged at 10,000 x g for 15 sec. After centrifugation, 2/3 of the absolute ethanol volume was added to the filtrate (266 μ l absolute ethanol for 400 μ l filtrate) and mixed thoroughly by inversion.

On the other hand, for total large RNA extraction, 1.25 volume of absolute ethanol was added to the aqueous phase (instead of 1/3 volume of absolute ethanol) and mixed by inversion. Both total small RNA and total RNA (from the previous step) plus 700 μ l of filtrate/ethanol mixture was passed through the new filter cartridge by centrifugation at 10,000 x g for 15 sec. The flow-through was discarded. Then, 700 μ l of miRNA wash solution 1 was added and centrifuged at 10,000 x g for 10 sec, with the flow-through being discarded. The filter was washed twice with 500 μ l of wash solution 2/3 with the flow-through discarded. The residual fluid was removed from the filter by centrifugation at 10,000 x g for 1 minute. The filter cartridge was then placed into a fresh collection tube. Then, 50 μ l of pre-heated (95 °C) elution solution was applied to the center of the filter and centrifuged at 10,000 x g for 1 minute. The eluate was applied again to the filter to maximize RNA recovery and then stored at -80 °C until use. The quality and quantity of RNA were determined using spectrophotometric denaturing polyacrylamide electrophoresis and the Agilent 2100 Bioanalyzer.

3.2.7.2 Small RNA library preparation and sequencing

In order to perform NGS of small RNA, cDNA libraries of small RNA from VP_{AHPND}-infected hemocyte under NLHS and NH at 0, 6, and 24 hpi were constructed using the TruSeq® Small RNA Sample Preparation Kit (Illumina) following 3' and 5' adapter ligation, reverse transcription, PCR amplification, and gel purification (Figure 35). Each small RNA library was separated by index sequence in the PCR amplification step. A 10 μ g of total small RNA in a total volume of 5 μ l was used. The 3' adapter ligation was performed by mixing 1 μ l of RNA 3' adapter (RA3) and 5 μ l of total RNA or total small RNA in a precooled nuclease-free 200 μ l PCR tube.

The reaction was then incubated in the thermal cycler at 70 °C for 2 min and immediately placed on ice. The master mix of 3' adapter ligation contained 2 µl of ligation buffer (HML), 1 µl of RNase inhibitor, and 1 µl of T4 RNA ligase 2 deletion mutant (Epicentre). Then, 4 µl of master mix was added into the reaction tube and incubated at 28 °C for 15 min. After this step, 5' adapter was prepared by pre-heating 1.1 µl of RNA 5' adapter (RA5) at 70 °C for 2 min and then immediately chilling the solution on ice, followed by 1.1 µl of 10 mM ATP and 1.1 µl of T4 RNA ligase being added to the heated RNA 5' adapter. To ligate the 5' adapter to small RNA, a mixture including RNA 5' adapter (3 µl) was added to 3' adapter ligation reaction and incubated at 28 °C for 1 hour. The 5' and 3' adapter-ligated RNA were stored at -80 °C.

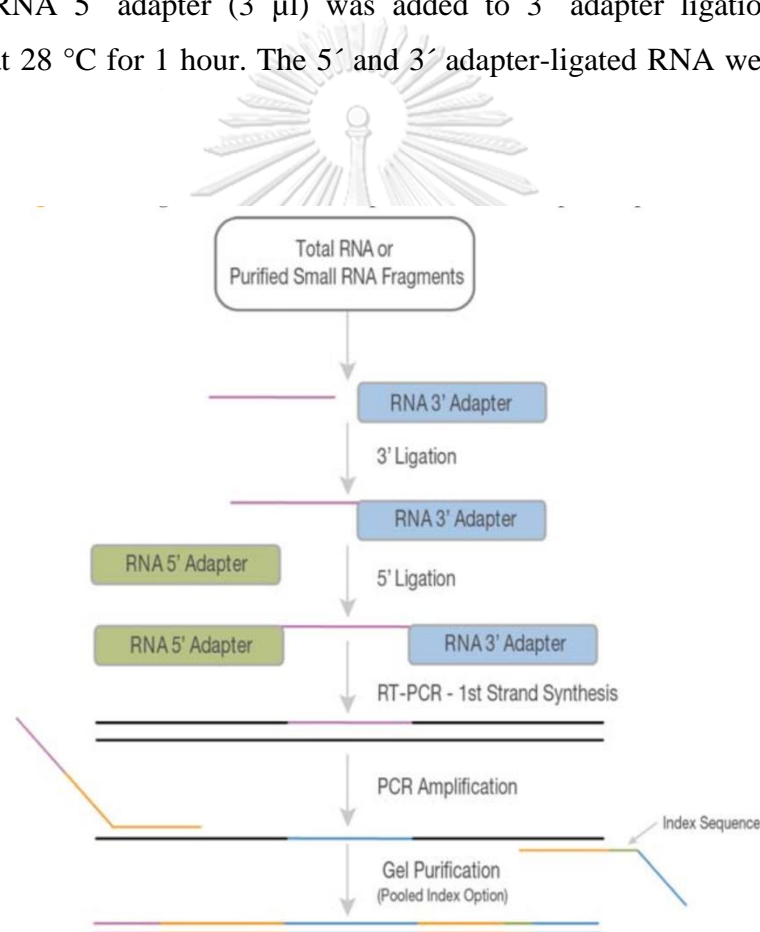


Figure 35 Small RNA library preparation workflow using the TruSeq® Small RNA Sample Preparation Kit.

Reverse transcription was performed by mixing 6 µl of 5' and 3' adapter-ligated RNA with 1 µl of RNA RT primer, followed by incubation at 70 °C for 2 min,

and then immediate placement on ice. The reverse transcription reaction contained 2 μ l of 5X first-strand buffer, 0.5 μ l of 12.5 mM dNTP mix, 1 μ l of 100 mM DTT, 1 μ l of RNase inhibitor, and 1 μ l of SuperScript III reverse transcriptase. Then, the reaction was incubated at 50 °C for 1 hour. In this step, the cDNA library was amplified by PCR in order to increase the copy number of the cDNA library to the appropriate amount as well as to index each library with a specific PCR primer (RIPX). RIPX contains unique sequences that help discriminate samples in pooled cDNA libraries. Each cDNA library was amplified by PCR. The PCR master mix (37.5 μ l), which contained 8.5 μ l of ultrapure water, 25 μ l of PCR mix (PML), 2 μ l of RNA PCR primer (RP1), and 2 μ l of RNA PCR primer (RPIX), was added to the aforementioned transcription reaction. The following PCR conditions were set on the thermal cycler: pre-heat lid to 100 °C, 98 °C for 30 sec, 15 cycles of 98 °C for 10 sec, 60 °C for 30 sec, 72 °C for 15 sec, 72 °C for 10 min, and 4 °C hold. The amplified cDNA libraries were stored at -20 °C until use. To purify the cDNA of corresponding mature miRNA, the PCR product was separated by 6% polyacrylamide gel electrophoresis (PAGE) in 1X TBE buffer (Tris-Borate-EDTA). The RNA ladders used for size selection were prepared by mixing 2 μ l of custom RNA ladder and 1 μ l of high-resolution ladder with 2 μ l and 1 μ l of DNA loading dye, respectively. All amplified cDNA was mixed with 10 μ l of DNA loading dye. After this step, 2 μ l of custom RNA ladder mixture and high-resolution ladder were loaded on the 6% PAGE gel into the wells flanking the samples. The gel was run for 60 min at 145 volts or until the blue front dye exited the gel. The gel was stained with 0.5 μ g/ml ethidium bromide for 2-3 min and viewed under a UV transilluminator. Then, cDNA sized between 145 and 160 bp was cut and placed into a 0.5 ml gel breaker tube. The first expected product of 147 bp was mature miRNA (approximately 22 nucleotides) ligated with 5' and 3' adapters (125 nucleotides). The second had an expected size of 157 bp and was mature miRNA with other regulatory small RNA molecules (approximately 32 nucleotides)-called piwi-interacting RNAs—ligated to the 5' and 3' adapters (125 nucleotides). Then, the gel breaker tube containing pieces of gel was centrifuged at 20,000 x g for 2 min. The small RNA library was eluted by 30-100 μ l of sterile water with shaking at room temperature overnight and transferred to the top

of a 5 µm filter and centrifuged for 10 sec at 600 x g. The small RNA library was concentrated using a vacuum concentrator and stored at -80 °C.

For NGS on MiSeq, an equal amount (2nM) of each small RNA library was mixed and denatured following the MiSeq sequencing protocol. First, 0.2 N fresh NaOH was prepared from 1.0 N NaOH stock. Then, 10 µl of 0.2 N NaOH was mixed with 10 µl of 2 nM pooled small RNA library from NLHS-VP at 0, 6, and 24 hpi and NH-VP at 0 and 6 hpi and vigorously vortexed. The mixture was incubated at room temperature for 5 min to denature the small RNA library to single-stranded DNA. After this step, 20 µl of the denatured small RNA library was combined with 980 µl of pre-chilled HT1 to make a final 20 pM concentration of the denatured small RNA library. The 20 pM denatured small RNA library was diluted to 7.5 pM in pre-chilled HT1, which—at a final volume of 1 ml—was immediately placed on ice. Then, the 1 ml of 7.5 pM denatured small RNA library was loaded into the MiSeq reagent cartridge. The flow cell and reagent bottle were put into the MiSeq machine before loading the sample-loaded cartridge, and the machine and program were started. PhiX control library, an adapter-ligated library, was used as a control for Illumina sequencing. It was recommended to combine the PhiX library with a small RNA library at 1% for most libraries, 5% for low diversity libraries, and $\geq 25\%$ for older versions of MiSeq software. In this study, 7.5% of the PhiX library was added to the pooled small RNA library.

3.2.7.3 Small RNA library preparation

After the small RNA libraries were sequenced using the MiSeq instrument, data was obtained in FASTQ format, which contained both nucleotide sequences and their corresponding quality scores. The 5'- and 3'-adapter trimming and quality control of raw reads were performed using tools in a Galaxy instance (<https://usegalaxy.org/>). High quality small RNA sequences with lengths shorter than 18 nucleotides and longer than 24 nucleotides were removed. A homology search of contaminating RNA (e.g. mRNA, rRNA, and tRNA) was conducted using BLASTn against the NCBI nucleotide and Rfam database. After discarding contaminating

RNA, remaining sequences were searched against miRBase 22.1 (<http://www.mirbase.org/>) in order to identify known miRNA homologs (Figure 36).

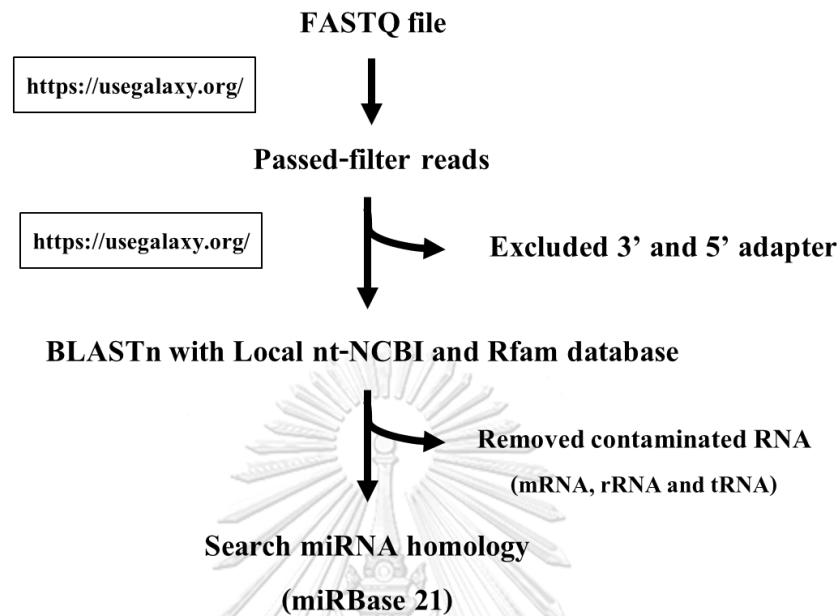


Figure 36 Small RNA data analysis workflow.

3.2.7.4 Stem-loop quantitative Real-time PCR analysis

The miRNAs of interest consisted of lva-miR-7170-5p, lva-miR-2169-3p, lva-miR-184, lva-miR-92b-5p, lva-miR-317, lva-miR-92a-3p, lva-miR-4901, lva-miR-61, lva-miR-2898, and lva-miR-6090, which were selected for expression analysis using stem-loop qRT-PCR. Pooled total small RNA from both VP_{AHPND}-infected, NLHS-treated, and control shrimp hemocyte at 0, 6, and 24 hpi was prepared using the mirVana miRNA Isolation Kit (Ambion, Life technologies). Extracted total small RNA was then used as a template for first-strand stem-loop cDNA synthesis. The stem-loop primer (Table 9) (CDS-3M primer: 5'-AAGCAGTGGTATCAACGCAGAGTGGCCGAGGCGGCCTTTTTTTTTTTTTTTT TTTTTVN-3') was used to synthesize first-strand cDNA using the RevertAid First-strand cDNA Synthesis Kit (Thermo Fisher Scientific). U6 gene expression was used as internal control. Stem-loop qRT-PCR was performed using an appropriate amount of cDNA for each gene, specific oligonucleotide primers (Table 2.5), and QPCR

Green Master Mix (Biotechrabbit) in the MiniOpticon™ Real-time PCR System (Bio-Rad) under the following conditions: 95 °C for 3 min, 40 cycles of 95 °C for 30 s, 60 °C for 30 s, and 72 °C for 30 s. Relative expression was calculated and data were analyzed using a paired-samples t-test, with data being presented as mean ± standard deviation. Statistical significance was considered at $P < 0.05$. The experiment was performed in triplicate.



Table 9 Primers used for qRT-PCR in stem-loop qRT-PCR

miRNA name	Primer name	Sequence
lva-miR-61	miR-61-F	GGGGTGA CTAGACTCTTAC
	miR-61_RT	GTTGGCTCTGGTGCAGGGTCCGAGGTATTCGCACCAGAGCCAACAGATGA
lva-miR-184	miR-184-F	GTTGTGGACGGAGAACTGA
	miR-184_RT	GTTGGCTCTGGTGCAGGGTCCGAGGTATTCGCACCAGAGCCAACCCCTTA
lva-miR-4901	miR-4901-F	GTTGGGGTA ACTTATTTTGG
	miR-4901_RT	GTTGGCTCTGGTGCAGGGTCCGAGGTATTCGCACCAGAGCCAACGTTGT
lva-miR-92a-3p	miR-92a-3p-F	GTTTTCGTCTCGTGTCTCG
	miR-92a-3p_RT	GTTGGCTCTGGTGCAGGGTCCGAGGTATTCGCACCAGAGCCAACCTAAGG
lva-miR-7170-5p	miR-7170-5p-F	GTTGAACTGGAGGCCGAA
	miR-7170-5p_RT	GTTGGCTCTGGTGCAGGGTCCGAGGTATTCGCACCAGAGCCAACAGTCCG
lva-miR-317	miR-317-F	GTTGAACACAGCTGGTGGT
	miR-317_RT	GTTGGCTCTGGTGCAGGGTCCGAGGTATTCGCACCAGAGCCA ACTGAGAT
lva-miR-92b-5p	miR-92b-5p-F	TTGTGGGGACGAGAAGCG
	miR-92b-5p_RT	GTTGGCTCTGGTGCAGGGTCCGAGGTATTCGCACCAGAGCCAACAAGCAC
lva-miR-2169-3p	miR-2169-3p-F	GTTTGATTTAAAGTGGTACGCG
	miR-2169-3p_RT	GTTGGCTCTGGTGCAGGGTCCGAGGTATTCGCACCAGAGCCAACCCAGCT
lva-miR-2898	miR-2898-F	TTGGGGTGGTGGAGATGC
	miR-2898_RT	GTTGGCTCTGGTGCAGGGTCCGAGGTATTCGCACCAGAGCCA ACTACCCC
lva-miR-6090	miR-6090-F	TTGTTGACTGGGCGAGG
	miR-6090_RT	GTTGGCTCTGGTGCAGGGTCCGAGGTATTCGCACCAGAGCCA ACTGGCCG
Universal primer		GTGCAGGGTCCGAGGT
U6	U6-qRTF	GTACTTGCTTCGGCAGTACATATAC
	U6-qRTR	TGGAACGCTTCACGATTTTGC

3.2.7.5 miRNA target prediction

The miRNA targets were identified by comparing with transcriptome data using CU-mir software that was previously developed by our research group (Kaewkascholkul et al., 2016) This software searched for locations on mRNA targets that seed sequences (2-8 nucleotides from 5' end) of miRNA and can bind with perfect complementary or 1 mismatch at identified seed sequences. Percent

complementary is calculated from the number of nucleotides that perfectly match the target mRNAs per total length of miRNA sequences. The percent complementarity cutoff was set at 55%. RNAhybrid (<http://bibiserv.techfak.uni-bielefeld.de/rnahybrid/>) was also used to predict genes targeted by miRNAs with the parameters of free energy < -15.0 kcal/mol (Kaewkascholkul et al., 2016).

3.2.7.6 miRNA/mRNA interaction network analysis

In order to define all possible miRNA-mRNA interactions involved in a specific dataset of immune-related genes, a miRNA-mRNA interaction network was constructed. Immune responsive genes from the transcriptome were specifically chosen for inclusion in the integrated analysis of the miRNA/mRNA network. The differentially expressed miRNAs from shrimp challenged with VP_{AHPND} under NLHS were used to identify mRNA targets and to construct the miRNA/mRNA network. Again, the binding of target mRNAs of differentially expressed miRNAs were predicted using RNAhybrid with the parameters of free energy < -15 kcal/mol. These target mRNAs were mapped against our RNA-Seq data to determine their immune-related functions.

3.3 Results

3.3.1 Effect of NLHS on shrimp survival upon VP_{AHPND} challenge

We have confirmed that treating shrimp with NLHS prior to VP_{AHPND} infection resulted in a significantly higher survival rate than the control, as previously demonstrated by Jungprung et al. (2017). This survival challenge experiment was set up by dividing shrimp into four groups of no treatment control (NH), NLHS control (NLHS), VP_{AHPND} challenge (NH-VP), and NLHS plus VP_{AHPND} challenge (NLHS-VP) (Figure 3.22). For each NLHS treatment, shrimp were placed in tanks with a temperature of 38 °C for 5 min daily for 7 days and allowed to recover in control tanks without any disturbance for 3 days. No mortality was observed until the end of the experiment in treatments without any VP_{AHPND} challenge. The observed survival rates were significantly different between NH-VP (24.53%) and NLHS-VP (58.33%) groups based on a Log-rank test, thereby indicating a possible modulation of the shrimp immune system to tolerate/fight against mortality related to bacterial infection (Figure 37).

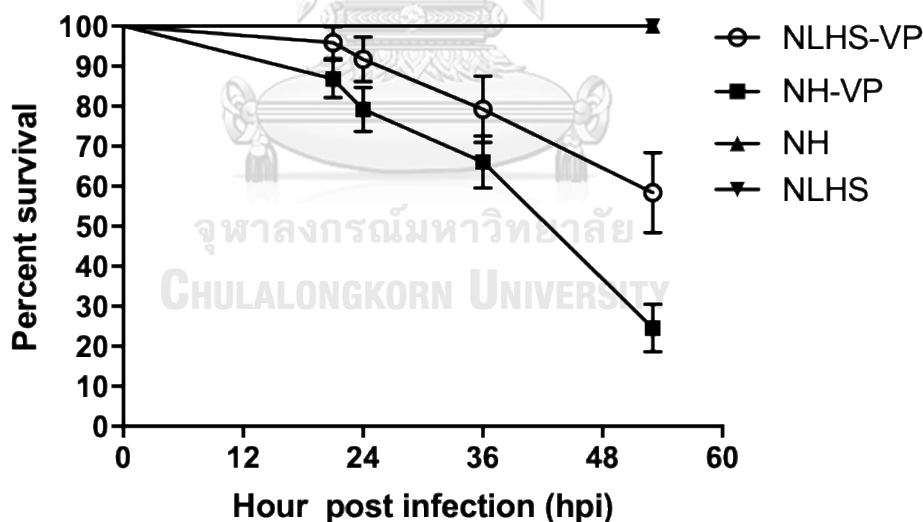


Figure 37 Effect of chronic heat stress on the survival of AHPND-challenged shrimp. The final observation of survival was performed at 53 h post immersion. All experiments were performed in triplicate. Survival percentage was calculated as mean \pm 1 S.E. at each time point.

3.3.2 Total small RNA preparation

Total small RNA was extracted from *P. vannamei* hemocyte of NLHS-VP and NH-VP at 0, 6, and 24 hpi using the mirVana™ miRNA Isolation Kit. The quality of total RNA and total small RNA sample were subsequently verified. The A_{260}/A_{280} ratio of the total RNA samples was 1.8-2.0, which was the expected ratio for acceptable RNA quality. The total small RNA samples were examined by electrophoresis on a denaturing acrylamide gel. The majority of bands are small RNAs whose sizes are below 500 nucleotides (Figure 38)

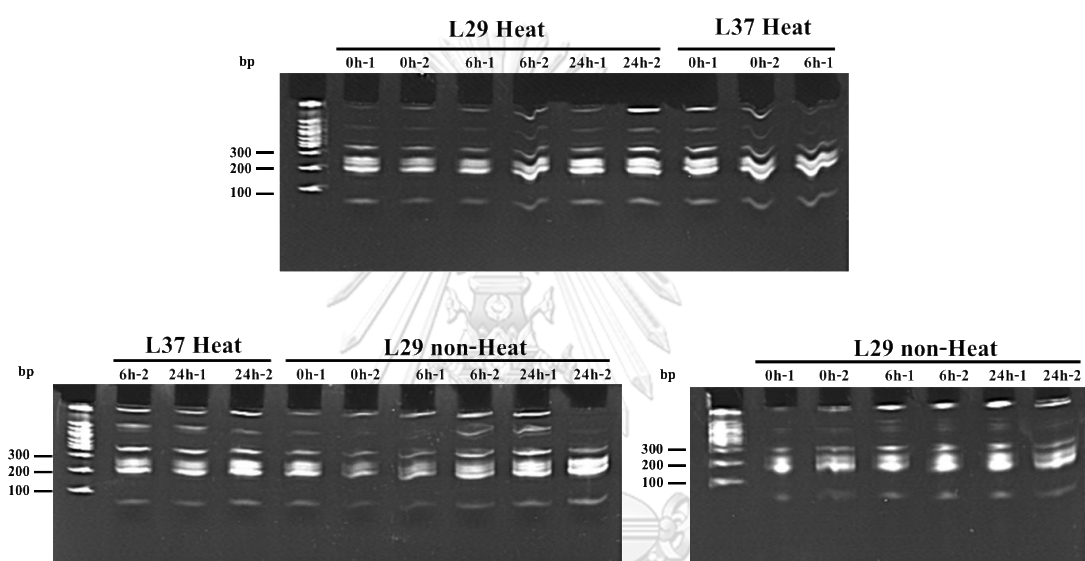


Figure 38 Verification of total small RNA quality by denaturing 15% acrylamide gel. The total small from 30 shrimp hemocyte upon VP_{AHPND} challenge under non-lethal heat shock (NLHS-VP) and normal conditions (NH-VP) was extracted and pooled per each lane. L29 and L37 represent shrimp family, Heat represents NLHS-VP, non-Heat represents NH-VP.

3.3.3 Sequence analysis of shrimp miRNAs

The global analysis of miRNA expression was used to determine regulators that may be associated with the observed gene expression. To achieve this, we analyzed miRNAs expressed in shrimp that were subjected to NLHS and VP_{AHPND} infection by sequencing them at various sampling times (0, 6, and 24 hpi for NLHS-VP and 0 and 6 hpi for NH-VP). High-throughput sequencing generated total raw reads of 5,264,595, including 1,086,629 in 0 NLHS-VP, 879,272 in 6 NLHS-VP, 1,114,328 in 24 NLHS-VP, 931,638 in 0 NH-VP, and 1,252,728 in 6 NH-VP. High

quality sequences that passed initial quality filters included 4,597,349 reads for all of the experimental group libraries. The results of analyses suggest that the majority of non-redundant sequences were composed of 20-22 nucleotides (nt) (Figure 39). Searching against the NCBI nucleotide database demonstrated that, on average, 25% of the sequences were likely contaminating RNAs (Figure 40). Following the removal of these contaminating mRNA, rRNA, and tRNA homologs, a final count of sequences resulted in a total of 78,000 sequences-77,415 of which were mappable to miRBase 22.1. The percentage of matched mature miRNA sequences for 0 hpi libraries was 93.86%, 93.93%, and 94.19%, respectively, for the 6 hpi and 24 hpi libraries. Sequences with unknown identities and homologs were listed (Table 10). A total of 41 miRNA homologs were identified from the NLHS-VP experimental group (Table 11), whereas 19 miRNA homologs were identified from the NH-VP experimental group (Table 12).

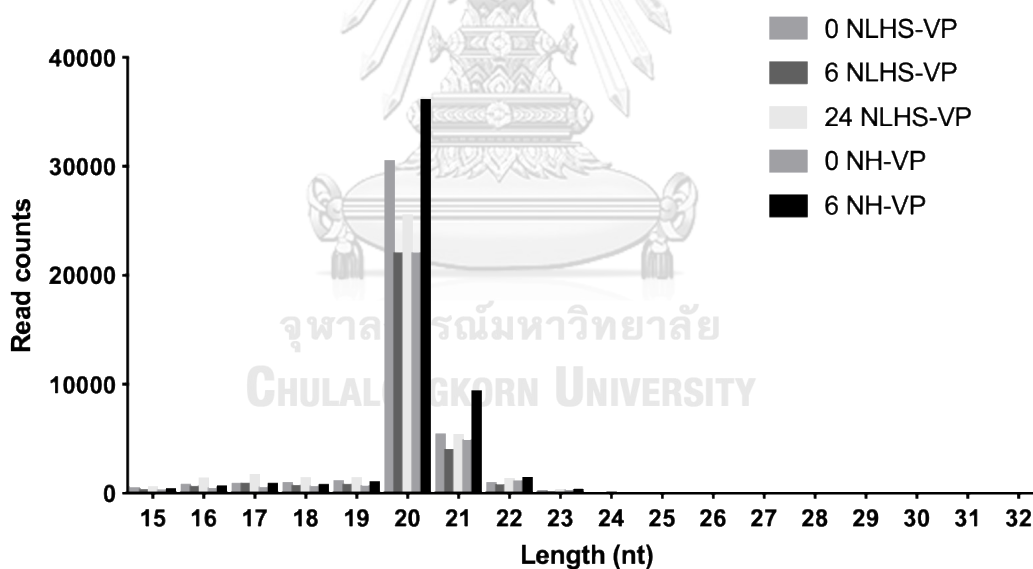


Figure 39 Length distribution and abundance of small RNAs in the small RNA libraries of 0 NLHS-VP, 6 NLHS-VP, 24 NLHS-VP, 0 NH-VP, and 6 NH-VP.

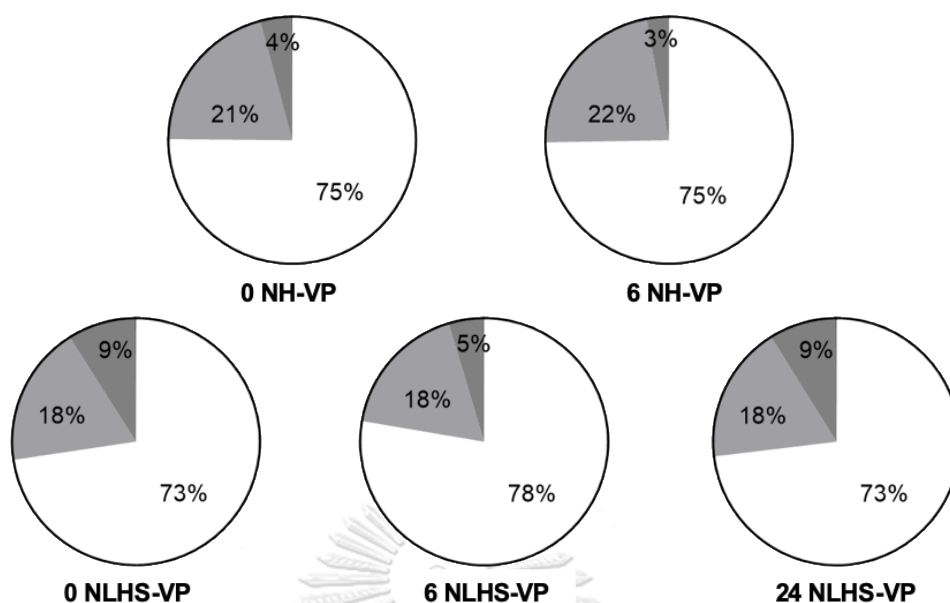


Figure 40 Composition of small RNAs in the small RNA NGS libraries.

Table 10 Summary of sequences identified from the small RNA libraries of *P. vannamei* hemocyte in the NLHS-VP condition at 0, 6, and 24 hpi, and in the NH-VP condition at 0 and 6 hpi

	Number of reads				
	NLHS-VP			NH-VP	
	0 NLHS-VP	6 NLHS-VP	24 NLHS-VP	0 NH-VP	6 NH-VP
Raw reads	1,086,629	879,272	1,114,328	931,638	1,252,728
Passed-filter reads	948,089	771,799	956,249	817,019	1,104,193
Trimmed 3' and 5' adapter	42,585	31,300	40,470	31,806	52,321
Size selection	39,874	29,009	36,134	30,117	49,815
Contaminating RNA	10,814	6,475	9,728	7,519	12,592
Mature microRNA homolog	29,060	22,534	26,406	22,598	37,223
pre-miRNA homolog	1,764	1,293	1,342	1,091	1,396
Unknown small RNA	136	162	287	103	156

Table 11 Nucleotide sequences of differentially expressed miRNA homologs identified in NLHS-VP-infected *P. vannamei* hemocytes.

miRNA name	Sequence	log ₂ (Fold change normalize with 0 NLHS-VP)	
		6/0 NLHS-VP	24/0 NLHS-VP
lva-miR-92b-5p	GGACGAGAAGCGGUGCUU	-2.86	
lva-miR8599	UUCUCGAGUUCUAACCUCAGCG	-2.45	-2.22
lva-miR9567-5p	AUUCAGAUUAUAGUUUGCC	-1.45	-2.22
lva-miR-7427-5p	AGAAACGCGGCACAGAAU	-1.45	-1.80
lva-miR-3689c	GGAGGUGUGAUAGCCUAGUG		-1.63
lva-miR9021-5p	UUUCAGAUUCUUCAUUGU		-1.63
lva-miR-2898	UGGUGGAGAUGCGGGGUA	-1.00	0.58
lva-miR-4850	AUAACAUGACUGAAAACAUUU	1.00	0.61
lva-miR-61	UGACUAGACUCUACUCAUCU	0.62	0.92
lva-miR-184	UGGACGGAGAACUGAUAAGGG		1.26
lva-miR-7373b-3p	GAGCUGCCAAUGAAGGGCU		1.54
lva-miR-2847	GUUGUCAGUCCGUUAU	1.14	1.69
lva-miR-9000	AAGCCCCAGUGGCGCAAUCG	1.36	1.78
lva-let-7-5p	UGAGGUAGUAGGUUGUAUAGUUU		1.95
lva-miR-9-3p	CAUACAGCUAGAUCACCAAAGA	1.14	1.95
lva-miR-2b	UAUCACAGCCACCUUGAUGAGCU	1.72	1.95
lva-miR-8415-3p	CGCGGCUAGACGGAAAGACC		2.37
lva-miR8552c	GGCCGUGAUCGUUAUGUG	1.88	2.48
lva-miR-13-3p	UAUCACAGCCUACUUGACGAGUU		2.69
lva-miR-305-3p	CGGCAUCUGUUGGAGUACAGUA		2.69
lva-miR-71	UGAAAGACAUGGGUAGUGAGAUGU	1.14	2.69
lva-miR-2a	UAUCACAGCCAGCUUGAUGAGCG		2.95
lva-miR-2525	UGCCUGGCGGCAAUAGCGAC	1.14	2.95
lva-miR-3826-3p	CCGUUCCCAUCGACUACGCCUU		3.17
lva-miR-2169-3p	AUUUAAAGUGGUACGCGAGCUGG	2.46	3.27
lva-miR-D9-3p	UUUCCAGAAUGUCCACU	1.14	3.54
lva-miR-6658-3p	GGCGGACGGGGGAACUAC		3.61
lva-miR-6090	GGACUGGGCGAGGGGCGGCCA	1.72	3.78
lva-miR-70	UGCCAACGACAUCUGGUGUUC		4.07
lva-miR6478	GGGAGAUUAGCUCAGUUG		4.07

miRNA name	Sequence	log ₂ (Fold change normalize with 0 NLHS-VP)	
		6/0 NLHS-VP	24/0 NLHS-VP
lva-miR-7278-5p	AAGGACUGGGCGAGGGGC		4.27
lva-miR-2238j-5p	UCGUCAGCUCCAUCCGCAAGG	3.72	4.37
lva-miR-7170-5p	AACUGGAGGACCGAACCGACU	2.46	4.39
lva-miR-6813-5p	GGUUUCAGGUUCUAUUUC	1.14	4.69
lva-miR-5395	GGCGAGCGAAAUUGGACUAGC		5.12
lva-miR-4901	UAACUUAUUUUUGGACAAAC		6.87
lva-miR-92a-3p	UCGUCUCGUGUCUCGGCCUAG	4.14	6.92
lva-miR319d-5p	UAUCAGUGAGAUUCUUCCUC	-2.18	
lva-miR-274-3p	CGGUGGCGAUCGCAACAG	-1.86	
lva-miR8623c	UCCCAUGGUGUCCAGCUAUA	-1.60	
lva-miR-317	UGAACACAGCUGGUGGUAUCUCA	-1.00	

Table 12 Nucleotide sequences of differentially expressed miRNA homologs identified in NH-VP-infected *P. vannamei* hemocytes

miRNA name	Sequence (5'-3')	log ₂ (Fold change 6/0 NH-VP)
lva-miR-2044-3p	GAAAAAUUAUCUUGAUAAGC	-4.2
lva-miR-71	UCUCACUACCUUGUCUUUCACG	-2.54
lva-miR-745-3p	GAGCUGCCCAAUGAAAGGCUG	-2.1
lva-miR-965	UAAGCGUAUGGCUUUUCCCU	-1.58
lva-miR-9000	AAGCCCCAGUGGCGCAAUCG	-1.32
lva-miR-100-5p	AACCCGUAGAUCCGAACUUGUG	-1.16
lva-miR-7427-5p	AGAAACGCGGCACAGAAU	-1.15
lva-miR-305	AUUGUACUUCAUCAGGUGCUCG	-1.12
lva-miR8552c	GGCCGUGAUCGUAUAGUG	-1.08
lva-miR-4850	AUAACAUGACUGAAAACAUUU	1.14
lva-miR7695-3p	CGAUUGUGCCACGGAGGCAU	1.14
lva-miR-2238j-5p	UCGUCAGCUCCAUCGCAAGG	1.26
lva-miR-5395	GGCGAGCGAAAUUGGACUAGC	1.26
lva-miR-2169-3p	AUUUAAAGUGGUACGCGAGCUGG	2.85
lva-miR-92a-3p	UCGUCUCGUGUCUCGGCCUAG	3.17
lva-miR-92b-5p	GGACGAGAAGCGGUGCUU	3.17
lva-miR-D9-3p	UUUCCAGAAUGUCCACU	3.79
lva-miR-7170-5p	AACUGGAGGACCGAACCGACU	4.22
lva-miR-4901	UAACUUAUUUUUGGACAAAC	5.96

CHULALONGKORN UNIVERSITY

3.3.4 Integrated analysis of miRNA and gene expression in the hemocytes of shrimp under the NLHS-VP condition

To investigate whether miRNA-gene interactions were involved in the enhancement of VP_{AHPND} tolerance in shrimp by NLHS, RNA-Seq data and small RNA NGS data were combined. The RNA-Seq analysis of shrimp hemocyte under NLHS-VP and NH-VP conditions at 0, 6, and 24 hpi were constructed by Dr. Benedict Arias Maralit (Unpublished data, Maralit et al.)

3.3.4.1 qRT-PCR validation of significant differentially expressed miRNAs (DEMs) and differentially expressed genes (DEGs)

In order to confirm the presence of the identified miRNAs and mRNAs as well as analyze the expression of *P. vannamei* miRNAs and mRNAs of interest in response to VP_{AHPND} infection under NLHS and control conditions, the expression profiles of 10 DEMs (lva-miR-7170-5p, lva-miR-2169-3p, lva-miR-184, lva-miR-92b-5p, lva-miR-317, lva-miR-92a-3p, lva-miR-4901, lva-miR-61, lva-miR-2898 and lva-miR-6090) and 8 DEGs identified from the NGS data (*Relish*, *Lipoprotein receptor*, *Dynamin*, *Importin7*, *Juvenile hormone epoxide hydroxylase 1*; *JHEH-1*, *DNAJ5*, *Prophenoloxidase 1*; *PO1* and *Prophenoloxidase 2*; *PO2*) were analyzed for their expression using qRT-PCR. In the NH-VP condition, *Relish* gene expression was significantly higher in all experimental groups compared to the respective controls. For the NLHS condition, *Dynamin* was up-regulated 2-fold at 6 hpi and down-regulated 2-fold at 24 hpi. The *lipoprotein receptor* was up-regulated at only 6 hpi by approximately 2-fold. *Importin7*, *JHEH-1*, *DNAJ5*, *PO1*, and *PO2* were significantly down-regulated by approximately 1.5- and 10-fold at 6 hpi and 24 hpi, respectively (Figure 41).

Meanwhile, the results of stem-loop qRT-PCR revealed that the expression levels of all 10 chosen DEMs were significantly differenced in shrimp hemocytes following VP_{AHPND} challenge under the NLHS condition by approximately 1.5- to 8-fold. For the NH-VP condition, only some of these DEMS exhibited significant changes in their expression levels; these include lva-miR-2898, lva-miR-2169-3p, lva-miR-7170-5p, and lva-miR-92b-5p, which were all up-regulated at 6 and 24 hpi by approximately 1.5- and 10-fold, respectively (Figure 42).

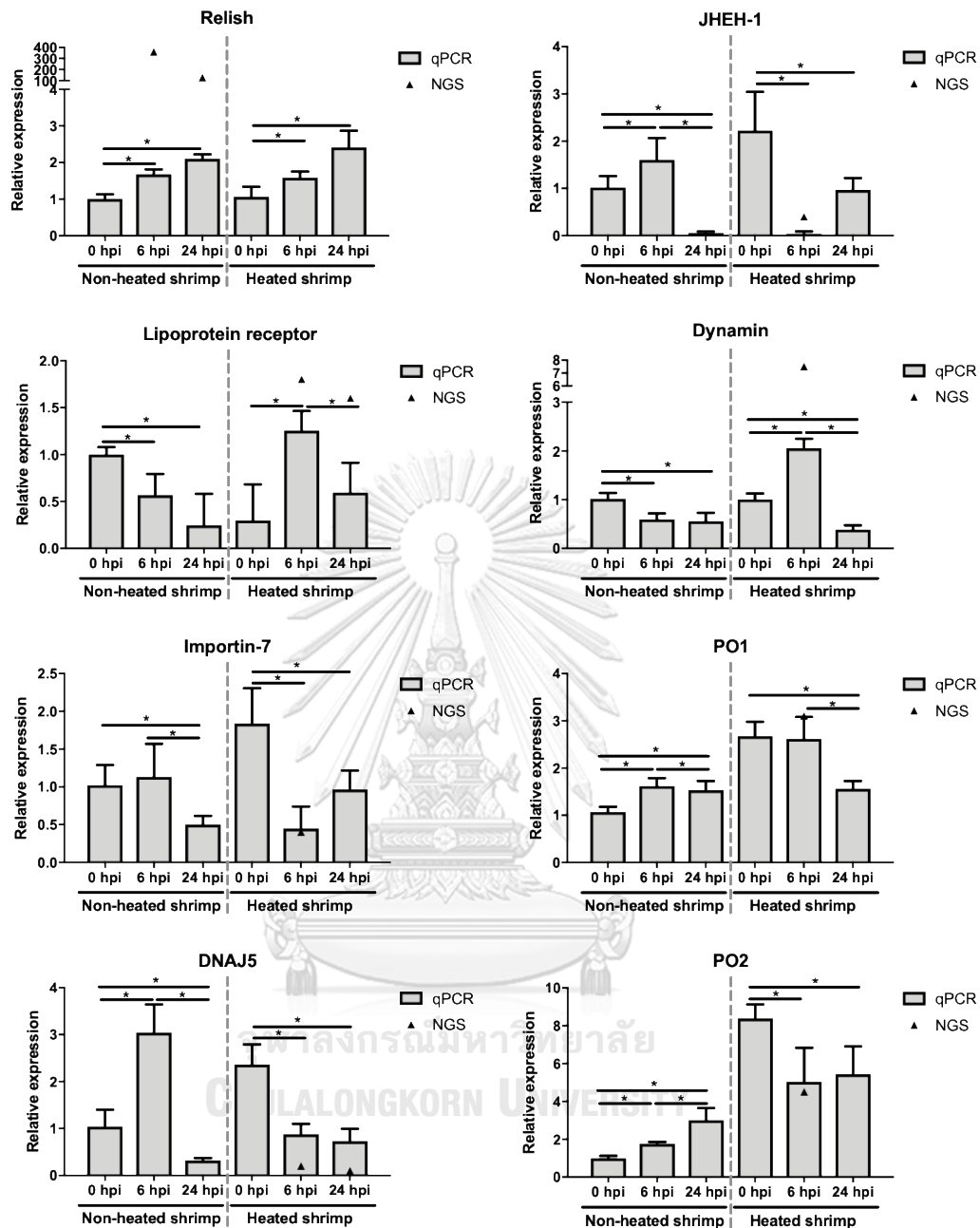


Figure 41 Validation of RNA-Seq using qRT-PCR

Eight genes (*Relish*, *Lipoprotein receptor*, *Dynamin*, *Importin7*, *Juvenile hormone epoxide hydroxylase 1*; *JHEH-1*, *DNAJ5*, *Prophenoloxidase 1*; *PO1* and *Prophenoloxidase 2*; *PO2*) were evaluated for their expression in shrimp hemocyte in response to VP_{AHPND} infection under NLHS and NH conditions. Total RNA from VP_{AHPND}-infected *P. vannamei* hemocyte at 0, 6 and 24 hpi under NH and NLHS conditions was used as template for cDNA synthesis. Relative expression levels of 8 transcripts were determined by qRT-PCR and standardized against EF-1 α , the internal reference. The relative expression ratio was calculated using the $2^{-\Delta\Delta CT}$ method. The bars are the data from qRT-PCR presented as means \pm standard deviations and the triangle marks (\blacktriangle) are the data from NGS. The experiment was done in triplicate. The expression level was calculated relative to that of the normal shrimp under NH

condition at 0 h after VP_{AHPND} challenge. Asterisks indicate significant difference ($P < 0.05$) from the respective VP_{AHPND} infected NH shrimp at 0 hpi.

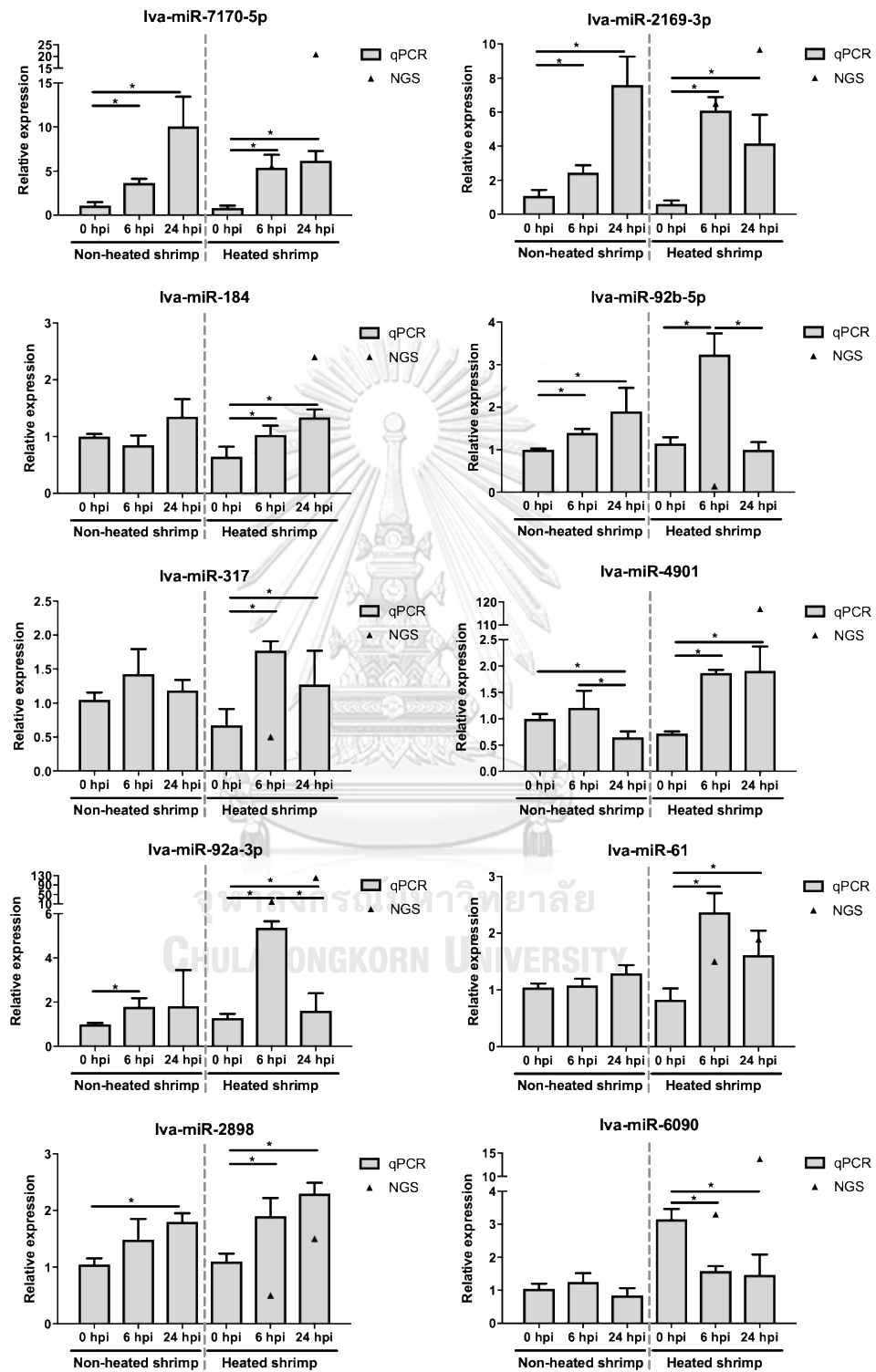


Figure 42 Relative expression analysis of miRNAs in response to VP_{AHPND} infection under heat and non-heat stress conditions. Total RNA from VP_{AHPND}-infected *P. vannamei* hemocyte under heat and non-heat stress conditions was used as a template

for specific stem-loop first-strand cDNA synthesis. The relative expression levels of 10 miRNAs were determined by qRT-PCR and standardized against U6 as the internal reference at 0, 6, and 24 hpi. The results were derived from triplicate experiments. Data are presented as means \pm standard deviations. Asterisks indicate significant differences at $P < 0.05$.

3.3.4.2 Correlation of DEMs and DEGs of shrimp in response to VP_{AHPND} infection under the heat stress condition

In order to analyze the interaction between miRNAs and their targets based on their differential expression profiles, the DEMs of NLHS-VP and NH-VP were combined. As with the expression profiles of the DEGs, Venn diagrams was used to highlight specific groupings of DEGs, such as NH-VP-responsive and NLHS-VP-responsive transcripts (Figure 43). A grouping composed of 2,664 DE transcripts was considered to represent NLHS-VP-responsive transcripts, while another grouping composed of 1,825 DE transcripts represented NH-VP-responsive transcripts. An intersection of 1,316 DE transcripts were considered both NH-VP- and NLHS-VP-responsive transcripts. Meanwhile, NLHS-VP-responsive transcripts were annotated using the NCBI GenBank database through BLASTX and mapped against available shrimp transcript databases to identify immune-related genes. Some identified immune-related genes include: prophenoloxidase1 (*PO1*) and prophenoloxidase2 (*PO2*) in the proPO system, ALF-AAK, *Penaeidin 4a*, and *AMP type2* in the AMP production system, and *transglutaminase* and *apoptosis inhibitor* in hemocyte homeostasis—all of which were up-regulated upon NLHS-VP. On the other hand, *caspase* was identified to be down-regulated upon NLHS-VP (Figure 45).

A Venn diagram was also created to highlight specific groupings of DEMs between the libraries of NLHS-VP and NH-VP. A total of 18 DEMs were specifically grouped into NLHS-VP, while only 2 DEMs were grouped into NH-VP (Figure 43). Those DEMs under the NLHS-VP condition (and their corresponding predicted target mRNAs from our sequencing dataset) were analyzed using in-house and RNAhybrid software for functionalizing their specific miRNA-mRNA interactions to provide details on the general regulatory mechanisms underlying the immune response of shrimp under NLHS and VP_{AHPND} infection. A total of 1,183 DEM-DEG pairs, with both positive and negative correlations, were identified (Figure 44A-B). Some of the

biological functions possibly regulated by NLHS-VP miRNAs include: “Defense & Homeostasis”, “Energy & Metabolism”, “Cell cycle & DNA Synthesis/repair”, “Gene expression & Protein synthesis/degradation”, “Receptor”, “Signaling & Communication”, “Transporter”, “Hypothetical protein”, and “Unknown”.

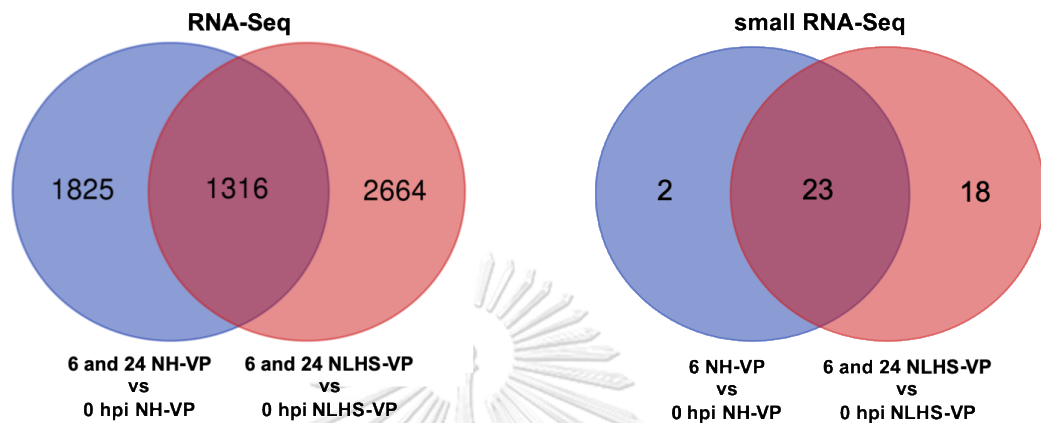


Figure 43 Venn diagrams represent unique and common shrimp mRNAs and miRNAs in response to VP_{AHPND} infection under heat and non-heat stress conditions.

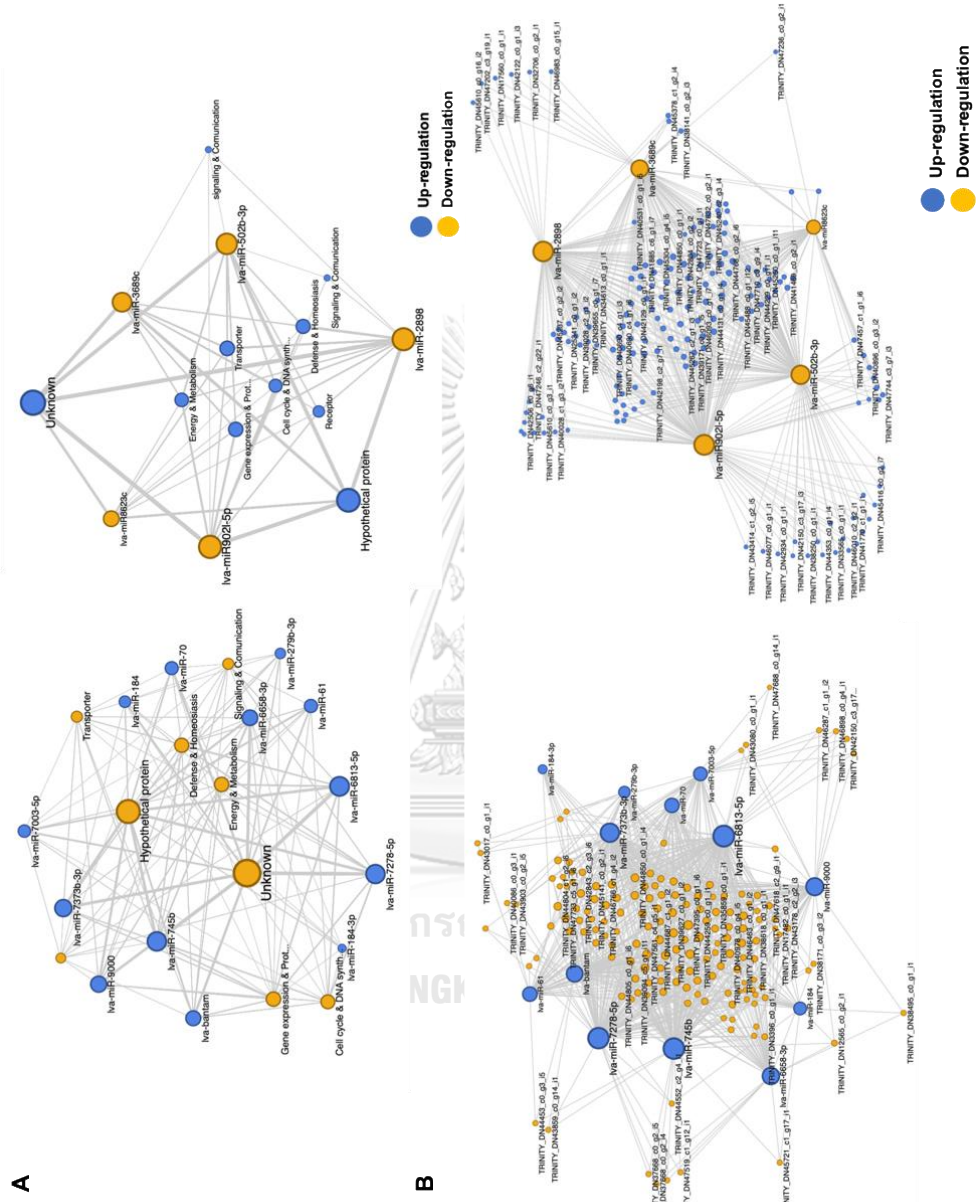


Figure 44 The miRNA-mRNA negative correlation network based on predicted miRNA target function (A) and unique isotig (B).

In order to further characterize the identified biological pathways, an enrichment analysis specific to immune-related pathways was performed for the identified DEGs of miRNA-mRNA pairs. These identified immune pathways that changed significantly ($P < 0.05$), were “hemocyte homeostasis”, “prophenoloxidase system”, and “AMP production”. The qRT-PCR analysis was used to quantify the expression profiles of some canonical members of the identified pathways (Figure 45). As expected, *PO1* and *PO2* in proPO pathway were highly up-regulated from 1.5- to 8-fold in the NLHS-VP group. In the IMD pathway, *IMD*, *IKK β* , and *Relish* exhibited higher gene expression, while expression of *Toll1*, *Toll2*, *Toll3*, *MyD88*, *TRAF6*, *Pelle*, and *Drosal* in the Toll pathway did not significantly change in the NLHS-VP group. For the hemocyte homeostasis pathway, *transglutaminase* and *inhibitor of apoptosis* were analyzed and found to be highly up-regulated, whereas *caspase* was down-regulated in NLHS-VP. These results confirmed the results of the pathway enrichment analysis, which finally suggests that the biological immune pathways “hemocyte homeostasis”, “prophenoloxidase system”, and “AMP production via IMD pathway” might serve important roles in the enhancement of shrimp antibacterial immunity against VP_{AHPND} upon modulation of NLHS (Figure 46).

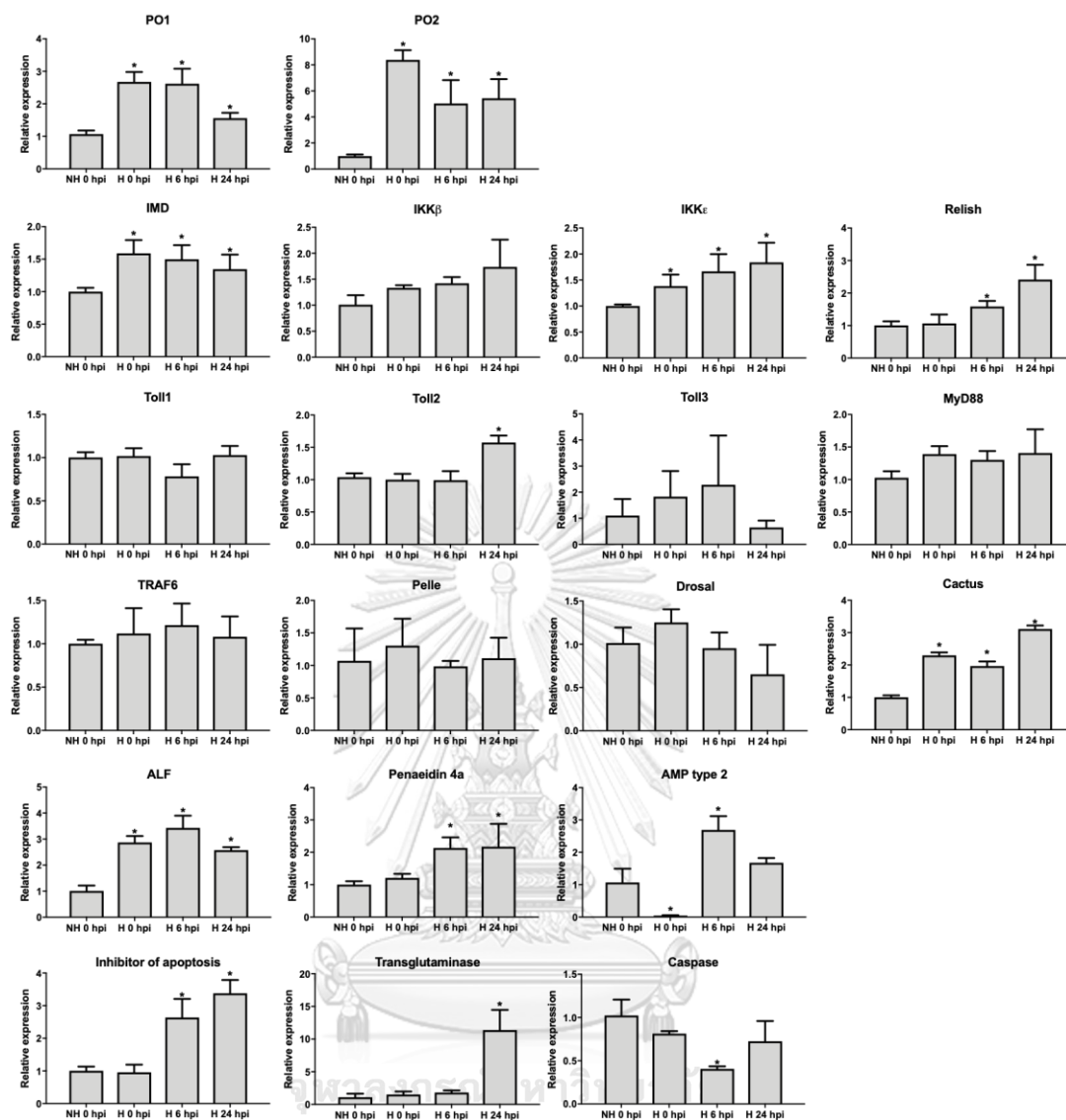


Figure 45 Relative expression analysis of genes in the NLSH modulated immune pathways processes.

Expression of genes in prophenoloxidase system, Toll pathway, IMD pathway, and hemocyte homeostasis in VP_{AHPND} -infected *P. vannamei* hemocyte following NLSH treatment were analyzed by qRT-PCR using the same cDNAs of the qRT-PCR validation experiment. Relative expression levels were normalized with NH-VP at 0 hpi to observe the effect of both NLSH and VP_{AHPND} challenge, and standardized against EF-1 α as the internal control. The results were derived from triplicate experiments. * indicate significant differences at $P < 0.05$. The expression profile of *PO1* and *PO2* under NLSH condition was modified and re-presented from Figure 3.41

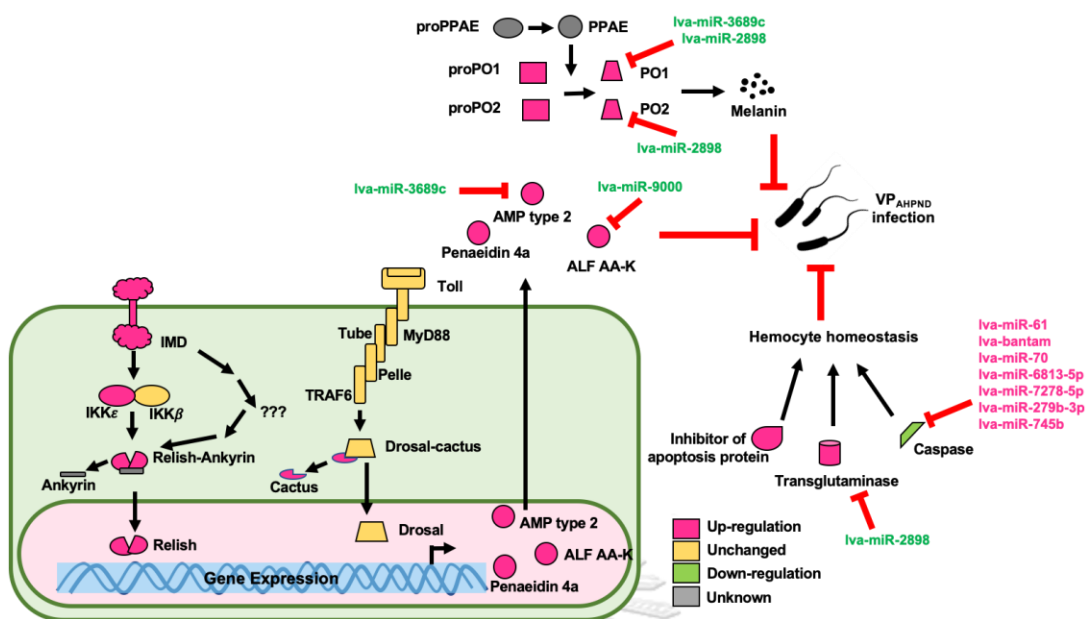


Figure 46 A schematic representation of the predicted interactions between the miRNAs and target immune genes of *P. vannamei* under the NLHS-VP condition.

3.4 Discussion

The previous observation that non-lethal heat shock may enhance production of heat shock proteins and then increase the expression of some immune-related genes resulting in enhanced immunity (Loc et al., 2013) has become a promising research interest because of its potential application in developing preventive strategies for diseases in shrimp. For instance, short-term hyperthermic treatment that was suggested to reduce gill-associated virus replication in *Penaeus monodon* (de la Vega et al., 2006) may prove to be a simple and efficient prophylactic strategy. In this study, we have observed that chronic heat stress improves the survival of *Penaeus vannamei*, which were challenged with AHPND-causing *V. parahaemolyticus* (VP_{AHPND}), revealing that non-lethal heat shock (NLHS) may indeed be an important immune-modulating factor to avoid mortalities caused by AHPND. However, *P. vannamei* tolerance to VP_{AHPND} infection was found to be influenced neither by Hsp70 accumulation nor the changes in tested immune-related proteins, such as proPO and hemocyanin (Loc et al., 2013). The mechanisms of tolerance to VP_{AHPND} infection under NLHS conditions, thus, still remain to be explored and explained by undescribed genes. To explore the microRNAs and gene networks that are involved in VP_{AHPND} infection and heat stress condition in *P. vannamei*, we performed small RNA sequencing analysis and RNA-Seq (by Dr. Benedict A. Maralit) during VP_{AHPND} infection under NLHS and control conditions.

The small RNA libraries prepared from VP_{AHPND}-infected *P. vannamei* hemocyte under NLHS (NLHS-VP) generated 3 million reads across 3 individual libraries and identified 41 DEMs of 27 up-regulated and 14 down-regulated miRNA in NLHS-VP. Previously, 47 up-regulated and 36 down-regulated miRNA homologs were identified from VP_{AHPND} challenged *P. vannamei* hemocyte (Zheng et al., 2018). This evidence suggests that miRNAs might play an important role as regulators of shrimp immune system upon pathogen infection.

The qRT-PCR results were used to validate mRNA and miRNA expression level in NLHS-VP and NH-VP conditions. Eight genes selected from NGS data including *Relish*, *Lipoprotein receptor*, *Dynamin*, *Importin7*, *Juvenile hormone epoxide hydroxylase 1*; *JHEH-1*, *DNAJ5*, *Prophenoloxidase 1*; *PO1* and *Prophenoloxidase 2*; *PO2* were analyzed. It was found that NLHS-VP- and NH-VP

responsive genes showed the expression profile similar to qRT-PCR. In the mean time, 10 differentially expressed NLHS-VP-responsive miRNAs were selected to validate their expression. The results showed that lva-miR-7170-5p, lva-miR-2898, lva-miR-184, lva-miR-2169-3p, lva-miR-4901, lva-miR-92a-3p and lva-miR-61 were significantly differenced in NLHS-VP condition as the same to our small RNA-Seq data.

The transcriptome reflects the mRNAs and miRNAs that are actively expressed under a particular condition. We attempted to acquire the miRNA-mRNA pairs through the use of DEMs and DEGs datasets and miRNA-targeting information. In most cases, the negative correlation between miRNAs and their target mRNAs is often considered proof of miRNA targeting (Alshalalfa et al., 2012). Previously, a total of 407 miRNA-mRNA interaction sites were predicted were identified to be involved in VP_{AHPND} infected *P. vannamei*. Among them, 11 DEMs might regulate 37 DE genes related to shrimp immune-responsive genes in response to VP_{AHPND} infection (Zheng et al., 2018). In the present study, a total of 779 pairs of NLHS-VP responsive miRNA-mRNA were identified with a negative correlation with the involvement of 19 DEMs and 707 DEGs. Among the interaction identified, only 11 heat-VP_{AHPND} responsive miRNAs might regulate shrimp immune-responsive genes/pathways such as hemocyte homeostasis, AMP production and prophenoloxidase system.

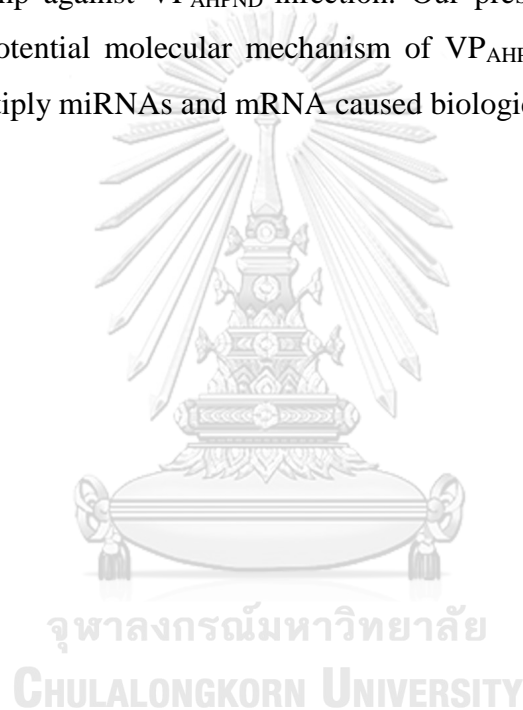
Caspase and transglutaminase (TGase) are 2 proteins that play important role in hemocyte homeostasis in crustacean species (Apitanyasai et al., 2015; Lin et al., 2008). Caspase is a key player in apoptosis (Fiandalo et al., 2012). In *Masupenaesus japonicus*, apoptosis pathway suppression using dsRNA could reduce the cumulative mortality of shrimp after challenge with *Vibrio alginolyticus* (Wang et al., 2018). TGase is known to be involved in blood coagulation, a conserved defense mechanism among invertebrates. In 2012, Fagutao et al. reported that suppression of TGase resulted in low haemocyte counts and high bacterial counts in *M. japonicus* (Fagutao et al., 2012). In our study, up-regulation of TGase and down-regulation of caspase identified from the NGS in shrimp hemocyte upon VP_{AHPND} infection under heat stress condition suggests that hemocyte homeostasis pathway might help shrimp tolerate to VP_{AHPND} infection after heat treatment.

Prophenoloxidase system is a major innate defense system in invertebrates that can kill pathogens and damaged shrimp tissues (Cerenius et al., 2004). Generally, phenoloxidase (PO), the key enzyme of the proPO-system, catalyzes the non-enzymatic conversion of phenolic substances to quinones, leading to the production of cytotoxic intermediates and melanin (Christensen et al., 2005). Proteinases and their inhibitor such as specific serine proteinases, non-catalytic serine proteinase homologs (SPH) as protein cofactors, and proteinase inhibitors cascade are the important cascade that regulated proPO-system to prevent excessive production of these toxic substances (Cerenius et al., 2004). In shrimp, suppression of proPO-system by gene silencing could increase susceptibility to bacterial infection (Charoensapsri et al., 2009). In 2018, it was found that the up-regulation of the two *Lv*proPO transcripts in shrimp *P. vannamei* might increase disease resistance to VP_{AHPND} (Chomwong et al., 2018). In this study, genes related-proPO system were highly up-regulated after VP_{AHPND} infection under heat treatment condition. This suggests that proPO-system plays crucial role in bacterial defense leading to shrimp tolerance to VP_{AHPND} infection.

The Toll and IMD pathways are regarded as the main pathways regulating the immune response of invertebrates. They play a key role in the response to pathogen infection by regulating a large set of genes including antimicrobial peptide genes, many small peptides with unknown function as well as components of the melanization and clotting cascades to fight against pathogen infection (Li et al., 2013). Anti-lipopolysaccharide factor is a type of antimicrobial peptides (AMPs) with a vital role in antimicrobial defense (Gu et al., 2018). In shrimp, it was found that ALF and AMP are regulated by Toll and IMD pathways (Tassanakajon et al., 2018). Silencing of *Lv*ALF along with VP_{AHPND} and VP_{AHPND} toxin challenge resulted in increasing of cumulative mortality rate (Tinwongger et al., 2019; Maralit et al., 2018). Similar to this study, AMPs were up-regulated in NLHS-VP condition. To proof that AMP gene upregulation is modulated through signaling pathway, genes in each Toll and IMD pathway were analyzed their expression under NLHS-VP condition. We found that genes in IMD pathway including *IMD*, *IKKε* and *Relish* were highly expressed in NLHS-VP condition. This suggests that NLHS treatment might modulate

the up-regulation of IMD pathway resulting in overexpression of AMP production system that play important role in bacterial defense.

In conclusions, the integrated analysis of miRNA and mRNA transcriptome analysis suggested that NLHS-VP miRNAs and their predicted target may have strong influence on tolerance to VP_{AHPND} infection under NLHS treatment method. In total, 3 immune-related pathways were identified based on the miRNA targets function, including proPO-system, IMD pathway, and hemocyte homeostasis. These findings improve our current understanding of the effect of NLHS treatment that mediate the immunity of shrimp against VP_{AHPND} infection. Our present study provides a new insight into the potential molecular mechanism of VP_{AHPND} infection under NLHS condition is a multiply miRNAs and mRNA caused biological change.



CHAPTER IV

Identification and functional characterization of miRNA in shrimp hemocyte in response to *Vibrio parahaemolyticus* AHPND (VP_{AHPND}) infection

The logo of Chulalongkorn University, featuring a central emblem with a crown and a sunburst, flanked by two figures, and a base with a banner.

จุฬาลงกรณ์มหาวิทยาลัย
CHULALONGKORN UNIVERSITY

4.1 Introduction

AHPND caused by VP_{AHPND} containing toxin-encoded plasmid has been responsible for important losses in the shrimp industry (Félix et al., 2017). Still, there are no effective approach to prevent VP_{AHPND} infection. The AHPND's characteristic symptoms were reported as a pale and atrophied hepatopancreas together with an empty stomach and midgut (Lightner et al., 2012). Histological examination of hepatopancreas as AHPND target tissue further showed that AHPND causes sloughing of the HP tubule epithelial cells into the HP tubule lumens (Tran et al., 2013). The metabolic capabilities analysis of VP_{AHPND} showed that VP_{AHPND} utilized 23 nutrient sources more efficiently than the other non-pathogenic VP strains (Williams et al., 2017).

miRNAs are small non-coding RNA molecules that function in RNA silencing and post-transcriptional regulation of gene expression. MiRNAs play important function in several biological processes including development, cellular differentiation, proliferation, apoptosis, hematopoiesis and immune system (Bartel, 2014). In miRNA biogenesis, the primary transcript (pri-miRNA) that contains hairpin loop domains is transcribed by RNA polymerase II. The pri-miRNA is cut by the RNase III enzyme Drosha to become a 60–70 nucleotide-long precursor miRNA (pre-miRNA), which is then exported to the cytoplasm by Exportin-5. The miRNA which is 18-24 double-stranded oligonucleotides is generated through cleavage of pre-miRNAs by the RNase-III enzyme, Dicer. The mature miRNA which is a single-

stranded RNA, called guide strand is integrated into an RNA-induced silencing complex (RISC). The interactions between the miRNA-RISC (miRISC) and mRNA targets involve binding between the “seed” region of the miRNA (typically nucleotides 2-8) and the complementary target sequence on the mRNA inducing mRNA degradation and translational repression (Azzam et al., 2012).

In animals, miRNA expression studies in response to various bacterial infections have revealed common miRNAs as key players in the host innate immune response (Eulalio et al., 2012). miR-146, along with miR-155, are found to be coordinately upregulated in immune cells in response to various bacterial pathogens including *Salmonella enterica* (Schulte et al., 2011; Sharbati et al., 2012), *Mycobacterium* species (Kumar et al., 2012; Rajaram et al., 2011; Sharbati et al., 2011; Spinelli et al., 2013; Wu et al., 2012), or *Francisella tularensis* (Cremer et al., 2009). miR-155 is induced by both bacterial and viral compounds through TLRs sensing bacterial and viral pathogens, and also by TNF- α and the antiviral interferons (O'Connell et al., 2007; Tili et al., 2007). In shrimp, miRNA was firstly identified upon viral infection in 2011. Thirty-five miRNAs including 15 miRNAs exhibited high homology to known miRNAs from other arthropods and other novel miRNAs were identified. Expression analysis of 22 miRNAs were determined upon WSSV infection (Ruan et al., 2011). The phagocytosis, apoptosis and phenoloxidase, are key immune reactions of shrimp immunity. Following activation or inhibition of these reactions in *Marsupenaeus japonicus*, the small RNA were sequenced and 24 miRNAs were seem to take great effects on phagocytosis, apoptosis or pro-phenoloxidase system (Yang et al., 2012). In bacterial infection, miRNAs in shrimp *M. japonicus* were identified in response to *V. alginolyticus* infection in 2016. Fifty-

five host miRNAs were identified from *V. alginolyticus* challenged shrimp. Apoptosis plays an important role in shrimp resistance against *V. alginolyticus* infection. The apoptosis-related miRNAs, miR-8, miR-965 and miR-S7 were significantly down-regulated after the infection and miR-S32 was significantly up-regulated at 48 h post infection (Zhu et al., 2016).

Previously the mRNA and miRNA expression profiles from the hemocyte of *P. vannamei* challenged with VP_{AHPND} following the NLHS and control conditions were determined by next-generation sequencing. A total of 2,662 mRNAs and 41 miRNAs were differentially expressed after the NLHS treatment and VP_{AHPND} infection. The relationship and probable interactions between miRNAs and mRNAs were studied by Target identification program. A miRNA-mRNA regulatory network was also conducted to illustrate the pathway interactions of miRNAs and the identified target genes. The results reveal that the NLHS treatment up-regulates the immune responses in *P. vannamei* hemocytes including the prophenoloxidase-activating system, hemocyte homeostasis, and antimicrobial peptide production (Boonchuen et al., Unpublished).

In the present study miRNAs involved in the immune response of *P. vannamei* to VP_{AHPND} infection, sequences and expression profiles of miRNAs in the hemocyte *P. vannamei* challenged with VP_{AHPND} at 0 and 6 h post infection (hpi) were obtained through the Illumina MiSeq high-throughput next-generation sequencing technique. Differentially expressed miRNAs were further verified by the real-time RT-PCR technique. The immune-related miRNA was selected for further functional characterization. The results provided basic information for the investigation of specific miRNAs involved in the response of *P. vannamei* to VP_{AHPND} infection.

4.2 Materials

4.2.1 Chemicals, reagents, enzymes and kits

*Nhe*I (NEB)

*Not*I-HF[®] (NEB)

Phusion high-fidelity (HF) PCR master mix with HF buffer (NEB)

RBC *Taq* DNA polymerase (RBC Bioscience)

RiboLock RNase inhibitor (Thermo Scientific)

Thermo Scientific™ RevertAid First Strand cDNA Synthesis Kit

*Xho*I (NEB)

4.2.2 Experimental shrimp, microorganisms, cells and viruses

Pacific white shrimp *Penaeus vannamei*

Escherichia coli strain XL-1blue

Vibrio parahaemolyticus (AHPND)

Human embryonic kidney 293T cells (HEK293T)

4.2.3 Software

BLAST[®] (<https://blast.ncbi.nlm.nih.gov/Blast.cgi>)

ExpASy-Translate tool (<https://web.expasy.org/translate/>)

Galaxy instance (<https://usegalaxy.org/>)

Geneious R11 (Biomatters, Ltd)

GraphPad Prism 6 (GraphPad Software)

miRBase 22.1 (<http://www.mirbase.org/>)

RNAhybrid (<http://bibiserv.techfak.uni-bielefeld.de/rnahybrid/>)

4.2.4 miRNA target prediction

The miRNA targets were identified by comparing with transcriptome data using CU-mir software that was previously developed by our research group (Kaewkascholkul et al., 2016) This software searched for locations on mRNA targets

that seed sequences (2-8 nucleotides from 5' end) of miRNA and can bind with perfect complementary or 1 mismatch at identified seed sequences. Percent complementary is calculated from the number of nucleotides that perfectly match the target mRNAs per total length of miRNA sequences. The percent complementarity cutoff was set at 55%. RNAhybrid (<http://bibiserv.techfak.uni-bielefeld.de/rnahybrid/>) was also used to predict genes targeted by miRNAs with the parameters of free energy < -15.0 kcal/mol (Kaewkascholkul et al., 2016).

4.2.5 miRNA/mRNA interaction network analysis

In order to define all possible miRNA-mRNA interactions involved in a specific dataset of immune-related genes, a miRNA-mRNA interaction network was constructed. Immune responsive genes from the transcriptome were specifically chosen for inclusion in the integrated analysis of the miRNA/mRNA network. The differentially expressed miRNAs from shrimp challenged with VP_{AHPND} under NLHS were used to identify mRNA targets and to construct the miRNA/mRNA network. Again, the binding of target mRNAs of differentially expressed miRNAs were predicted using RNAhybrid with the parameters of free energy < -15 kcal/mol. These target mRNAs were mapped against our RNA-Seq data to determine their immune-related functions.

4.2.6 Dual-luciferase reporter assay

The luciferase reporter system was used in order to confirm the interaction between miRNAs of interest and their target genes. The lva-miR-4850 was predicted to target PO2 that was also of interest. Gene-specific primers for target mRNA amplification were designed (Table 2.6). The PO2 sequence at 3'UTR containing the predicted lva-miR-4850 target site were amplified from the cDNA of the VP_{AHPND} *P. vannamei* hemocyte. The PCR products of each target sequence were cloned into pmiRGLO plasmid (Promega) producing pmirGLO-PO2 plasmid.

To construct the experimental control, the binding element at position 2-8 nucleotide was mutated by using QuikChange II XL Site-Directed Mutagenesis Kit (Agilent Technology). Briefly, the primers were designed by switching the bases of a

seed sequence from purine to pyrimidine or pyrimidine to purine with a melting temperature (T_m) of ≥ 78 °C. Then, the recombinant pmiRGLO-PO2 was amplified by *PfuUltra* HF DNA polymerase and then, the PCR product was treated with *DpnI* restriction enzyme. The treated PCR product was transformed into *E. coli* Top10. The mutant plasmids were then randomly chosen and sequenced.

After validating the sequences, 200 ng of plasmids were co-transfected into HEK293-T cells along with 20 pmol of lva-miR-4850 mimic (5'-AUAACAUGACUGAAAACAUUU-3') (GenePhama) or miR-4850 scramble (5'-GUUAAUACCUAAGAUUAACAA-3') (GenePhama) using the Effectene transfection reagent (Qiagen). After 48 h post transfection, the luciferase activity of Firefly and Renilla luciferases were measured by the Dual-Luciferase® Reporter assay system (Promega) following the manufacturer's instructions. Three independent experiments were performed. GraphPad Prism 6.0 software was used for statistical analyses including a paired-samples t-test, with data presented as means \pm standard deviations.

4.2.7 Mimic, scramble mimic, anti-miRNA oligonucleotide (AMO), and AMO scramble

To investigate whether lva-miR-4850 is involved in the prophenoloxidase system of shrimp, *in vivo* RNAi experiments were performed. The mimic, scramble mimic, anti-miRNA oligonucleotide (AMO), and AMO scramble RNA of lva-miR-4850 were synthesized by Shanghai GenePharma Co., Ltd., P.R. China (Table 13).

Table 13 Mimic, scramble mimic, anti-miRNA oligonucleotide (AMO), and AMO scramble RNA sequences

Gene	Name	Sequence	
		Sense (5'-3')	Antisense (5'-3')
Lva-miR-4850	Mimic	AUAACAUGACUGAAAACAUUU	AUGUUUUCAGUCAUGUUUUU
	Scramble mimic	GUUAAUACCUAAGAUUAACAA	GUAUAUCUUAGGUAUUAACUU
	AMO	AAAUGUUUUCAGUCAUGUUU	
	AMO scramble	GAUUUAUCCAUAUUGAUUAGU	

4.2.8 *In vivo* lva-miR-4850 introducing and silencing in shrimp

Shrimp (2-3 g) were divided into five groups of three individuals each. Experimental shrimp were intramuscularly injected with 50 μ l of 0.85% NaCl solution containing 2 nmole of mimics-lva-miR-4850 or AMO-lva-miR-4850, while the control group was injected with 2 nmole of scramble mimics-lva-miR-4850 or AMO-lva-miR-4850 scramble or 50 μ l of 0.85% NaCl. After 24 h post injection, VP_{AHPND} was challenged as described in Section 2.3. At 24 h post challenge, shrimp hemolymph was collected. Total RNA was extracted and used for first-strand cDNA production. The expression levels of lva-miR-4850 and *PO2* were determined by qRT-PCR, as described in section 3.1.4.

On the other hand, stomach and hepatopancreas were individually collected from 3 shrimp per group, crushed, and serially 10-fold diluted in sterile 0.85% NaCl. The diluted hemolymph samples (at 10⁻ to 10⁶-fold) were dropped onto TCBS agar and incubated at 30 °C for 12-14 h. The bacterial colonies were then counted and calculated as CFU/ml. All experiments were performed in triplicate, and statistical analyses were performed using one-way ANOVA followed by Duncan's new multiple range test and presented as means \pm standard deviations. Statistical significance was set at $P < 0.05$.

4.2.9 Phenoloxidase activity assay

Phenoloxidase (PO) activity was determined in the hemolymph of VP_{AHPND}-infected shrimp. The shrimp hemolymph from each siRNA-injected group (as described in Section 2.24.3) were collected at 24 h post VP_{AHPND} infection. PO activity was measured using a method modified from Sutthangkul et al. (2017). Briefly, 50 μ l of hemolymph was mixed with 25 μ l of 3 mg/mL freshly prepared L-3, 4-dihydroxyphenylalanine (L-DOPA; Fluka), and 25 μ L of 20 mM Tris-HCl (pH 8.0). The absorbance at 490 nm was monitored. The amount of hemolymph proteins was measured using the Bradford method. PO activity was recorded as A₄₉₀/mg total protein/min.

4.3 Results

4.3.1 miRNA expression analysis upon VP_{AHPND} infection using stem-loop real-time PCR

In order to confirm the presence of the identified miRNAs and to analyze the expression of *P. vannamei* miRNA in response to VP_{AHPND} infection, the expression levels of 10 selected NH-VP responsive miRNAs (lva-miR-9000, lva-miR-8522c, lva-miR-2169-3p, lva-miR-4850, lva-miR-92b-5p, lva-miR-D9-3p, lva-miR-184, lva-miR-4901, lva-miR-7170-5p, and lva-miR-92a-3p) were evaluated using stem-loop RT-PCR. The relative expression levels of miRNAs were determined in VP_{AHPND}-infected *P. vannamei* hemocyte at 0, 6, and 24 hpi, using U6 as the internal reference (Figure 47). The results indicated that the expression levels in 8 out of 10 miRNAs were altered in shrimp hemocyte following VP_{AHPND} challenge. The expression levels of lva-miR-8522c and lva-miR-184 remained unchanged at 6 and 24 hpi. For lva-miR-9000, the expression level at 6 and 24 hpi were down-regulated by approximately 1.5- and 1.75-fold, respectively. Moreover, the expression level of lva-miR-D9-3p and lva-miR-4850 remained unchanged at 6 hpi but were then down-regulated by approximately 2-fold at 24 hpi. For lva-miR-2169-3p and lva-miR-7170-5p, the expression level was up-regulated by approximately 2- and 3-fold at 6 hpi and 2.5- and 10-fold at 24 hpi, respectively. For lva-miR-4901, the expression level was down-regulated by 1.7-fold at 6 hpi and remained unchanged at 24 hpi. The expression level of lva-miR-92a-3p increased by approximately 2-fold at 6 hpi and remained unchanged at 24 hpi. The expression level of lva-miR-92b-5p was unchanged at 6 hpi but increased by approximately 1.75-fold at 24 hpi.

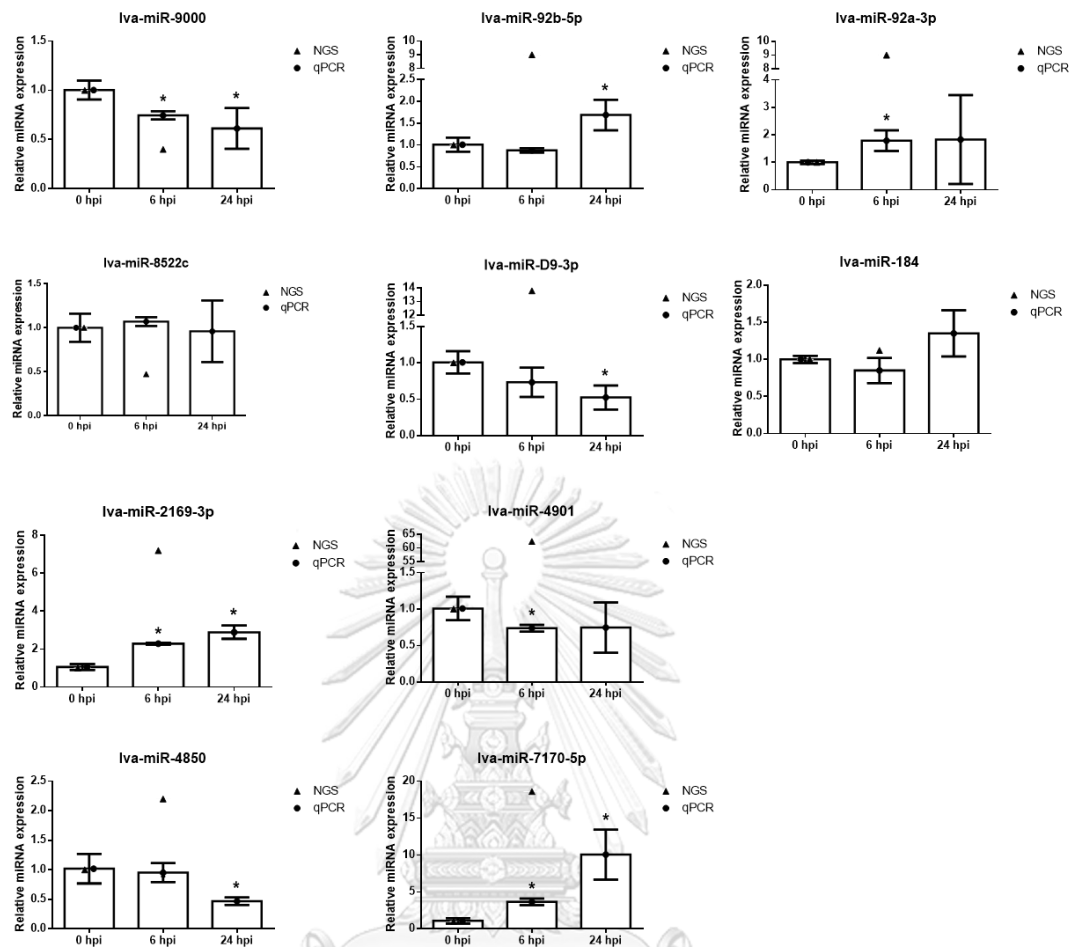


Figure 47 Relative expression analysis of miRNAs in response to VP_{AHPND} infection. Total RNA from VP_{AHPND}-infected *P. vannamei* hemocyte was used as a template for specific stem-loop first-strand cDNA synthesis. The relative expression levels of 10 miRNAs were determined by qRT-PCR and standardized against U6 as the internal reference at 0, 6, and 24 hpi. Results were derived from triplicate experiments. Data are presented as means \pm standard deviations. Asterisks indicate significant differences at $P < 0.05$.

4.3.2 miRNA target prediction

The function of miRNA on gene expression regulation depends on its ability to directly bind the target mRNA. Therefore, identification of the target mRNA of each miRNA could provide clues regarding the role of miRNA in shrimp immune response against VP_{AHPND} infection. The transcriptome database of VP_{AHPND}-infected *P. vannamei* was used for mRNA target prediction using the developed miRNA target prediction program (Kaewkascholkul et al., 2016). The criteria for searching miRNA

targets included: the presence of a seed sequence (2-8 nucleotides from the 5' end) of miRNA with perfect complementarity or 1 mismatch position to mRNA at any different region; an open reading frame (ORF); 3'-UTR and 5'-UTR; and an overall complementarity of miRNA to target mRNA no lower than 65%. It was determined that VP_{AHPND}-responsive miRNAs might target several shrimp immune-related genes (Figure 48).



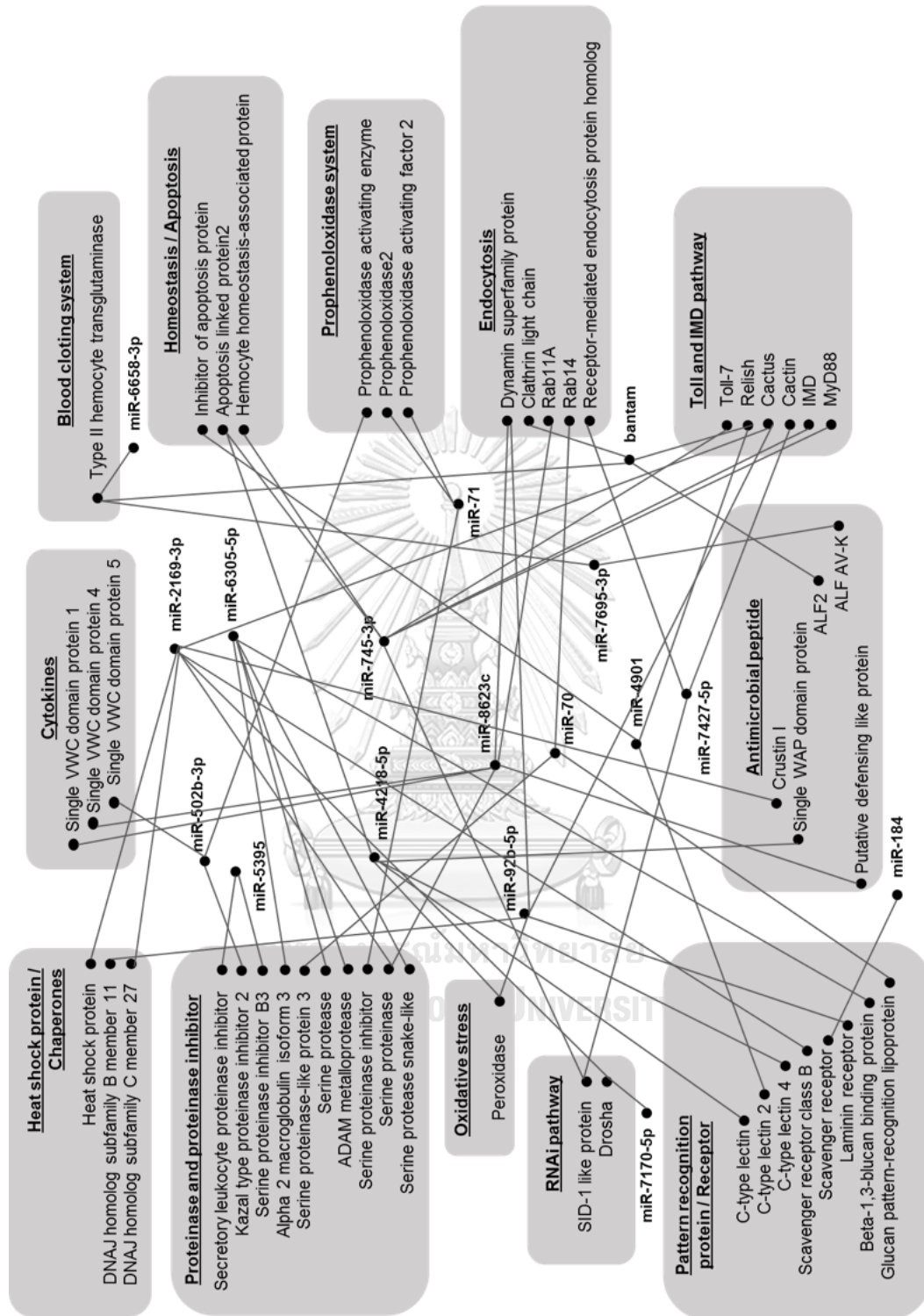


Figure 48 The predicted interactions between miRNAs and target *P. vannamei* immune genes.

The target genes of VP_{AHPND}-responsive miRNAs were predicted against the *P. vannamei* transcriptome database using the developed miRNA target prediction program. Target genes were grouped according to immune-related function.

4.3.3 Expression analysis of the target mRNA of lva-miR4850 in *P. vannamei* shrimp by qRT-PCR

Based on the results presented in Section 3.12.2, lva-miR4850 was selected for further miRNA/target interaction analysis. Notably, lva-miR4850 was predicted to target the 3'-UTR of *PO2* at position 2319 to 2338 and *Dicer1* at position 11,779 to 11,795, which were a gene in the prophenoloxidase system and RNA interference pathway, respectively (Figure 49A-B). The expression analysis of putative lva-miR4850 target genes revealed that *PO2* and *Dicer1* were up-regulated after VP_{AHPND} infection in *P. vannamei* hemocyte by approximately 1.8- to 3-fold (Figure 49C). The results suggested that *PO2* and *Dicer1* might be lva-miR4850 target genes.

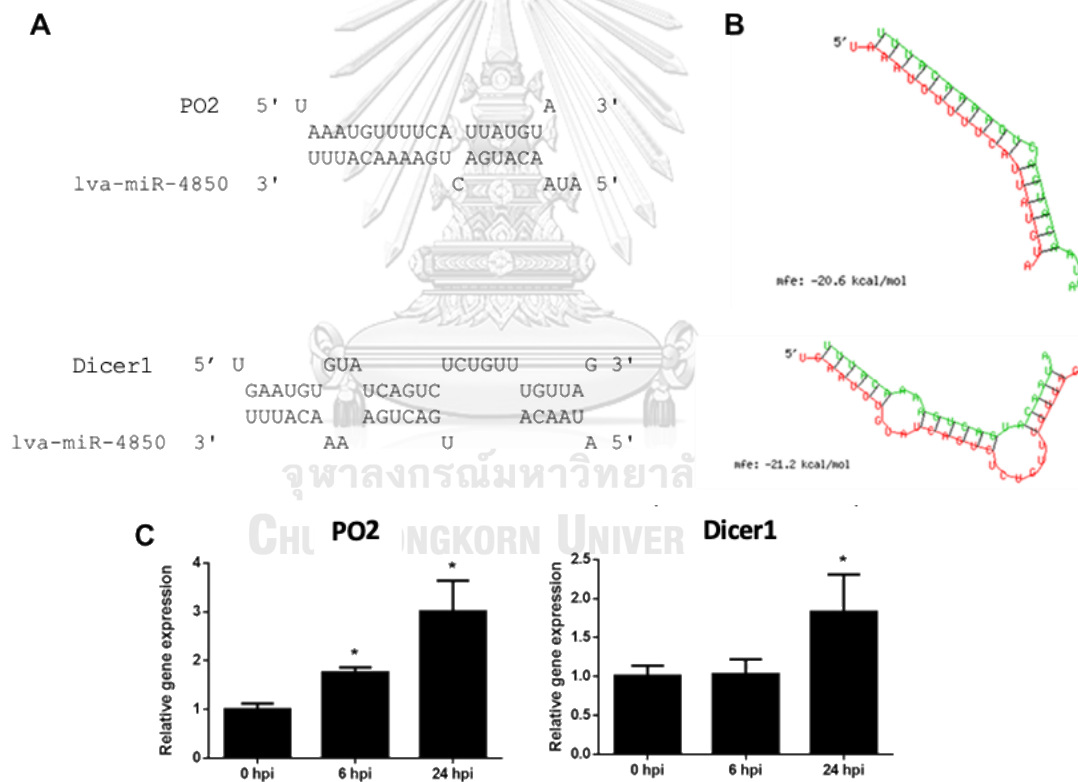


Figure 49 Prediction of target genes, miRNA binding site and expression analysis of lva-miR-4850.

The binding of lva-miR-4850 to target mRNA were predicted using in-house software (A) and RNAhybrid software (B). Relative expression analysis of the mRNA targets of lva-miR-4850 in response to VP_{AHPND} infection in *P. vannamei* hemocyte. Relative expression levels were determined by qRT-PCR and standardized against EF-1 α as the internal control. Results were derived from triplicate experiments. Asterisks indicate significant differences at $P < 0.05$.

4.3.4 Confirmation of target mRNA of lva-miR4850 by dual-luciferase reporter assay

PO2 is one of key enzyme in the melanization cascade that also participates in cuticle sclerotization and wound healing. Sclerotized cuticle presents a barrier to infection, and melanization around pathogens help to kill invading pathogens (Amparyup et al., 2013). In this study, *PO2* was predicted as the lva-miR-4850 target gene. Therefore, *PO2* and lva-miR-4850 interaction was further characterized

To confirm the miRNA/target interaction, DNA fragments corresponding to the putative miRNA-binding region of the *PO2* gene was cloned into a pmirGLO vector downstream of the firefly luciferase gene (Figure 50) and used as the parental construct (pmirGLO-*PO2*). Then, it was mutated at the seed region (pmirGLO-*PO2*-mutant-mutant) and used for the experiment. Reporter constructs were then transfected into HEK293-T cells with either respective miRNA mimics or scramble. The results showed that the luciferase activity of pmirGLO-*PO2* was reduced by approximately 35% (Figure 51). The reduction of firefly luciferase expression indicates the binding of miRNA to the cloned miRNA target sequence. On the other hand, the mutated seed sequence of lva-miR-4850 did not affect luciferase activity compared to that of the control group (Figure 51). These results indicated that the *PO2* gene was a target gene of lva-miR-4850.

```

PO2 -WT          GCGGT TT CTG TA TTA GAG TT AGAAA TG GCT AT TGT GT ACA TT TCT TT TGT AT CTG TT TAA 60
PO2 -mutant     GCGGT TT CTG TA TTA GAG TT AGAAA TG GCT AT TGT GT ACA TT TCT TT TGT AT CTG TT TAA 60
*****

PO2 -WT          TATTT GG ATT TT GGT AC ATT GT TGT AT AAT AT ATT TT GTA TC TGC AGATA CAGAA AT ACT 120
PO2 -mutant     TATTT GG ATT TT GGT AC ATT GT TGT AT AAT AT ATT TT GTA TC TGC AGATA CAGAA AT ACT 120
*****

PO2 -WT          AAATG TT TTC AT TAT GT A TAAAATG TG AAA AC TGT GT TCC CT GTA AT ACT GT ATT AT CTG 180
PO2 -mutant     AAATG TT TTC Aaata ca A TAAAATG TG AAA AC TGT GT TCC CT GTA AT ACT GT ATT AT CTG 180
*****

PO2 -WT          TAATA AC TAC TT ACA CA TAT CAG TA TT AGA TAG TT GT ATA TT TTA TT CAT TA TAA TC ATG 240
PO2 -mutant     TAATA AC TAC TT ACA CA TAT CAG TA TT AGA TAG TT GT ATA TT TTA TT CAT TA TAA TC ATG 240
*****

PO2 -WT          ATATT TGA AC AG AC GAA ATG CG TTT AAATA A      271
PO2 -mutant     ATATT TGA AC AG AC GAA ATG CG TTT AAATA A      271
*****

```

Figure 50 Sequence alignment of the *lva*-miR-4850 binding site for the PO2 gene between the wild type and mutated seed sequence. Yellow highlight represents the *lva*-miR-4850 binding sequence.

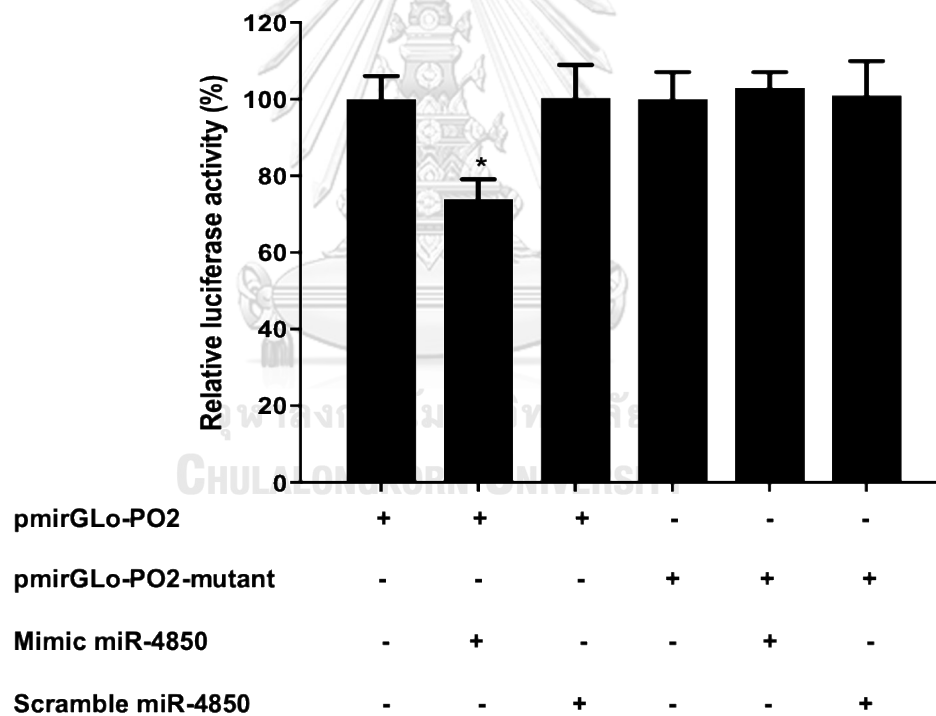


Figure 51 *In vitro* miRNA/target interaction analysis.

Synthetic *lva*-miR-4850 or *lva*-miR-4850 scramble were co-transfected with pmirGLO-PO2 or pmirGLO-PO2 mutant into HEK293-T cells. Luciferase activity was measured at 48 h after transfection. The experiments were performed triplicate. Asterisk indicates significant differences at $P < 0.05$.

4.3.5 Regulation of *PO2* gene and proPO activating system by lva-miR-4850 in VP_{AHPND}-infected shrimp

To investigate whether lva-miR-4850 regulates *PO2* gene in shrimp, *in vivo* RNAi experiments were performed. Shrimp were injected with either mimic-lva-miR-4850, scramble mimic-lva-miR-4850, AMO-lva-miR-4850, scramble AMO-lva-miR-4850, or 0.85% NaCl. After 24 hpi, each injected shrimp was challenged with VP_{AHPND}. The total RNA was extracted from the hemocyte at 24 h post VP_{AHPND} challenge and subjected to qRT-PCR analysis and phenoloxidase activity assay. The qRT-PCR analysis showed that the lva-miR-4850 transcription level increased significantly by approximately 2-fold in mimic-lva-miR-4850 injected shrimp, when compared to the scramble mimic-lva-miR-4850 and 0.85% NaCl-injected shrimp. The transcription level of *PO2* exhibited a negative correlation to that of lva-miR-4850. The *PO2* expression level was significantly decreased by approximately 4-fold in mimic-lva-miR-4850-injected shrimp as compared to the control of scramble mimic-lva-miR-4850- and 0.85% NaCl-injected shrimp (Figure 52). As the same trend of *PO2* expression, injection of mimic-lva-miR-4850 showed a negative correlation to lva-miR-4850 expression. The prophenoloxidase activity was significantly decreased by about 2-fold when compared to the control of scramble mimic-lva-miR-4850- and 0.85% NaCl-injected shrimp (Figure 53).

On the other hand, shrimp injected with AMO-lva-miR-4850 to inhibit lva-miR-4850 and challenged with VP_{AHPND} exhibited significant reduction of lva-miR-4850 expression level (approximately 1.5-fold), when compared to the scramble AMO-lva-miR-4850- and 0.85% NaCl-injected shrimp. Considering *PO2* expression level, the inversed relationship between lva-miR-4850 and *PO2* was observed. AMO-lva-miR-4850 injected shrimp increased significantly approximately by 1.5-fold in AMO-lva-miR-4850-injected shrimp but decreased significantly by 4-fold in the mimic-lva-miR-4850 injection (Figure 52). In addition, shrimp injected with AMO-lva-miR-4850 challenged with VP_{AHPND} increased prophenoloxidase activity by approximately 1.5-fold, when compared to the scramble AMO-lva-miR-4850- and 0.85% NaCl-injected shrimp (Figure 53).

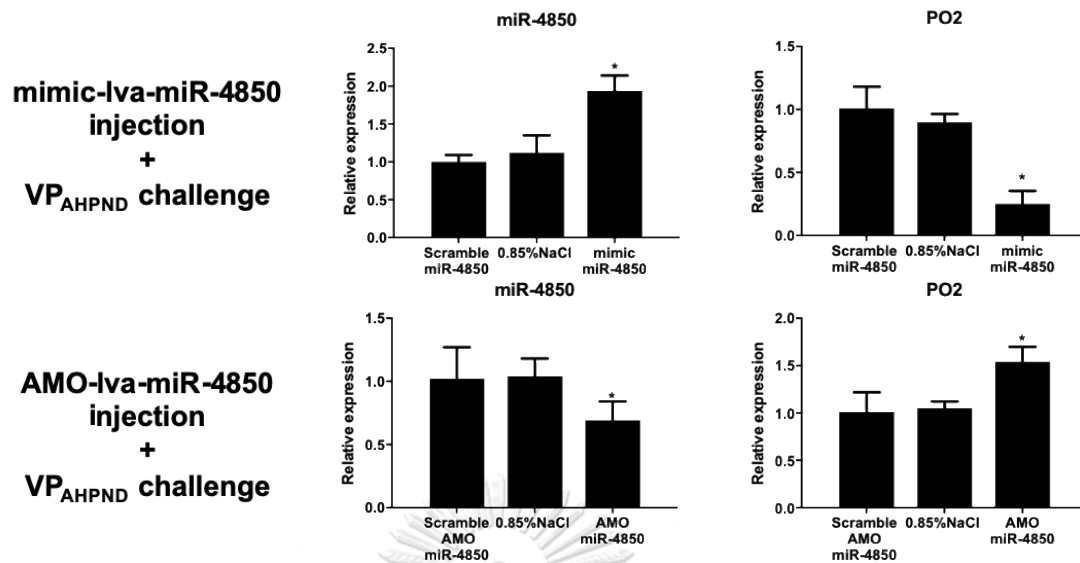


Figure 52 Regulation of *PO2* gene by lva-miR-4850 in VP_{AHPND} infected shrimp. Expression analysis of lva-miR-4850 and *PO2* in mimic-lva-miR-4850-, scramble mimic-lva-miR-4850-, AMO-lva-miR-4850-, scramble AMO-lva-miR-4850-, or 0.85% NaCl-injected shrimp challenged with VP_{AHPND}. The experiment was performed in triplicate. Data are presented as means \pm standard deviations. Asterisks indicate significant differences between data for scramble mimic- or scramble AMO-injected shrimp at $P < 0.05$.

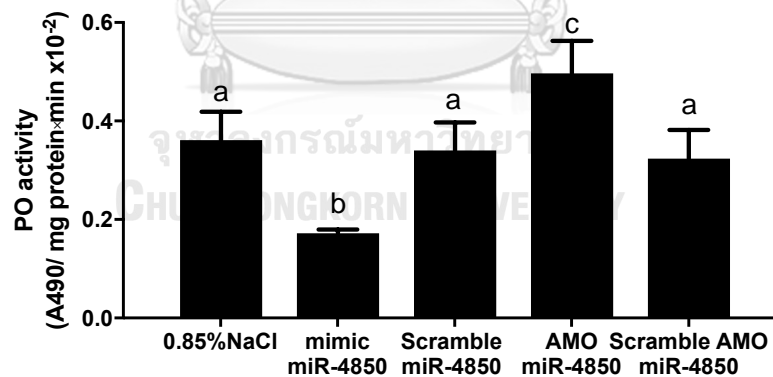


Figure 53 Regulation of proPO activating system by lva-miR-4850 in VP_{AHPND} infected shrimp.

Phenoloxidase activity of mimic-lva-miR-4850-, scramble mimic-lva-miR-4850-, AMO-lva-miR-4850-, scramble AMO-lva-miR-4850-, or 0.85% NaCl-injected shrimp challenged with VP_{AHPND} was determined in hemolymph collected at 24 h post VP_{AHPND} challenge. The experiment was performed in triplicate. Data are presented as means \pm standard deviations. Different small letters indicate significant differences between data at $P < 0.05$.

4.3.6 Effect of mimic and AMO lva-miR-4850 on the number of bacteria in stomach and hepatopancreas of VP_{AHPND}-infected shrimp

Based on the results of the challenge test for mimic-lva-miR-4850- and AMO lva-miR-4850-injected shrimp, we further investigated whether they had an effect on the number of bacterial cells in VP_{AHPND} targeted shrimp tissues, stomach and hepatopancreas. The amount of total *Vibrio* in shrimp stomach and hepatopancreas was counted after either mimic-lva-miR-4850, scramble mimic-lva-miR-4850, AMO-lva-miR-4850, scramble AMO-lva-miR-4850, or 0.85% NaCl injection and VP_{AHPND} challenge. The results revealed that the number of green colonies in both stomach and hepatopancreas increased in shrimp injected with mimic-lva-miR-4850. The number of VP_{AHPND} (CFU/ml) in AMO-lva-miR-4850 injected shrimp was reduced by approximately 10-fold compared to the scramble AMO-lva-miR-4850- and 0.85% NaCl-injected groups (Figure 54).

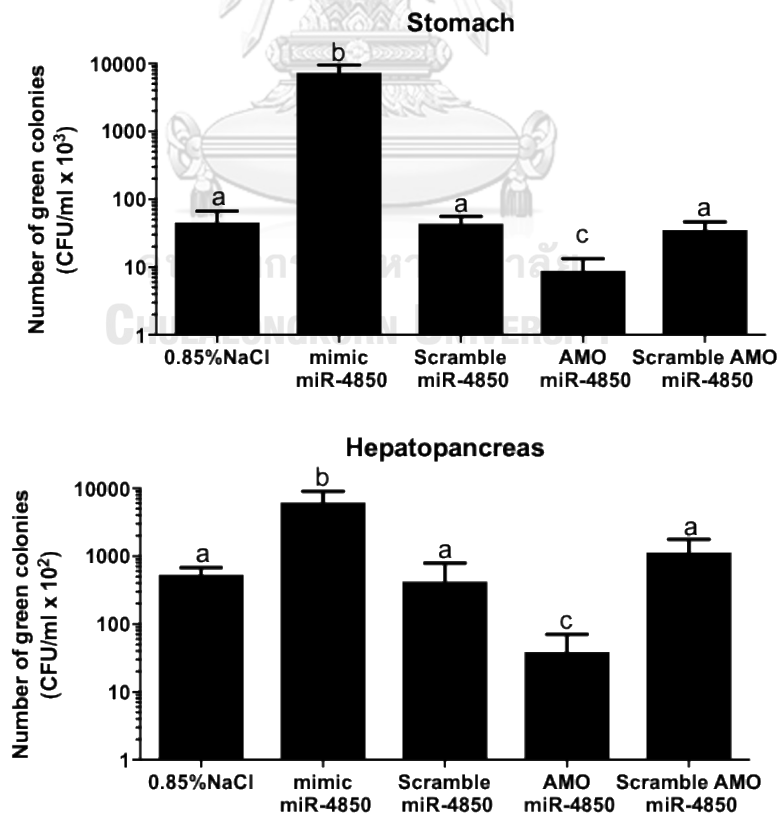


Figure 54 Effects of mimic and AMO lva-miR-4850 on the number of bacteria in stomach and hepatopancreas of VP_{AHPND}-infected shrimp.

Shrimp were injected with mimic-lva-miR-4850, scramble mimic-lva-miR-4850, AMO-lva-miR-4850, scramble AMO-lva-miR-4850, or 0.85% NaCl. After 24 h, shrimp were infected with 1×10^6 CFU/ml VP_{AHPND} by immersion. Stomach and hepatopancreas were individually collected to determine the amount of VP_{AHPND} by dotting on TCBS agar at 24 h post VP_{AHPND} challenge. Following overnight incubation, the total number of viable green colonies (CFUs) were evaluated. The experiment was performed in triplicate. Data are presented as means \pm standard deviations. The letters indicate significant differences at $P < 0.05$.

4.4 Discussion

In this study, we used next-generation sequencing to survey the miRNA and miRNA expression profiles in VP_{AHPND}-infected group and a control group of shrimp *P. vannamei*. Previously, the innate immune response was activated in *P. vannamei* infected with VP_{AHPND} (Boonchuen et al., Unpublished). This lead us to further determine the degree of changes in gene expression and miRNA expression. These results also allowed us to predict the miRNA-mRNA regulatory network of *P. vannamei* upon VP_{AHPND} infection. In this study, we further analyzed expression of VP_{AHPND} responsive miRNA of *P. vannamei* hemocyte to better understand function of miRNA in antibacterial immune response. Previously in *Scylla paramamosain*, 161 miRNAs were significantly differentially expressed during the VP_{AHPND} challenge and the potential targets of these differentially expressed miRNAs were predicted as genes in innate immunity (Li et al., 2013). In shrimp *P. vannamei*, a total of 83 miRNAs were significantly differentially expressed in *P. vannamei* upon VP_{AHPND} infection (Zheng et al., 2018). In our study, 19 miRNAs were identified as a differentially expressed miRNA homologs in shrimp hemocyte upon VP_{AHPND} infection. Our study identified miRNA homologs against vertebrate and invertebrate species whereas the NGS from Zheng et al., 2018 identified miRNA homologs against only invertebrate

species. Among both NGS data, only lva-miR-71 shared the same trend of the expression profiles. In our study, the qRT-PCR results were used to validate miRNA expression level in VP_{AHPND} challenge shrimp hemocyte. It was found that 4 from 10 miRNAs including lva-miR-9000, lva-miR-7170-5p, lva-miR-92a-3p and lva-miR-2169-3p were significantly different expressed in shrimp hemocyte upon VP_{AHPND} infection at 6 hpi as same as our small RNA-Seq data. Among the expression analysis, the 10 miRNAs were differentially expressed after VP_{AHPND} challenge.

According to Zheng et al., 2018, 12 miRNAs and their predicted target genes are possibly involved in modulating several immune-related processes in the pathogenesis of AHPND. In our study, the differentially expressed miRNAs were predicted against the transcriptomic data of VP_{AHPND} challenge *P. vannamei*. It was found that VP_{AHPND} responsive miRNAs might regulate several shrimp immune genes. Based on miRNA target function, the miR-4850 targeting *PO2* gene was characterized.

Upon bacterial infection, the shrimp proPO system takes part in shrimp antibacterial immunity by producing melanin and cytotoxic intermediate for bacterial sequestration (Li et al., 2008). The phenoloxidase (PO) is a key enzyme in the melanization cascade that also participates in cuticle sclerotization and wound healing. Sclerotized cuticle presents a barrier to infection, and melanization around pathogens help to kill invading pathogens (Amparyup et al., 2013). *PO2* was significantly increased after 6 and 24 h post-VP_{AHPND} infection. As expected, the negative correlation of lva-miR-4850 expression and *PO2* gene expression was observed in hemocytes after VP_{AHPND} infection. According to Jaree et al., 2018, pmo-miR-315 in *P. monodon* functioned in enhancing viral replication by regulating the

proPO system through the inhibition of *PmPPAE3* gene expression. In our study, an increase in the bacterial number in hepatopancreas and stomach of VP_{AHPND}-infected shrimp after lva-miR-4850 mimic injection indicated that the lva-miR-4850 might plays role in enhancing VP_{AHPND}-infection by regulating the proPO system through the inhibition of PO2 gene expression. On the other hand, the amount of AMO-lva-miR-4850 challenged shrimp was lower than that of VP_{AHPND}-infected shrimp challenged with exogenous lva-miR-4850. In conclusions, the lva-miR-4850 was reduced in shrimp hemocyte after VP_{AHPND} infection resulted in increasing of PO2 gene in prophenoloxidase system.



CHAPTER V

Identification of miRNAs and their interacting partners from WSSV-infected *P. vannamei* hemocyte using psoralen analysis of RNA interactions and structures (PARIS)



5.1 Introduction

Viral and bacterial diseases have caused high mortalities and lead to a serious economics loss in shrimp aquaculture worldwide. WSSV outbreaks can reach a cumulative mortality of up to 100% within 3 to 7 days of infection. Basically, to fight against infection, shrimp use innate immunity including several immune effectors and pathways, for example, Toll and IMD pathways, apoptosis and RNA interference pathway (RNAi). RNAi is the pathway that regulates the target gene expression by the regulators, microRNA (miRNA).

The miRNA which is small non-coding RNA (20-22 nucleotides long) that is transcribed from host genome yielding the primary miRNA (pri-miRNA) then, it is cleaved by Drosha to be precursor miRNA (pre-miRNA) and it is transported from nucleus to cytoplasm via Exportin-5 where the pre-miRNA is cleaved again by Dicer resulting in short double strand miRNA. After that, a single strand miRNA in cooperate with RNA induced silencing complex (RISC) which is driven by Argonaute proteins (Bartel, 2004). MiRNA acts as a guide that can complementarily bind to its target gene, which is recognized at the seed region (position 2-8 on miRNA sequence). Then, the miRNA/target gene leading to repress the translational process and/or cleavage the target genes. Although, several genes that are responded to the diseases caused by bacteria and viruses have been identified, the knowledge on shrimp immune responses and regulation is still limited.

Currently, there are many reports suggested that miRNA is involved in regulating genes of host/or viruses upon viral infection (Yaodong et al., 2014 and Jaree et al., 2018). However, the miRNA-mRNA target was used only computational method for miRNA-mRNA target prediction. In 2018, the Psoralen Analysis of RNA Interactions and Structures (PARIS) method was used to study RNA interaction in living cell (Lu et al., 2018). Previously, The PARIS method was used to study the structure and interaction mapping on four Dengue (DENV) and Zika (ZIKV) virus strains in infected cells. It was found that many pair-wise interactions, 40% of which form alternative structures, was observed. These results suggested the extensive structural heterogeneity of both viruses (Huber et al., 2019).

In this study, the miRNAs from our ongoing research in hemocyte of WSSV-infected *P. vannamei* by method will also be functionally characterized. PARIS is a

method for mapping RNA duplex. The RNA that was treated by psoralen and was exposed by UV making the crosslinking RNA (Lu et al., 2018). Then, the isolated RNA/RNA will be subjected to NGS. Hence, this research aims to study the function of miRNAs and target genes related to the antiviral immune response in shrimp.

5.2 Materials

5.2.1 Equipment

High-voltage electrophoresis power supply
 qPCR machine (Stratagene Mx3005p, capable of removal of individual samples amid reaction)
 Stratalinker 2400 model UV Crosslinker (Stratagene)
 Thermomixer (Eppendorf)

5.2.2 Chemicals and reagents

Absolute ethanol, $\text{CH}_3\text{CH}_2\text{OH}$ (HAYMAN)
 Acrylamide page (GE Healthcare)
 Ammonium persulfate (APS; Thomas Scientific)
 Chloroform, CHCl_3 (RCI Labscan)
 D-Biotin (Molecular Probes)
 Deoxycholic acid sodium salt (Fisher Scientific)
 Diethyl pyrocarbonate (DEPC), $\text{C}_6\text{H}_{10}\text{O}_5$ (SIGMA)
 Dithiothreitol (DTT), $\text{C}_4\text{H}_{10}\text{O}_2\text{S}_2$ (BIO BASIC INC.)
 Dynabeads MyOne streptavidin C1 (Life Technologies)
 Ethylene diaminetetraacetic acid disodium salt dehydrate, EDTA (Ajax Finechem)
 Gel loading dye, orange, 6X (NEB)
 Isopropanol, $\text{C}_3\text{H}_7\text{OH}$ (MERCK)
 Magnesium chloride, MgCl_2 (MERCK)
 Methanol, CH_3OH (Burdick&Jackson)

N-Lauroylsarcosine sodium salt solution (20%, for molecular biology; Sigma-Aldrich)

Opti-MEM (Life Technologies)

PBS (Life Technologies)

RedSafe™ Nucleic Acid Staining Solution (iNtRON Biotechnology)

SYBR Gold nucleic acid gel stain, 10,000× (Life Technologies)

SYBR Green I nucleic acid gel stain, 10,000X (Life Technologies)

T4 RNA ligase 1 (ssRNA ligase), high concentration (NEB)

Thermo Scientific™ dNTP Set 100 mM Solutions

Trizol LS reagent (Life Technologies)

Ultrapure TEMED (Invitrogen)

Yeast extract powder (HIMEDIA)

5.2.3 Enzymes and kits

5' Deadenylase (NEB)

CircLigase II ssDNA ligase (Epicentre)

DNA ladder, 25 bp (Invitrogen)

DNA Clean & Concentrator-5 columns (Zymo Research)

Phusion high-fidelity (HF) PCR master mix with HF buffer (NEB)

Proteinase K (NEB)

S1 nuclease (ThermoFisher)

SequaGel UreaGel System, (National Diagnostics)

ShortCut RNase III (NEB)

SuperScript III reverse transcriptase (Invitrogen)

RecJf exonuclease (NEB)

RiboLock RNase inhibitor (Thermo Scientific)

RNA Clean & Concentrator-5 columns (Zymo Research)

RNase cocktail enzyme mix (Ambion)

RNase H (NEB)

T4 DNA ligase (NEB)

5.2.4 Experimental shrimp, microorganisms, cells and viruses

Pacific white shrimp *Penaeus vannamei*

White spot syndrome virus

5.2.5 PARIS library construction

The psoralen analysis of RNA interactions and structures (PARIS) is a new method that combines four critical techniques: psoralen crosslinking, 2D gel purification, proximity ligation, and high-throughput sequencing. The PARIS method employs a cell-permeable and reversible photo-crosslinker AMT (4'aminomethyltrioxsalen) to covalently link RNA duplexes in living cells. The crosslinked RNA are partially digested with RNase and run through 2-dimensional gels to selectively purify crosslinked RNA fragments, which make up a small fraction of all RNA fragments. Then, proximity ligation is used to join the trimmed duplexes, while the resulting chimeras can be sequenced and used to determine RNA structure and interaction (Figure 55).

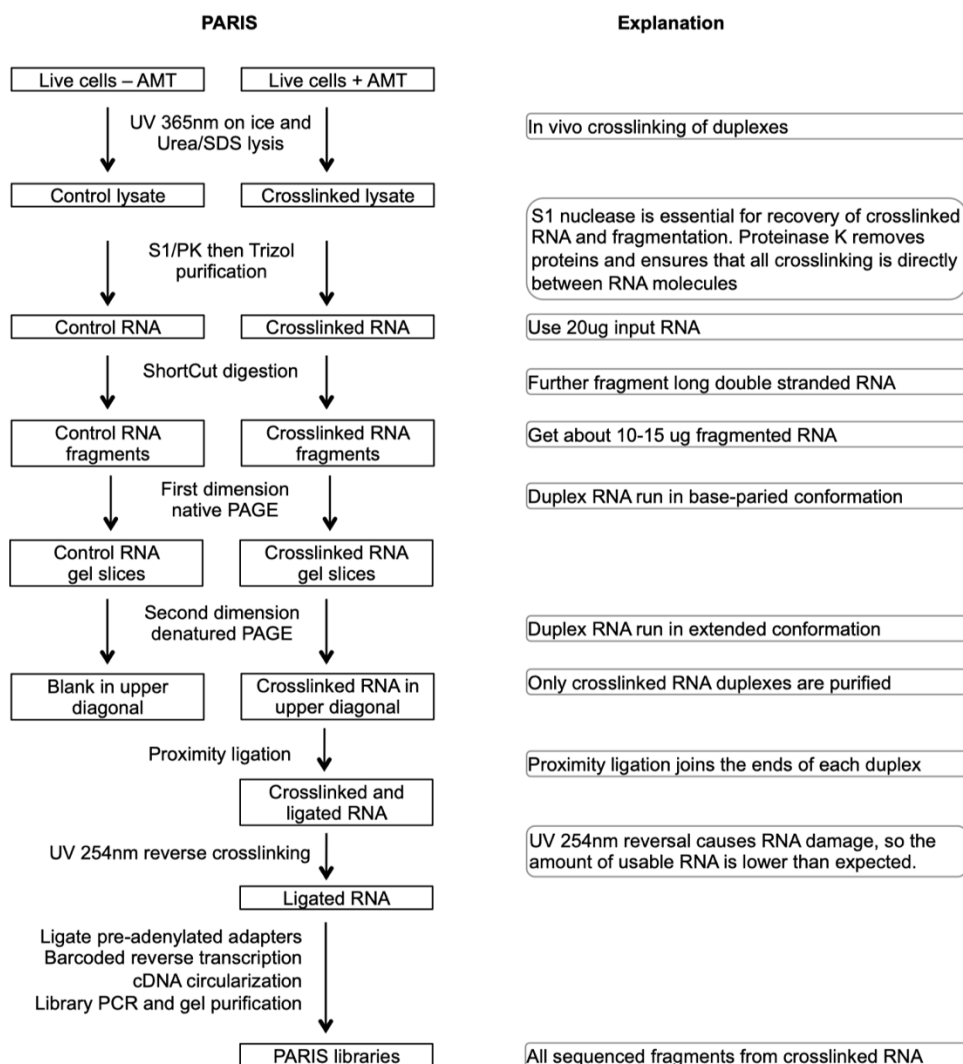


Figure 55 Outline of the PARIS experimental strategy. Major steps are explained on the right side (Lu et al., 2018).

The crosslinked RNA from WSSV- or 0.85% NaCl-injected shrimp hemocyte were performed by Miss Chantaka Wongdontri. Briefly, each 1×10^7 hemocyte cell from 15 WSSV- or 0.85% NaCl-injected shrimp was collected, washed by MAS solution, and incubated with 125 μ l 2 mg/ml AMT (Sigma, cat. no. A4330) adjusted to a volume of 250 μ l with MAS solution in 6-well plate for 30 min at room temperature. Then, AMT-incubated hemocyte were exposed under UVA at 365 nm for 30 min on ice trays in the UV chamber crosslinker. The plates were swirled every 10 min and kept horizontal so that the liquid covers all the cells. After scraping off cells in 1 ml chilled MAS solution, transferring to 1.5 ml tubes, and centrifuging at 4

°C and 400 x g for 5 min, the cell pellets were snap frozen on dry ice, and stored as pellets at 80 °C.

The AMT crosslinked cell pellets were lysed by 200 µl urea/SDS solution. Then, the cell lysate was added to 60 µl 5× S1 nuclease buffer, 2 µl S1 nuclease (Thermo), and incubated at room temperature for 20 min. Then, 33 µl 10% SDS (final concentration 1%) and 2 µl proteinase K (PK, 20 mg/mL, final 0.1 µg/µl) were added to the S1 digested lysate and incubated at 50 °C for 30 min in a thermomixer at 1000 rpm. The crosslinked RNA was extracted using TRIzol reagent. The purified crosslinked RNA were analyzed for their quality using a bioanalyzer with the Agilent RNA 6000 Pico Kit. Then, 25 µg of crosslinked RNA from each group were treated with ShortCut RNase III (NEB) to decrease the crosslinked RNA length by adding 4 µl ShortCut RNase III, 5 µl 200 mM MnCl₂, and 5 µl ShortCut buffer for a 50 µl total volume. After incubating at 37 °C for 20 min, the RNase III-treated RNA were extracted using TRIzol reagent. The purified RNase III-treated RNA were analyzed for their quality using a bioanalyzer with the Agilent Small RNA Kit. To obtain only crosslinked RNA, the 2-dimensional polyacrylamide gel electrophoresis (2D gel) was used. For the first dimension, 12% 1.5 mm thick native TBE-polyacrylamide gel electrophoresis was prepared and run at 100 V for 70 min in 0.5× TBE. After electrophoresis was complete, the gel was stained with 2 µl SYBR Gold in 20 ml 0.5× TBE and incubated for 5 min. The gel was imaged using 300 nm transillumination. Then, each lane was excised between 30 and 150 nt from the first-dimension gel. The second-dimension gel was a 20% 1.5 mm thick urea denatured gel using the UreaGel system (16 ml UreaGel concentrate, 2 ml UreaGel diluent, 2 ml UreaGel buffer, 8 µl TEMED, and 160 µl 10% APS). To make the second-dimension gel, the excised gel pieces were put in a “head-to-toe” manner with a 2-5 mm gap between them, and the gel solution was poured from the bottom of the plates. Then, the 0.5× TBE buffer was pre-warmed to 60 °C and used to fill the electrophoresis chamber. The second-dimension gel was then run at 30W for 40 min to maintain high temperature and promote denaturation. After electrophoresis was complete, the gel was stained with 2 µl SYBR Gold in 20 mL 0.5× TBE, then incubated for 5 min. The gel was imaged using 300 nm transillumination and contained crosslinked RNA cut from the 2D gel

(Figure 56). The RNA extracted from 2D gel were analyzed for their quality by a bioanalyzer using the Agilent Small RNA Kit.

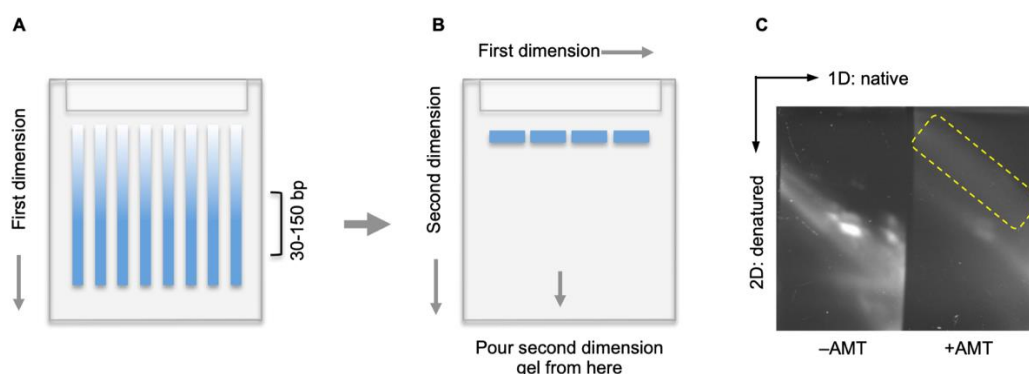


Figure 56 Diagram and example result for 2D gel purification of crosslinked and digested RNA.

(A) First-dimension native gel. Gel slices containing RNA approximately 30 – 150 bp are usually cut out from the first dimension for the second dimension. (B) Second-dimension denatured gel. Gel slices are aligned between the glass plates before pouring the urea denatured gel solution at the bottom of the gel plates (as indicated by the arrow in the middle). (C) An example second-dimension gel. The yellow boxed area indicates the crosslinked RNA to be extracted for library preparation.

Then, 10 μ l of 2D gel-extracted RNA was added to 10 μ l proximity ligation reagent (2 μ l 10 \times T4 RNA ligase buffer, 5 μ l T4 RNA ligase (high concentration), 1 μ l SUPERaseIn, 1 μ l 10 mM ATP, and 1 μ l water), then incubated at room temperature overnight. After boiling the ligation mixture at 95 $^{\circ}$ C for 2 min, ethanol precipitation was performed (resuspending RNA pellets in 12 μ l water). To reverse the AMT crosslinking, ligated RNA was placed on the clean surfaces of 12-well plates on ice trays in a crosslinking UV chamber and irradiated with 254 nm UV for 15 min. The recovered 10 μ l RNA was added to 10 μ l ligation mixture (2 μ l 10 \times T4 RNA ligase buffer, 1 μ l 0.1M DTT, 5 μ l 50% PEG8000 (50% vol/vol), 1 μ l 10 μ M pre-adenylated, 3'-biotinylated RNA adapter (/5rApp/AGATCGGAAGAGCGGTTCAG/3Biotin/) and 1 μ l high concentration T4 RNA ligase I) and incubated 3 h at room temperature. Following adapter ligation, the free adapters were removed by adding 3 μ l 10 \times RecJf buffer (NEB buffer 2), 2 μ l RecJf, 1 μ l 5'deadenylase, 1 μ l SUPERaseIn, and 3 μ l water and incubating at 37 $^{\circ}$ C for 1 hour. Then, the RNA solution was purified with Zymo RNA clean and

Concentrator-5. The purified RNA was added to 1 μ l of custom RT primer (with barcode; Table 14), heated to 70 °C for 5 min in a PCR block, cooled to 25 °C by stepping down 1 °C every 1 sec (50 steps), and held at 25 °C. The heated RNA was added to 8 μ l of reverse transcriptase enzyme mix (4 μ l 5 \times First-strand buffer, 0.75 μ l RiboLock (40 U/ μ l), 1 μ l 100 mM DTT, 1 μ l dNTPs (10 mM each), and 1.25 μ l SuperScript III reverse transcriptase) and incubated at 25 °C for 3 min, 42 °C for 5 min, 52 °C for 30 min, and held at 4 °C. Then, Dynabeads MyOne streptavidin C1 (Life Technologies) was used to purify the first-strand cDNA product. After incubating the first-strand cDNA product with C1 beads, 50 μ l of RNaseA/T1/H elution mix was resuspended with immobilized beads and incubated at 37 °C for 30 min at 1000 rpm in a thermomixer. DNA Clean & Concentrator-5 columns (Zymo Research) were used to purify the cDNA product.

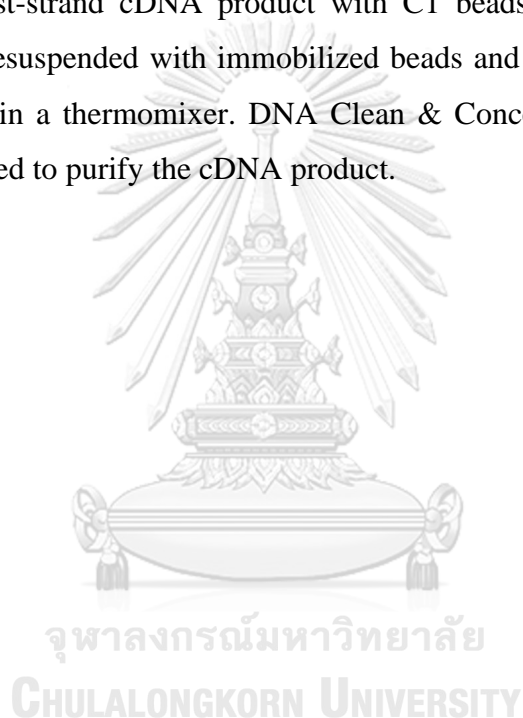


Table 14 The custom RT primer sequence

RT primer index	Sequence (5' to 3')
Index 1	/5phos/WWWNNNATCACGNNNNNTACCCTTCGCTTCACACACAAG/iSp18/GGATCC/iSp18/TACTGAAC CGC
Index 2	/5phos/WWWNNNCGATGTNNNNNTACCCTTCGCTTCACACACAAG/iSp18/GGATCC/iSp18/TACTGAAC CGC
Index 3	/5phos/WWWNNNTTAGGCNNNNNTACCCTTCGCTTCACACACAAG/iSp18/GGATCC/iSp18/TACTGAAC CGC
Index 4	/5phos/WWWNNNTGACCANNNNNTACCCTTCGCTTCACACACAAG/iSp18/GGATCC/iSp18/TACTGAAC CGC
Index 5	/5phos/WWWNNNACAGTGNNNNTACCCTTCGCTTCACACACAAG/iSp18/GGATCC/iSp18/TACTGAAC CGC
Index 6	/5phos/WWWNNNGCCAATNNNNNTACCCTTCGCTTCACACACAAG/iSp18/GGATCC/iSp18/TACTGAAC CGC
Index 7	/5phos/WWWNNNCAGATCNNNNNTACCCTTCGCTTCACACACAAG/iSp18/GGATCC/iSp18/TACTGAAC CGC
Index 8	/5phos/WWWNNNACTTGANNNNNTACCCTTCGCTTCACACACAAG/iSp18/GGATCC/iSp18/TACTGAAC CGC
Index 9	/5phos/WWWNNNGATCAGNNNNNTACCCTTCGCTTCACACACAAG/iSp18/GGATCC/iSp18/TACTGAAC CGC
Index 10	/5phos/WWWNNNTAGCTTNNNNNTACCCTTCGCTTCACACACAAG/iSp18/GGATCC/iSp18/TACTGAAC CGC
Index 11	/5phos/WWWNNNGGCTACNNNNNTACCCTTCGCTTCACACACAAG/iSp18/GGATCC/iSp18/TACTGAAC CGC
Index 12	/5phos/WWWNNNCTGTANNNNNTACCCTTCGCTTCACACACAAG/iSp18/GGATCC/iSp18/TACTGAAC CGC
Index 13	/5phos/WWWNNNAGTCAANNNNNTACCCTTCGCTTCACACACAAG/iSp18/GGATCC/iSp18/TACTGAAC CGC
Index 14	/5phos/WWWNNNAGTCCNNNNNTACCCTTCGCTTCACACACAAG/iSp18/GGATCC/iSp18/TACTGAAC CGC
Index 15	/5phos/WWWNNNATGTCANNNNNTACCCTTCGCTTCACACACAAG/iSp18/GGATCC/iSp18/TACTGAAC CGC
Index 16	/5phos/WWWNNNCCGTCCNNNNNTACCCTTCGCTTCACACACAAG/iSp18/GGATCC/iSp18/TACTGAAC CGC
Index 17	/5phos/WWWNNNGTCCGCNNNNNTACCCTTCGCTTCACACACAAG/iSp18/GGATCC/iSp18/TACTGAAC CGC
Index 18	/5phos/WWWNNNGTGAAANNNNNTACCCTTCGCTTCACACACAAG/iSp18/GGATCC/iSp18/TACTGAAC CGC
Index 19	/5phos/WWWNNNGTGCCNNNNNTACCCTTCGCTTCACACACAAG/iSp18/GGATCC/iSp18/TACTGAAC CGC
Index 20	/5phos/WWWNNNGTTTCGNNNNNTACCCTTCGCTTCACACACAAG/iSp18/GGATCC/iSp18/TACTGAAC CGC
Index 21	/5phos/WWWNNNCGTACGNNNNNTACCCTTCGCTTCACACACAAG/iSp18/GGATCC/iSp18/TACTGAAC CGC
Index 22	/5phos/WWWNNNGAGTGNNNNNTACCCTTCGCTTCACACACAAG/iSp18/GGATCC/iSp18/TACTGAAC CGC
Index 23	/5phos/WWWNNNACTGATNNNNNTACCCTTCGCTTCACACACAAG/iSp18/GGATCC/iSp18/TACTGAAC CGC
Index 24	/5phos/WWWNNNATTCCTNNNNNTACCCTTCGCTTCACACACAAG/iSp18/GGATCC/iSp18/TACTGAAC CGC
/5phos/ = 5' Phosphorylation; /iSp18/ = A spacer to prevent PCR from forming concatemers; W = A/T and N = A/T/G/C	

To circularize the cDNA library, 4 μ l of circularization reaction mix (2 μ l 10 \times CircLigase II buffer, 1 μ l 50 mM MnCl₂, and 1 μ l CircLigase II) was added and incubated at 60 °C for 100 min, followed by 80 °C for 10 min. Then, the circularized cDNA was added with qPCR reaction mixture (10 μ l 2 \times Phusion HF PCR master mix, 0.2 μ l 25 \times SYBR Green I, 0.25 μ l P3/P6 TaII v4 PCR primer mix (20 μ M forward and 20 μ M reverse)) and amplified by qPCR machine using 10 cycles of 95 °C for 15 sec, 65 °C for 30 sec, and 72 °C for 45 sec. The Ampure XP beads were used for the cDNA library purification. To add the universal Illumina sequence annealing onto the cartridge, P3/P6 Solexa PCR primers were used for amplification of the cDNA library (P3-Solexa PCR primer: 5'-CAAGCAGAAGACGGCATAACGAGATCGGTCTCGGCATTCCTGCTGAACCGCTCTTCCGATCT-3' and P6-Solexa PCR primer: 5'-AATGATACGGCGACCACCGAGATCT-3'). The cDNA library was added 20 μ l 2 \times Phusion HF master mix and 2 μ l 20 μ M P3/P6 Solexa PCR primer (final 1 μ M) and a PCR reaction was run (95 °C, 45"; 3 cycles of 95 °C, 15"; 65 °C, 20"; 72 °C, 45"; and 4 °C on hold). DNA Clean & Concentrator-5 columns (Zymo Research) were used to purify the cDNA product. Then, 6% native TBE gel was run to separate the cDNA library at 100V for 75 min. Then, the cDNA with sizes above 150 bp were excised and eluted by adding 300 μ l water during shaking at 55 °C and 1000 rpm overnight on a thermomixer. DNA Clean & Concentrator-5 columns (Zymo Research) were then used to purify the cDNA library. Lastly, the library was sequenced on an Illumina sequencer using standard conditions and the P6_Custom_seq primer (CACTC TTTCC CTTG TGTGT GAAGC GAAGG GTA). The 70 nt single end sequencing reaction is sufficient for PARIS.

5.3 Results

The PARIS method was used to directly identify base-paired helices (the most basic elements in RNA structures) and RNA-RNA interactions using nucleic acid crosslinker psoralen-derivative 4'-aminomethyltrioxsalen (AMT) to fix base pairs in living cells (Lu et al., 2018).

5.3.1 Establishment of mRNAs and small RNA of WSSV-infected *P. vannamei* hemocyte by the Next generation sequencing and used as reference

5.3.1.1 Next generation sequencing

The NGS of RNA-Seq and small RNA-Seq of WSSV-infected shrimp was performed in the Hi-Seq Illumina platform in order to gain more deep transcript data. Total RNA from WSSV- or 0.85% NaCl-injected shrimp hemocyte at 24 hpi were prepared by Miss Chantaka Wongdontri. The purified total RNA were analyzed for their quality by Bioanalyzer using the Agilent RNA 6000 Pico Kit. The obtained electropherogram (a plot of migration time against fluorescence unit [FU]) and gel-like images of total RNA samples revealed a predominant band of 18S rRNA of approximately 1.9 kb in size as well as some small RNA (Figure 57). The RNA-Seq and small RNA-Seq were performed by Novogene Corporation, USA.

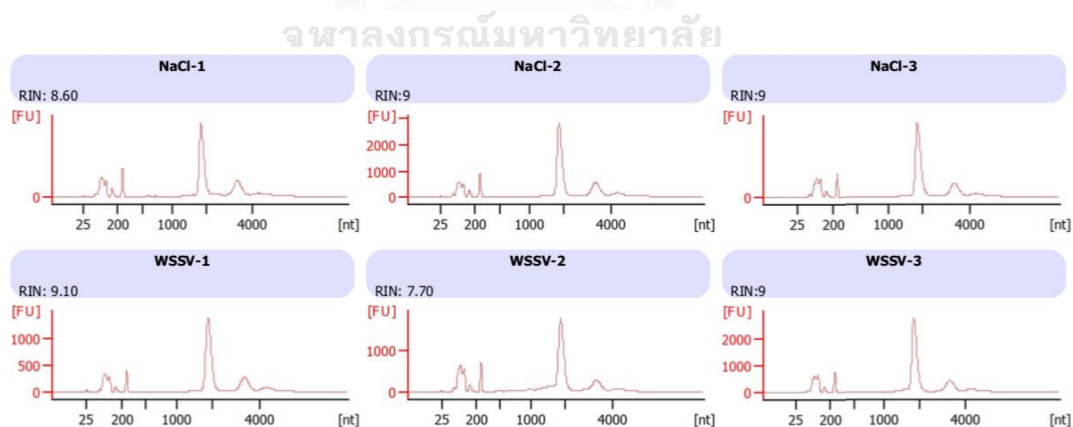


Figure 57 Analysis of total RNA quality using a Bioanalyzer.

The total RNA of WSSV- or 0.85% NaCl-injected shrimp at 24 h were analyzed by Agilent RNA 6000 Pico Kit on bioanalyzer instrument.

5.3.1.2 Differential expression of genes in *P. vannamei* hemocyte upon WSSV infection

Biological replicates are necessary for any biological experiment, including those involving RNA-Seq technology (Hansen et al., 2011). In RNA-Seq, replicates have a two-fold purpose. First, they demonstrate whether the experiment is repeatable. Secondly, they can reveal differences in gene expression between samples. The correlation between samples is an important indicator for testing the reliability of an experiment. The closer the correlation coefficient to 1, the greater the similarity of the samples. The results of the present study suggested that the square of the Pearson correlation coefficient was larger than 0.8 in both NaCl and WSSV (Figure 58). DEGs in *P. vannamei* hemocyte upon WSSV infection were then identified by pairwise comparisons between relevant groups of three biological replicates and expressed as fold-changes against a specific group. The overall results of FPKM cluster analysis are presented in Figure 59. Among the DEGs, only shrimp immune-related genes were identified (Table 15).

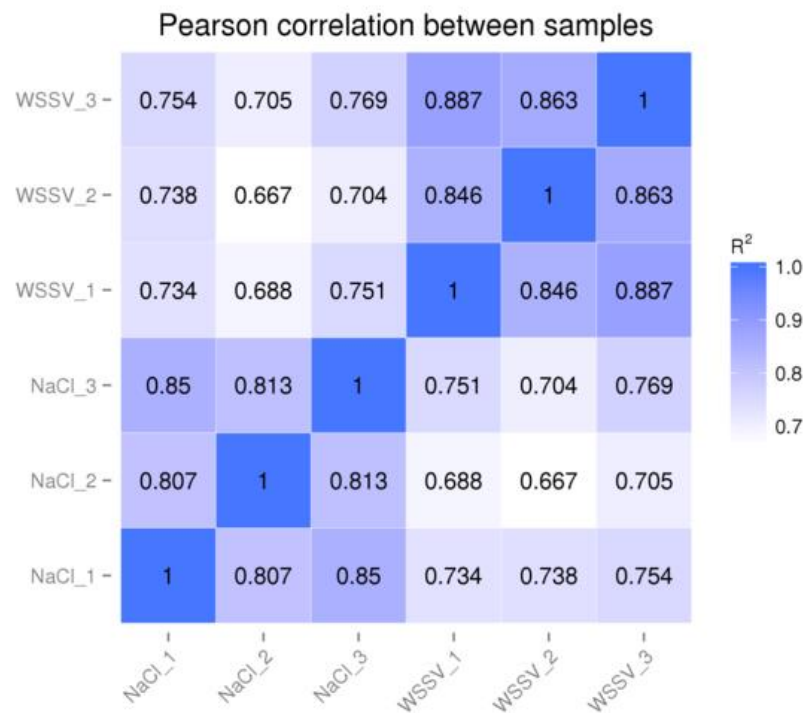


Figure 58 Sample correlation analysis by Pearson correlation. The differences in gene expression between NaCl and WSSV libraries that were differentially expressed

($P < 0.05$) by at least 2-fold were generated as a matrix table. The unigenes from each library were counted. Sample correlations were calculated using ENCODE software.

Cluster analysis of differentially expressed genes

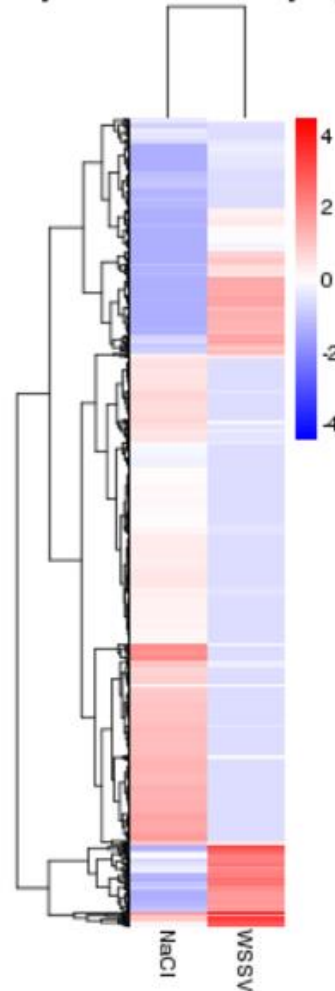


Figure 59 The overall results of FPKM cluster analysis based on clustering using the $\log_{10}(\text{FPKM}+1)$ value.

Red denotes genes with high expression levels, while blue denotes genes with low expression levels. The color range from red to blue represents $\log_{10}(\text{FPKM}+1)$ values from large to small.

Table 15 Differentially expressed genes from shrimp hemocyte upon WSSV infection that were involved in shrimp immunity

gene_id	log2(FoldChange)	Gene homolog
Cluster-57413.43823	-13.13	dynammin-like 120 kDa protein
Cluster-23090.0	-5.09	clathrin interactor 1-like isoform X4
Cluster-57413.20659	-3.06	rho guanine nucleotide exchange factor 7-like
Cluster-57413.15816	-2.65	alpha2 macroglobulin isoform 3
Cluster-57413.19142	-2.62	heat shock protein 67B2
Cluster-41969.0	-1.49	heat shock protein isoform 12Ai1
Cluster-57413.24830	1.45	heat shock protein HSP 90-alpha
Cluster-19343.2	1.82	hemocyte homeostasis-associated protein
Cluster-57413.31631	2.65	caspase 5
Cluster-57413.44885	2.78	heat shock protein 60
Cluster-37376.1	2.81	chitinase
Cluster-45976.4	3.02	heat shock factor 1
Cluster-4786.4	3.1	innexin inx2-like (LOC113830071), mRNA
Cluster-57413.9261	5.5	caspase
Cluster-57413.33109	11.6	<i>Penaeus vannamei</i> hsc70-interacting protein-like
Cluster-57413.22736	12.38	E3 ubiquitin-protein ligase RNF103-like
Cluster-57413.28405	15.59	cytochrome c (LOC113825161),

5.3.1.3 Small RNA-Seq data analysis

High-throughput sequencing generated total raw reads for six libraries including 29,026,777 in NaCl-1, 31,354,307 in NaCl-2, 28,971,867 in NaCl-3, 33,861,122 in WSSV-1, 32,409,633 in WSSV-2, and 132,641,660 in WSSV-3. High quality sequences that passed initial quality filters included 165,725,975 reads for all the experimental group libraries. Among these, a total of 136,826,232 reads from all experimental group were 18-24 nt (Table 16). A hierarchy-clustered heatmap revealed the correlation of triplicated small RNA libraries of NaCl- and WSSV-injected shrimp by comparing both NaCl and WSSV libraries (Figure 60). A total of 74 miRNA homologs were identified from the WSSV-infected *P. vannamei* hemocytes (Table 17).

Table 16 Summary of sequences identified from the small RNA libraries of *P. vannamei* hemocyte infected with WSSV at 24 hpi

Library name	Raw reads	Clean reads (Q30)	3' Adapter clipping	5' Adapter clipping	18-24 nt
NaCl-1	29,026,777	25,482,879	24,129,236	23,343,138	20,142,702
NaCl-2	31,354,307	27,644,958	26,631,410	25,801,627	22,831,679
NaCl-3	28,971,867	25,525,917	23,262,364	22,510,281	20,027,675
WSSV-1	33,861,122	30,014,895	29,315,688	28,303,217	25,161,190
WSSV-2	32,409,633	28,608,896	27,682,533	27,040,455	24,535,564
WSSV-3	32,641,660	28,448,430	27,371,106	26,598,375	24,127,422

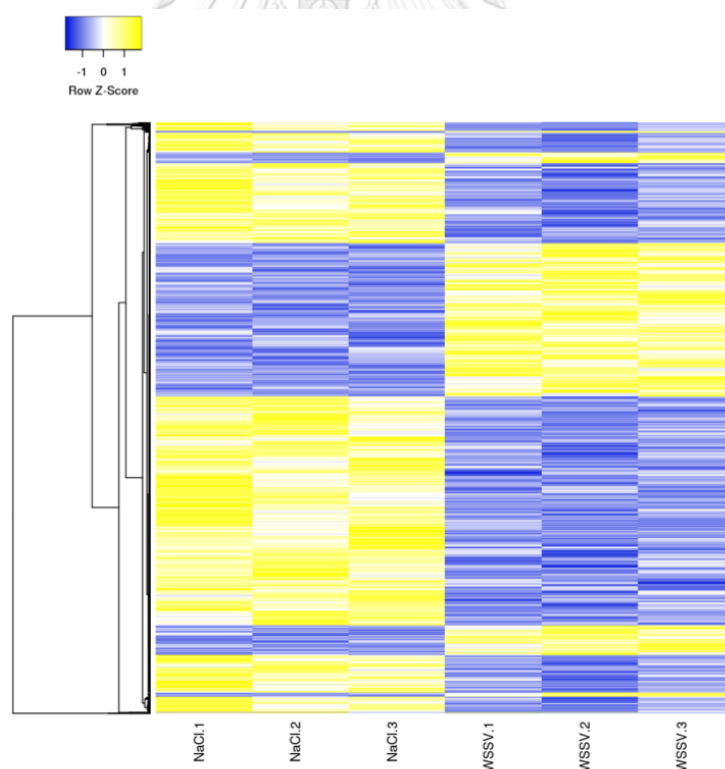


Figure 60 Hierarchy-clustered heatmap of (TMM-normalized) FPKM expression values for miRNAs (represented in rows) that were at least 2-fold differentially expressed ($P < 0.05$).

Table 17 Nucleotide sequences of differentially expressed miRNA homologs identified in WSSV-infected *P. vannamei* hemocytes

miRNA homolog	Sequence	log ₂ (Fold change)
lva-miR-6493-3p	AAGGGGGAAACCGCGCTGAGC	-2.32
lva-miR-3334	GTGCATGGAATGATGGAAC	-2.01
lva-miR-7977	TCGTTTCCCGGCCGACGCACCA	-1.93
lva-miR5719	TATTGTGATGATACATTTA	-1.91
lva-miR7532b	AGCCTCTGGTCGATAGATC	-1.87
lva-miR-12457-3p	ATCCCGGGTCTGGGCACCA	-1.76
lva-miR-36e-5p	TTTCACCAAGCGTAGGATT	-1.68
lva-miR-9344	AGAACCCTGTAGAGAGAGTTCAAG	-1.64
lva-miR-6763-3p	CTCGGGCAAAGGCCGGGGTTTCCC	-1.64
lva-miR5049-3p	CTTCCCTCCGATCCCCTGG	-1.62
lva-miR-1421k-3p	ATCCCGTGACCTGCCCTGT	-1.61
lva--miR-m01-2-3p	CCATCGACGTGTCTGAACGC	-1.6
lva-miR-10550-3p	TTGAAAATCTTCTAAACTGAAC	-1.6
lva-miR11108p-5p	TTGAATGATGAGAATGAATT	-1.56
lva-miR-4443	TCTCTCAGGAGGCGTGGGT	-1.54
lva-miR-8920	GCCGGGCCCGCGGCCGCTCTGCGC	-1.53
lva-miR-8364f-3p	AGGAAAATGAAGATTCTGATA	-1.49
lva-miR-100e-3p	GACGGGGTTCGGGTCCCGCGAGC	-1.48
lva-miR5023	GCTTGGTCGTGGATAAGTCGGC	-1.48
lva-miR-10010-5p	CTCTCACCCGCGAGGCCCGG	-1.48
lva-miR-28a-3p	GTGAGATTGTGATCTGCTGGGAGC	-1.48
lva-miR-148a-5p	AGACGGCCGTCTCAGAACT	-1.47
lva-miR-279c-5p	GGTAAGTGGAACCTTGTTTCATG	-1.45
lva-miR-8447-3p	GAGCAATGATGAGTGTCTGTG	-1.45
lva-miR7749-5p	TAAACGGGCGGAGATTCTGA	-1.44
lva-miR-12023	AAAAAGGGGGGAGGGAGGAGC	-1.4
lva-miR-12060	ACGGACCAGGGGAATCCGACT	-1.39
lva-miR-7286b-5p	GTGAGATTGTGATCTGTTGGG	-1.36
lva-miR-8236-3p	TTTAGACTGCAAGTGACATGAACA	-1.36
lva-miR-10607	GCCCAGTGCTCTGAATGTCAAAGT	-1.35
lva-miR-7382-5p	GAAGGCTCTTCTCGAGTGTCTGTG	-1.34

miRNA homolog	Sequence	log₂(Fold change)
lva-miR-7911c-5p	CGTTTCCCGGCCGATGCACCA	-1.32
lva-miR156h-3p	ATGTCGGCTCTTCCTATCATT	-1.29
lva-miR8719	ATTACTTGGATAACTGTGGTA	-1.27
lva-miR-125a	TCCCTGAGACCCTTTCTTG	-1.25
lva-miR6112	ACTTTTTGACACCTGAAA	-1.24
lva-miR-1-3p	TGGAATGTAAAGAAGTATGGAAA	-1.23
lva-miR5801c-3p	GACTCTGAATCCAACAATC	-1.22
lva-miR-10366a-2-5p	ATATCGGCTGGGGTGTGTACCGG	-1.2
lva-miR-5988	CGTGATTCCATCGACGTGTC	-1.16
lva-miR-1550-5p	CGCTTTGGGGGTGTAGCTC	-1.15
lva-miR482c-5p	TGTACTTGTCCGGTAGCTC	-1.11
lva-miR-10485-5p	TCATTTCCCGGACAGGCCCCCA	-1.11
lva-miR-981-5p	CCCGAAACCCGGTCGTCGTGC	-1.1
lva-miR-1193-3p	CCTGTCACGCGGGAGACCGGGG	-1.1
lva-miR-190-5p	TGATTTTCGTGGTCACTGATA	-1.09
lva-miR-12200-5p	AGTGTGAGCCTCTGAGCGGAAGC	-1.09
lva-miR2275a	ATATTATGAAGGAAACCGAAG	-1.08
lva-miR-7144-3p	TCGGGACAAGGATTGGCTCT	-1.08
lva-miR-1995	CCCACCATCGCATTGTGACCG	-1.08
lva-miR169i-5p.2	CGACTGGGGGTGTAGCTCT	-1.06
lva-miR-975-3p	GAGTGGGGTTCGTTGGCCGTA	-1.06
lva-miR-143-3p	TGAGATGAAGCACTGTAGCTCGT	-1.05
lva-miR-184-5p	CCTTATCATTTCGTCACTCCAG	-1.01
lva-miR-10353	ATAGTCGACGGATCTCAACC	-1
lva-miR-9e-5p	TCTTTGGTGATCTAGTTGTGTGA	-1
lva-miR-11204d-3p	GTGGAGCAAAAAGGTCTTT	1.06
lva-miR-4882a	GCTCTCCTGTAAGGATTCTCTT	1.07
lva-miR-100	AACCCGTAGATCCGAACCTTGTTTC	1.09
lva-let-7a	TGAGGTAATAGGTTGTATAGTC	1.14
lva-miR-2a-3p	TATCACAGCCTACTTGACGTGT	1.16
lva-miR-7a-5p	TGGAAGACTAGTGATCTTGTGTGC	1.21
lva-miR-279b-3p	TGACTAGATTAGCACTCGCT	1.22
lva-miR-87-5p	TGACTAGGCTCTTGCTCATCT	1.23
lva-miR-9226-5p	CCCTGTTCCGGCGAACACTTT	1.24
lva-miR-9618-5p	TGGCAGAGGGCCCATGGTTTT	1.29

miRNA homolog	Sequence	log ₂ (Fold change)
lva-miR-61a-3p	TGACTAGACTCTTACTAATCC	1.32
lva-miR-7-5p	TGGAAGACTAGTGATTTTCGTTGTC	1.42
lva-miR-279b	TCTGACTAGACTCCTACTCATCT	1.44
lva-miR-3689c	GGAGGTGTGATAGCCTAGTG	1.49
lva-miR8574	TGACTATACTCTTACTCATCC	1.79
lva-miR-10931	GTGGTGACTCTTTTCTCT	2.14
lva-miR-6489-5p	CCGGACTGGCGCCCTGGAGCT	2.24
lva-miR5225b	TCTGTCTGAAGGTGGACGTCTTT	2.66

5.3.2 PARIS library construction

The crosslinking of RNA from WSSV- or 0.85% NaCl-injected shrimp hemocyte were prepared by Miss Chantaka Wongdontri. The purified crosslinked RNA was analyzed for their quality by Bioanalyzer using the Agilent RNA 6000 Pico Kit. The obtained electropherogram (a plot of migration time against fluorescence unit [FU]) and gel-like images of total RNA samples revealed a predominant peak of crosslinked RNA size of approximately 1000-4000 nt (Figure 61). Then, 25 µg of the crosslinked RNA from each group was treated with ShortCut RNase III to decrease the crosslinked RNA length. The RNase III-treated RNA were then extracted using TRIzol reagent. The purified RNase III-treated RNA were analyzed for their quality by a Bioanalyzer using the Agilent Small RNA Kit. The bioanalyzer identified a predominant peak of crosslinked RNA size of approximately 4-150 nt (Figure 62). To obtain only crosslinked RNA, a 2-dimensional polyacrylamide gel electrophoresis (2D gel) was used (Figure 63). The extracted RNA from the 2D gel were analyzed for their quality by Bioanalyzer using the Agilent Small RNA Kit. The crosslinked RNA size range of approximately 20-150 nt was found only in the AMT-incubated hemocyte (Figure 64).

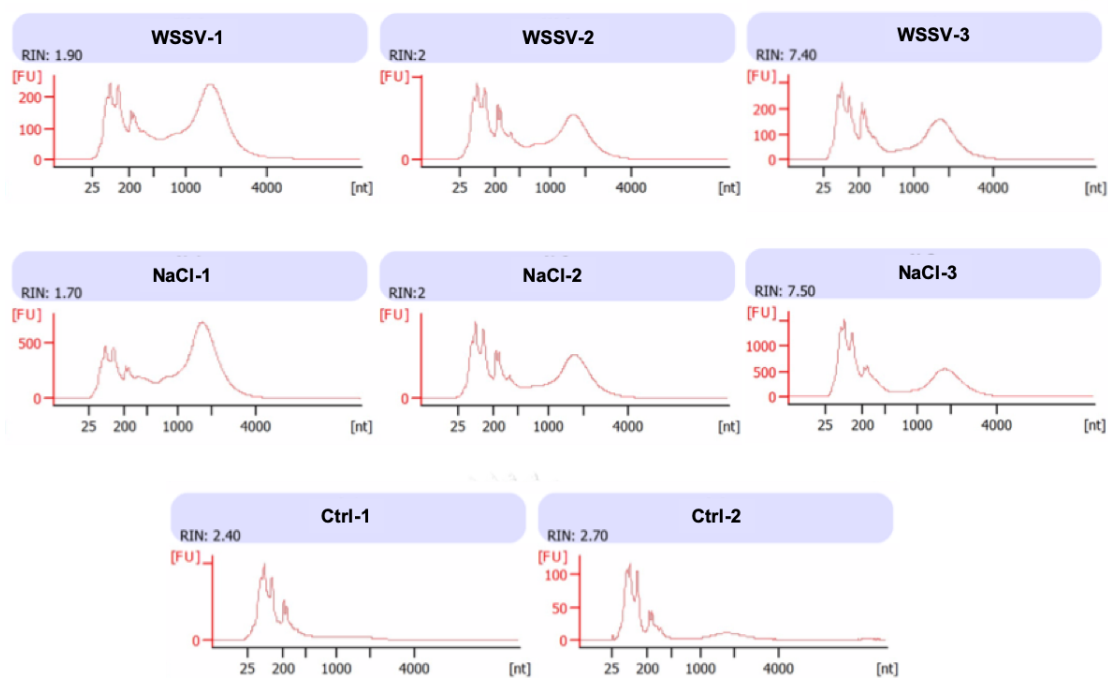


Figure 61 Analysis of crosslinked RNA quality using a Bioanalyzer. The crosslinked RNA of WSSV- or 0.85% NaCl-injected shrimp at 24 h were analyzed by Agilent RNA 6000 Pico Kit on a bioanalyzer instrument. The un-crosslinked RNA was used as a control.

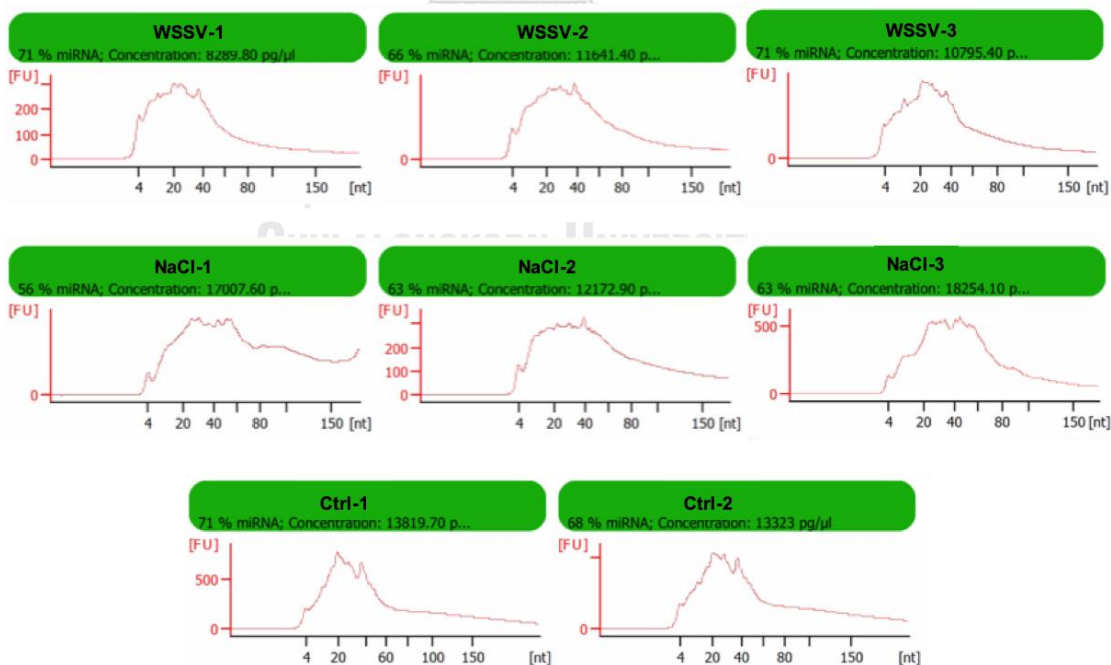


Figure 62 Analysis of purified RNase III-treated RNA quality using a Bioanalyzer. The RNase III-treated RNA of WSSV- or 0.85% NaCl-injected shrimp at 24 h were analyzed by Agilent Small RNA Kit on a bioanalyzer instrument. The un-crosslinked RNA were used as a control.

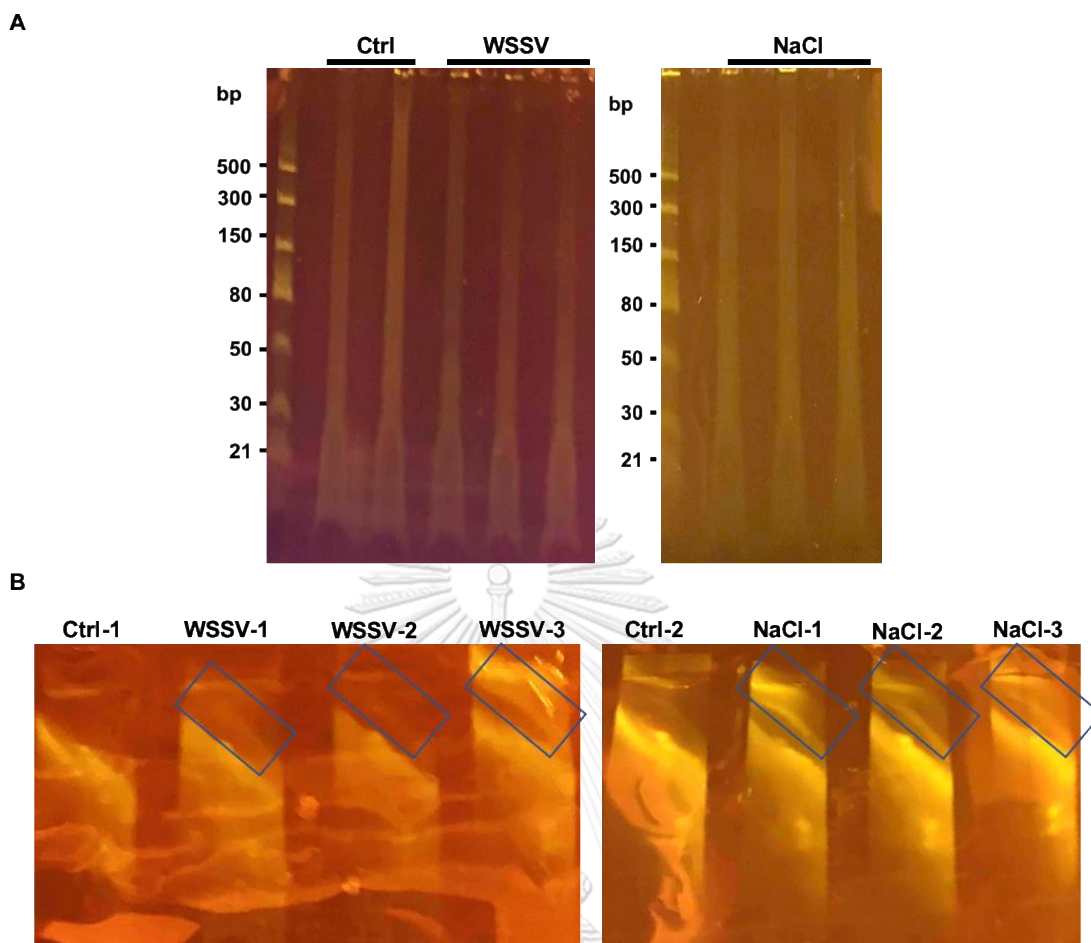


Figure 63 Analysis of crosslinked RNA libraries constructed by 2D gel.

RNase III-treated RNA was run using native 6% acrylamide gel electrophoresis for 75 min (A). Only the RNA size of about 30-150 nt were cut. The gel pieces of length-selected RNA were loaded and run using denatured 8% acrylamide gel electrophoresis (urea system) for 40 min (B). The blue squares show the crosslinked RNA area.

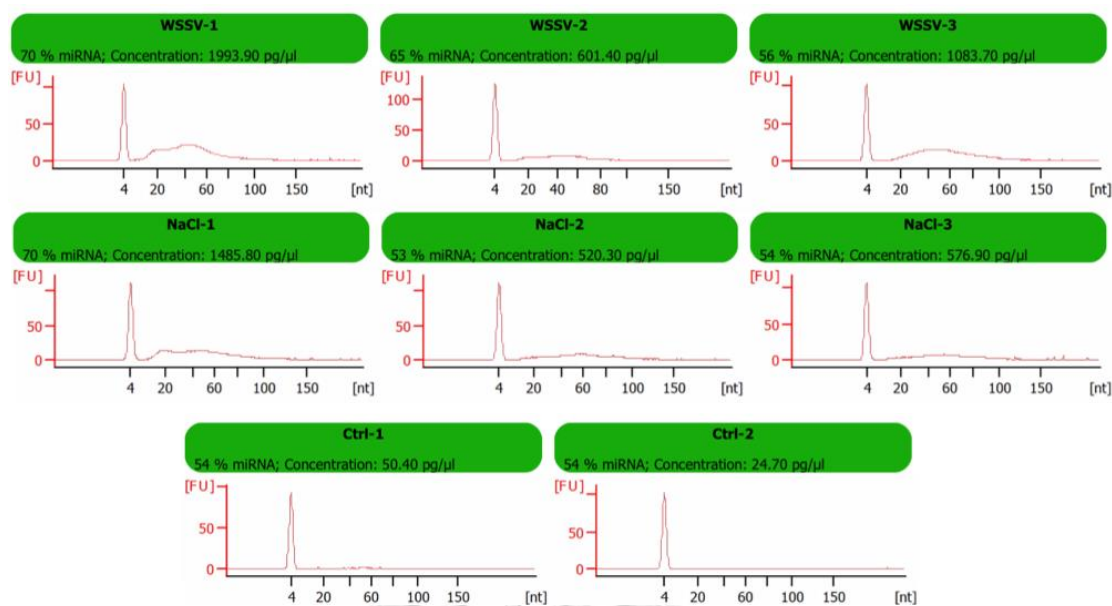


Figure 64 Analysis of extracted RNA quality using a Bioanalyzer.

The RNase III-treated RNA of WSSV- or 0.85% NaCl-injected shrimp at 24 h were analyzed using an Agilent Small RNA Kit and bioanalyzer instrument. The uncrosslinked RNA was used as a control.

For PARIS construction, the crosslinked RNA extracted from 2D gel were ligated using T4 ssRNA ligase, reverse crosslinked under UV at 254 nm, ligated adaptor, reverse transcription, and amplification following the PARIS protocol. A total of six PARIS libraries of WSSV- and 0.85% NaCl-injected shrimp hemocyte was successfully constructed. The amplified cDNAs were analyzed by a bioanalyzer using a high-sensitivity DNA kit. The Bioanalyzer 2100 output data indicated that the PARIS libraries had an expected size of approximately 150-300 nucleotides; however, the contaminated sequence of the adapter (75 nucleotides fragment) was found in WSSV-1 and WSSV-3 (Figure 65). Then, the cDNA libraries will be sequenced using Hi-Seq Illumina platform at Novogene Corporation Inc., Sacramento, CA, USA.

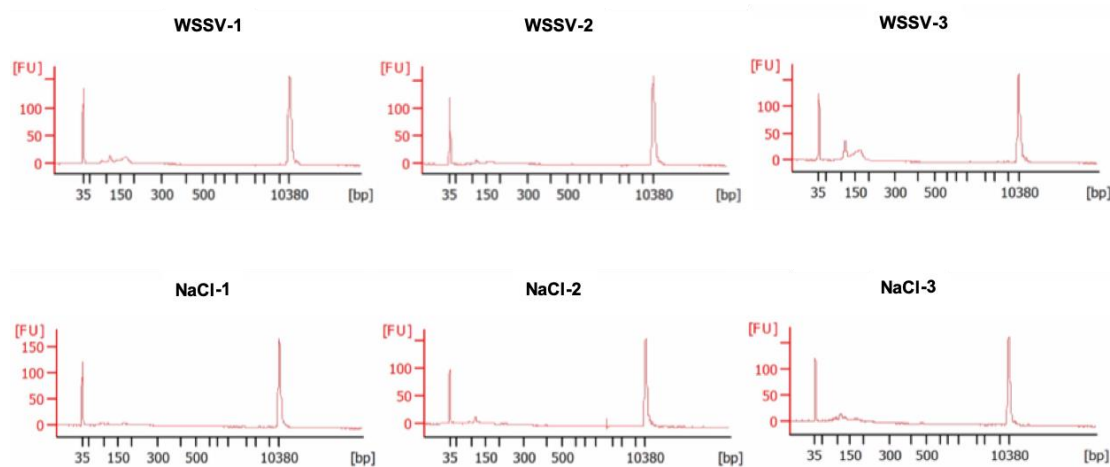


Figure 65 Quantitative analysis of PARIS libraries using bioanalyzer. The amplified products of PARIS libraries (WSSV-1, WSSV-2, WSSV-3, NaCl-1, NaCl-2, and NaCl-3) were electrophoresed using an Agilent High-sensitivity DNA Kit.



5.4 Discussion

RNA has the intrinsic property to base pair and form complex structures fundamental to its diverse functions. The psoralen analysis of RNA interactions and structures (PARIS), a method based on reversible psoralen-crosslinking for global mapping of RNA duplexes with base-pair resolution in living cells, was developed (Lu et al., 2017). In this study, the PARIS was used to identify the global analysis of small RNAs and their partner RNA targets from shrimp upon WSSV infection. Previously, RNA-RNA interaction assay using PARIS was used to identify global RNA interaction in human cell upon viral infection (Huber et al., 2019). It was found that a network of pairwise interactions within the viral genome that likely work together to support and facilitate virus fitness leading to guide the design of broad-based RNA therapeutics that target the critical RNA structures of these pathogenic viruses

Since the shrimp genome has not been well annotated, the NGS of RNA-Seq and small RNA-Seq were performed and the transcriptome database will be used as reference sequences for PARIS analysis. In 2013, the transcriptome profiles in hemocytes of unchallenged and WSSV-challenged shrimp *P. vannamei* were performed. Among all the annotation, the 1,179 unigenes were associated with shrimp immune-related genes (Xue et al., 2013). In our study, 17 differentially expressed unigenes were identified from NGS data as immune-related genes. Among both libraries, cytochrome c, hemocyte homeostasis-associated protein, heat shock protein 90 and heat shock 60 were differentially expressed after WSSV infection on the other hand, A total of 74 miRNA homologs were identified from the WSSV-infected *P. vannamei* hemocytes. According to Sun et al., 2016, Sixteen or twenty-one differential miRNAs were up- or down-regulated respectively. Only miR-278 was shared the same trend between both NGS data.

CHAPTER VI

CONCLUSIONS

1. Identification and functional characterization of genes from *P. vannamei* hemocyte and hepatopancreas in response to *Vibrio parahaemolyticus* AHPND (VP_{AHPND}) infection by suppression subtractive hybridization (SSH).

1.1 Using SSH, genes that are up-regulated at the early and late phases of VP_{AHPND} infection in *Penaeus vannamei* hemocyte and hepatopancreas were identified, and the indeed up-regulation of the VP_{AHPND}-responsive genes was verified by qRT-PCR.

1.2 In hepatopancreas, 5 hemocyanin isoforms were identified as DEGs. *HMC* was up-regulated at early phase of VP_{AHPND} infection whereas *HMCL3* and *HMCL4* were induced in response to VP_{AHPND} toxin at the early phase of injection. Immune-related function study showed that hemocyanin could induce bacterial agglutination and neutralize VP_{AHPND} toxin via PirA interaction resulting in the reduction of shrimp mortality.

1.3 *Vago5* was up-regulated in *P. vannamei* hemocyte at early phase of VP_{AHPND} infection and played a crucial role in shrimp antibacterial immunity as its gene knockdown led to the increase in bacterial number and cumulative mortality in VP_{AHPND}-infected *P. vannamei*.

2. Integrated analysis of microRNA and mRNA expression profiles in *P. vannamei* hemocyte challenged with VP_{AHPND} under non-lethal heat shock (NLHS) condition

2.1 The differentially expressed miRNAs (DEMs) and genes (DEGs) upon VP_{AHPND} infection under non-lethal heat shock (NLHS) and normal (NH) conditions were successfully identified by NGS and validated by qRT-PCR.

2.2 A total number of NLHS-VP-responsive transcripts are 3,980 and of NH-VP responsive transcripts are 3,141. Eighteen NLHS-VP-responsive miRNAs and 2 NH-VP responsive miRNAs were identified.

- 2.3 The miRNA-mRNA interaction prediction based on their expression profiles in NLHS-treated *P. vannamei* hemocyte challenged with VP_{AHPND} identified 183 DEMs -DEGs pairs with negative correlation. DEMs that have high degrees of connectivity to DEGs are lva-miR-7278-5p, lva-miR-6831-5p, lva-miR-745b, lva-miR-9041-5p, lva-miR-502b-3p and lva-miR-2898.
- 2.4 Taken together, the NLHS modulates several immune genes involved prophenoloxidase system, hemocyte homeostasis, and antimicrobial peptide production via the IMD pathway in *P. vannamei* hemocyte.

3. Identification and functional characterization of miRNAs in shrimp hemocyte of VP_{AHPND}-infected *P. vannamei*

- 3.1 NGS could identify DEMs from VP_{AHPND}-infected hemocyte and their expression levels were confirmed by stem-loop qRT-PCR.
- 3.2 The predicted target genes of these DEMs are involved in Toll pathway, IMD pathway, endocytosis, prophenoloxidase, apoptosis, heat shock protein, pattern recognition receptor, cytokines, proteinases and proteinases inhibitors.
- 3.3 The direct interaction between the interesting miRNA, lva-miR-4850, and the target sequence at 3'-UTR of PO2 gene was confirmed.
- 3.4 Introducing the mimic lva-miR-4850 into the VP_{AHPND}-infected shrimp caused the reduction of the PO2 transcript level and PO activity whereas the bacterial number in the shrimp stomach and hepatopancreas were increased. These results suggested that lva-miR-4850 is a regulator of prophenoloxidase system.

4. Identification of miRNAs and their interacting partners from WSSV-infected *P. vannamei* hemocyte using psoralen analysis of RNA interactions and structures (PARIS).

- 4.1 Deep transcriptomic data of mRNAs and small RNAs of WSSV-infected *P. vannamei* hemocyte was obtained by the NGS and used as reference databases for miRNAs and their interacting partners identification.
- 4.2 The RNA from WSSV-infected *P. vannamei* hemocyte was successfully crosslinked by psoralen.

4.3 The PARIS cDNA libraries were successfully constructed from the psoralen-crosslinked RNA for miRNAs and their interacting partners identification.



REFERENCES

- Adams A. Response of penaeid shrimp to exposure to *Vibrio* species. *Fish & Shellfish Immunology*. 1991 Jan 1;1(1):59-70.
- Afgan E, Baker D, Van den Beek M, Blankenberg D, Bouvier D, Čech M, Chilton J, Clements D, Coraor N, Eberhard C, Grüning B. The Galaxy platform for accessible, reproducible and collaborative biomedical analyses: 2016 update. *Nucleic acids research*. 2016 May 2;44(W1):W3-10.
- Alshalalfa M. MicroRNA response elements-mediated miRNA-miRNA interactions in prostate cancer. *Advances in bioinformatics*. 2012;2012.
- Altschul SF, Gish W, Miller W, Myers EW, Lipman DJ. Basic local alignment search tool. *Journal of molecular biology*. 1990 Oct 5;215(3):403-10.
- Amparyup P, Charoensapsri W, Tassanakajon A. Prophenoloxidase system and its role in shrimp immune responses against major pathogens. *Fish & shellfish immunology*. 2013 Apr 1;34(4):990-1001.
- Amparyup P, Charoensapsri W, Tassanakajon A. Prophenoloxidase system and its role in shrimp immune responses against major pathogens. *Fish & shellfish immunology*. 2013 Apr 1;34(4):990-1001.
- Apitanyasai K, Amparyup P, Charoensapsri W, Senapin S, Tassanakajon A. Role of *Penaeus monodon* hemocyte homeostasis associated protein (*Pm*HHAP) in regulation of caspase-mediated apoptosis. *Developmental & Comparative Immunology*. 2015 Nov 1;53(1):234-43.
- Ashburner M, Ball CA, Blake JA, Botstein D, Butler H, Cherry JM, Davis AP, Dolinski K, Dwight SS, Eppig JT, Harris MA. Gene ontology: tool for the unification of biology. *Nature genetics*. 2000 May 1;25(1):25.
- Assavalapsakul W, Smith DR, Panyim S. Identification and characterization of a *Penaeus monodon* lymphoid cell-expressed receptor for the yellow head virus. *Journal of virology*. 2006 Jan 1;80(1):262-9.
- Assavalapsakul W, Tirasophon W, Panyim S. Antiserum to the gp116 glycoprotein of yellow head virus neutralizes infectivity in primary lymphoid organ cells of *Penaeus monodon*. *Diseases of aquatic organisms*. 2005 Jan 25;63(1):85-8.
- Austin B, Zhang XH. *Vibrio harveyi*: a significant pathogen of marine vertebrates and invertebrates. *Letters in applied microbiology*. 2006 Aug;43(2):119-24
- Azzam G, Smibert P, Lai EC, Liu JL. *Drosophila* Argonaute 1 and its miRNA biogenesis partners are required for oocyte formation and germline cell division. *Developmental biology*. 2012 May 15;365(2):384-94.
- Bartel DP. MicroRNAs: genomics, biogenesis, mechanism, and function. *cell*. 2004 Jan 23;116(2):281-97.
- Baruah K, Norouzitallab P, Linayati L, Sorgeloos P, Bossier P. Reactive oxygen species generated by a heat shock protein (Hsp) inducing product contributes to Hsp70 production and Hsp70-mediated protective immunity in *Artemia franciscana* against pathogenic vibrios. *Developmental & Comparative Immunology*. 2014 Oct 1;46(2):470-9.

- Bonami JR, Hasson KW, Mari J, Poulos BT, Lightner DV. Taura syndrome of marine penaeid shrimp: characterization of the viral agent. *Journal of General Virology*. 1997 Feb 1;78(2):313-9.
- Bradford MM. A rapid and sensitive method for the quantitation of microgram quantities of protein utilizing the principle of protein-dye binding. *Anal Biochem* (1976);72(1-2):248-54. doi: 10.1016/0003-2697(76)90527-3
- Bratvold D, Lu J, Browdy CL. Disinfection, microbial community establishment and shrimp production in a prototype biosecure pond. *Journal of the World Aquaculture Society*. 1999 Dec;30(4):422-32.
- Bravo A, Gómez I, Conde J, Muñoz-Garay C, Sánchez J, Miranda R, Zhuang M, Gill SS, Soberón M. Oligomerization triggers binding of a *Bacillus thuringiensis* Cry1Ab pore-forming toxin to aminopeptidase N receptor leading to insertion into membrane microdomains. *Biochimica et Biophysica Acta (BBA)-Biomembranes*. 2004 Nov 17;1667(1):38-46.
- Brock JA, Lightner DV. Diseases caused by microorganisms. *Diseases of marine animals*. 1990;3:245-349.
- Brümmer A, Hausser J. MicroRNA binding sites in the coding region of mRNAs: Extending the repertoire of post-transcriptional gene regulation. *Bioessays*. 2014 Jun;36(6):617-26.
- Cerenius L, Söderhäll K. The prophenoloxidase-activating system in invertebrates. *Immunological reviews*. 2004 Apr;198(1):116-26.
- Chang CC, Yeh MS, Lin HK, Cheng W. The effect of *Vibrio alginolyticus* infection on caspase-3 expression and activity in white shrimp *Litopenaeus vannamei*. *Fish & shellfish immunology*. 2008 Nov 1;25(5):672-8.
- Chang Y, Xing J, Tang X, Sheng X, Zhan W. Haemocyanin content of shrimp (*Fenneropenaeus chinensis*) associated with white spot syndrome virus and *Vibrio harveyi* infection process. *Fish & shellfish immunology*. 2016 Jan 1;48:185-9.
- Chantanachookin C, Boonyaratpalin S, Kasornchandra J, Direkbusarakom S, Ekpanithanpong U, Supamataya K, Sriurairatana S, Flegel TW. Histology and ultrastructure reveal a new granulosis-like virus in *Penaeus monodon* affected by yellow-head disease. *Diseases of Aquatic Organisms*. 1993 Nov 18;17:145-.
- Charoensapsri W, Amparyup P, Hirono I, Aoki T, Tassanakajon A. Gene silencing of a prophenoloxidase activating enzyme in the shrimp, *Penaeus monodon*, increases susceptibility to *Vibrio harveyi* infection. *Developmental & Comparative Immunology*. 2009 Jul 1;33(7):811-20.
- Charoensapsri W, Amparyup P, Hirono I, Aoki T, Tassanakajon A. *PmPPAE2*, a new class of crustacean prophenoloxidase (proPO)-activating enzyme and its role in PO activation. *Developmental & Comparative Immunology*. 2011 Jan 1;35(1):115-24.
- Chen H, Sun H, You F, Sun W, Zhou X, Chen L, Yang J, Wang Y, Tang H, Guan Y, Xia W. Activation of STAT6 by STING is critical for antiviral innate immunity. *Cell*. 2011 Oct 14;147(2):436-46.
- Chen LL, Lo CF, Chiu YL, Chang CF, Kou GH. Natural and experimental infection of white spot syndrome virus (WSSV) in benthic larvae of mud crab *Scylla serrata*. *Diseases of aquatic organisms*. 2000 Mar 14;40(2):157-61.

- Chomwong S, Charoensapsri W, Amparyup P, Tassanakajon A. Two host gut-derived lactic acid bacteria activate the proPO system and increase resistance to an AHPND-causing strain of *Vibrio parahaemolyticus* in the shrimp *Litopenaeus vannamei*. *Developmental & Comparative Immunology*. 2018 Dec 1;89:54-65.
- Christensen BM, Li J, Chen CC, Nappi AJ. Melanization immune responses in mosquito vectors. *Trends in parasitology*. 2005 Apr 1;21(4):192-9.
- Coates CJ, Nairn J. Diverse immune functions of hemocyanins. *Developmental & Comparative Immunology*. 2014 Jul 1;45(1):43-55.
- Conesa A, Götz S, García-Gómez JM, Terol J, Talón M, Robles M. Blast2GO: a universal tool for annotation, visualization and analysis in functional genomics research. *Bioinformatics*. 2005 Aug 4;21(18):3674-6.
- Cremer TJ, Ravneberg DH, Clay CD, Piper-Hunter MG, Marsh CB, Elton TS, Gunn JS, Amer A, Kanneganti TD, Schlesinger LS, Butchar JP. MiR-155 induction by *F. novicida* but not the virulent *F. tularensis* results in SHIP down-regulation and enhanced pro-inflammatory cytokine response. *PloS one*. 2009 Dec 30;4(12):e8508.
- Deddouche S, Matt N, Budd A, Mueller S, Kemp C, Galiana-Arnoux D, Dostert C, Antoniewski C, Hoffmann JA, Imler JL. The DExD/H-box helicase Dicer-2 mediates the induction of antiviral activity in drosophila. *Nature immunology*. 2008 Dec;9(12):1425.
- Destoumieux-Garzón D, Saulnier D, Garnier J, Jouffrey C, Bulet P, Bachère E. Crustacean immunity antifungal peptides are generated from the c terminus of shrimp hemocyanin in response to microbial challenge. *Journal of Biological Chemistry*. 2001 Dec 14;276(50):47070-7.
- de la Vega E, Hall MR, Degnan BM, Wilson KJ. Short-term hyperthermic treatment of *Penaeus monodon* increases expression of heat shock protein 70 (HSP70) and reduces replication of gill associated virus (GAV). *Aquaculture*. 2006 Mar 31;253(1-4):82-90.
- De Schryver P, Defoirdt T, Sorgeloos P. Early mortality syndrome outbreaks: a microbial management issue in shrimp farming?. *PLoS Pathogens*. 2014 Apr 24;10(4):e1003919.
- Decker H, Ryan M, Jaenicke E, Terwilliger N. SDS-induced Phenoloxidase Activity of Hemocyanins from *Limulus polyphemus*, *Eurypelma californicum*, and *Cancer magister*. *Journal of Biological Chemistry*. 2001 May 25;276(21):17796-9.
- Eulalio A, Schulte L, Vogel J. The mammalian microRNA response to bacterial infections. *RNA biology*. 2012 Jun 1;9(6):742-50.
- Fagutao FF, Maningas MB, Kondo H, Aoki T, Hirono I. Transglutaminase regulates immune-related genes in shrimp. *Fish & shellfish immunology*. 2012 May 1;32(5):711-5.
- Félix DM, Elías JA, Córdova ÁI, Córdova LR, González AL, Jacinto EC, Aldaz NH, Mendoza FC, Zazueta MG. Survival of *Litopenaeus vannamei* shrimp fed on diets supplemented with *Dunaliella* sp. is improved after challenges by *Vibrio parahaemolyticus*. *Journal of invertebrate pathology*. 2017 Sep 1;148:118-23.

- Fiandalo MV, Kyprianou N. Caspase control: protagonists of cancer cell apoptosis. *Experimental oncology*. 2012 Oct;34(3):165.
- Finn RD, Clements J, Eddy SR. HMMER web server: interactive sequence similarity searching. *Nucleic acids research*. 2011 May 18;39(suppl_2):W29-37.
- Flegel TW. Major viral diseases of the black tiger prawn (*Penaeus monodon*) in Thailand. *World Journal of Microbiology and Biotechnology*. 1997 Jul 1;13(4):433-42.
- Gao Y, Zhang X, Wei J, Sun X, Yuan J, Li F, Xiang J. Whole transcriptome analysis provides insights into molecular mechanisms for molting in *Litopenaeus vannamei*. *PloS one*. 2015 Dec 9;10(12):e0144350
- Gollas-Galván T, Sotelo-Mundo RR, Yepiz-Plascencia G, Vargas-Requena C, Vargas-Albores F. Purification and characterization of α 2-macroglobulin from the white shrimp (*Penaeus vannamei*). *Comparative Biochemistry and Physiology Part C: Toxicology & Pharmacology*. 2003 Apr 1;134(4):431-8.
- Gong Y, Ju C, Zhang X. The miR-1000-p53 pathway regulates apoptosis and virus infection in shrimp. *Fish & shellfish immunology*. 2015 Oct 1;46(2):516-22.
- Grabherr MG, Haas BJ, Yassour M, Levin JZ, Thompson DA, Amit I, Adiconis X, Fan L, Raychowdhury R, Zeng Q, Chen Z. Full-length transcriptome assembly from RNA-Seq data without a reference genome. *Nature biotechnology*. 2011 Jul;29(7):644.
- Gu HJ, Sun QL, Jiang S, Zhang J, Sun L. First characterization of an anti-lipopolysaccharide factor (ALF) from hydrothermal vent shrimp: Insights into the immune function of deep-sea crustacean ALF. *Developmental & Comparative Immunology*. 2018 Jul 1;84:382-95.
- Han JE, Tang KF, Pantoja CR, White BL, Lightner DV. qPCR assay for detecting and quantifying a virulence plasmid in acute hepatopancreatic necrosis disease (AHPND) due to pathogenic *Vibrio parahaemolyticus*. *Aquaculture*. 2015 May 1;442:12-5.
- Han JE, Tang KF, Tran LH, Lightner DV. Photorhabdus insect-related (Pir) toxin-like genes in a plasmid of *Vibrio parahaemolyticus*, the causative agent of acute hepatopancreatic necrosis disease (AHPND) of shrimp. *Diseases of aquatic organisms*. 2015 Feb 10;113(1):33-40.
- Hausser J, Syed AP, Bilen B, Zavolan M. Analysis of CDS-located miRNA target sites suggests that they can effectively inhibit translation. *Genome research*. 2013 Apr 1;23(4):604-15.
- He Y, Yang K, Zhang X. Viral microRNAs targeting virus genes promote virus infection in shrimp *in vivo*. *Journal of virology*. 2014 Jan 15;88(2):1104-12.
- Hong XP, Xu D, Zhuo Y, Liu HQ, Lu LQ. Identification and pathogenicity of *Vibrio parahaemolyticus* isolates and immune responses of *Penaeus (Litopenaeus) vannamei* (Boone). *Journal of fish diseases*. 2016 Sep;39(9):1085-97.
- Hou F, He S, Liu Y, Zhu X, Sun C, Liu X. RNAi knock-down of shrimp *Litopenaeus vannamei* Toll gene and immune deficiency gene reveals their difference in regulating antimicrobial peptides transcription. *Developmental & Comparative Immunology*. 2014 Jun 1;44(2):255-60.
- Huang PH, Lu SC, Yang SH, Cai PS, Lo CF, Chang LK. Regulation of the immediate-early genes of white spot syndrome virus by *Litopenaeus*

- vannamei* Kruppel-like factor (*LvKLF*). *Developmental & Comparative Immunology*. 2014 Oct 1;46(2):364-72.
- Huang T, Cui Y, Zhang X. Involvement of viral microRNA in the regulation of antiviral apoptosis in shrimp. *Journal of virology*. 2014 Mar 1;88(5):2544-54.
- Huang T, Xu D, Zhang X. Characterization of host microRNAs that respond to DNA virus infection in a crustacean. *Bmc Genomics*. 2012 Dec;13(1):159.
- Huang Y, Wang W, Ren Q. Two host microRNAs influence WSSV replication via STAT gene regulation. *Scientific reports*. 2016 Mar 31;6:23643.
- Huang Y, Han K, Wang W, Ren Q. Host microRNA-217 promotes white spot syndrome virus infection by targeting tube in the Chinese mitten crab (*Eriocheir sinensis*). *Frontiers in cellular and infection microbiology*. 2017 May 4;7:164.
- Huber RG, Lim XN, Ng WC, Sim AY, Poh HX, Shen Y, Lim SY, Sundstrom KB, Sun X, Aw JG, Too HK. Structure mapping of dengue and Zika viruses reveals functional long-range interactions. *Nature communications*. 2019 Mar 29;10(1):1408.
- Jaree P, Wongdontri C, Somboonwiwat K. White spot syndrome virus-induced shrimp miR-315 attenuates prophenoloxidase activation via PPAE3 gene suppression. *Frontiers in immunology*. 2018;9:2184.
- Jiang N, Tan NS, Ho B, Ding JL. Respiratory protein-generated reactive oxygen species as an antimicrobial strategy. *Nature immunology*. 2007 Oct;8(10):1114.
- Jin S, Fu H, Sun S, Jiang S, Xiong Y, Gong Y, Qiao H, Zhang W, Wu Y. Integrated analysis of microRNA and mRNA expression profiles during the sex-differentiation sensitive period in oriental river prawn, *Macrobrachium nipponense*. *Scientific reports*. 2017 Sep 20;7(1):12011.
- Jitrapakdee S, Unajak S, Sittidilokratna N, Hodgson RA, Cowley JA, Walker PJ, Panyim S, Boonsaeng V. Identification and analysis of gp116 and gp64 structural glycoproteins of yellow head nidovirus of *Penaeus monodon* shrimp. *Journal of general virology*. 2003 Apr 1;84(4):863-73.
- Junprung W, Supungul P, Tassanakajon A. HSP70 and HSP90 are involved in shrimp *Penaeus vannamei* tolerance to AHPND-causing strain of *Vibrio parahaemolyticus* after non-lethal heat shock. *Fish & shellfish immunology*. 2017 Jan 1;60:237-46.
- Kaewkascholkul N, Somboonwiwat K, Asakawa S, Hirono I, Tassanakajon A, Somboonwiwat K. Shrimp miRNAs regulate innate immune response against white spot syndrome virus infection. *Developmental & Comparative Immunology*. 2016 Jul 1;60:191-201.
- Kamsaeng P, Tassanakajon A, Somboonwiwat K. Regulation of antilipopolysaccharide factors, ALFPm3 and ALFPm6, in *Penaeus monodon*. *Scientific reports*. 2017 Oct 4;7(1):12694.
- Kanehisa M, Goto S, Sato Y, Furumichi M, Tanabe M. KEGG for integration and interpretation of large-scale molecular data sets. *Nucleic acids research*. 2011 Nov 10;40(D1):D109-14.
- Krogh A, Larsson B, Von Heijne G, Sonnhammer EL. Predicting transmembrane protein topology with a hidden Markov model: application to complete genomes. *Journal of molecular biology*. 2001 Jan 19;305(3):567-80.

- Krüger J, Rehmsmeier M. RNAhybrid: microRNA target prediction easy, fast and flexible. *Nucleic acids research*. 2006 Jul 1;34(suppl_2):W451-4.
- Kumar S, Stecher G, Tamura K. MEGA7: molecular evolutionary genetics analysis version 7.0 for bigger datasets. *Molecular biology and evolution*. 2016 Mar 22;33(7):1870-4.
- Kumar A, Kumar A, Devi S, Patil S, Payal C, Negi S. Isolation, screening and characterization of bacteria from Rhizospheric soils for different plant growth promotion (PGP) activities: an in vitro study. *Recent research in science and technology*. 2012 Jan 17;4(1).
- Lai HC, Ng TH, Ando M, Lee CT, Chen IT, Chuang JC, Mavichak R, Chang SH, Yeh MD, Chiang YA, Takeyama H. Pathogenesis of acute hepatopancreatic necrosis disease (AHPND) in shrimp. *Fish & shellfish immunology*. 2015 Dec 1;47(2):1006-14.
- Lavilla-Pitogo CR, Leñaño EM, Paner MG. Mortalities of pond-cultured juvenile shrimp, *Penaeus monodon*, associated with dominance of luminescent vibrios in the rearing environment. *Aquaculture*. 1998 May 1;164(1-4):337-49.
- Leñaño EM, Mohan CV. Early mortality syndrome threatens Asia's shrimp farms. *Global Aquaculture Advocate*. 2012 Jul;2012(7/8):38-9.
- Lee CT, Chen IT, Yang YT, Ko TP, Huang YT, Huang JY, Huang MF, Lin SJ, Chen CY, Lin SS, Lightner DV. The opportunistic marine pathogen *Vibrio parahaemolyticus* becomes virulent by acquiring a plasmid that expresses a deadly toxin. *Proceedings of the National Academy of Sciences*. 2015 Aug 25;112(34):10798-803.
- Lee SY, Lee BL, Söderhäll K. Processing of an antibacterial peptide from hemocyanin of the freshwater crayfish *Pacifastacus leniusculus*. *Journal of Biological Chemistry*. 2003 Mar 7;278(10):7927-33.
- Leu JH, Chen SH, Wang YB, Chen YC, Su SY, Lin CY, Ho JM, Lo CF. A review of the major penaeid shrimp EST studies and the construction of a shrimp transcriptome database based on the ESTs from four penaeid shrimp. *Marine Biotechnology*. 2011 Aug 1;13(4):608-21.
- Li X, Meng X, Luo K, Luan S, Shi X, Cao B, Kong J. The identification of microRNAs involved in the response of Chinese shrimp *Fenneropenaeus chinensis* to white spot syndrome virus infection. *Fish & shellfish immunology*. 2017 Sep 1;68:220-31.
- Li F, Xiang J. Signaling pathways regulating innate immune responses in shrimp. *Fish & shellfish immunology*. 2013 Apr 1;34(4):973-80.
- Lightner DV, Hasson KW, White BL, Redman RM. Experimental infection of western hemisphere penaeid shrimp with Asian white spot syndrome virus and Asian yellow head virus. *Journal of aquatic animal health*. 1998 Sep;10(3):271-81.
- Lightner DV, editor. *A handbook of shrimp pathology and diagnostic procedures for diseases of cultured penaeid shrimp*. Baton Rouge: World Aquaculture Society; 1996.
- Lightner DV, Redman RM, Pantoja CR, Tang KF, Noble BL, Schofield P, Mohney LL, Nunan LM, Navarro SA. Historic emergence, impact and current status

- of shrimp pathogens in the Americas. *Journal of invertebrate pathology*. 2012 Jun 1;110(2):174-83.
- Lin X, Söderhäll K, Söderhäll I. Transglutaminase activity in the hematopoietic tissue of a crustacean, *Pacifastacus leniusculus*, importance in hemocyte homeostasis. *BMC immunology*. 2008 Dec;9(1):58.
- Liu Y, Song L, Sun Y, Liu T, Hou F, Liu X. Comparison of immune response in Pacific white shrimp, *Litopenaeus vannamei*, after knock down of Toll and IMD gene in vivo. *Developmental & Comparative Immunology*. 2016 Jul 1;60:41-52.
- Loc NH, MacRae TH, Musa N, Abdullah MD, Wahid ME, Sung YY. Non-lethal heat shock increased Hsp70 and immune protein transcripts but not *Vibrio* tolerance in the white-leg shrimp. *PloS one*. 2013 Sep 9;8(9):e73199.
- Lu X, Lu H, Guo L, Zhang Z, Zhao X, Zhong M, Li S, Zhang Y. Cloning and characterization of a novel hemocyanin variant *LvHMCV4* from shrimp *Litopenaeus vannamei*. *Fish & shellfish immunology*. 2015 Oct 1;46(2):398-405.
- Lu Y, Tapay LM, Gose RB, Brock JA, Loh PC. Infectivity of yellow head virus (YHV) and the Chinese baculo-like virus (CBV) in two species of penaeid shrimp *Penaeus stylirostris* (Stimpson) and *Penaeus vannamei* (Boone). *Diseases in Asian Aquaculture III*. 1997:297-304.
- Lu Y, Tapay LM, Loh PC, Brock JA, Gose RB. Distribution of yellow-head virus in selected tissues and organs of penaeid shrimp *Penaeus vannamei*. *Diseases of aquatic organisms*. 1995 Sep 14;23(1):67-70.
- Maralit BA, Jaree P, Boonchuen P, Tassanakajon A, Somboonwiwat K. Differentially expressed genes in hemocytes of *Litopenaeus vannamei* challenged with *Vibrio parahaemolyticus* AHPND (VP_{AHPND}) and VP_{AHPND} toxin. *Fish & shellfish immunology*. 2018 Oct 1;81:284-96.
- Marcato P, Griener TP, Mulvey GL, Armstrong GD. Recombinant Shiga toxin B-subunit-keyhole limpet hemocyanin conjugate vaccine protects mice from Shigatoxemia. *Infection and immunity*. 2005 Oct 1;73(10):6523-9.
- Mendoza-Cano F, Sánchez-Paz A. Development and validation of a quantitative real-time polymerase chain assay for universal detection of the White Spot Syndrome Virus in marine crustaceans. *Virology journal*. 2013 Dec;10(1):186
- Nagai T, Osaki T, Kawabata SI. Functional conversion of hemocyanin to phenoloxidase by horseshoe crab antimicrobial peptides. *Journal of Biological Chemistry*. 2001 Jul 20;276(29):27166-70.
- O'Connell RM, Taganov KD, Boldin MP, Cheng G, Baltimore D. MicroRNA-155 is induced during the macrophage inflammatory response. *Proceedings of the National Academy of Sciences*. 2007 Jan 30;104(5):1604-9.
- Paradkar PN, Trinidad L, Voysey R, Duchemin JB, Walker PJ. Secreted Vago restricts West Nile virus infection in *Culex mosquito* cells by activating the Jak-STAT pathway. *Proceedings of the National Academy of Sciences*. 2012 Nov 13;109(46):18915-20.
- Petersen TN, Brunak S, Von Heijne G, Nielsen H. SignalP 4.0: discriminating signal peptides from transmembrane regions. *Nature methods*. 2011 Oct;8(10):785.

- Pfaffl MW. A new mathematical model for relative quantification in real-time RT-PCR. *Nucleic acids research*. 2001 May 1;29(9):e45-.
- Pongsomboon S, Wongpanya R, Tang S, Chalorsrikul A, Tassanakajon A. Abundantly expressed transcripts in the lymphoid organ of the black tiger shrimp, *Penaeus monodon*, and their implication in immune function. *Fish & shellfish immunology*. 2008 Nov 1;25(5):485-93.
- Powell S, Szklarczyk D, Trachana K, Roth A, Kuhn M, Muller J, Arnold R, Rattei T, Letunic I, Doerks T, Jensen LJ. eggNOG v3. 0: orthologous groups covering 1133 organisms at 41 different taxonomic ranges. *Nucleic acids research*. 2011 Nov 16;40(D1):D284-9.
- Punta M, Coghill PC, Eberhardt RY, Mistry J, Tate J, Boursnell C, Pang N, Forslund K, Ceric G, Clements J, Heger A. The Pfam protein families database. *Nucleic acids research*. 2011 Nov 29;40(D1):D290-301.
- Qian Z, Liu X, Wang L, Wang X, Li Y, Xiang J, Wang P. Gene expression profiles of four heat shock proteins in response to different acute stresses in shrimp, *Litopenaeus vannamei*. *Comparative Biochemistry and Physiology Part C: Toxicology & Pharmacology*. 2012 Nov 1;156(3-4):211-20.
- Qiu C, Sun J, Liu M, Wang B, Jiang K, Sun S, Meng X, Luo Z, Wang L. Molecular cloning of hemocyanin cDNA from *Fenneropenaeus chinensis* and antimicrobial analysis of two C-terminal fragments. *Marine biotechnology*. 2014 Feb 1;16(1):46-53.
- Rajaram MV, Ni B, Morris JD, Brooks MN, Carlson TK, Bakthavachalu B, Schoenberg DR, Torrelles JB, Schlesinger LS. *Mycobacterium tuberculosis* lipomannan blocks TNF biosynthesis by regulating macrophage MAPK-activated protein kinase 2 (MK2) and microRNA miR-125b. *Proceedings of the national academy of sciences*. 2011 Oct 18;108(42):17408-13.
- Rao R, Zhu YB, Alinejad T, Tiruvayipati S, Thong KL, Wang J, Bhasu S. RNA-seq analysis of *Macrobrachium rosenbergii* hepatopancreas in response to *Vibrio parahaemolyticus* infection. *Gut pathogens*. 2015 Dec;7(1):6.
- Robinson MD, McCarthy DJ, Smyth GK. edgeR: a Bioconductor package for differential expression analysis of digital gene expression data. *Bioinformatics*. 2010 Jan 1;26(1):139-40.
- Ruan L, Bian X, Ji Y, Li M, Li F, Yan X. Isolation and identification of novel microRNAs from *Marsupenaeus japonicus*. *Fish & shellfish immunology*. 2011 Aug 1;31(2):334-40.
- Rungrasamee W, Leelatanawit R, Jiravanichpaisal P, Klinbunga S, Karoonuthaisiri N. Expression and distribution of three heat shock protein genes under heat shock stress and under exposure to *Vibrio harveyi* in *Penaeus monodon*. *Developmental & Comparative Immunology*. 2010 Oct 1;34(10):1082-9.
- Santos CA, Blanck DV, de Freitas PD. RNA-seq as a powerful tool for penaeid shrimp genetic progress. *Frontiers in genetics*. 2014 Aug 28;5:298.
- Schulte LN, Westermann AJ, Vogel J. Differential activation and functional specialization of miR-146 and miR-155 in innate immune sensing. *Nucleic acids research*. 2012 Nov 7;41(1):542-53.
- Sharbati J, Lewin A, Kutz-Lohroff B, Kamal E, Einspanier R, Sharbati S. Integrated microRNA-mRNA-analysis of human monocyte derived macrophages upon

- Mycobacterium avium* subsp. hominissuis infection. PloS one. 2011 May 24;6(5):e20258.
- Sharbati S, Sharbati J, Hoeke L, Bohmer M, Einspanier R. Quantification and accurate normalisation of small RNAs through new custom RT-qPCR arrays demonstrates Salmonella-induced microRNAs in human monocytes. BMC genomics. 2012 Dec;13(1):23.
- Shu L, Li C, Zhang X. The role of shrimp miR-965 in virus infection. Fish & shellfish immunology. 2016 Jul 1;54:427-34.
- Silver SJ, Hagen JW, Okamura K, Perrimon N, Lai EC. Functional screening identifies miR-315 as a potent activator of Wingless signaling. Proceedings of the National Academy of Sciences. 2007 Nov 13;104(46):18151-6.
- Sirikharin R, Taengchaiyaphum S, Sanguanrut P, Chi TD, Mavichak R, Proespraiwong P, Nuangsaeng B, Thitamadee S, Flegel TW, Sritunyalucksana K. Characterization and PCR detection of binary, Pir-like toxins from *Vibrio parahaemolyticus* isolates that cause acute hepatopancreatic necrosis disease (AHPND) in shrimp. PloS one. 2015 May 27;10(5):e0126987.
- Somboonwiwat K, Chaikerasitak V, Wang HC, Lo CF, Tassanakajon A. Proteomic analysis of differentially expressed proteins in *Penaeus monodon* hemocytes after *Vibrio harveyi* infection. Proteome science. 2010 Dec;8(1):39.
- Somboonwiwat K, Marcos M, Tassanakajon A, Klinbunga S, Aumelas A, Romestand B, Gueguen Y, Boze H, Moulin G, Bachère E. Recombinant expression and anti-microbial activity of anti-lipopolysaccharide factor (ALF) from the black tiger shrimp *Penaeus monodon*. Developmental & Comparative Immunology. 2005 Jan 1;29(10):841-51.
- Soonthornchai W, Chaiyapechara S, Klinbunga S, Thongda W, Tangphatsornruang S, Yoocha T, Jarayabhand P, Jiravanichpaisal P. Differentially expressed transcripts in stomach of *Penaeus monodon* in response to AHPND infection. Developmental & Comparative Immunology. 2016 Dec 1;65:53-63.
- Spann KM, Donaldson RA, Cowley JA, Walker PJ. Differences in the susceptibility of some penaeid prawn species to gill-associated virus (GAV) infection. Diseases of aquatic organisms. 2000 Sep 28;42(3):221-5.
- Spann KM, McCulloch RJ, Cowley JA, East IJ, Walker PJ. Detection of gill-associated virus (GAV) by in situ hybridization during acute and chronic infections of *Penaeus monodon* and *P. esculentus*. Diseases of aquatic organisms. 2003 Aug 15;56(1):1-0.
- Spinelli SV, Diaz A, D'Attilio L, Marchesini MM, Bogue C, Bay ML, Bottasso OA. Altered microRNA expression levels in mononuclear cells of patients with pulmonary and pleural tuberculosis and their relation with components of the immune response. Molecular immunology. 2013 Mar 1;53(3):265-9.
- Sritunyalucksana K, Utairungsee T, Sirikharin R, Srisala J. Virus-binding proteins and their roles in shrimp innate immunity. Fish & shellfish immunology. 2012 Dec 1;33(6):1269-75.
- Sun X, Liu QH, Yang B, Huang J. Differential expression of microRNAs of *Litopenaeus vannamei* in response to different virulence WSSV infection. Fish & shellfish immunology. 2016 Nov 1;58:18-23.

- Sung YY, Van Damme EJ, Sorgeloos P, Bossier P. Non-lethal heat shock protects gnotobiotic *Artemia franciscana* larvae against virulent Vibrios. *Fish & shellfish immunology*. 2007 Apr 1;22(4):318-26.
- Sutthangkul J, Amparyup P, Eum JH, Strand MR, Tassanakajon A. Anti-melanization mechanism of the white spot syndrome viral protein, WSSV453, via interaction with shrimp proPO-activating enzyme, PmpProPPAE2. *Journal of General Virology*. 2017 Apr 28;98(4):769-78.
- Sutthangkul J, Amparyup P, Charoensapsri W, Senapin S, Phiwsaiya K, Tassanakajon A. Suppression of shrimp melanization during white spot syndrome virus infection. *Journal of Biological Chemistry*. 2015 Mar 6;290(10):6470-81.
- Tassanakajon A. Innate immune system of shrimp. *Fish Shellfish Immunol*. 2013 Apr;34(4):953.
- Tassanakajon A, Rimphanitchayakit V, Visetnan S, Amparyup P, Somboonwiwat K, Charoensapsri W, Tang S. Shrimp humoral responses against pathogens: antimicrobial peptides and melanization. *Developmental & Comparative Immunology*. 2018 Mar 1;80:81-93.
- Tinwongger S, Thawonsuwan J, Kondo H, Hirono I. Identification of an anti-lipopolysaccharide factor AV-R isoform (LvALF AV-R) related to Vp_PirAB-like toxin resistance in *Litopenaeus vannamei*. *Fish & shellfish immunology*. 2019 Jan 1;84:178-88.
- Tili E, Michaille JJ, Wernicke D, Alder H, Costinean S, Volinia S, Croce CM. Mutator activity induced by microRNA-155 (miR-155) links inflammation and cancer. *Proceedings of the National Academy of Sciences*. 2011 Mar 22;108(12):4908-13.
- Tran L, Nunan L, Redman RM, Mohney LL, Pantoja CR, Fitzsimmons K, Lightner DV. Determination of the infectious nature of the agent of acute hepatopancreatic necrosis syndrome affecting penaeid shrimp. *Diseases of aquatic organisms*. 2013 Jul 9;105(1):45-55.
- Untergasser A, Cutcutache I, Koressaar T, Ye J, Faircloth BC, Remm M, Rozen SG. Primer3-new capabilities and interfaces. *Nucleic acids research*. 2012 Jun 21;40(15):e115-.
- Wang B, Li F, Dong B, Zhang X, Zhang C, Xiang J. Discovery of the genes in response to white spot syndrome virus (WSSV) infection in *Fenneropenaeus chinensis* through cDNA microarray. *Marine Biotechnology*. 2006 Oct 1;8(5):491-500.
- Wang J, Zhang FY, Song W, Fang YB, Hu JH, Zhao M, Jiang KJ, Ma LB. Characterization of hemocyanin from the mud crab *Scylla paramamosain* and its expression analysis in different tissues, at various stages, and under *Vibrio parahaemolyticus* infection. *Genetics and Molecular Research*. 2015 Dec 11;14(4):16639-51
- Wang L, Zhi B, Wu W, Zhang X. Requirement for shrimp caspase in apoptosis against virus infection. *Developmental & Comparative Immunology*. 2008 Jan 1;32(6):706-15.
- Wang Z, Sun B, Zhu F. The shrimp hormone receptor acts as an anti-apoptosis and anti-inflammatory factor in innate immunity. *Fish & shellfish immunology*. 2018 Jan 1;72:581-92.

- Wang Z, Zhu F. MicroRNA-100 is involved in shrimp immune response to white spot syndrome virus (WSSV) and *Vibrio alginolyticus* infection. *Scientific reports*. 2017 Feb 9;7:42334.
- Wijegoonawardane PK, Cowley JA, Phan T, Hodgson RA, Nielsen L, Kiatpathomchai W, Walker PJ. Genetic diversity in the yellow head nidovirus complex. *Virology*. 2008 Oct 25;380(2):213-25.
- Williams SL, Jensen RV, Kuhn DD, Stevens AM. Analyzing the metabolic capabilities of a *Vibrio parahaemolyticus* strain that causes early mortality syndrome in shrimp. *Aquaculture*. 2017 Jul 1;476:44-8.
- Wongteerasupaya C, Sriurairatana S, Vickers JE, Akrajarn A, Boonsaeng V, Panyim S, Tassanakajon A, Withyachumnarnkul B, Flegel TW. Yellow-head virus of *Penaeus monodon* is an RNA virus. *Diseases of Aquatic Organisms*. 1995 May 4;22(1):45-50.
- Wu J, Lu C, Diao N, Zhang S, Wang S, Wang F, Gao Y, Chen J, Shao L, Lu J, Zhang X. Analysis of microRNA expression profiling identifies miR-155 and miR-155* as potential diagnostic markers for active tuberculosis: a preliminary study. *Human immunology*. 2012 Jan 1;73(1):31-7.
- Xu J, Ruan L, Li Z, Yu X, Li S, Shi H, Xu X. Characterization of four hemocyanin isoforms in *Litopenaeus vannamei*. *Acta Oceanologica Sinica*. 2015 Feb 1;34(2):36-44.
- Xu X, Yuan J, Yang L, Weng S, He J, Zuo H. The Dorsal/miR-1959/Cactus feedback loop facilitates the infection of WSSV in *Litopenaeus vannamei*. *Fish & shellfish immunology*. 2016 Sep 1;56:397-401.
- Yang YT, Chen IT, Lee CT, Chen CY, Lin SS, Hor LI, Tseng TC, Huang YT, Sritunyalucksana K, Thitamadee S, Wang HC. Draft genome sequences of four strains of *Vibrio parahaemolyticus*, three of which cause early mortality syndrome/acute hepatopancreatic necrosis disease in shrimp in China and Thailand. *Genome Announc.*. 2014 Oct 30;2(5):e00816-14.
- Yang L, Yang G, Zhang X. The miR-100-mediated pathway regulates apoptosis against virus infection in shrimp. *Fish & shellfish immunology*. 2014 Sep 1;40(1):146-53.
- Yang G, Yang L, Zhao Z, Wang J, Zhang X. Signature miRNAs involved in the innate immunity of invertebrates. *PloS one*. 2012 Jun 19;7(6):e39015.
- Yeh MD. Characterization and involvement of toll and IMD pathways in AHPND-infected shrimp. 2016.
- Young MD, Wakefield MJ, Smyth GK, Oshlack A. Gene ontology analysis for RNA-seq: accounting for selection bias. *Genome biology*. 2010 Feb;11(2):R14.
- Zeng D, Chen X, Xie D, Zhao Y, Yang Q, Wang H, Li Y, Chen X. Identification of highly expressed host microRNAs that respond to white spot syndrome virus infection in the Pacific white shrimp *Litopenaeus vannamei* (Penaeidae). *Genet Mol Res*. 2015 Oct;14(2):4818-28.
- Zhang X, Huang C, Qin Q. Antiviral properties of hemocyanin isolated from shrimp *Penaeus monodon*. *Antiviral research*. 2004 Feb 1;61(2):93-9.
- Zhang Y, Wang S, Xu A, Chen J, Lin B, Peng X. Affinity proteomic Approach for identification of an IgA-like protein in *Litopenaeus vannamei* and study on

- its Agglutination characterization. *Journal of proteome research*. 2006 Apr 7;5(4):815-21.
- Zheng Z, Aweya JJ, Wang F, Yao D, Lun J, Li S, Ma H, Zhang Y. Acute Hepatopancreatic Necrosis Disease (AHPND) related microRNAs in *Litopenaeus vannamei* infected with AHPND-causing strain of *Vibrio parahaemolyticus*. *BMC genomics*. 2018 Dec;19(1):335.
- Zhou J, Wang WN, He WY, Zheng Y, Wang L, Xin Y, Liu Y, Wang AL. Expression of HSP60 and HSP70 in white shrimp, *Litopenaeus vannamei* in response to bacterial challenge. *Journal of invertebrate pathology*. 2010 Mar 1;103(3):170-8.
- Zhao S, Lu X, Zhang Y, Zhao X, Zhong M, Li S, Lun J. Identification of a novel alternative splicing variant of hemocyanin from shrimp *Litopenaeus vannamei*. *Immunology letters*. 2013 Jul 1;154(1-2):1-6.
- Zhao X, Guo L, Lu X, Lu H, Wang F, Zhong M, Chen J, Zhang Y. Evidences of abundant hemocyanin variants in shrimp *Litopenaeus vannamei*. *Molecular immunology*. 2016 Sep 1;77:103-12.
- Zheng Z, Aweya JJ, Wang F, Yao D, Lun J, Li S, Ma H, Zhang Y. Acute Hepatopancreatic Necrosis Disease (AHPND) related microRNAs in *Litopenaeus vannamei* infected with AHPND-causing strain of *Vibrio parahaemolyticus*. *BMC genomics*. 2018 Dec;19(1):335.
- Zhou J, Wang WN, He WY, Zheng Y, Wang L, Xin Y, Liu Y, Wang AL. Expression of HSP60 and HSP70 in white shrimp, *Litopenaeus vannamei* in response to bacterial challenge. *Journal of invertebrate pathology*. 2010 Mar 1;103(3):170-8.
- Zhu F, Wang Z, Sun BZ. Differential expression of microRNAs in shrimp *Marsupenaeus japonicus* in response to *Vibrio alginolyticus* infection. *Developmental & Comparative Immunology*. 2016 Feb 1;55:76-9.

CURRICULUM VITAE

Name: Mr.Pakpoom Boonchuen

Tel: (+66) 9-8192-7800

Date of Birth: October 1st, 1991

Email: mr.boonchuen@gmail.com

Institutional Affiliation: Center of Excellence for Molecular Biology and Genomics of Shrimp, Department of Biochemistry, Faculty of Science, Chulalongkorn University, Bangkok 10330

Education:

2010 - 2013 B.Sc. (2nd Class Honor in Biochemistry), Chulalongkorn University

2014 - Present Ph.D. (Biochemistry), Chulalongkorn University

Scholarships:

2012 The King Bhumibol Scholarship

2014 - 2015 The 100th Anniversary Chulalongkorn University Fund for Doctoral Scholarship, Chulalongkorn University, Thailand

2015 - Present The Royal Golden Jubilee Ph.D. Program Scholarship for Ph.D. degree, Thailand Research Fund, Thailand

2016 - Present The 90th Anniversary of Chulalongkorn University Fund (Ratchadaphiseksomphot Endowment Fund), Chulalongkorn University, Thailand

Publications:

1. Methatham T, **Boonchuen P**, Jaree P, Tassanakajon A, Somboonwiwat K. Antiviral action of the antimicrobial peptide ALFPm3 from *Penaeus monodon* against white spot syndrome virus. (2017). Dev Comp Immunol., Volume 69, pp. 23-32. [Impact Factor: 3.218]
2. **Boonchuen P**, Jaree P, Tassanakajon A, Somboonwiwat K. Hemocyanin of *Litopenaeus vannamei* agglutinates *Vibrio parahaemolyticus* AHPND (VP_{AHPND})

- and neutralizes its toxin. (2018). *Dev Comp Immunol.*, Volume 84, pp. 371-381. [Impact Factor: 3.218]
3. Mararit B.A., Jaree P, **Boonchuen P**, Tassanakajon A, Somboonwiwat K. Differentially expressed genes in hemocytes of *Litopenaeus vannamei* challenged with *Vibrio parahaemolyticus* AHPND (VP_{AHPND}) and VP_{AHPND} toxin. (2018). *Fish Shellfish Immunol.*, Volume 81, pp 284-296. [Impact Factor: 3.298]
 4. **Boonchuen P**, Mararit B.A., Jaree P., Tassanakajon A, Somboonwiwat K. MicroRNA and mRNA interactions contribute to coordinating the immune response in chronic non-lethal heat stressed *Litopenaeus vannamei* against acute hepatopancreatic necrosis disease-causing strain of *Vibrio parahaemolyticus*. (Submitted)
 5. **Boonchuen P**, Sakhor H, Jaree P, Tassanakajon A, Somboonwiwat, K. Functional characterization of the Vago5 gene in *Vibrio parahaemolyticus* AHPND-infected *Penaeus vannamei*. (manuscript preparation)
 6. **Boonchuen P**, Somboonviwat K., Tassanakajon A, Somboonwiwat K. Identification of miRNAs from *Penaeus vannamei* in response to *Vibrio parahaemolyticus* AHPND infection. (manuscript preparation)

Presentations Awards:

- 2018 Outstanding poster presentation, The 6th International Conference on Biochemistry and Molecular Biology (BMB), 20-22 June 2018
- 2017 The 2nd Winner Poster Presentation, 10th Symposium on Diseases in Asian Aquaculture (DAA10), the Anvaya Beach Resort, Kuta, Bali, Indonesia
- 2016 The Third Place Award Oral presentation, 21st Biological Sciences Graduate Congress (BSGC), University of Malaya, Kuala Lumpur, Malaysia.
- 2014 The second prize of the poster presentation, The Joint 7th AOHUPO Congress and 9th International Symposium of the Protein Society of Thailand (7th AOHUPO/9th PST), Bangkok, Thailand.
- 2014 The First prize of the poster presentation, Session: Biological Sciences, The Science Forum 2014, Chulalongkorn University, Thailand

Oral Presentation

1. **Boonchuen, P.**, Jaree P, Tassanakajon, A., Somboonwiwat, K., Identification of miRNAs from *Penaeus vannamei* in response to *Vibrio parahaemolyticus* AHPND infection and heat stress. 22nd Biological Sciences Graduate Congress (BSGC), University Town, National University of Singapore (2017).
2. **Boonchuen, P.**, Maralit, B.A., Luangtrakul, W., Jaree P, Tassanakajon, A., Somboonwiwat, K., Effect of chronic heat stress on hemocyte transcriptome of *Penaeus vannamei* challenged with *Vibrio parahaemolyticus* AHPND. The 5th Thailand Research Fund (TRF) Senior Scholar Group Annual Meeting 2017 (2017).
3. **Boonchuen, P.**, Methatham T, Jaree P, Tassanakajon, A., Somboonwiwat, K., Antiviral action of ALFPm3 on WSSV. The 3rd Thailand Research Fund (TRF) Senior Scholar Group Annual Meeting 2015 (2015).
4. **Boonchuen, P.**, Methatham, T., Tassanakajon, A., Somboonwiwat, K., Antiviral action of antilipoplysaccharide factor isoform 3 on white spot syndrome virus. 20th Biological Sciences Graduate Congress (BSGC), Chulalongkorn University, Bangkok, Thailand (2015).
5. **Boonchuen, P.**, Tassanakajon, A., Somboonwiwat, K., Protein-Protein interaction assay between proteins of white spot syndrome virus and *Penaeus monodon* Antilipoplysaccharide factor Isoform 3 (ALFPm3)., The Hitachi Trophy 2014, The Science Forum 2014, Chulalongkorn University, Bangkok, Thailand (2014).

Poster Presentation

1. **Boonchuen, P.** and Somboonwiwat, K. (2018). Identification of miRNAs from *Penaeus vannamei* in response to *Vibrio parahaemolyticus* AHPND infection. The 6th International Conference on Biochemistry and Molecular Biology (BMB), 20-22 June, 2018, Rayong, Thailand.
2. **Boonchuen, P.**, Methatham T, Jaree P, Tassanakajon, A., Somboonwiwat, K., Hemocyanin of *Litopenaeus vannamei* agglutinates *Vibrio parahaemolyticus* AHPND (VP_{AHPND}) and neutralizes VP_{AHPND} toxin. 10th Symposium on Diseases in Asian Aquaculture (DAA10), the Anvaya Beach Resort, Kuta, Bali, Indonesia (2017).

3. **Boonchuen, P.**, Methatham T, Jaree P, Tassanakajon, A., Somboonwiwat, K., Antiviral action of ALFPm3 on WSSV. The 3rd Thailand Research Fund (TRF) Senior Scholar Group Annual Meeting 2015 (2015).
4. **Boonchuen, P.**, Methatham T, Jaree P, Tassanakajon, A., Somboonwiwat, K., *Penaeus monodon* anti-lipoplysaccharide factor isoform 3 (ALFPm3) exhibits anti-WSSV activity through the interactions with WSSV proteins. The Joint 7th AOHUPO Congress and 9th International Symposium of the Protein Society of Thailand (7th AOHUPO/9th PST) (2014).
5. **Boonchuen, P.**, Tassanakajon, A., Somboonwiwat, K., Protein-Protein interaction assay between proteins of white spot syndrome virus and *Penaeus monodon* Anti-lipoplysaccharide factor Isoform 3 (ALFPm3). The 4th International Biochemistry and Molecular Biology Conference 2014, Bangkok, Thailand (2014).
6. **Boonchuen, P.**, Tassanakajon, A., Somboonwiwat, K., Protein-Protein interaction assay between proteins of white spot syndrome virus and *Penaeus monodon* Anti-lipoplysaccharide factor isoform 3 (ALFPm3). The Science Forum 2014, Chulalongkorn University, Bangkok, Thailand (2014).

Research Experiences

Senior project research (Bachelor degree)

Advisor: Asst. Prof. Dr. Kunlaya Somboonwiwat

- Construction and expression of the recombinant WSSV186 and WSSV395 proteins in *E. coli* system then, the protein-protein interaction between WSSV proteins and ALFPm3, anti-lipoplysaccharide factor isoform 3, were studied.

Ph.D. research:

Advisor: Asst. Prof. Dr. Kunlaya Somboonwiwat

Co-advisor: Prof. Dr. Anchalee Tassanakajon

- Identification and functional characterization of genes and microRNAs from *Penaeus vannamei* in response to *Vibrio parahaemolyticus* AHPND infection and heat stress.

Activities

1. An organizing committee of the 6th International Conference on Biochemistry and Molecular Biology (BMB), Rayong, Thailand (20-22 June, 2018)
2. An organizing committee of the 20th Biological Sciences Graduate Congress (BSGC), Chulalongkorn University, Bangkok, Thailand (9-11 December 2015)
3. A trainee in Center of Excellence in Clinical Virology, faculty of Medicine, Chulalongkorn University (25 March – 30 April 2013)
4. An organizing committee of CU Academic Expo 2012 in faculty of Science Chulalongkorn University (14-18 November 2012)
5. An organizing committee of Young Leader Scientist Camp #19 at Rayong, Thailand (25 August 2012)
6. An organizing committee of Science Quiz Competition 2012 Faculty of Science Chulalongkorn University (16-20 October 2012)
7. An organizing committee of Knowledge Sharing Camp # 13, Faculty of Science Chulalongkorn University (20-22 April 2012)

REFERENCES

จุฬาลงกรณ์มหาวิทยาลัย
CHULALONGKORN UNIVERSITY



จุฬาลงกรณ์มหาวิทยาลัย
CHULALONGKORN UNIVERSITY

VITA

NAME	Pakpoom Boonchuen
DATE OF BIRTH	01 October 1991
PLACE OF BIRTH	Nakhornratchasima
INSTITUTIONS ATTENDED	- Department of Biochemistry, Faculty of Science, Chulalongkorn University, Thailand. - Department of Microbiology and Immunology, School of Medicine, Stanford University, USA.
HOME ADDRESS	444/266 Condolette IZE ratchatewi, Phayathai Rd. Ratchatewi, Bangkok, 10330 Thailand
PUBLICATION	<ol style="list-style-type: none"> 1. Methatham T, Boonchuen P, Jaree P, Tassanakajon A, Somboonwiwat K. Antiviral action of the antimicrobial peptide ALFPm3 from <i>Penaeus monodon</i> against white spot syndrome virus. (2017). <i>Dev Comp Immunol.</i>, Volume 69, pp. 23-32. [Impact Factor: 3.218] 2. Boonchuen P, Jaree P, Tassanakajon A, Somboonwiwat K. Hemocyanin of <i>Litopenaeus vannamei</i> agglutinates <i>Vibrio parahaemolyticus</i> AHPND (VPAHPND) and neutralizes its toxin. (2018). <i>Dev Comp Immunol.</i>, Volume 84, pp. 371-381. [Impact Factor: 3.218] 3. Mararit B.A., Jaree P, Boonchuen P, Tassanakajon A, Somboonwiwat K. Differentially expressed genes in hemocytes of <i>Litopenaeus vannamei</i> challenged with <i>Vibrio parahaemolyticus</i> AHPND (VPAHPND) and VPAHPND toxin. (2018). <i>Fish Shellfish Immunol.</i>, Volume 81, pp 284-296. [Impact Factor: 3.298] 4. Boonchuen P, Mararit B.A., Jaree P., Tassanakajon A, Somboonwiwat K. MicroRNA and mRNA interactions contribute to coordinating the immune response in chronic non-lethal heat stressed <i>Litopenaeus vannamei</i> against acute hepatopancreatic necrosis disease-causing strain of <i>Vibrio parahaemolyticus</i>. (Submitted) 5. Boonchuen P, Sakhor H, Jaree P, Tassanakajon A, Somboonwiwat, K. Functional characterization of the Vago5 gene in <i>Vibrio parahaemolyticus</i> AHPND-infected <i>Penaeus vannamei</i>. (manuscript preparation) 6. Boonchuen P, Somboonwiwat K., Tassanakajon A, Somboonwiwat K. Identification of miRNAs from <i>Penaeus vannamei</i> in response to <i>Vibrio parahaemolyticus</i> AHPND infection. (manuscript preparation)
AWARD RECEIVED	2018 Outstanding poster presentation, The 6th International Conference on Biochemistry and Molecular

Biology (BMB), 20-22 June 2018

2017 The 2nd Winner Poster Presentation, 10th Symposium on Diseases in Asian Aquaculture (DAA10), the Anvaya Beach Resort, Kuta, Bali, Indonesia

2016 The Third Place Award Oral presentation, 21st Biological Sciences Graduate Congress (BSGC), University of Malaya, Kuala Lumpur, Malaysia.

2014 The second prize of the poster presentation, The Joint 7th AOHUPO Congress and 9th International Symposium of the Protein Society of Thailand (7th AOHUPO/9th PST), Bangkok, Thailand.

2014 The First prize of the poster presentation, Session: Biological Sciences, The Science Forum 2014, Chulalongkorn University, Thailand



จุฬาลงกรณ์มหาวิทยาลัย
CHULALONGKORN UNIVERSITY